Busy Burst Technology Applied to OFDMA–TDD Systems

Birendra Ghimire

A thesis submitted for the degree of Doctor of Philosophy.
The University of Edinburgh.
February 2010

Abstract

The most significant bottleneck in wireless communication systems is an ever-increasing disproportion between the bandwidth demand and the available spectrum. A major challenge in the field of wireless communications is to maximise the spatial reuse of resources whilst avoiding detrimental co-channel interference (CCI). To this end, frequency planning and centralised coordination approaches are widely used in wireless networks. However, the networks for the next generation of wireless communications are often envisioned to be decentralised, randomly distributed in space, hierarchical and support heterogeneous traffic and service types. Fixed frequency allocation would not cater for the heterogeneous demands and centralised resource allocation would be cumbersome and require a lot of signalling. Decentralised radio resource allocation based on locally available information is considered the key.

In this context, the busy burst (BB) signalling concept is identified as a potential mechanism for decentralised interference management in future generation networks. Interference aware allocation of time-frequency slots (chunks) is accomplished by letting receivers transmit a BB in a time-multiplexed mini-slot, upon successful reception of data. Exploiting channel reciprocity of the time division duplex (TDD) mode, the transmitters avoid reusing the chunks where the received BB power is above a pre-determined threshold so as to limit the CCI caused towards the reserved chunks to a threshold value. In this thesis, the performance of BB signalling mechanism in orthogonal frequency division multiple access - time division duplexing (OFDMA-TDD) systems is evaluated by means of system level simulations in networks operating in *ad hoc* and cellular scenarios. Comparisons are made against the state-of-the-art centralised CCI avoidance and mitigation methods, *viz.* frequency planning, fractional frequency reuse, and antenna array with switched grid of beams, as well as decentralised methods such as the carrier sense multiple access method that attempt to avoid CCI by avoiding transmission on chunks deemed busy. The results demonstrate that with an appropriate choice of threshold parameter, BB-based techniques outperform all of the above state-of-the-art methods. Moreover, it is demonstrated that by adjusting the BB-specific threshold parameter, the system throughput can be traded off for improving throughput for links with worse channel condition, both in the *ad hoc* and cellular scenario. Moreover, by utilising a variable BB power that allows a receiver to signal the maximum CCI it can tolerate, it is shown that a more favourable trade-off between total system throughput and link throughput can be made. Furthermore, by performing link adaptation, it is demonstrated that the spatial reuse and the energy efficiency can be traded off by adjusting the threshold parameter. Although the BB signalling mechanism is shown to be effective in avoiding detrimental CCI, it cannot mitigate CCI by itself. On the other hand, multiple antenna techniques such as adaptive beamforming or switched beam approaches allow CCI to be mitigated but suffer from hidden node problems. The final contribution of this thesis is that by combining the BB signalling mechanism with multiple antenna techniques, it is demonstrated that the hybrid approach enhances spatial reusability of resources whilst avoiding detrimental CCI.

In summary, this thesis has demonstrated that BB provides a flexible radio resource mechanism that is suitable for future generation networks.

Declaration of originality

I hereby declare that the research recorded in this thesis and the thesis itself was composed and originated entirely by myself in the School of Engineering and Science at Jacobs University Bremen and at the Institute for Digital Communications at The University of Edinburgh, with the following exception:

Initial code developed for modelling the time variant and frequency selective channel was written by Dr. Van Duc Nguyen.

Birendra Ghimire

Acknowledgements

First and foremost, I would like to wholeheartedly thank my supervisor Harald Haas for accepting me as his PhD student and for his continuous guidance and constructive feedback that I received throughout the PhD process.

Second, I would like to thank School of Engineering and Science at Jacobs University Bremen and School of Engineering at the University of Edinburgh for the scholarship during the course of PhD. I acknowledge the financial support from the Deutsche Forschungsgemeinschaft (DFG) for the initial part of the work and DOCOMO Eurolabs for the latter part. In this context, I would also like to thank Gunther Auer from DOCOMO Eurolabs for many fruitful discussions and constructive feedback. I acknowledge Stefan Videv's assistance in cross checking and optimizing the code used for [1] and his part in the development of CESAR concept [2, 3] as a part of joint research project with DOCOMO Eurolabs.

I would like to thank my colleagues at the Institute for Digital Communication for helpful advices. In particular, I would like to mention (in alphabetical order) Ellina, Mostafa, Rami, Sinan and Zubin for friendly help and constructive feedbacks. I would also like to acknowledge the use of computational resources provided by CLAMV at Jacobs University Bremen, TLC lab and the IDCOM computer pool, without which this PhD project would not have completed. In this respect, I would like to thank Achim Gelessus from Jacobs University Bremen, Dave Laurenson from IDCOM and the IT team at School of Engineering for supporting the computing facilities. I would also like to thank Nicola Ferguson for the administrative formalities involved.

Last but not least, I would like to thank my family for their continuous support. I would like to especially thank my wife, Shanta, for her love and understanding at all times without which this thesis would not have been possible.

Finally, I would like to dedicate this thesis in the memory of my late grandfather, who unfortunately passed away while I was preparing this thesis. May his soul rest in eternal peace.

Contents

List of figures

List of tables

Acronyms and abbreviations

2G	Second generation
3G	Third generation
3GPP	Third generation partnership project
4G	Fourth generation
ACH	Access channel
ACI	Adjacent channel interference
ACK	Acknowledgement
AoA	Angle of arrival
AoD	Angle of departure
BB	Busy burst
BPSK	Binary phase shift keying
BS	Base station
BT	Busy tone
BSBS	Blind score-based scheduler
CCI	Co-channel interference
cdf	Cumulative distribution function
CESAR	Cellular slot allocation and reservation
CSMA	Carrier sense multiple access
CSMA/CA	CSMA with collision avoidance
CSMA/CD	CSMA with collision detection
CTF	Channel transfer function
CTS	Clear to send
DBTMA	Dual busy tone multiple access
DCF	Distributed coordination function
DFT	Discrete Fourier transform
DL	Downlink
DS	Data sending
ECH	Echo channel
ESPRIT	Estimation of signal parameter by rotational invariant techniques

FDD	Frequency division duplexing
FDMA	Frequency division multiple access
FEC	Forward error correction
FIFO	First in first out
FFT	Fast Fourier transform
FFR	Fractional frequency reuse
FSBS	Fair score-based scheduler
Gbps	Giga bits per second
GSM	Global system for mobile telecommunications
HARQ	Hybrid automatic repeat request
HII	Heavy interference indicator
HSPA	High speed packet access
HSPA+	HSPA evolved
HSDPA	High speed downlink packet access
HSUPA	High speed uplink packet access
ICI	Inter-carrier interference
ICIC	Inter-cell interference coordination
IDFT	Inverse discrete Fourier transform
IEEE	Institute for electrical and electronics engineers
i.i.d	Independent and identically distributed
IFFT	Inverse fast Fourier transform
ISM	Industrial, scientific and medical
kbps	Kilo bit per second
LA	Link adaptation
LAN	Local area network
LoS	Line of sight
LTE	Long term evolution
MAC	Medium access control
MACA	Multiple Access with Collision Avoidance
MACA-W	Multiple Access with Collision Avoidance - Wireless
MAI	Multiple access interference
Mbps	Megabits per second
MS	Mobile station

MIMO	Multiple input multiple output
MUSIC	Multiple signal classification
NLoS	Non line of sight
OI	Overload indicator
OFDM	Orthogonal frequency division multiplexing
OFDMA	Orthogonal frequency division multiple access
PCF	Point coordination function
QAM	Quadrature amplitude modulation
QoS	Quality of service
QPSK	Quadrature phase shift keying
PCF	Point coordination function
PSTN	Public switched trunked network
RF	Radio frequency
rms	Root mean squared
RTS	Ready to send
SC	Sub-carrier.
SINR	Signal to interference and noise ratio
SNR	Signal to noise ratio
SUC	Satisfied user criterion
TCH	Traffic channel
TDD	Time division duplexing
TDMA	Time division multiple access
TV	Television
UL	Uplink
UMTS	Universal mobile telecommunications system
W-CHAMB	Wireless channel oriented *ad hoc* multihop protocol
WINNER	Wireless world initiative new radio
WLAN	Wireless local area network

List of Principal Symbols

$a_\nu[n,k]$	Binary variable denoting chunks accessed by user ν
A_e	Elemental antenna gains of an anisotropic phased array
A_f	Antenna factor
A_o	Overall antenna gain for an anisotropic phased array
$b_\nu[n,k]$	Binary variable denoting successful transmission for user ν on chunk (n,k)
$\chi_\mathbf{y}[n,k]$	Binary variable denoting whether or not the transmitter $\mathbf{y}$ was allowed to access the chunk (n,k)
B	System bandwidth
B_sc	Bandwidth of a subcarrier
$C_{\nu,\beta}[n,k]$	Instantaneous capacity user ν connected to BS β on chunk (n,k)
α	Receiver of active link (μ,α)
β	Receiver of competing link (ν,β)
d	Distance between MS and BS
d_1	Distance from BS to street crossing in Manhattan scenario
d_2	Distance from street crossing to MS in Manhattan scenario
d_t	Distance of t^th element of antenna array from a reference point
d_BP	Distance at which the path loss exponent changes from lower exponent to higher exponent
Δ_f	Separation between two adjacent subcarriers
Δ_FFR	Scaling factor applied to median pathloss for cell-center boundary in FFR
E	Energy consumption per bit
$\epsilon_{\nu,\beta}[n,k]$	Access control indicator indicating whether or not user ν is admitted in cell β
η_FFR	Fraction of resources allocated to cell-edge users
$f_{\mathrm{D},\ell}$	Doppler's frequency shift for ℓ^th multipath component
G_min	Minimum channel gain necessary for admitting a link
$G_{\mu,r}$	Channel gain between transmitter μ and receiver r
$\mathbf{x}$	Transmitter or receiver (depending on context) of link (μ,r)
$\mathbf{y}$	Transmitter or receiver of interfering link (ν,q).
$G_\mathbf{xy}$	Channel gain between transmitter $\mathbf{y}$ and receiver $\mathbf{x}$

$G_{\mathbf{x}}$	Intended channel gains, equivalent to $G_{\mathbf{x}x}$
$G^{\mathrm{ls}}_{\mu,\alpha}$	Large scale channel gain between transmitter μ and receiver α
$\gamma_\nu[n,k]$	SINR achieved for user ν on chunk (n,k)
Γ	Set of SINR targets corresponding to $\mathcal{M}$
Γ_m	SINR target corresponding to m level modulation scheme
$\Gamma_{\min}$	Minimum SINR required for reserving a chunk
$H_{\mathbf{xy}}$	Channel transfer function between transmitter x and receiver y in MIMO system
$h_{\mathbf{xy}}$	Channel transfer function between transmitter x and receiver y in MISO system
i	Beam index
$I^{\mathrm{b}}_{\mathbf{x}}$	Interfering BB power received at transmitter $\mathbf{x}$
$I^{\mathrm{d}}_{\mathbf{x}}$	Cochannel interference power at the receiver $\mathbf{x}$
I_{th}	Interference threshold
$I^{\mathrm{tol}}_{\mathbf{x}}$	Interference tolerance at receiver $\mathbf{x}$
k	Frame index of chunk (n,k)
K	Cluster size
K_{D}	Number of diffused components within a multipath echo
L	Number of multipath components
λ	Carrier wavelength
m	Number of bits per symbol
$m_\nu[n,k]$	Number of bit per symbol used by user ν chunk (n,k)
$\hat{m}_\nu[n,k]$	Estimated number of bit per symbol that can be used by user ν chunk (n,k)
μ	Transmitter of active link (μ,α)
$\mathcal{M}$	Set of available modulation formats in the system
ν	Transmitter of competing link (ν,β)
n	Frequency index of chunk (n,k)
n_{os}	Number of OFDM symbols per chunk
n_{sc}	Number of subcarriers per chunk
(n,k)	Chunk index
N	Noise power
N_{B}	Number of base stations
N_{C}	Number of chunks within system bandwidth
N_{L}	Number of links in an *ad hoc* scenario
N_{M}	Number of mobile stations in the system

N_{R}	Number of receive antennas
N_{T}	Number of transmit antennas
p	Probability of accessing unreserved chunk
$P^{\mathrm{ls}}_{\mu,\alpha}$	Path loss between transmitter μ and receiver α
p_{LoS}	Probability of line of sight
$\Psi_{\nu,\beta}$	Priority penalty factor for user ν
ϕ_{T}	Angle of departure at BS
ϕ_{R}	Angle of arrival at MS
$R^{\mathrm{d}}_{\mathbf{x}}$	Intended signal power at receiver $\mathbf{x}$.
$R^{\mathrm{b}}_{\mathbf{x}}$	Busy burst transmit power used by receiver $\mathbf{x}$
$s_{\nu,\beta}[n,k]$	Score of user ν connected to BS β on chunk (n,k)
σ	Standard deviation of log-normal shadowing
T_{S}	OFDM symbol duration
T_{ν}	Throughput of user ν
T_{sys}	Total system throughput
$\mathcal{T}$	Set of all active receivers
τ_{ℓ}	Propagation delay of the ℓ^{th} multipath component
$T^{\mathrm{d}}_{\mathbf{x}}$	Data transmit power used by transmitter $\mathbf{x}$
$T^{\mathrm{b}}_{\mathbf{x}}$	Busy burst transmit power used by receiver $\mathbf{x}$
$T^{\mathrm{b}}_{\mathrm{max}}$	Maximum busy burst transmit power
$\mathcal{T}$	Set of all active transmitters
θ_{ℓ}	Initial phase of the ℓ^{th} multipath component
θ	Angle between normal of antenna array and transmitter direction in far field
$\mathcal{U}$	Set of all users within the system
Υ_{ν}	Binary variable indicating reservation of chunk (n,k) for user ν
$\mathbf{v}^{(\mathbf{i})}$	Vector of complex coefficients for activating i^{th} beam
v_t	Complex coefficient applied to t^{th} antenna of an array
w	Width of street in Manhattan scenario
$\mathbf{x}$	Transmitter or receiver of tagged link
$\mathbf{y}$	Transmitter or receiver that interferes with $\mathbf{x}$
ξ	Random variable modelling log-normal shadowing
$\zeta_{\beta}[n,k]$	The user that is allocated chunk (n,k) in cell β

Chapter 1
Introduction

1.1 Trends in mobile communications

The last decade has witnessed an unprecedented growth in the mobile communications industry. This is evident from an increase in the number of mobile subscribers worldwide from 1.5 billions in the year 2003 to 4 billions towards the end of the year 2008 [4]. In the United Kingdom itself, the number of active mobile connections per 100 of population stands at 126.1 in 2008 compared to 88.8 in 2003 [4]. Together with the growth of the market, the industry has started experiencing the paradigm shift from primarily voice oriented services towards data oriented communication. Applications such as high speed internet and email access, multimedia upload and downloads are some of the services traditionally sought from wired telecommunications that have penetrated into the domain of expected services from wireless communication networks in recent years. Indeed, mobile devices that combine entertainment, communications and navigation into one product are already widely available in the high street. These are already paving the way towards realising the *anything*, *anytime* and *anywhere* paradigm.

The increase in the number of services sought from wireless networks increases the requirements in terms of data rate. In the early universal mobile telecommunications system (UMTS) networks, the peak data rates envisioned were 144 kpbs in vehicular, 384 kpbs in outdoor-to-indoor environment [5]. The peak data rates expected from third generation (3G) cellular networks enhanced to 14 Mbps using high speed packet access (HSPA) [6] and 28 Mbps using HSPA evolved (HSPA+) [7]. In the fourth generation, (4G) networks, typical peak data rates envisioned are 100 Mbps for mobile and 1 Gbps for fixed wireless links [8, 9]. The major bottleneck in realising the above goals is the availability of wireless spectrum, which is generally considered a scarce resource and is often auctioned off at very high prices. An example of this is the recent spectrum auction in 2003 in the United Kingdom for the 40 MHz of spectrum in the 3.4 GHz band, which was auctioned off for GBP 6,955,000 [10] for fixed wireless broadband access. Given the limited availability of spectrum and high cost of spectrum, two of the major challenges for the wireless network operator are first, to be able to meet the ever increasing

traffic demand in the limited available spectrum and second, to reduce the cost of transmission per bit.

1.2 Bottleneck in mobile communications

Mobile communication faces a trend of ever increasing data rates while the available spectrum increases at a much slower pace. The only solution to the emerging bottleneck is a significant increase of system spectral efficiency (by factors). In general terms, this can be achieved by increasing the frequency reuse. On the physical layer, *e.g.* multiple-input-multiple-output (MIMO) transmissions achieve this goal via spatial multiplexing [11–13] or beamforming [14, 15]. On the system/networking level, this goal is achieved by smaller cell radii through the introduction of femtocells [16, 17] or *ad hoc* communication [18, 19] and at the same time allowing all cells/links to access all frequency channels. Extensions of this concept are cognitive radio approaches which expand the accessible set of frequency channels beyond the frequency bandwidth allocated to a particular system [20], *e.g.* to enable mobile communication systems to benefit from unused TV channels.

Common to all these techniques is that they generate interference. Such interference is called inter-channel interference (ICI) for multiple input multiple output (MIMO) systems whereas the interference in system arising from an increased system frequency reuse is called co-channel interference (CCI). In order to avoid increased interference, it is imperative that powerful interference mitigation techniques are employed. Smaller cell radii and random link deployments such as in femtocell and *ad hoc* networks render effective interference coordination techniques difficult since central control is not possible and the system, in fact, relies on self-organisation which requires the entities in the network to make own decisions based on local information. When multiple links share the same time-frequency resources, the problems of collisions can be debilitating – especially since the vulnerable receiver cannot be 'sensed' by new transmitters entering the network - giving rise to the *hidden node* and *exposed node* problems, which is discussed further in Section 2.7.2.3.

Two or more links may reuse the spectrum as long as they are able to decode the transmitted information correctly. Due to interference and noise, the received bits may differ from the originally transmitted bits, giving rise to bit errors. The bit errors may either be detected using error detection schemes such as parity checks, check sums, cyclic redundancy checks and

Hamming distance based checks and retransmission may be requested or some of the bit errors may be corrected using forward error correction (FEC) codes such as convolutional coding. The ratio between incorrectly received bits to the number of bits transmitted is called the bit error ratio (BER). The maximum tolerable BER depends on application and the typical BER figures are 10^{-3} for voice and between 10^{-7} and 10^{-5} for data applications. There exists a one-to-one mapping between the BER and the signal to interference and noise ratio (SINR) where in general the BER decreases as the SINR increases [21, 22]. The maximum amount of interference that can be admitted whilst ensuring that the BER remains below the maximum permitted for satisfying the QoS constraint is called an 'interference tolerance' threshold. Different approaches have been proposed to maximise spectral reuse whilst attempting to keep the interference below the interference tolerance threshold, the detailed discussion of such interference avoidance mechanisms is done in Chapter 2.

1.3 Interference management

Interference may broadly be classified into inter-system interference and intra-system interference based on the source and the victim of interference. Inter-system interference arises when two systems operate in the same or the adjacent bandwidths. A typical example of inter-system interference is the interference caused among the systems operating in the industrial, scientific and medical (ISM) bands, such as Bluetooth signal interfering with wireless local area network (WLAN) signal. Likewise, Doppler shift can cause interference between two systems even if they are transmitting at mutually orthogonal frequencies. Inter system interference is generally avoided by planning the use of the spectrum and licensing to a particular system for use. The licensee holds the exclusive right to transmit within the licensed spectrum but must ensure that the spillage to adjacent channels is kept within the limits. For unlicensed spectrum, cognitive approaches that detect and avoid the use of the spectrum are generally used [23] or the approaches that preemptively avoid collisions such as through random channel hopping [24].

By contrast, the reuse of spectrum within the same system gives rise to intra system interference. Intra system interference is typically an issue in cellular and *ad hoc* systems operating within the licensed bands where the licensee is the sole user of the particular bandwidth. However, the licensee endeavours to maximise the spectral reuse in order to increase the number of bits transmitted in the available spectrum. The interference arising from imperfections in hardware design or Doppler shift give rise to adjacent channel interference (ACI). In cellu-

lar systems, ACI arises due to sharing of the available bandwidth between multiple users and is called multiple access interference (MAI) which may be mitigated by improving time and frequency synchronisation or frequency correction.

The co-channel interference (CCI) which arises from frequency reuse may be mitigated by careful allocation of radio resources. The received signal power on average decreases exponentially with distance, typically with an exponent factor between 2 (free space model) and 4 (in urban environment). As long as the receiver is 'sufficiently' away from an interfering transmitter, the radio resource may be reused. This principle is used in cellular networks with fixed infrastructure used for mobile telecommunications system. In cellular networks, the mobile stations (MSs) communicate with the base stations (BSs) using the frequency bands assigned by the BS. The BSs are generally assumed to be uniformly distributed. Two BSs that use the same set of frequencies are called co-channel cells. A large spatial separation between co-channel cells reduces CCI caused to victim receivers and vice versa. However, increasing the spatial separation decreases the number of times the frequency is reused within the network which can *potentially* lower the spectral efficiency of the wireless networks. The 'reuse factor' is chosen based on the maximum CCI acceptable in the network. Clearly, such approach results in a 'hard reuse' and cannot cater for load imbalance across different sites or exploit the frequency selectivity and time variance of the channel.

Moreover, frequency planning is generally not feasible for CCI mitigation in *ad hoc* networks that have no fixed infrastructure and centralised control. In such networks, the MSs typically need to coordinate among themselves on how they communicate with one another and/or how they access the network resources. One of the most widely used CCI avoidance approaches used in *ad hoc* networks such as WLANs using IEEE 802.11 protocol is the carrier sensing approach. The transmitting entity attempts to determine the presence of another transmitter by sensing any ongoing activity on the frequency band the new transmitter intends to use. Such approaches are 'preemptive' in nature and do not solve the 'hidden' and the 'exposed' node problem (discussed in Chapter 2) depending on the location of an interfering transmitter with respect to the receiver and the transmitter respectively of an active link.

The aforesaid problems with the hidden and the exposed node or inflexible resource allocation in cellular network can be solved if the transmitter has an *a priori* knowledge of the amount of interference the transmitter would cause to the receiver of pre-established links. Likewise, in cellular networks such knowledge would reduce the loss in spectral efficiency due to hard

frequency reuse whilst still maintaining that the interference is kept within the tolerable limits. The frequency bands can be allocated to different cells in an 'on demand basis', thereby allowing flexible operation in the network. One way to obtain such knowledge is using the busy burst (BB) signalling [25–27], where the receiver of an already established link transmits a BB in a time-multiplexed mini-slot following a successful reception of data. Provided that the transmitter is obliged to sense the BB slot before transmission, it can infer the amount of interference it causes to an active link if it were to transmit by utilising the channel reciprocity property of the TDD mode. Exclusion region around the victim receiver is established by requiring a transmitter to avoid transmissions where the transmitter senses that it potentially causes detrimental CCI (*i.e.* larger than a threshold value) towards the active receiver. The application of the BB approach in *ad hoc* and cellular deployments is addressed in this thesis.

1.4 Thesis contributions

The aim of this thesis is to investigate the BB signalling mechanism for dynamic chunk allocation in orthogonal frequency division multiple access (OFDMA) – time division duplexing (TDD) systems operating in *ad hoc* and cellular scenarios. The performance of chunk allocation using BB signalling is evaluated against the state-of-the-art chunk allocation methods used in wireless networks such as carrier sense multiple access (CSMA) in *ad hoc* networks or full frequency reuse and frequency reuse planning methods in cellular networks. The system performance is evaluated by means of system level simulations [28] using a MATLAB-based simulator written for this purpose. It is widely accepted that the optimal allocation of power and spatial reuse of bandwidth in a multi-link scenario is a non-convex problem in general form [29–31]. Therefore, dynamic chunk allocation algorithm cannot be analysed in a closed form. Hence, a simulation approach is used for investigating the BB signalling mechanism in this thesis.

Early work with BB signalling [27] demonstrated that the total system throughput can be maximised by an appropriate choice of the threshold parameter in a system that used fixed modulation scheme systemwide. In this thesis, it is demonstrated that when the threshold is set so as to enhance the system throughput, the radio resources are primarily allocated to the links with better channel condition at an expense of the links with worse channel conditions, assuming a full-buffer traffic. In this context, it is demonstrated that the system throughput may be traded

off for an enhanced throughput at the lower 10^{th} percentile of link throughput[1] by adjusting the threshold parameter. The lower 10^{th} percentile of user throughput is chosen as a measure of guaranteed link throughput in a network. Furthermore, in a system utilising fixed modulation scheme systemwide, it is demonstrated that the trade off between link throughput and system throughput is more favourable if each receiver broadcasts a BB of variable power that signals the maximum amount of CCI that the receiver can tolerate whilst meeting the SINR target. In a system performing link adaptation, it is demonstrated that a high threshold enforces a high spatial reuse, which reduces the achieved SINRs at the receiver. By utilising feedback from the receiver, the transmitter selects lower order modulation schemes. Provided that a fixed transmit power per chunk is used systemwide, it is demonstrated that the energy per bit required for transmission can be adjusted by varying the threshold in an interference limited scenario.

In the context of the cellular system, due to point-to-multipoint transmissions in the downlink (DL) and multipoint-to-point transmissions in the uplink (UL), high CCI is coupled with low intended signals in the DL; whereas in the UL high CCI can equally affect the links with low or high levels of intended signal power, giving rise to what is termed as *interference diversity*. Consequently, it is identified that the average SINRs are lower in the DL than in the UL provided that chunks are fully reused. This results in a higher guaranteed link throughput in the UL than in the DL with full frequency reuse. By lowering the threshold, it is demonstrated that the dominant component of the CCI in the DL is eliminated. As a result, the achieved SINR at the cell-edge improve and the guaranteed link throughput improves at the cost of the achievable system throughput. By contrast, lowering the threshold in the uplink reduces the number of chunks used in adjacent cell that can be used by cell-edge user in the tagged cell. Consequently, the improvement in the SINR achieved by lowering the threshold is counteracted by the reduction in the number of chunks available to cell-edge users. Therefore, it is demonstrated that the trade off is more favourable in the DL than in the UL. Furthermore, the impact of prioritising users with fewer reserved chunks was investigated in the context of the cellular systems and it was shown that user prioritisation improves user throughput when CCI protection is enforced. However, when CCI protection is compromised by increasing the threshold, it is demonstrated that user prioritisation increases collisions and compromises the total system throughput.

The final contribution of this thesis is that it combines the interference awareness property

[1]The term user throughput and link throughput are used synonymously in this thesis. The former is preferred in the context of cellular networks and the latter in the context of *ad hoc* networks.

of the BB protocol with CCI mitigation achieved using multiple antennas at the BS. In the literature, it has been demonstrated that multiple antennas at the base station (BS) such as a switched beam approach [15] or adaptive beamforming with opportunistic scheduling [14, 32] provide powerful basic mechanisms to mitigate the effects of CCI and enhance the reusability of radio resources. The key problem is that the interfering gains between the transmitting BS of the tagged cell and the receiving MSs in adjacent cells is not known in a short time basis without significant signalling overhead. This problem is solved by combining BB protocol with a switched beam approach. The impact of contention avoidance with $p-$persistence and contention free approach proposed in [2] combined with BB protocol are investigated and it is demonstrated that the latter improves both the system and the user throughput. Finally, the impact of the number of antennas at the BS and the number of users served by a BS are investigated. It is shown that the BB-enabled switched beam approach improves the system performance beyond that provided by the switched beam approach, regardless of the number of antennas utilised. In light of these results, it is demonstrated that the BB protocol and beamforming techniques perfectly complement each other enabling a high frequency reuse in the system while mitigating CCI.

1.5 Thesis structure

This chapter provided a brief motivation and highlighted the importance of CCI avoidance and mitigation in future generation networks. The remainder of this thesis is structured as follows.

Chapter 2 introduces different classes of wireless networks and methods of accessing channel for bidirectional communication (duplexing) as well as methods of sharing the available bandwidth among multiple users (multiple access). Centralised CCI mitigation approaches such as frequency planning, fractional frequency reuse and beamforming using multiple antennas typically applied to cellular networks are discussed next. The issue of scheduling and fairness is discussed. Finally, decentralised CCI mitigation approaches such as carrier sense multiple access, two-way handshake protocols and their variants as well as busy signal approaches are discussed next. This leads to the concept of busy burst signalling which is the concept explored further in this thesis.

Chapter 3 describes the dynamic chunk allocation mechanism using BB signalling and investigates the performance of BB signalling in self organising *ad hoc* networks using the parameters

from the TDD mode of wireless world initiative new radio (WINNER) in an indoor deployment scenario. Comparisons are made against random chunk allocation approaches and the state-of-the-art CSMA/CA approach.

Chapter 4 considers BB signalling together with user scheduling in cellular systems operating in Manhattan and hexagonal cellular deployments. Comparisons are made against the full-frequency reuse scheme that does not attempt to avoid interference. The impact of blind and fair user scheduling and the impact of performing link adaptation are considered.

Chapter 5 addresses chunk allocation in cellular network that are equipped with multiple antennas at the BS and utilise transmit beamforming in the downlink (DL) mode. The impact of an increase in the number of antennas and the number of users in the system performance is investigated. Likewise, the impact of utilising *a priori* estimate of the SINR for user scheduling in the DL mode is investigated. Finally, the impact of collision free approach and $p-$persistent approach in allocating unreserved chunks is presented.

Chapter 6 draws conclusion from the work recorded in this thesis and discusses the key limitations and suggests future works that needs to be done.

Chapter 2
Background

The paradigm shift from conventional telephony in the second generation (2G) towards multimedia applications that are envisioned for the fourth generation (4G) networks has made radio resource allocation in wireless networks more challenging than ever before. Services such as email access, high-speed Internet access, downloading music and videos, video telephony and so forth that were traditionally considered to be wireline applications are common in mobile devices. Novel services such as television (TV) on demand, video-conferencing and navigation are constantly being added to mobile services. Such applications have stringent and heterogeneous demand in terms of data rate, delay tolerance, bit error ratio (BER) and security. Research and development efforts are ongoing to develop a system that is capable of meeting the ambitious goals for the fourth generation networks. The key objectives that 4G networks are envisioned to fulfil, according to the international telecommunications union (ITU) are as follows [33]

1. To achieve a data rate of 100 Mbps in vehicular speeds and 1 Gbps for fixed and stationary links [33, 34].
2. To achieve appropriate quality at reasonable cost [33].
3. To limit delays in the order of less than 20 ms to 200 ms depending on service class [35].
4. To have a seamless handover and interoperability among networks in different continents [33, 34].
5. To have networks running on an internet protocol (IP)-based packet switched network.

An efficient utilisation of the available spectrum is one of the most important necessity in meeting most of the above objectives. On the one hand, reuse of the spectrum increases the amount of bandwidth available in the system *potentially* increasing the system spectral efficiency whereas on the other hand the reuse of spectrum increases the co-channel interference

(CCI) caused to the receiver. The impact of CCI can be debilitating on links that suffer from high channel attenuation, potentially resulting in an outage [36]. CCI mitigation and avoidance is therefore regarded as the key to reducing outage and improving spectral efficiency. In this chapter, existing CCI avoidance and mitigation approaches proposed and/or utilised in different types of network ranging from self organising *ad hoc* network to cellular networks which may be centrally coordinated are discussed. Furthermore, this chapter also provides background on the channel access methods and in particular on the orthogonal frequency division multiple access (OFDMA) - time division duplex (TDD) system and motivates how it is suitable for the 4G networks.

2.1 Wireless communications networks

Wireless communications networks for personal and commercial use may be classified into the following three main types based on the type of infrastructure and control - *viz.* the cellular networks, wireless hotspots and the *ad hoc* networks.

2.1.1 Cellular networks

In cellular networks, the wireless service provider typically provides coverage to the subscribers by providing access points to which the subscriber units can connect to using electromagnetic waves. In an ideal sense, such access points are distributed uniformly over the intended geographical coverage area and the subscriber units connect to the access point that provides the maximum channel gain. In practice, the wireless network operator places the access points so that it covers a certain percentage of population within the geographical area. This may results in holes where no signal may be received. The wireless access points are connected to a core network that interconnects with either the public switched trunked network (PSTN) or the Internet. The subscriber units are called mobile stations (MSs) and the access points that act as intermediaries between the communication network and the subscriber units are called base stations (BSs)[1]. The wireless interface between the MSs and the BSs is the last hop (or first hop) of the communication chain. As the system relies on a fixed infrastructure, the frequency bandwidth used for communication between the BS and the MS may be coordinated centrally

[1] In the third generation partnership project (3GPP) long term evolution (LTE) terminology, BS is called enhanced node B (eNodeB) and MS is called user equipment (UE) [37]. In this thesis, the terminology BS and MS is used.

or in a distributed manner so as to mitigate the effects of CCI. One of the commonly utilised means to mitigate CCI is frequency planning, discussed further in Section 2.6.1.

2.1.2 Wireless hotspots

The wireless hotspots are isolated BSs that provide coverage to subscriber units located within their coverage area. Examples of such wireless hotspots include the wireless local area network (WLAN) access points or femtocells [16, 17] envisioned to extend the cellular coverage to indoor users. Provided that the BS is isolated from other BSs, the only source of interference arises when multiple users attempt to transmit to the BS. This problem can be solved using polling [38] which is used as a part of the point coordination function (PCF) in the IEEE 802.11 standard.

However, the signal originating from transmitters located within one hotspot interferes with receivers located within another hotspot. WLAN access points and femtocells are typically installed by the subscribers at their premises and have no knowledge of the position of an interfering node. In such scenario, pre-mediated positioning of such access points as done in cellular network so as to mitigate CCI is often not feasible. In such networks, centralised frequency planning would be too cumbersome and would require a large amount of signalling.

2.1.3 *Ad hoc* networks

Ad hoc networks, by definition, are the networks formed in an 'on demand' basis to fulfil a particular purpose. The characteristic feature of such networks is that they lack centralised infrastructure and rigorous control. As such, the communicating nodes typically coordinate among themselves how they communicate with one another and/or how the access the network resources. Although classical use of such *ad hoc* networks included military communications, disaster relief scenarios or the sensor networks, the popularity of such networks in home and commercial applications is growing. The network formed by communicating devices that use the Bluetooth interface is a good example of *ad hoc* network. Likewise, wireless home digital interface [39] that aims to connect video devices wirelessly by providing data of 3 Gbps on a 40 MHz bandwidth in a short range is another recent example of *ad hoc* network in a typical home scenario. Common to all *ad hoc* networks above is an absence of a global controller that coordinates the usage of radio resources. As such, the nodes must utilise information available

locally so as to communicate successfully with one another.

2.2 Channel access methods

In a wireless communication network, the available bandwidth is shared to enable bidirectional communications (duplexing). Moreover, in each duplex direction, the available radio resource must be shared among multiple competing users (multiple access) whilst avoiding (ideally) any interference between two users. Interference is avoided when orthogonality between the radio resources assigned to two users (in multiple access) or between the two directions (duplexing) is maintained. This is achieved by separating the signals in time, frequency, code or space domain. In this section, a general overview of duplexing and multiple access techniques is presented.

2.2.1 Duplexing techniques

Duplexing is a means to provide bidirectional communication between two communicating terminals. In the context of a cellular system, the BS transmits to the MS in the downlink (DL) mode while the MS transmits to the BS in the uplink (UL) mode. Duplexing is typically performed by separating the signals either along the time domain or along the frequency domain.

In the frequency division duplexing (FDD), separate frequency bands are used for transmitting or receiving when viewed from a user's perspective as depicted in Figure 2.1(a). A channel used in the transmit mode is paired uniquely with another channel in the receive mode and the transceivers transmit and receive simultaneously. The transmit band and the receive bands are well separated from one another so as to avoid self-interference problem due to non-ideal filters used at the RF frontend.

2.2.1.1 Time division duplexing

In the time division duplex (TDD) mode, transmissions in both directions are carried out using the same frequency band in mutually orthogonal time slots as depicted in Figure 2.1(b). A key property of the TDD is that the channel is reciprocal during the transmit mode and the receive mode as long as the separation time is much lower than the coherence time. Coherence

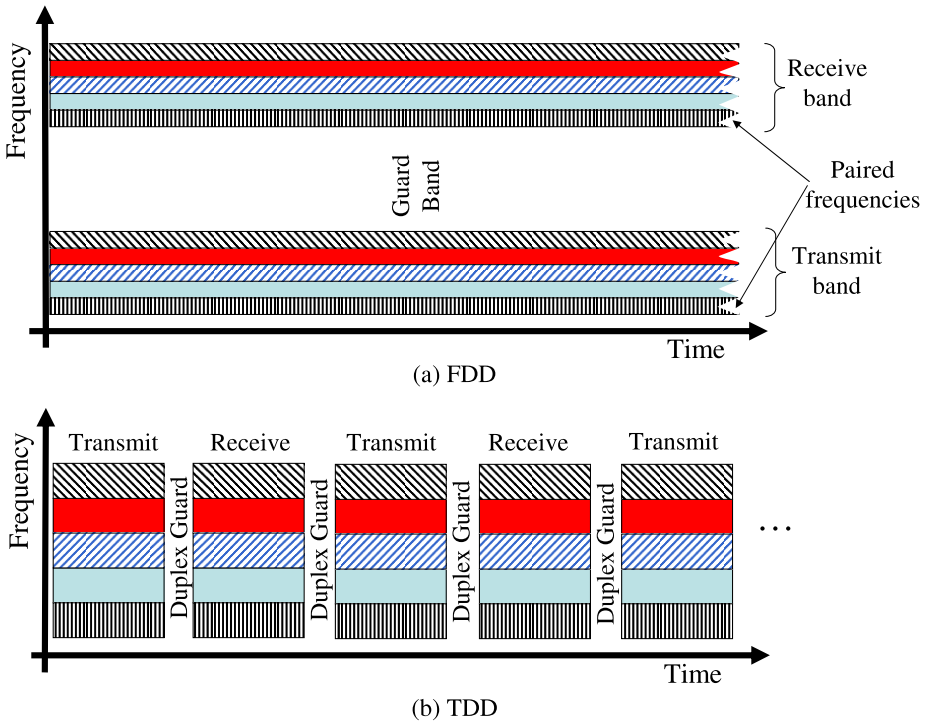

Figure 2.1: *Depiction of TDD mode where bidirectional communication is carried out using two orthogonal time slots or two different frequencies. The different colours represent different users sharing the available bandwidth.*

time is the period of time during which the channel appears to be time invariant [40]. The channel reciprocity property can be utilised for important system functions such as acquiring the knowledge of channel with low signalling overhead. In particular, channel sounding pilots can be used for estimating the channel in the TDD mode [41] whereas the in the FDD mode, the channel state information has to be explicitly signalled back to the transmitter using data feedback [41, 42]

A key feature of the TDD system is that a guard interval between the transmission and the reception slots should be maintained so as to take into account the propagation delays as well as to allow the transceiver to change from the transmit mode to the receive mode. The time taken for a signal to travel a distance of kilometre is 5.4 μs, using velocity of radio waves as 3×10^8 m/s. To avoid transmitted information from being lost, it is essential that the signal originating from the farthest user is still received before the receiver duplexes into the transmit mode. The key advantages of TDD over FDD are briefly presented below.

1. The TDD mode provides a better support for services that have asymmetric bandwidth requirements. The bandwidth can be conveniently scaled to suit the traffic demand imposed on the network by simply changing the ratio of the transmit slots to the receive slots. This property is quite important for 4G systems where the traffic is envisioned to be primarily composed of multimedia applications.

2. The RF components such as the antenna, the duplexer, the mixer and the filter can be shared between the transmit mode and the receive mode as the same frequency is used for transmission as well as reception. By contrast, the FDD mode requires separate duplexers, filters and mixers. Sharing the components results in a reduction in cost and complexity of the hardware units for an RF unit designed for the TDD mode compared to that of the FDD mode.

3. In a TDD system, the signalling overhead required for obtaining the knowledge of the channel at the transmitter or receiver is much lower compared to that of the FDD system. In TDD system, this can be achieved by inserting channel sounding pilots within the MAC frame. However, in the FDD system separate channel sounding pilots must be used in both directions and explicit feedback of information is required.

The main drawbacks of TDD compared to FDD are as follows

1. The duration of guard interval needs to increase as the distance between the transmitter and receiver is large. Such guard interval decreases the spectral efficiency for long distance communications. This is the reason why TDD is preferred for short distance communications such as in microcells and FDD for longer distance communications.

2. In scenarios where *instantaneous* traffic asymmetry is different across cells and provided that the cells switch the duplex directions independently to cater for such traffic asymmetry, interference between BS to BS and MS to MS arises. This is particularly prohibitive because the interfering channel gains can often surpass desired channel gains, which is especially true for MS to MS interference particularly at the cell-edge. The capacity loss due to interference can exceed the gains obtained through such flexible load balancing approach.

3. Time synchronisation is critical to ensure that the transmitted information is received before the receiver switches the duplex direction.

2.2.2 Multiple access

The available radio resources may be shared among multiple users without causing significant interference as long as the radio resources are shared orthogonally among the users. The users may be separated in time, code, space or frequency dimensions or the combination of any two or more of the aforesaid dimensions. In the following, sharing of resources along the time domain and along the frequency domain is discussed.

2.2.2.1 Time division multiple access

The time division multiple access (TDMA) scheme accommodates multiple users by separating them along the time dimension. At any time instant, the entire available bandwidth is accessed by one user as depicted in Figure 2.2(a). With TDMA, it is critical that the users are time-synchronised. Otherwise, the transmissions from two users overlap in time resulting in an undesired interference. This overlap may be remedied by either adding a guard time or using a technique called timing advance, where different users commence their transmission at different time instants depending on the location of the user.

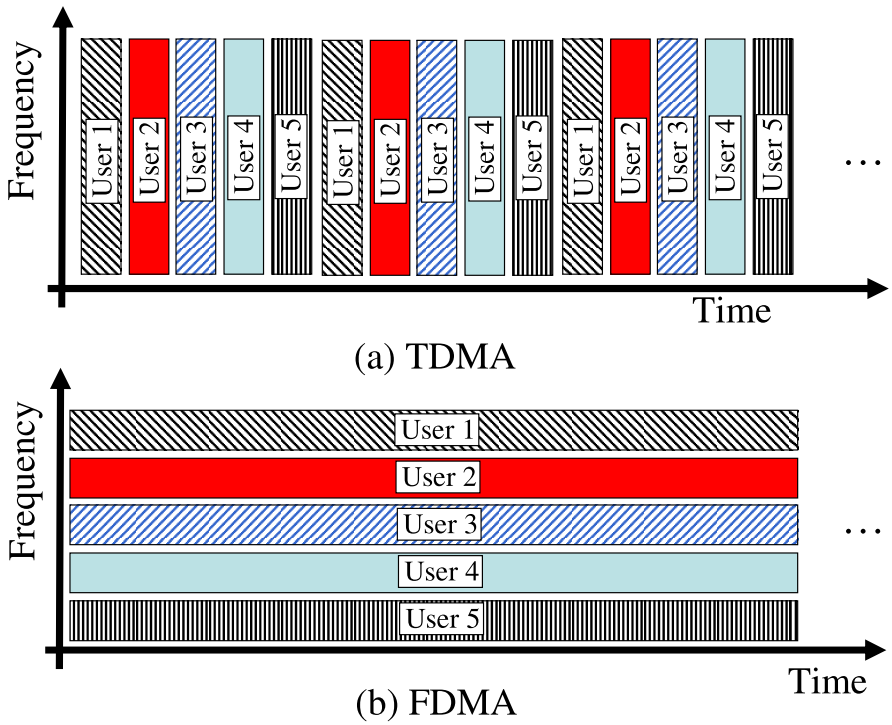

Figure 2.2: *Multiple users coordinated by a common central entity are orthogonalised in time (TDMA) or frequency (FDMA).*

2.2.2.2 Frequency division multiple access

The frequency division multiple access (FDMA) separates users from one another along the frequency dimension. The available bandwidth is divided into smaller sub-bands and each band is allocated to a unique user. The user transmits on the allocated chunk for the entire time duration as depicted in Figure 2.2(b). The interference from one sub-band to another is mitigated by using guard bands. The necessity of guard band arises because an ideal filter with rectangular transfer function is a non-causal system.

FDMA is often used in combination with TDMA for resource allocation. A relevant example is radio resource allocation in the global system of mobile telecommunications (GSM) where the available system bandwidth of 25 MHz is divided into channels having bandwidth of 200 kHz (FDMA) and each of the 200 kHz channels are partitioned into 8 orthogonal slots (TDMA) [43].

2.2.2.3 Orthogonal frequency division multiple access

Orthogonal frequency division multiple access (OFDMA) is a multiple access technique that combines modulation using orthogonal frequency division multiplexing (OFDM) and utilises FDMA to assign subcarriers (SCs) to multiple users. OFDMA is more spectrally efficient than conventional FDMA because the necessity of using guard bands is obviated with OFDM technique and the subcarriers can overlap as long as the orthogonality between the SCs is ensured. Orthogonality between the SCs is maintained by utilising the frequencies of the sinusoidal functions whose inner product is 0 over a symbol duration as the carrier frequencies for the respective SCs. In the following paragraphs, a brief motivation of using OFDM for data transmission and brief description of data transmission using the OFDM technique is provided.

2.2.2.4 Orthogonal frequency division multiplexing

OFDM is a multi-carrier technique in which the information is carried along a number of SCs, where the central carrier frequency of each subcarrier is an integer multiple of the fundamental carrier frequency. Data transmission using OFDM was first proposed in [44], where it was demonstrated that the spectra of the SCs may overlap without interfering with one another. OFDM in its current form utilises inverse discrete Fourier transform (IDFT) for modulation and discrete Fourier transform (DFT) for demodulation as proposed in [45] and incorporates a cyclic prefix [46], which provides means to combat the inter symbol interference (ISI) and inter carrier interference (ICI), which shall be discussed shortly. The importance of multicarrier transmissions and in particular OFDM for 4G networks is motivated as follows in the light of the data rates envisioned for 4G system. If the information were transmitted serially, then the symbol duration would be 10 ns and 1 ns for the data rates of 100 Mbps and 1 Gbps respectively, assuming a single carrier modulation (SCM) and 1 bit per symbol. There are three key problems with transmitting symbols of such small duration. First, the transmitted symbol (often several consecutive symbols) is/are corrupted by the impulse noise which has a pulse duration of 250 ns and an effective burst duration of 1 μs [47]. Second, due to multipath propagation in a wireless environment, the depth of inter-symbol interference (ISI) can exceed hundreds of symbols, which requires additional equalisers that complicate the receiver design. Third, a large bandwidth (in the order of tens to hundreds of MHz), which is required for such high data rate transmission is subject to frequency selective fading and therefore requires channel equalisation. These key drawbacks can be avoided by converting the high data rate serial transmission

into several parallel transmissions, each transmitting at the much lower data rate compared to the original serial data rate.

Given N_{SC} SCs are used for transmission, the resulting symbol duration is $T_{\mathrm{S}} = N_{\mathrm{SC}}T_{\mathrm{ser}}$, where T_{ser} is the symbol duration in a system utilising serial transmissions. Likewise, the bandwidth of each frequency slot becomes $B_{\mathrm{sc}} = B/N_{\mathrm{SC}}$. While this would mitigate the problems associated with impulse noise and depth of ISI, this still requires the use of guard bands because a causal filter has a non-rectangular frequency response. As a result, a part of the spectrum which could otherwise have been utilised remains wasted. Furthermore, each subcarrier requires a separate oscillator and a separate filter which increases the hardware complexity at the transceiver.

To address the above shortcomings, OFDM utilises functions that are orthogonal to one another over a fundamental period for modulation and demodulation so as to maintain orthogonality among the SCs. The complex exponentials $e^{j2\pi f_\ell t}$ and $e^{j2\pi f_m t}$, where f_ℓ and f_m are the central frequency of sub-carriers with indices ℓ and m such that $mf_\ell = \ell f_m$, are orthogonal to each another when integrated over the symbol duration (T_{S}), given by

$$\frac{1}{T_{\mathrm{S}}}\int_0^{T_{\mathrm{S}}} e^{j2\pi f_\ell t}e^{-j2\pi f_m t}dt = \begin{cases} 1 & l = m \\ 0 & l \neq m \end{cases}. \tag{2.1}$$

This property allows the complex exponentials $e^{j2\pi f_\ell t}$ and $e^{-j2\pi f_\ell t}$ to be utilised as the modulator function and the demodulator function respectively on the ℓ^{th} SC. For (2.1) to hold, the carrier spacing required between two adjacent subcarriers is

$$\Delta_f = f_{\ell+1} - f_\ell = \frac{1}{T_{\mathrm{S}}}. \tag{2.2}$$

Let $s_\ell(\iota)$ be a baseband symbol transmitted on the ℓ^{th} subcarrier on the ι^{th} OFDM symbol. The OFDM symbol (output of OFDM modulator shown in Figure 2.3(a)) is given by

$$x(t) = \left(\sum_{\ell=0}^{N_{\mathrm{SC}}-1} s_\ell(\iota)e^{j2\pi f_\ell t}\right)\mathrm{rect}\left(\frac{t-(\iota+0.5)T_{\mathrm{S}}}{T_{\mathrm{S}}}\right), \tag{2.3}$$

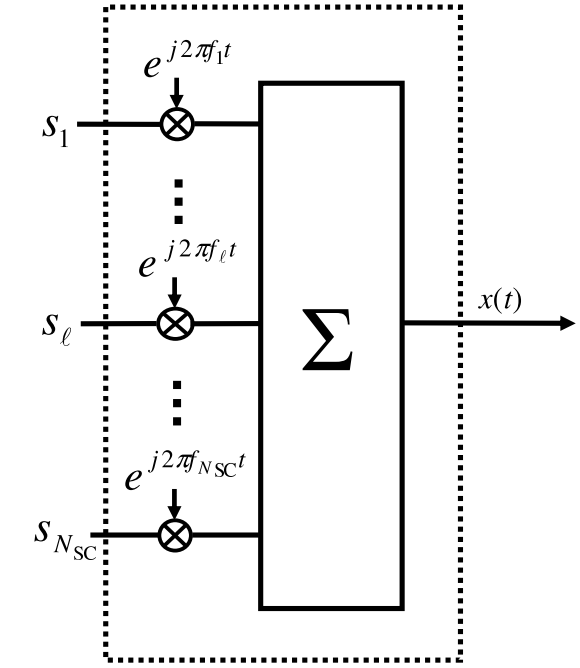

(a) OFDM modulator

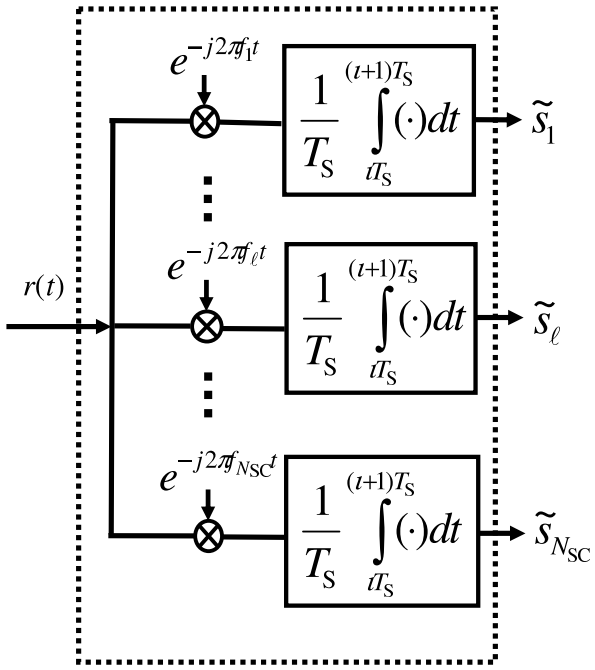

(b) OFDM demodulator

Figure 2.3: *Analogue representation of OFDM modulation and demodulation.*

where the $\mathrm{rect}(\cdot)$ is a rectangular pulse defined as

$$\mathrm{rect}\left(\frac{t-(\iota+0.5)T_{\mathrm{S}}}{T_{\mathrm{S}}}\right) = \begin{cases} 1\,, & \iota T_{\mathrm{S}} \leq t < (\iota+1)T_{\mathrm{S}} \\ 0\,, & \text{elsewhere}\,. \end{cases} \tag{2.4}$$

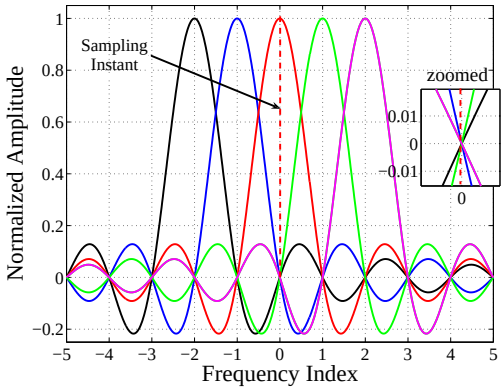

Figure 2.4: *Spectra of OFDM symbol before RF conversion for an OFDM symbol centered around $t = 0$. In an ideal channel (the channel with unit impulse response), at the sampling instant for subcarrier l, the signal of all other SCs $m \neq \ell$ pass through 0.*

The spectra of the modulated OFDM symbol $x(t)$ in the baseband can be obtained by taking the Fourier transform of $x(t)$ and is denoted as $X(f, \iota T_{\mathrm{S}})$, given by

$$X(f, \iota T_{\mathrm{S}}) = \frac{1}{T_{\mathrm{S}}} \int_{\iota T_{\mathrm{S}}}^{(\iota+1)T_{\mathrm{S}}} x(t) e^{-j2\pi f t} dt \tag{2.5}$$

$$= \sum_{\ell=0}^{N_{\mathrm{SC}}-1} s_{\ell}(\iota) \mathrm{sinc}(fT_{\mathrm{S}} - \ell) e^{-j2\pi(fT_{\mathrm{S}}-\ell)(\iota+0.5)T_{\mathrm{S}}}. \tag{2.6}$$

The spectrum of each of the SCs is a sinc function as depicted in Figure 2.4. The transmitted symbols $s_{\ell}(\iota)$ can be obtained by sampling $X(f, \iota T_{\mathrm{S}})$ at $f = \frac{\ell}{T_{\mathrm{S}}}$ as follows

$$X\left(\frac{\ell}{T_{\mathrm{S}}}, \iota T_{\mathrm{S}}\right) = s_{\ell}(\iota), \quad \ell = 0, 1, \cdots, N_{\mathrm{SC}} - 1 \tag{2.7}$$

It is clear from Figure 2.4 that at the sampling instant, the contribution of all other SCs except the subcarrier being sampled is 0 towards the total received signal. Thus, in an ideal channel (a channel with a unit impulse response), interference is avoided even when the spectra of individual carriers overlap and the requirements of using the guard bands and filters is obviated.

However, the transmitted OFDM symbol propagates through the (wireless) channel where it is subject to interference and noise which corrupts the transmitted signal. The received signal is given by $y(t) = x(t) + z(t)$, where $z(t)$ is the interference and noise added to the received signal. The receiver performs a correlation of the received waveform with the demodulator function and integrate over the symbol duration as shown in Figure 2.3(b). The output of the OFDM demodulator is given by

$$Y_\ell(f, \iota T_\mathrm{S}) = \frac{1}{T_\mathrm{S}} \int_{\iota T_\mathrm{S}}^{(\iota+1)T_\mathrm{S}} y(t) e^{-j2\pi\ell\frac{t}{T_\mathrm{S}}} dt \tag{2.8}$$

$$= s_\ell(\iota) + Z_\ell(f, \iota T_\mathrm{S}) \tag{2.9}$$

where $Z_\ell(f, \iota T_\mathrm{S})$ is the Fourier transform of the interference and noise component of $y(t)$.

In the current systems utilising OFDM, modulation is carried out by using inverse discrete Fourier transform (IDFT) and demodulation is carried out using discrete Fourier transform (DFT) as shown in Figure 2.5. Assuming N_SC SCs in the system, the modulation and demodulation can be carried out using a N_SC point IDFT and DFT respectively. The modulation (IDFT) and demodulation (DFT) operations can be expressed as

$$x[\ell] = x\left(\frac{\ell T_\mathrm{S}}{N_\mathrm{SC}}\right) = \left(\sum_{\kappa=0}^{N_\mathrm{SC}-1} s_\ell e^{j2\pi\frac{\kappa}{N_\mathrm{SC}}\ell}\right) \quad \text{(IDFT)} \quad \text{and} \tag{2.10}$$

$$Y[\ell] = Y\left(\frac{\ell}{T_\mathrm{S}}\right) = \frac{1}{N_\mathrm{SC}} \left(\sum_{\kappa=0}^{N_\mathrm{SC}-1} y\left(\frac{\ell T_\mathrm{S}}{N_\mathrm{SC}}\right) e^{-j2\pi\frac{\kappa}{N_\mathrm{SC}}\ell}\right) \quad \text{(DFT)} \tag{2.11}$$

The discrete representation of modulation (2.10) and demodulation (2.11) are signals sampled at $\frac{\ell T_\mathrm{S}}{N_\mathrm{SC}}$ of the analogue representation of OFDM modulation (2.3) and demodulation (2.8) [48]. In (2.11) and (2.10), the index of OFDM symbol (ι) is dropped to simplify notation, as it is clear from the context that we are dealing with the ι^{th} OFDM symbol. At the transmitter side, the discrete sequence of complex numbers is converted into an analogue waveform using a digital to analogue (D/A) converter, which is typically a low pass filter with cutoff frequency at B, where B is the signal bandwidth of the OFDM signal. At the receiver side, the signal is sampled at the rate $N_\mathrm{SC}/T_\mathrm{S}$ to obtain to the discrete symbols $y[\ell]$ required for DFT. Provided that N_SC can be expressed as a power of 2, the IDFT and DFT can be realised efficiently using inverse fast Fourier transform (IFFT) and fast Fourier transform (FFT) algorithms for which efficient implementations exist [49, 50]. Thus, it is demonstrated that the OFDM allows the spectra

of different subcarriers to overlap in an ideal channel (channel with unit impulse response). In such channel, there is no intersymbol interference (ISI) and intercarrier interference (ICI). However, a wireless channel with L multipath components behaves like a filter containing L taps and therefore the signal received at the receiver is the sum of multiple scaled and shifted copies of the original symbol. A shift by τ in the time domain introduces a phase shift in the frequency domain because of which the carriers are shifted with respect to one another. As a result, at the sampling instant, the contribution from other SCs is non-zero. This is rectified by adding a cyclic prefix [46] of length T_{G}, which is nothing but T_{G} samples from the tail end of IDFT output copied to the beginning of the IDFT output as depicted in Figure 2.5. The cyclic prefix is discarded at the receiver and the rest of the samples are passed to the DFT for OFDM demodulation. As the channel with L taps has a memory of L, copying $T_{\mathrm{G}} = L$ samples from the end of the IDFT output sequence (*i.e.* end of the OFDM symbol) to immediately before the beginning of the IDFT output sequence makes the OFDM symbol appear cyclic to the channel. Therefore, the linear convolution of OFDM symbol with the channel filter appears to be cyclic. Thus, channel equalisation is reduced to a scalar multiplication by inverse of the channel transfer function. This frequency domain equalisation technique is called zero forcing [51]. A detailed mathematical description of cyclic prefix and how it solves the ICI and ISI problem is beyond the scope of this thesis and is not discussed further. Interested readers are referred to [52] for the same.

The communication chain depicted in Figure 2.5 depicts OFDM transmission of a single link. In an OFDMA system, the available SCs are shared among multiple users. Adjacent SCs and OFDM symbols are grouped together to form a time-frequency slot called a *chunk*. A chunk is a unit of radio resource allocation in OFDMA systems.

2.3 Signal fading in wireless channels

The transmitted signal propagates from the transmitter to the receiver along a number of multiple paths as shown in Figure 2.6(a). The mobile radio channel consists of two effects - the large scale fading effects and the small scale fading effects [40]. The large scale fading results due to the distance between the transmitter and the receiver and obstruction of the signal paths by large object such as mountains, buildings and so on. The parameters of the large scale fading change on a much slower scale than the small scale fading parameters that they are generally considered to be static in the short-term. The average path gain between a transmitter μ and a

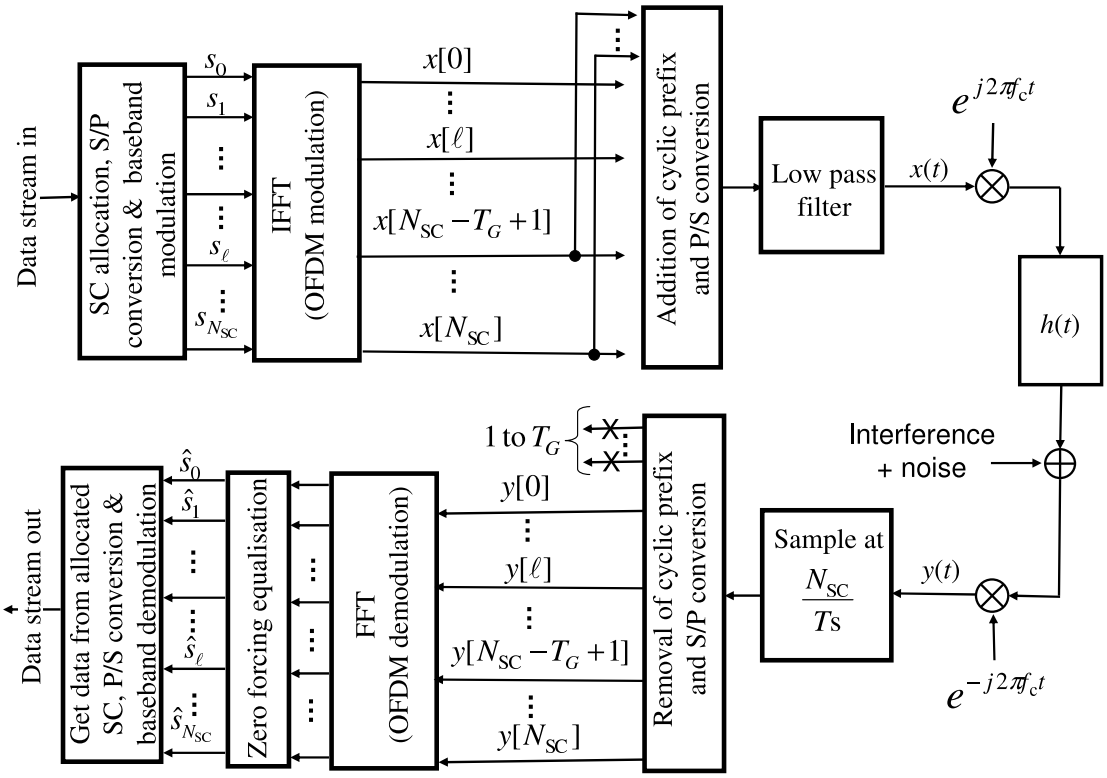

Figure 2.5: *OFDM transmission chain.*

receiver α can be expressed as

$$G_{\mu,\alpha}^{\text{ls}} = 10^{\frac{-P_{\mu,\alpha}^{\text{ls}}}{10}}, \tag{2.12}$$

where $P_{\mu,\alpha}^{\text{ls}}$ is the path loss between transmitter μ and receiver α. The general form of the path loss equation is given by

$$P_{\mu,\alpha}^{\text{ls}} = \max\left(A_{\text{pl}}\log_{10}(d_{\mu,\alpha}) + B_{\text{pl}} + C_{\text{pl}}\log_{10}\left(\frac{f_{\text{c}}}{5}\right) + X_{\text{pl}} + \mathcal{N}(0,\sigma^2), P_{\mu,\alpha}^{\text{free}}\right), \tag{2.13}$$

where A_{pl} and B_{pl} are constants specific to the deployment scenario chosen, which are obtained from empirical measurements, $d_{\mu,\alpha}$ is the distance between transmitter μ and receiver α expressed in meters and σ is the standard deviation of the random variable that models the log-normal shadowing between the transmitter and the receiver. The term f_{c} expressed in GHz represents the central carrier frequency and the constant C_{pl} allows the path loss model to be extended over a wider range of frequencies centered around the frequency where the measurements were originally made. In the wireless world initiative new radio (WINNER) project, the measurements were made at 5 GHz. The term X_{pl} is an additional adjustment made to the path loss equation to take into account other deployment or scenario specific parameters, such as

propagation through the walls. When no such adjustments are required, X_{pl} is set to 0. Finally, $P_{\mu,\alpha}^{\mathrm{free}}$ refers to the free space path loss between μ and α, which models the propagation in a LoS scenario in the free space, which sets the lower limit on the path loss possible in any deployment scenario. The free space path loss is given by

$$P_{\mu,\alpha}^{\mathrm{free}} = 20\log_{10}(d_{\mu,\alpha}) + 46.4 + 20\log_{10}\left(\frac{f_{\mathrm{c}}}{5.0}\right). \tag{2.14}$$

By contrast, the small scale fading causes the received signal to fluctuate along the time domain or along the frequency domain at a much shorter scale than the large scale fading. Small scale fading occurs due to two effects - multipath propagation and the Doppler shift. Due to multipath, time shifted and weighted replicas of the original signal are received at the receiver. The received signals are time shifted because of the difference in the length of each of the paths the signal propagates through and weighted due to attenuation of signal along each of the paths.

The time shift results in constructive interference at some frequencies and destructive interference at other frequencies, resulting in a frequency selective channel. Likewise, the Doppler shift results due to relative motion between the transmitter and the receiver. As the signal can arrive at the receiver from all angles, the Doppler shift is distributed from $-f_{\mathrm{D}}$ to f_{D}, where f_{D} is the maximum Doppler shift between the transmitter and the receiver and occurs when the receiver is moving towards the transmitter. A shift in the frequency results in a phase rotation in time, due to which the signal undergoes constructive interference at certain time instants and destructive interference at some other time instants. As a result, a time variant channel is obtained. A detailed treatment of mobile fading channel can be found in [40, 52–54].

In this thesis, the mobile channel is modelled according to the approach in [55, 56]. In this model, the channel impulse response consists of L echoes, that have a distinct arrival time (τ_ℓ) and attenuation ρ_ℓ, where ℓ is an index in the range 1 to L. The average phase of each echo is modelled as a uniformly distributed random variable in interval $[0 : 2\pi]$. Each echo consists of K_{D} diffused components received with a different Doppler shift ($f_{\kappa,\ell}^{\mathrm{D}}$), where κ is an index in the range $[0 : K_{\mathrm{D}}]$ for the diffused component within the ℓ^{th} echo. It is assumed that the number of diffused components within an echo K_{D} is 10. Using the notation above, the time-variant and frequency-selective channel is modelled as

$$G_{\mu,\alpha}(f,t) = \left|\left|\sqrt{\frac{G_{\mu,\alpha}^{\mathrm{ls}}}{L}}\sum_{\ell=1}^{L}\frac{1}{K_{\mathrm{D}}}\sum_{\kappa=1}^{K_{\mathrm{D}}}\rho_\ell \exp\left(j\theta_{\ell,\kappa} + j2\pi[f_{\kappa,\ell}^{\mathrm{D}}t - \tau_\ell f]\right)\right|\right|. \tag{2.15}$$

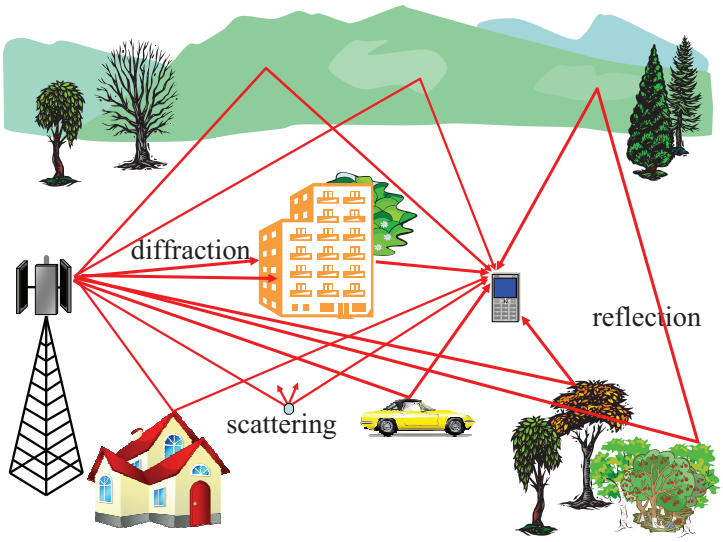

(a) Multipath propagation

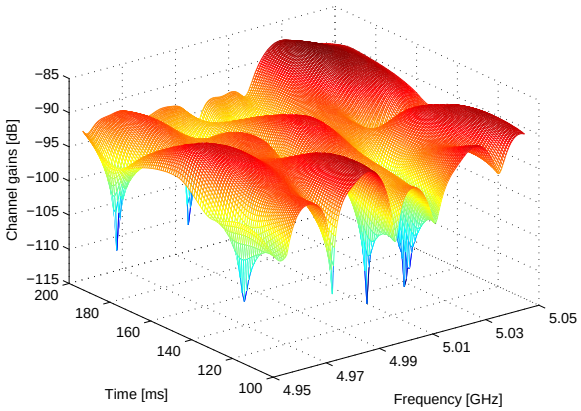

(b) Time variant and frequency selective channel

Figure 2.6: *Illustration of multipath and channel transfer function.*

An instant of a channel modelled using (2.15) is depicted in Figure 2.6(b). In this figure, the channel gains are obtained using typical path loss for a non line of sight (NLoS) scenario obtained at a distance of 20 m in an indoor office environment. Note that in (2.15) the term $\exp(j2\pi(f^{\mathrm{D}}_{\kappa,\ell})t)$ arises from shift by $f^{\mathrm{D}}_{\kappa,\ell}$ in the frequency domain which results in a multiplication by a complex exponential in the time domain. Likewise, the term $\exp(j2\pi\tau f)$ models a multiplication by a complex exponential in the frequency domain which arises due to a delay in the time domain.

As already mentioned earlier, the resources in OFDMA system are allocated in blocks which consists of n_{os} adjacent OFDM symbols and n_{sc} subcarriers (see Figure 3.1 and Figure 4.1), referred to as a *chunk*. The size of a chunk is selected such that the fluctuation of channel gains are negligible over both frequency and time axis within the chunk[2]. For computational efficiency, (2.15) is calculated at discrete intervals in time and frequency, such that the channel gain variations between adjacent chunks in time and frequency are taken into account but the fluctuations within the chunk are neglected. This approximation is valid as long as the chunk dimensions are significantly smaller than coherence time and coherence bandwidth [57]. The coherence time T_{C} and coherence bandwidth B_{C} are calculated using the following rule of thumb [58]

$$T_{\mathrm{C}} = \sqrt{\frac{9}{16\pi(f^{\mathrm{D}}_{\max})^2}}\,, \tag{2.16}$$

$$B_{\mathrm{C}} = \frac{1}{50\sigma_\tau}\,, \tag{2.17}$$

where $f^{\mathrm{D}}_{\max}$ is the maximum Doppler shift, and σ_τ is the root mean square (rms) delay spread. Therefore, by replacing t with $kn_{\mathrm{os}}T_{\mathrm{S}}$ and f with $f_{\mathrm{l}}+nn_{\mathrm{sc}}\Delta_f$, where f_{l} is the lowest frequency within the system bandwidth, in (2.15), we obtain a representation of channel gains that are constant over a chunk size. A chunk is denoted (n,k) consistently in this thesis, where n refers to the frequency index and k refers to the time index[3]. The channel gain for the chunk (n,k)

[2] In wireless world initiative new radio (WINNER) system, a chunk consists of 8 SC and 15 OFDM symbols.

[3] The author is aware that in signal processing literature, n typically denotes the time index and k typically denotes the frame index. The alternative notation is used consistently throughout this thesis to keep the notations consistent with the publications attached to this thesis.

can be written as

$$G_{\mu,\alpha}[n,k] = \left|\left| \sqrt{\frac{G^{\mathrm{ls}}_{\mu,\alpha}}{L}} \sum_{\ell=1}^{L} \frac{1}{K_{\mathrm{D}}} \sum_{\kappa=1}^{K_{\mathrm{D}}} \rho_{\ell} \exp\left(j\theta_{\ell,\kappa} + j2\pi[f^{\mathrm{D}}_{\ell,\kappa} k n_{\mathrm{os}} T_{\mathrm{S}} - \tau_{\ell}(f_{\mathrm{l}} + n n_{\mathrm{sc}} \Delta_f)]\right) \right|\right|. \tag{2.18}$$

As the components θ_{ℓ}, $f^{\mathrm{D}}_{\ell,\kappa}$ are modelled as independent random processes, they are not identical for two users, as long as the users are not co-located. Therefore, for two users $\mu \neq \nu$, $G_{\mu,\alpha}(n,k)$ and $G_{\nu,\alpha}(n,k)$ vary independently of one another, which allow the fluctuations in the channel gains to be exploited for user scheduling which will be discussed in Section 2.4.

2.4 User scheduling in cellular systems

Provided that the channel fading of each user is an independent process, as discussed in Section 2.3, the statistics of channel fading can be exploited to enhance the sum throughput or fairness in the system. User scheduling in an OFDMA system involves distributing N_{C} chunks available at the serving BS to U users served by the considered BS. The user that is scheduled at BS β on chunk (n,k) is denoted $\zeta_{\beta}[n,k]$. In the following, a brief discussion of the schedulers commonly used in wireless communications systems is provided. Interested readers are referred to [59] for a more comprehensive treatment of schedulers in wireless networks.

2.4.1 Maximum throughput scheduling

A maximum throughput scheduler is a greedy scheduling algorithm that allocates a chunk (n,k) to the user ν that maximises the data rate on chunk (n,k) among U competing users. Let $C_{\nu,\beta}[n,k]$ be the data rate of user ν on cell β, the maximum throughput scheduler is defined as

$$\zeta_{\beta}[n,k] = \underset{\nu = 1,\ldots,U}{\arg\max}\ C_{\nu,\beta}[n,k]. \tag{2.19}$$

In a cellular system, the users located closer to the serving BS achieve channel gains that are typically tens of dB higher than those closer to the cell-edge. Thus, maximum throughput scheduling mechanism leads to an unfair distribution of radio resources where most of the radio resources are allocated to a few of the users closer to the cell-centre and result in starvation of the users closer to the cell-edge.

2.4.2 Round robin scheduling

A round robin scheduler allocates chunk to each user in strict rotation, in a manner similar to the first in first out (FIFO) queue. The user that is allocated the chunk (n, k) is given by

$$\zeta_{\beta}[n, k] = \mod (k, U) + 1 \tag{2.20}$$

A round robin scheduler results in a fair allocation of resources but fails to opportunistically exploit channel fluctuations.

2.4.3 Min-max fair scheduling

Min-max fair scheduling refers to a broader category of algorithms that maximise the minimum of the considered considered quality of service (QoS) parameter in the system [60–64]. The QoS parameter may refer to the achieved signal to interference and noise ratio (SINR), achieved data rates, delay and so forth. When min-max fair scheduling is achieved, the achieved level of QoS cannot be increased in any link without compromising the level of achieved QoS in other links.

A simple min-max fair scheduler allocates chunk to different users in strict rotation until the demands of at least one user is met. The remaining chunks are distributed among the remaining users until all of the users are satisfied or there are no more chunks. Such scheduler proposed in [64] is presented in Algorithm 1. In the presented algorithm, D_{ν} refers to the demand of user ν, N_{C} is the number of chunks available within the system bandwidth and i is a dummy variable. All other notations are consistent with earlier definitions.

Input: $U, N_{\mathrm{C}}, D_{\nu}$

Output: $\zeta_{\beta[n,k]}$

initialization;

satisfied_users $\leftarrow 0$;

unsatisfied_users $\leftarrow U$;

$n \leftarrow 1$;

$i \leftarrow 1$;

while $n \leq N_{\mathrm{C}}$ **do**

  $\nu \leftarrow$ *satisfied_users* + mod($i-1$,*unsatisfied_users*)+1;

  $\zeta_{\beta[n,k]} \leftarrow \nu$;

  allocated_chunks $\leftarrow \sum_{l=1}^{n} \mathbb{I}_{\zeta_{\beta[l,k]=\nu}}$;

  if *allocated_chunks* = D_{ν} **then**

    satisfied_users $\leftarrow$ *satisfied_users*;

    unsatisfied_users $\leftarrow$ *unsatisfied_users*-1;

    $i \leftarrow 1$;

  else

    $i \leftarrow i+1$;

  end

  $n \leftarrow n+1$;

  if *satisfied_users* = U **then**

    Break;

  end

end

Algorithm 1: Min-max fair scheduling algorithm.

A min-max fair scheduling mechanism results in a performance identical to that of round robin scheduling if all of the users have the same demand. Like the round robin scheme, min-max fairness scheme also fails to exploit channel fluctuations opportunistically as it allocates chunks in strict rotation.

2.4.4 Proportional fair scheduling

The notion of proportional fair scheduling was first introduced in [65] as a mechanism to allocate data rates to different users on the basis of charge they are willing to pay. The proportional fair scheduling criteria has been widely used in the literature [14, 66–69], where attempts to av-

erage the data rate allocated to different users are made by allocating the chunk to the user that maximises the priority factor. The priority factor is the ratio of the current data rate $C_{\nu,\beta}[n,k]$ to its exponentially smoothed average data rate $\breve{C}_{\nu,\beta}[n,k]$. The scheduled user on chunk (n,k) is given by

$$\zeta_\beta[n,k] = \underset{\nu=1,\ldots,U}{\arg\max} \frac{C_{\nu,\beta}[n,k]}{\breve{C}_{\nu,\beta}[n,k]} \tag{2.21}$$

where $\breve{C}_{\nu,\beta}[n,k]$ is an exponentially averaged user throughput given by

$$\breve{C}_{\nu,\beta}[n,k] = (1-\frac{1}{t_\mathrm{c}})\breve{C}_{\nu,\beta}[n,k-1] + \frac{1}{t_\mathrm{c}} C_{\nu,\beta}[n,k-1]\mathbb{I}_{\zeta_\beta[n,k-1]=\nu}, \tag{2.22}$$

where $\mathbb{I}_x$ takes value 1 or 0 depending on whether the condition x is true or false respectively. In (2.22), the term $\mathbb{I}_{\zeta_\beta[n,k-1]=\nu}$ ensures that the data rate potentially achievable by user ν on chunk $(n,k-1)$ is taken into account only if the user ν was actually scheduled during that slot. The term t_c is a weighting factor that serves as the system memory in calculating the exponentially smoothened average. A smaller value of t_c allows highest weighting to the most recent data rate achieved and vice versa. Thus, the system can trade off fairness in the short term (using small t_c) to enhance multiuser diversity (using large t_c).

2.4.5 Score-based scheduling

Score-based scheduler proposed in [70] ranks the slots according to the considered QoS metric. The QoS metric can be the intended channel gains of the users, the *a priori* estimate of the SINR, instantaneous data rates and so forth. In this section, the instantaneous data rates are used as a basis of score. The rationale behind score-based scheduling is that the received signal strength fluctuates in time and frequency as discussed earlier in Section 2.3. The fluctuations of signal power leads to fluctuations in instantaneous data rates achievable on the link. By ranking the chunks according to the amount of data achievable on each link, the chunk can be allocated when the achieved data rates attain the highest when compared to the history of the instantaneous data rates achievable within an observation window of size W. In essence, a channel is allocated to a particular user when the considered QoS metric is highest on its own link. Score-based scheduling utilises the fact that the channel gains of two users fade independently so as to perform user scheduling. The score for user ν, provided that the current

data rate is used as a scheduling criteria, is given by

$$s_{\nu,\beta}[n,k] = 1 + \sum_{\ell=1}^{W-1} \mathbb{I}_{\{C_{\nu,\beta}[n,k]<C_{\nu,\beta}[n,\ell]\}} + \sum_{\ell=1}^{W-1} \mathbb{I}_{\{C_{\nu,\beta}[n,k]=C_{\nu,\beta}[n,\ell]\}} X_\ell \,, \tag{2.23}$$

where X_ℓ is an independent and identically distributed (i.i.d.) random variable on $\{0,1\}$ with $\Pr(X_\ell = 0) = \frac{1}{2}$. The user that is allocated the chunk is given by

$$\zeta_q[n,k] = \underset{\nu\,=\,1,\ldots,U}{\arg\min}\; s_{\nu,\beta}[n,k] \tag{2.24}$$

The score for user ν given by (2.23) is the minimum (*i.e.* 1) on chunk (n,k) when the instantaneous data rate, $C_{\nu,\beta}[n,k]$ attains its highest value within the observation window. Provided that the channel fading of each user is independent of the channel fading of all other users, the score attained by a user ν on chunk (n,k) is different from the score attained by a user μ on chunk (n,k). Provided that $W \gg U$ holds, it is less likely that two users will attain the same score. Therefore, (4.7) exploits multi user diversity so as to ensures that the chunk is allocated to the user that attains the highest data rate in relation to its past data rates. Moreover, as the scores are calculated for each link are based on its own history of achievable data rate using (2.23), the cell-edge users have the same likelihood of being scheduled on a certain chunk as the users located closer to the serving BS. However, as the chunks are allocated when the instantaneous data rates within the observation window attain the maximum value (see (2.24)), the minimum data rate achieved by each link is maximised.

However, the score-based scheduler in [70] does not allow for reservations. In this thesis, a modified version of score-based scheduler [71] is proposed so that it suits a cellular system that allows multiple access with reservation. The modified score-based scheduler is presented later in Section 4.3.

2.5 Interference in OFDMA-TDD networks

Interference scenario in OFDMA-TDD networks result both from spectrum sharing as well as leakage of signal transmitted in one frequency band towards another. The multiple access interference (MAI) in OFDMA network results due to loss of orthogonality between subcarriers, as depicted in Figure 2.7. The major reasons for the loss of orthogonality in OFDMA-TDD

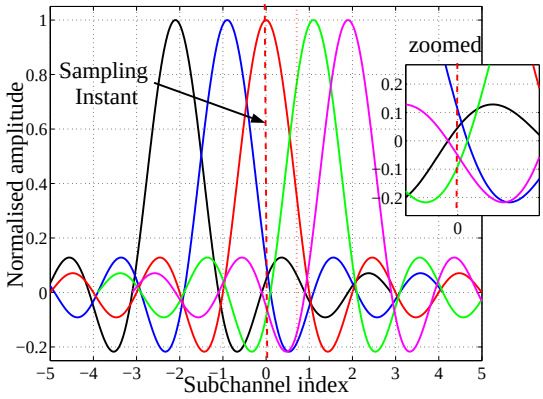

Figure 2.7: *MAI caused due to imperfect frequency synchronisation in OFDMA system.*

networks are due to the Doppler shift, frequency offset in oscillator and synchronisation errors [72]. In the DL, the Doppler and frequency offset is either positive or negative for the entire signal bandwidth. Therefore, it is relatively easier to mitigate such interference by applying appropriate correction factor in the DL compared to UL [73]. In the latter, the Doppler and frequency offsets tend to have positive errors for some users whereas it will have negative errors for other users, which makes it more challenging for MAI mitigation.

The CCI results due to spectrum sharing and can be mitigated by careful allocation of radio resources. Since the focus of this thesis is on CCI mitigation in OFDMA-TDD system, a MAI-free system is assumed. This assumption necessitates a perfect time and frequency synchronisation and a perfect Doppler shift correction. Frequency synchronisation is typically performed using frequency offset estimation and correction approaches [74, 75]. Likewise, time synchronisation can be carried out using the network time protocol, which is used to synchronise the clock of the nodes connected to the Internet, or using global positioning system (GPS) receivers, which provide precise time stamp to receivers that are able to receive signals from GPS satellites. The network time protocol can be easily utilised in networks where the access points are connected to the backbone network. Likewise, synchronisation using GPS receivers can be achieved provided that the user terminals are outdoors and are able to receive GPS signals. Moreover, the user terminals can synchronise themselves to the access points using synchronisation sequences such as Barker codes that are used in IEEE 802.11 networks. In decentralised and self-organising networks, time synchronisation is carried out by listening to regular beacons broadcasted by a master node, such as in Bluetooth and Zigbee networks. Finally, in fully decentralised networks, time synchronisation can be achieved using biologically inspired

synchronisation methods such as firefly synchronisation [76]. However, it is recognised that a perfect synchronisation in time and frequency may not always be possible across the network due to propagation delays and estimation errors which results in additional interference at the receiver. The impact of imperfect time and frequency synchronisation is not considered in this thesis as the focus of this thesis is on decentralised CCI management in wireless networks. Interested readers are referred to [77, 78] for further details on time-frequency synchronisation in OFDMA systems.

2.6 Centralised CCI mitigation and avoidance approaches

Provided that a centralised infrastructure exists, the allocation of radio resources can be computed centrally such that the CCI is mitigated. Such techniques can either be static frequency planning approaches or dynamic frequency approaches. Static frequency planning methods generally tend to be rigid and usually waste the available capacity due to preemptive approach in mitigating CCI. By contrast, dynamic frequency allocation approaches tend to more flexible and result in a better utilisation of channel capacity by utilising the channel state information and traffic demands. Admittedly, such techniques require signalling from different transmitting and receiving entities in the network, which can result in extra overhead. Such signalling in the context of long term evolution (LTE) system include heavy interference indicator (HII), overload indicator (OI) that are transmitted over the X2 interface or interference bitmap that are transmitted across BSs (eNode B in LTE terminology) for reconfiguring frequency allocation. An X2 interface is a mechanism for inter BS communication in the LTE standard. As already noted, such signalling results in extra overheads and are usually transmitted no more frequently that every 20 ms in a long time evolution (LTE) system [37].

In the following, centralised and static methods for mitigating CCI in cellular networks are discussed.

2.6.1 Static frequency planning

Static frequency planning involves distributing the available frequency in the system to different cells such that any two cells reusing the same frequency are separated by minimum reuse distance D. The set of available frequencies in the system $\mathcal{F}$ is divided into K disjoint subsets where each set of frequency is allocated to one cell in a group of K closely located cells called

a *cluster* [40, 54]. Two or more cells that reuse the same set of frequency resources are referred to as co-channel cells. The cluster is repeated as often as necessary within the geographical area to cover the required area served by the system. An example of static frequency planning is depicted in Figure 2.8 where a cluster size of 7 in a hexagonal cellular structure is assumed. It should be noted that increasing K increases D thereby decreasing the CCI caused by transmitter in one cell towards the receiver in another co-channel cell. However, increasing K at the same time decreases the spatial reuse of frequency resources, thereby potentially reducing the system capacity.

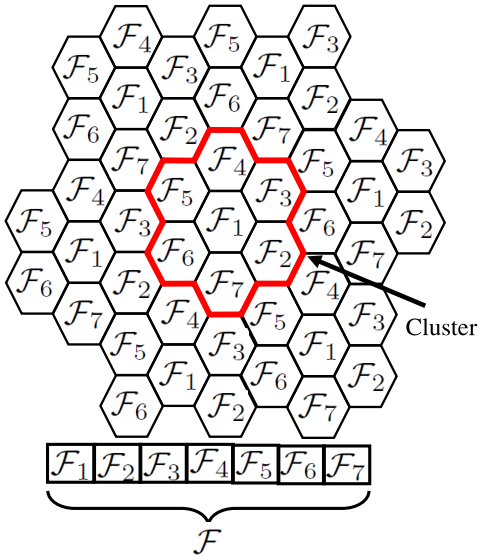

Figure 2.8: *Frequency planning in a cellular structure with reuse factor of* 7.

At one extreme, $K = 1$ refers to a full frequency reuse (also known as universal frequency reuse), where the entire system bandwidth is used in each cell. While the spatial reuse of frequency attains the maximum value, the CCI is also highest which can potentially decrease the system throughput. On the other extreme, $K = N_{\mathrm{B}}$, where N_{B} is the number of BSs in the system, refers to a CCI free system where the desired channel gains determine the system capacity, assuming that an adaptive modulation is performed. However, as the frequencies are not reused in the system, the system capacity is potentially wasted. A careful choice of K during frequency planning that balances the spatial reuse of frequency with the level of CCI tolerated in the system is essential, so as to maximise the spatial reuse whilst reducing outage, especially at the cell-edge.

Furthermore, it should be noted that the static frequency planning results in a *hard reuse* of radio resources. The frequencies assigned to a particular cell remain fixed. As a result, it is likely

that the capacity is wasted in one cell while the other cell is unable to serve user demands, in a system with heterogeneous user distribution. As a result, fixed frequency planning cannot cater for imbalance in user distribution across different cells or imbalance in traffic demands.

2.6.2 Fractional frequency reuse

In a cellular system where the BSs are distributed in an isotropic manner, the users closest to the cell-boundary have higher desired channel gain to the intended BS. Therefore, the resources assigned to users in the inner region of the cells can potentially be allocated in adjacent cells, but remain wasted with frequency planning approach discussed in Section 2.6.1. Fractional frequency reuse (FFR) [79–82] addresses this issue by realising that in the cellular networks, CCI predominantly affects users near the cell boundary. FFR typically involves a sub-band with full frequency reuse that is exempt from any slot assignment restrictions. The allocation of the remaining sub-bands is coordinated among neighbouring cells, in a way that the users in the given cell are denied access to sub-bands assigned to the cell-edge users in the adjacent cells.

Fractional frequency reuse in cellular system are extensively studied [80, 81, 83, 84] in the literature. Two major variants are depicted in Figure 2.9. In both cases, the set of frequencies ($\mathcal{F}_1$) where full reuse is considered is allocated to the cell-centre user. In the first variant, shown in Figure 2.9(a) the set of frequencies whose allocation is coordinated among adjacent cells may only be allocated to the cell-edge user. In the second variant, depicted in Figure 2.9(b), the set of frequencies whose allocation is coordinated among the adjacent cells may be assigned flexibly within the cell to both the cell center and cell-edge users. The region within the cell where the set of frequencies in the coordinated frequency bands may be allocated is depicted using small arrows. For resource allocation, a user may be classified as a cell-edge user or a cell-center user based on its path loss to its serving BS [80].

2.6.3 Soft frequency reuse

The CCI caused towards the victim receivers can be mitigated by using power mask in a coordinated manner [80], mainly in DL mode. A full reuse of resources in each cell is considered. The available frequencies are partitioned into different sub-bands. Full power is used for transmission in one of the sub-bands and this part is exclusively allocated to the cell-centre users. The rest of the sub-bands are used to serve the cell-edge users. Only one cell within a cluster is

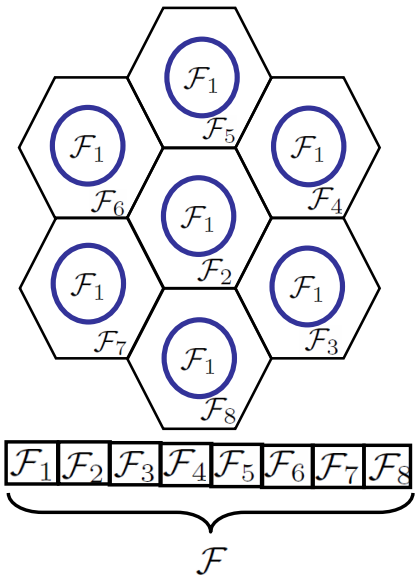

(a) Coordinated frequency band allocated exclusively to cell-edge users.

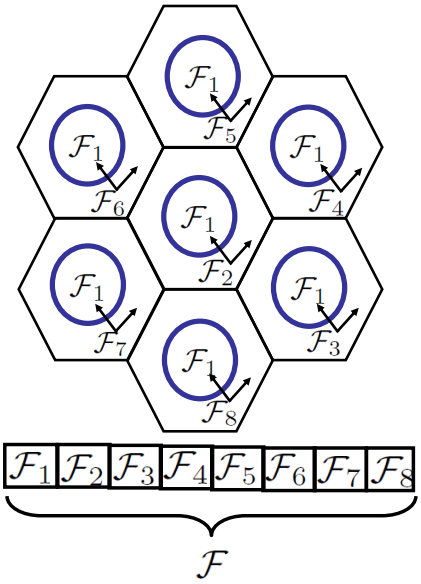

(b) Coordinated frequency band allocated both to cell-edge and cell-centre users.

Figure 2.9: *Depiction of fractional frequency planning in a cellular scenario. A subset of the available set of frequencies is universally reused while the allocation of the remaining subsets are coordinated dynamically among the cells within a cluster. In (a) the set of frequencies in the coordinated frequency band are allocated exclusively to the cell-edge users. In (b), the set of frequencies in the coordinated frequency band point to both the cell-edge region as well as the cell-center region denoting that the resources may be allocated flexibly within the cell, to either cell-edge or cell-center users.*

allowed to transmit with full power on the coordinated sub-bands whereas the other cells must utilise a lower transmit power. It is important that user scheduling is considered jointly with transmit power allocation is such system, such that the links utilising lower transmit power are not noise limited.

2.6.4 Beamforming

Provided that the BSs are equipped with multiple antennas, the BS can apply transmit precoding to perform spatial filtering of signals. This enables the transceivers to enhance signals originating from (or transmitted towards) a particular direction and attenuate signals originating from (or transmitted towards) other directions. The resulting radiation pattern is called a beam, which is depicted in Figure 2.10. The lobe in the direction where the antenna gain is the highest is called the *main lobe* and the lobes in the other directions are called the *side lobes*, with lower antenna gains compared to the main lobe. Provided that the main lobe of the antenna array does not point towards the victim receiver (or interfering transmitter), the CCI caused towards a victim receiver can be mitigated.

Figure 2.10 depicts beamforming using an antenna array. Let x represent the signal transmitted from the far-field of an antenna array. The signal received on t^{th} antenna element of the array is given by x_t. Likewise, d_t represents the distance of antenna t from a reference point considered. From the geometry of the array, the delay observed at antenna t with respect to the reference point is $d_t \sin(\theta)$, where θ is the angle made by the transmitter located in the far field of the array with respect to the normal of the antenna array as shown in Figure 2.10. This induces a phase shift of $e^{-j\frac{2\pi}{\lambda}d_t \sin(\theta)}$ at the antenna element t. Let $\mathbf{v} = [v_1, \dots v_{N_\text{T}}]$ be the steering vector, where v_t is the complex coefficient multiplying the received signal at antenna t. The output of the antenna array is expressed as [85]

$$\begin{aligned} y &= \sum_{t=1}^{N_\text{T}} x_t v_t \\ &= \sum_{t=1}^{N_\text{T}} \underbrace{x e^{-j\frac{2\pi}{\lambda}d_t \sin(\theta)}}_{x_t} v_t \end{aligned} \tag{2.25}$$

In a uniform linear array, the antenna array attains a maximum gain along the direction ϕ provided that v_t cancels the phase of x_t. In this case, the coefficients are $v_t = e^{j\frac{2\pi}{\lambda}d_t \sin(\phi)}$.

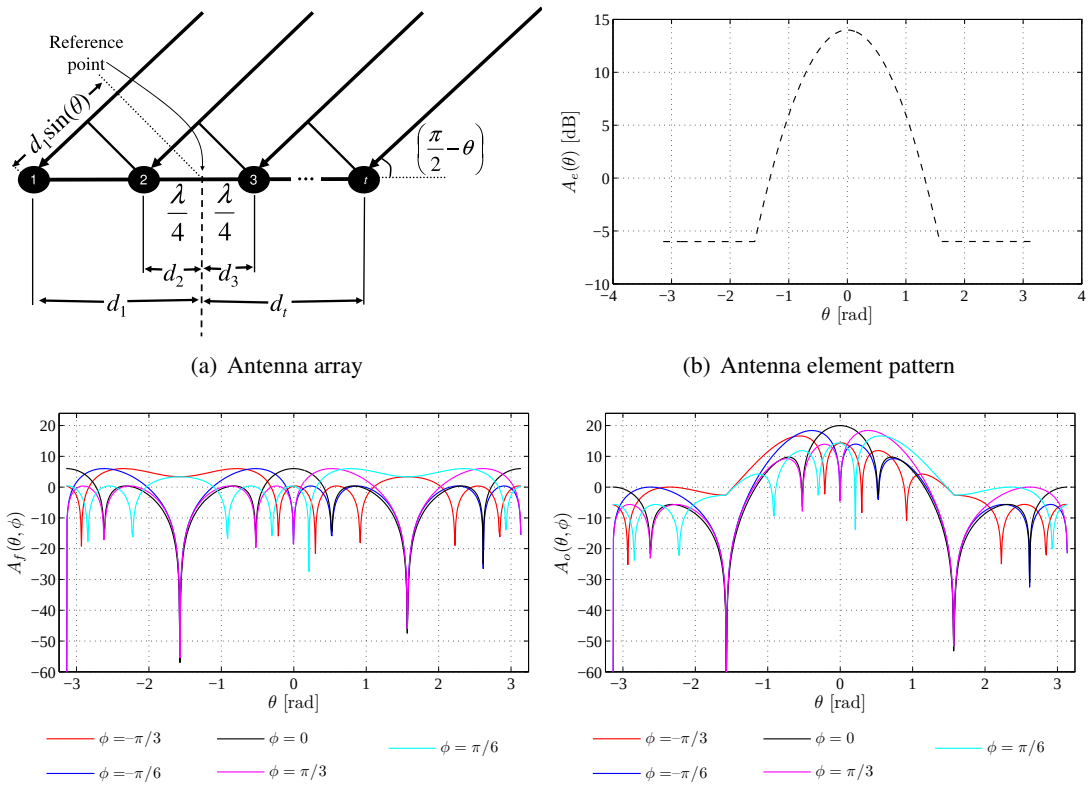

(a) Antenna array

(b) Antenna element pattern

(c) Array gain (isotropic antenna elements)

(d) Array gain (anisotropic antenna elements)

Figure 2.10: *Beamforming using multiple antennas at the transmitter. A uniform linear array of with 4 antenna elements is shown in (a). The radiation pattern of an individual antenna element (b) is multiplied with array factor (c), which is calculated using* (2.28) *to give the overall radiation pattern of an array (d), which is calculated using* (2.29)*.*

Thus, (2.25) may be rephrased as

$$y = \sum_{t=1}^{N_{\mathrm{T}}} x e^{-j\frac{2\pi}{\lambda}d_t(\sin(\theta)-\sin(\phi))} \tag{2.26}$$

The array factor, expressed as $A_{\mathrm{f}}(\theta,\phi) = y/x$, is expressed as

$$A_{\mathrm{f}}(\theta,\phi) = \sum_{t=1}^{N_{\mathrm{T}}} e^{-j\frac{2\pi}{\lambda}d_t(\sin(\theta)-\sin(\phi))} \tag{2.27}$$

For a uniform linear array, $d_t = t\Delta_t$, (2.27) reduces to [86]

$$\begin{aligned} A_{\mathrm{f}}(\theta,\phi) &= \sum_{t=1}^{N_{\mathrm{T}}} e^{-j\frac{2\pi t\Delta_t}{\lambda}(\sin(\theta)-\sin(\phi))} \\ &= e^{\frac{-j(N-1)\Delta_t\pi(\sin(\theta)-\sin(\phi))}{\lambda}} \left(\frac{\sin\left(\frac{\pi N\Delta_t}{\lambda}(\sin(\theta)-\sin(\phi))\right)}{\sin\left(\frac{\pi\Delta_t}{\lambda}(\sin(\theta)-\sin(\phi))\right)} \right) \end{aligned} \tag{2.28}$$

In (2.28), $A_{\mathrm{f}}(\theta,\phi)$ attains its maximum if $\phi = \theta$. Therefore, by adjusting ϕ, the main lobe of the beam can be electronically steered. It should be noted that (2.28) is valid for antenna array where all antenna elements are isotropic radiators. However, the overall array pattern for array $A_{\mathrm{o}}(\theta,\phi)$ where individual elements are anisotropic radiators with radiation pattern given by $A_{\mathrm{e}}(\theta)$ can be obtained using pattern multiplication [86] as follows

$$A_{\mathrm{o}}(\theta,\phi) = A_{\mathrm{f}}(\theta,\phi)A_{\mathrm{e}}(\theta). \tag{2.29}$$

For serving a MS located within the coverage region, the BS needs to estimate the angle of arrival (AoA) of the signal from the MS. Well known techniques such as estimation of signal parameter by rotational invariant techniques (ESPRIT) [87, 88] or multiple signal classification (MUSIC) [89], can be used which allow good estimation of the AoA parameter.

2.6.4.1 Fixed beamforming

With the fixed beamforming method, the steering vector for generating a beam is pre-computed and applied to the antenna array to activate such beam. By adjusting the coefficients applied to the antenna elements, the main lobe of the antenna radiation pattern can be steered. Provided

that the area of coverage for a given cell can be fully served by utilising N_{beam} beams, the coefficients required for generating such beams can be pre-computed and stored at the BS. The BS estimates the angle of arrival (AoA) and determines the beam that provides such user with the best channel gain. The precoding vector appropriate for activating such beam is then applied to the array. In such a system, when the angular difference between the direction of main lobe (ϕ) and direction of user θ increases, the antenna gain decreases. When the gain provided by switching on a neighbouring beam exceeds the gain achieved by the current beam, beam switching occurs.

2.6.4.2 Adaptive beamforming

Unlike fixed beamforming, the coefficients for adaptive beamforming are computed in real time. Adaptive beamforming may be performed such that the maximum gain of the radiation pattern is formed towards the intended user, referred to as user tracking and/or create nulls towards the victim receivers, referred to as null steering [90]. As the location of both intended and interfering users may change with time, adaptive beamforming techniques require that the coefficients are computed in real time. Thus, there is a trade off between performance and complexity of transceiver units. The advantage of adaptive beamforming is that either the intended user can be positioned at the location providing maximum antenna gain within main lobe, provided that its location is precisely known or up to $N_{\mathrm{int}} = N_{\mathrm{T}}$ interferers can be nulled.

2.6.5 Centralised coordination

In unicellular wireless network like that of a WLAN where a centralised receiver is within the hearability range of all transmitters, the central node may coordinate allocation of radio resources. In the uplink, it coordinates transmissions originating from different users such that no two users transmit using the same radio resources. Polling [91] is one of the contention free allocation strategy which is also implemented in IEEE 802.11 WLANs. This procedure is termed as point coordination function (PCF) so as to provide quality of service (QoS) guarantee. An alternative centralised coordination approach [91] is that when a transmitter begins transmission to the centralised receiver, the centralised receiver broadcasts a busy signal barring all other users from accessing the channel.

2.7 Decentralised CCI mitigation and avoidance approaches

This class of CCI mitigation approaches may utilise the locally available information to mitigate CCI caused towards other links.

2.7.1 ALOHA and slotted ALOHA

ALOHA is a 'best effort' multiple access protocol used in wireless networks, which was developed in the 1970s at the University of Hawaii. It makes no attempt to mitigate CCI caused towards the victim receiver. In the wireless network using ALOHA protocol, the transmitter begins data transmission as soon as it has data to transmit. If collisions are detected, the data is retransmitted after a random backoff. It has been demonstrated that the peak throughput of ALOHA protocol is approximately 18% [40, 92] assuming that the collisions are hard and the traffic is Poisson distributed.

In order to reduce the collisions, the time axis is slotted and the transmitter can only transmit at the beginning of the slot. This avoids collision of the data frames that partially overlap with one another. With identical assumptions as the *pure* ALOHA system, it has been demonstrated [40, 92] that the slotted ALOHA achieves 37% of the channel capacity.

2.7.2 Carrier Sense Multiple Access

The carrier sense multiple access (CSMA) [40, 92] improves the performance of the 'best effort' ALOHA protocol by requiring the transmitter that has data to transmit to sense whether the channel is 'busy' or 'idle' before transmission. If the signal from another transmitter is detected, it is understood that the channel is in use, *i.e.* busy, otherwise it is considered idle and may be used for transmission. Provided that no ongoing transmissions are detected, the transmitter transmits data to its intended receiver using the free channel. Depending the reaction of the transmitter upon learning that the channel is idle, the CSMA protocol is classified as

- $1-$persistent CSMA: The transmitter continuously senses the channel and transmits immediately upon learning that the channel is free. The problem with $1-$persistent CSMA is that two or more transmitters can simultaneously detect the channel free and proceed with transmission, resulting in collisions.
- Non persistent CSMA: The non-persistent CSMA attempts to reduce the collision due

to simultaneous access of the channel by refraining from sensing the channel for a random period of time. This reduces collisions because the likelihood that two terminals simultaneously sense the channel free and proceed with transmission is lower than that of $1-$persistent CSMA.

However, it should be noted that collision may still occur within time duration τ_{p} where τ_p is the time it takes for the signal from the transmitter to propagate to all users within the range of the transmitter.

- $p-$persistent CSMA: The $p-$persistent approach is used in systems where a transmitter may only begin its transmission at the beginning of a discrete time slot. If the time slot is sensed free, it transmits with a probability p. If either the time slot was not sensed free or if the transmitter did not transmit on the slot sensed free (which happens with a probability of $1 - p$, the transmitter waits until the next time slot when it is allowed to sense the channel again. The process is repeated until either the transmitter successfully transmits its data or another transmitter successfully allocates the slot and the slot is sensed busy.

Although the likelihood of collision is reduced by the CSMA approach compared to the ALOHA protocols, collisions can still occur. When collision occurs, the transmitted data would be destroyed. By stopping such transmissions immediately upon learning that the collisions have occurred, wastage of channel capacity can be reduced. This is accomplished by either collision detection or collision avoidance techniques.

2.7.2.1 CSMA with collision detection

CSMA with collision detection (CSMA/CD) is a widely used medium access technique used in the IEEE 802.3 networks, popularly known as the Ethernet [92]. The CSMA/CD technique requires the transmitters to listen to the channel simultaneously whilst transmitting. If the transmitter detects signal originating from a different transmitter, it infers that a collision has occurred. The key assumption made with CSMA/CD is that all transmitters and receivers within the network are within the hearability range of one another.

In wireless networks, implementing collision detection is not feasible for two reasons. First, it is unrealistic to assume that all transmitters and receivers are within the hearability range of one another. Second, the signals originating from other transmitters are indistinguishable given

that its own transmission is received at a much higher signal power. Virtual collision detection methods have been proposed that allow collision to be detected by pausing own transmission randomly to listen to ongoing transmissions [93] or using time slots of different durations [94]. Furthermore, in wireless medium, not all transmitting and receiving nodes are within the hearability range of one another, due to which the classical hidden and expose node problems (see Section 2.7.2.3) arise. To solve this problem, the task of detecting the collision and informing the transmitter about the collision has been delegated to the receiver, where the receiver transmits a collision detection signal on a designated feedback channel [95, 96].

2.7.2.2 CSMA with collision avoidance

In CSMA with collision avoidance (CSMA/CA), a channel is allocated when the transmitter detects the data slot as idle. If the channel is sensed busy, the transmitter refrains from sensing the slot again for certain period of time randomly chosen in an interval between 0 and k_{bo}. The time k_{bo} is distributed according to a truncated binary exponential distribution, given by $k_{\mathrm{bo}} = \min(2^i - 1, k_{\max})$, where i is the number of times collision is encountered in succession and $k_{\max}$ is the maximum number of time slot a transmitter has to backoff, regardless of the number of times the collision was encountered.

Current implementation of CSMA/CA include channel probing using ready-to-send (RTS) and reservation using clear-to-send (CTS) to avoid collisions, when the packet to be transmitted is larger than a certain threshold. The threshold on packet size for enabling RTS/CTS packet exchange is enforced to reduce signalling overhead for smaller packets. However, RTS/CTS packet exchange is an optional part in the state-of-the-art implementations of WLAN access points and not all WLAN hardware can support this feature.

2.7.2.3 Hidden and exposed node problem

A hidden node problem occurs when a new transmitter is out of the hearability region of an active transmitter but is within the hearability region of the receiver. As the new transmitter does not detect the presence of the active transmitter, it incorrectly infers that the channel is free and therefore causes detrimental CCI to the active receiver in its vicinity. By contrast, an exposed node problem results from the transmitter being over-cautious when it senses the medium as busy even when its own transmission would not hurt the ongoing transmission. Fig-

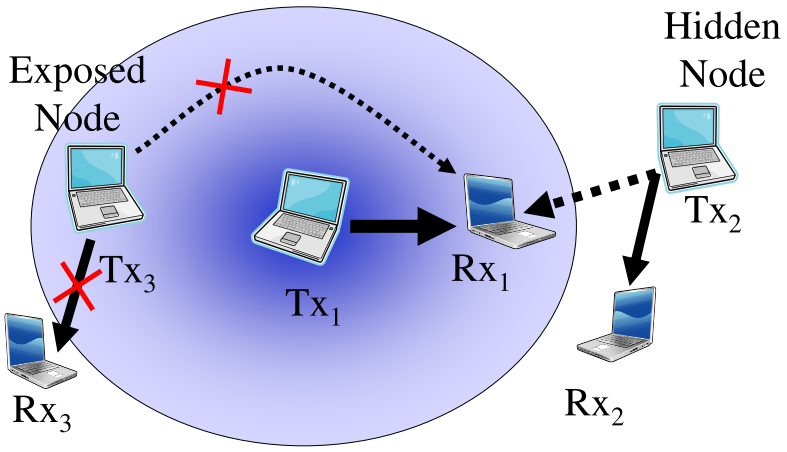

Figure 2.11: *Illustration of the hidden and the exposed node problem. The intended links are denoted with solid lines whereas the interfering links are denoted with dashed lines. The oval indicate the region over which the carrier signal is detected above the threshold. The transmitting node Tx_2 does not hear the transmitting node Tx_1 and commences transmission which causes excessive CCI towards Rx_1 (hidden node). By contrast, Tx_3 avoids transmitting even though it is outside hearability range of Rx_1 (exposed node). The links that are not activated are crossed.*

ure 2.11 depicts the hidden node and the exposed node problem. In the considered example, the transmission between transmitting node Tx_1 and receiving node Rx_1 is ongoing. Tx_2 which happens to be in the vicinity of Rx_1 but outside the hearability range of from Tx_1 commences transmission, thereby causing strong CCI towards Rx_1. As Tx_2 cannot hear the ongoing transmission, it is called the hidden node. By contrast, Tx_3 which happens to be in the vicinity of Tx_1 but shielded from Rx_1 refrains from transmission, giving rise to exposed node problem.

2.7.3 IEEE RTS/CTS handshake

The transmitter that has data to transmit sends an RTS packet. If the channel is not busy at the receiver end, the receiver replies with a CTS packet. A competing transmitter that hears an RTS packet must remain silent until the deadline for receiving the CTS packet expires. If the RTS packet is received but not the CTS packet, the transmitter infers that it is an exposed node and may transmit its own RTS packet. Likewise, a transmitter that receives a CTS packet but not an RTS packet infers that it is a hidden node and remains silent until the packet is transmitted. Thus the RTS/CTS handshake solves the hidden node problem as long as the potential transmitter is within the packet decoding distance of an active receiver. However, it was correctly identified in [97] that the transmitters could still interfere with the ongoing transmission because the

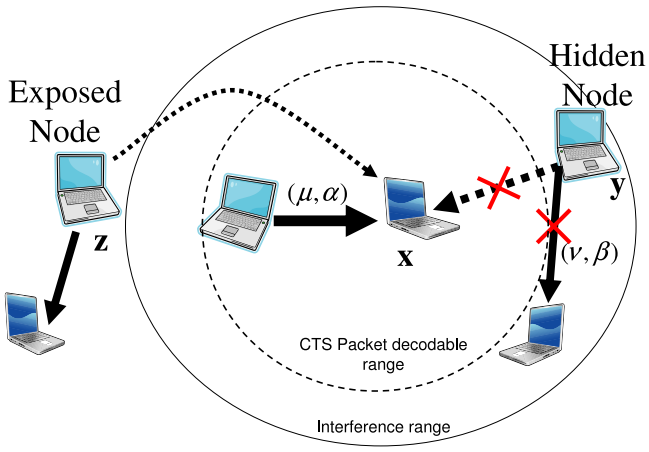

Figure 2.12: *Illustration of interference range vs. CTS range. The receiver of an active link, denoted* $\mathbf{x}$*, transmits a CTS packet. The region around the receiver* $\mathbf{x}$ *where the CTS packet can be decoded is demarked with a dashed oval. Any node lying within the CTS packet decodable range avoids reusing the chunk so as to avoid CCI. The node* $\mathbf{y}$ *lies outside the region where CTS packet cannot be decoded but within the range where it causes significant interference towards* $\mathbf{x}$ *(hidden node). Therefore, the hidden problem is mitigated with RTS/CTS handshake mechanism but not completely eliminated.*

distance at which the CTS packet can be decoded correctly is usually smaller than the distance from which the transmission may cause detrimental CCI at the receiver of an active link. The working mechanism of IEEE RTS/CTS mechanism is depicted in Figure 2.12. A transmitter or a receiver of link (μ, α) is denoted $\mathbf{x}$ and the transmitter or receiver of link (ν, β) is denoted $\mathbf{y}$. It is assumed that the transmitter μ transmits an RTS packet to receiver α. The receiver $\mathbf{x}$ (*i.e.* α) replies with a CTS packet. The transmitter $\mathbf{y}$ which lies outside the range where the CTS packet can be decoded, believes that the channel is free and proceeds with the transmission. However, as $\mathbf{y}$ is still within the range of $\mathbf{x}$ within which any transmitters will cause severe interference to $\mathbf{x}$, the hidden node problem is not resolved fully. Adding CSMA may improve on avoiding hidden node problem, but it can aggravate the exposed node problem because with CSMA mechanism the exposed node never gets an opportunity to transmit the RTS packet. For example, in Figure 2.12, the node $\mathbf{z}$ will not get a chance to transmit the RTS packet as it will sense the carrier from transmitter of link (μ, α). Finally, as the RTS, CTS and data packets all share the common bandwidth, a node that has heard a CTS cannot respond to the RTS packets addressed to it. Therefore the RTS/CTS mechanism does not completely solve the exposed node problem.

The original RTS/CTS handshake, called Multiple Access with Collision Avoidance (MACA),

which was proposed by Karn [98], was modified in [99] to suit the wireless environment. The new algorithm was called MACA-W (MACA-Wireless). In the MACA-W algorithm, data sending (DS) packet preceding the data transmission to avoid transmitting data to a receiver which is at that instant in a transmit mode. In addition, acknowledgment (ACK) following successful data transmission were added to facilitate fast retransmissions at the link layer itself rather than wait until the errors were detected by higher layers of the protocol stack. However, similar to the MACA protocol, the MACA-W protocol does not completely eliminate the hidden node problem.

The RTS/CTS handshake is extended to systems where multiple users share multiple channels available in the system, where both the transmitter and the receiver monitor the channel usage [100, 101] of neighbouring nodes and deduce the free slots from channel usage. In the variants of RTS/CTS signalling incorporating these improvements added to the original RTS/CTS handshake mechanism, the transmitter announces free slots at the transmitter with the RTS packet and the receiver replies with free channels at the receiver with the CTS packet.

2.7.4 Busy Signal approach

The busy signal concept solves the hidden node problem by allowing the receivers to transmit a busy signal in either a dedicated out-of-band channel [102] or in an in-band channel [27]. These busy signals inform a potential transmitter about the instantaneous CCI it causes to the 'victim' receivers, which enables the transmitter to take appropriate steps to avoid interference, such as deferring its own transmission to another time-frequency slot.

2.7.4.1 Dual busy tone multiple access

The dual busy tone multiple access (DBTMA) protocol [102] and its variants [103] solve the problem associated with incorporating CTS into the data slot. This is accomplished by incorporating two narrowband channels where two types of busy tones (BT), $\mathrm{BT_t}$ and $\mathrm{BT_r}$ are transmitted, which will be discussed shortly. The channel access request is made using RTS packet. A transmitter is permitted to transmit an RTS packet only if it hears no $\mathrm{BT_t}$ and $\mathrm{BT_r}$ signals on the respective control channels. Whilst the transmitter transmits RTS packet, it also transmits a busy tone $\mathrm{BT_t}$ to ensure that no other transmitter begins to transmit an RTS packet. This enhances the reliable detection of RTS at the receiver. The receiver after receiving the RTS

packet sets up the BT_r to signal CTS, which signals the competing transmitters to withhold their RTS packets. The intended transmitter implicitly understands that the channel is reserved and begins the data transmission. After successful data transmission, the receiver stops broadcasting the BT_r and releases the channel.

It should be clear that the DBTMA avoids the problem observed with MACA and MACA-W protocol that a receiving node of a competing link that heard CTS (any node that lie within the CTS hearability range in Figure 2.12) would be barred from responding to its RTS packet. This is because there is no explicit CTS packet transmitted but CTS is implied by the BT_r transmitted on a dedicated channel. However, the shortcoming with MACA and MACA-W is addressed at a cost of separate channels dedicated for out-of-band signalling. Furthermore, as the protocol requires the transceivers to listen to the out-of-band busy tones whilst transmitting, complex radio frequency (RF) units are required due to additional filters and duplexers involved. This may pose difficulties for terminals designed for mobile applications that have space and energy constraints. Moreover, the DBTMA does not allow frequency selectivity to be exploited for multiuser diversity.

2.7.4.2 Wireless Channel Oriented *ad hoc* multihop protocol

The wireless channel oriented *ad hoc* multihop protocol (W-CHAMB) [104, 105] is also a busy signal based approach for solving the hidden node problem. Unlike the DBTMA protocol which uses out of band signalling, the W-CHAMB multiplexes the busy signals with the data signal along the time dimension. The air interface consists of TDMA frames, each of which is divided into three types of channels - access channel (ACH), traffic channel (TCH) and echo channel (ECH). The access channel is used for coordinating access among the terminals competing for channel access taking into account priority of the service class and fairness constraints. The TCH contains transmitted data and the ECH contains the busy signal. The transmitter that succeeds to obtain the right to transmit must determine the free TCH in the MAC frame to transmit. For determining the free TCH slots and solving the hidden node problem, the ECH slot comes into play. A MAC frame contains the same number of ECH slots and TCH slots with a one-to-one mapping between them. A transmitter must sense the channel to determine free TCH. A slot is considered free if it detects no carrier in the TCH slot as well as it detects no busy signal in its corresponding ECH slot. The transmitter sends a packet request on the slots where busy signal is not detected. The receiver checks the packet request and if the slots are

free at the receiver side, it sends a busy signal on the ECH. This ECH serves two purposes, first it avoids any transmitter within the vicinity of the receiver from transmitting, thus effectively solving the hidden node problem and second,it informs the transmitter that it can commence transmission.

It should be noted that although W-CHAMB protocol solves the hidden node problem, it does not solve the exposed node problem. This is primarily because the free slots at the transmitter are determined by carrier sense mechanism. Furthermore, it does not exploit the frequency selectivity in broadband wireless networks due to the TDMA air interface.

2.7.4.3 Busy burst signalling

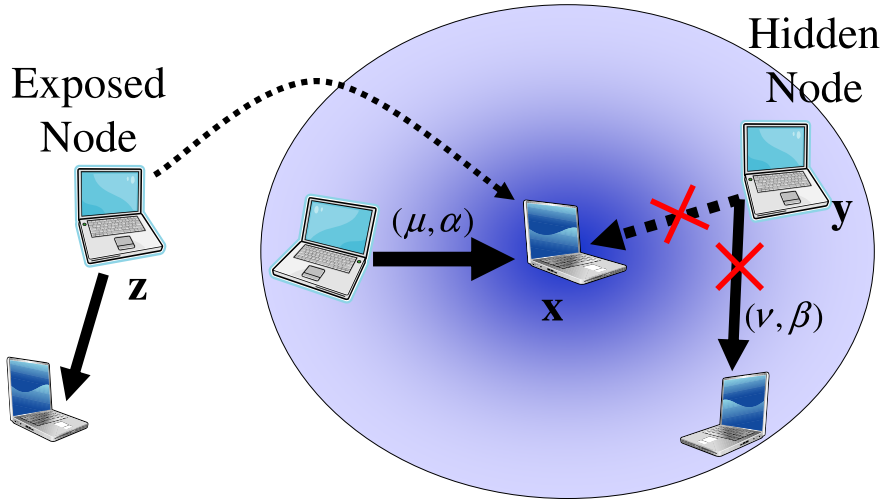

Figure 2.13: *Elimination of hidden and the exposed nodes using BB signalling. The oval indicates the exclusion region established around the active receiver. The intended link and interfering link are denoted are denoted by solid and dashed lines respectively. The transmitter* **y** *which is a hidden node to receiver* **x** *detects BB above a threshold and avoids transmission. The link is crossed to show that it was not activated. By contrast, the transmitter* **z** *may reuse the radio resource used by* **y** *as it receives BB below the threshold.*

The busy burst (BB) signalling mechanism [25–27, 71] utilises the channel reciprocity property of the TDD mode [106] to solve the hidden and the exposed node problem is a self organising network. The target is to limit the amount of CCI caused to the receiver of the active links to a threshold value I_{th}, which is fixed systemwide. This goal can be achieved if the transmitter is aware of the amount of CCI it potentially causes towards a pre-established active link before it actually transmits. This knowledge allows the transmitter to decide autonomously whether

or not it should allocate the considered radio resource so that the CCI at the victim receiver is capped at the threshold.

The channel reciprocity property of the TDD mode is utilised to convey the *a priori* knowledge of CCI. The transmit power utilised for transmitting data is T^{d} and the transmit power utilised for transmitting feedback information in the reverse direction (*i.e.* BB signal) is T^{b}. An intended link is denoted as a pair (μ, α) and an another link is denoted (ν, β) that reuses the same radio resource used by link (μ, α). For notational convenience, $\mathbf{x}$ represents a transmitter or a receiver of link (μ, α). Another link (ν, β), where $\mu \neq \nu$ and $\alpha \neq \beta$ is an interfering link, whose transmitter or receiver is designated $\mathbf{y}$. With this notation, the term $G_{\mathbf{x}}$ represents the channel gains of an intended link and is equivalent to $G_{\mu,\alpha}$. Likewise, the term $G_{\mathbf{y}}$ represents the intended channel gains of a competing link and is equivalent to $G_{\nu,\beta}$. The term $G_{\mathbf{xy}}$ represents channel gains of the interfering link between transmitter $\mathbf{x}$ and receiver $\mathbf{y}$. $G_{\mathbf{xy}}$ is equivalent to $G_{\mu,\beta}$ if the interference caused by the transmitter of link (μ, α) to the receiver of link (ν, β) is modelled. It is assumed that the receiver $\mathbf{x}$ has transmitted BB to reserve the radio resource for the next time slot. The received BB power at transmitter $\mathbf{y}$ is

$$I_{\mathbf{y}}^{\mathrm{b}} = T^{\mathrm{b}} G_{\mathbf{xy}}. \tag{2.30}$$

Likewise, the CCI caused to receiver $\mathbf{x}$ if $\mathbf{y}$ were to transmit is

$$I_{\mathbf{x}}^{\mathrm{d}} = T^{\mathrm{d}} G_{\mathbf{yx}}. \tag{2.31}$$

Combining (2.30) and (2.31) and exploiting channel reciprocity of the TDD mode, *i.e.* $G_{\mathbf{yx}} = G_{\mathbf{xy}}$, the amount of CCI caused towards the victim receiver $\mathbf{x}$ is given by

$$I_{\mathbf{x}}^{\mathrm{d}} = \left(\frac{T^{\mathrm{d}}}{T^{\mathrm{b}}}\right) I_{\mathbf{y}}^{\mathrm{b}}. \tag{2.32}$$

To limit $I_{\mathbf{x}}^{\mathrm{d}}$ to a threshold value, the potential transmitter $\mathbf{y}$ must check if

$$\left(\frac{T^{\mathrm{d}}}{T^{\mathrm{b}}}\right) I_{\mathbf{y}}^{\mathrm{d}} < I_{\mathrm{th}} \tag{2.33}$$

holds true. If (2.33) holds true, transmitter $\mathbf{y}$ allocates the considered radio resource for transmission. Otherwise, the transmitter refrains from using such radio resource.

To allow the transmitter to evaluate (2.33), the medium access control (MAC) frame is divided into 'data slot' and a 'BB minislot'. Each data slot is uniquely paired with the preceding BB slot, which the potential transmitter is obliged to scan to check if (2.33) holds. Likewise, after receiving data with the minimum SINR target required, the receiver must broadcast a BB to reserve the radio resource for the next time slot. This enables the transmitter to check whether or not the transmitter lies within the exclusion region of the receiver. It should be noted that with the BB mechanism, the potential transmitter infers the amount of CCI by measuring the received BB power. Therefore, this effectively avoids the problem faced with IEEE RTS/CTS mechanism (see Section 2.7.3) that the interference range of a potential interferer can be further away than the packet reception range for CTS packet. Consequently, the BB mechanism completely avoids the hidden and the exposed node problem.

The earlier work on BB signalling was performed for a TDMA-TDD air interface [25, 26]. By extending the concept to interference aware chunk allocation in wireless system where multiple users share a set of parallel frequency slots of a broadband frequency-selective radio channel, such as the 100MHz channel of the WINNER-TDD mode [28]. By extending the BB concept to OFDMA [27, 107], the channel reciprocity of TDD [106] is exploited for decentralised interference management such that the chunks can be dynamically assigned on a short-term basis. For this purpose, the exclusion region is established individually for each chunk. The chunks where the interfering channel gains are attenuated are spatially reused by the competing link whereas those chunks that have high interfering channel gains are avoided. Detailed description of this concept is deferred to later chapters in this thesis for different types of network, namely *ad hoc*, cellular networks with omnidirectional antennas and cellular networks that utilise transmit beamforming.

2.7.5 Other CCI mitigation approaches

Other techniques to mitigate the detrimental effect of CCI include interference cancellation, frequency hopping or spread spectrum techniques. For completeness, these techniques are briefly presented in the following paragraphs.

2.7.5.1 Interference cancellation

Interference cancellation involves predicting the transmitted signal in presence of other signals. The predicted signal is then subtracted from the residual signal . A decision feedback equaliser (DFE) is an example of interference cancellation technique used for cancelling the inter symbol interference (ISI) due to multipath in single carrier systems. Likewise, successive interference cancellation [108–110] and parallel interference cancellation [110, 111] are used for decoding signals transmitted across multiple streams in MIMO systems. A requirement for performing interference cancellation is that sufficient degrees of freedom for signal separation at the receiver must exist. Such degrees of freedom may be provided by multiple receiving antennas at the receiver that are spatially uncorrelated (ideally) or by using spreading codes.

2.7.5.2 Spread spectrum techniques

In spread spectrum technique, the transmitted data is spread over a larger frequency bandwidth than what would be necessary in a conventional FDMA system. Depending on the mechanism used to scramble the data, two main types of spread spectrum techniques widely used are as follows:

Frequency hopping Frequency hopping mitigates CCI by reducing the duration of strong CCI. In the system implementing frequency hopping, the transmitter selects a channel which is a small fraction of the available system bandwidth in each time slot [24]. In the next time slot, the transmission in carried out by selecting a different set of channels. By hopping from one frequency channel to another, the impact of CCI is averaged out over time. Bluetooth [112] is an example of a system that performs frequency hopping.

Direct sequence spread spectrum In direct sequence spread spectrum, the transmitter spreads the data by convolving it with spreading code that has a higher bandwidth than the data itself. The receiver retrieves the transmitted data by correlating it with the code used for transmission. The spreading may be done either using orthogonal codes (*e.g.* Walsh sequences [113] which may be generated using Hadamard matrix [114]) or using pseudo noise codes that have autocorrelation properties similar to the orthogonal code [40, 115]. By spreading the signal during transmission and despreading during reception, CCI caused by narrowband interferers can be effectively mitigated. Furthermore, by using different codes multiple users can be accom-

modated within the same frequency bandwidth, which is the basis of CDMA (code division multiple access) technique widely used in the current 3G based cellular telecommunications (*e.g.* universal mobile telecommunications system (UMTS)).

2.8 Summary

This chapter provided a brief overview of wireless networks commonly deployed for communications. The concept of multiple access to accommodate multiple users within a shared bandwidth as well as duplexing concept to provide bidirectional communication is discussed. In this context, it was motivated why OFDMA-TDD is suitable for the next generation wireless networks where the traffic is inherently bursty and the bandwidth is frequency selective. A brief discussion of interference management in cellular networks where resource allocation is coordinated by the BS is presented. In this context, three approaches widely used in cellular networks - *viz.* frequency planning, interference mitigation using beamforming and power allocation were discussed. It was motivated that such methods are either inflexible or require a large amount of signalling which makes it difficult to realise reconfigurable frequency reuse on short time scale. Likewise, for systems performing decentralised radio resource allocation, it was motivated how the solutions such as sensing the activity of another transmitter lead to the hidden and the exposed node problem and fail to avoid CCI. It was briefly discussed that the BB signalling mechanism solves the above shortcomings and allows a reconfigurable frequency reuse on a short time basis by utilising receiver feedback in forms of BB signal and exploiting channel reciprocity property of the TDD mode.

Chapter 3
Busy Burst Enabled Interference Avoidance in *ad hoc* Scenario

3.1 Introduction

The term *ad hoc* network refers intrinsically to the class of wireless networks that lack rigorous centralised infrastructure and control. *Ad hoc* networks were classically used for communication in scenarios where a network with centralised infrastructure would be difficult to realise, such as in a disaster rescue area, military applications or as sensor networks. Likewise, another example of *ad hoc* networks is two or more computers communicating with one another using wireless local area network (WLAN) in an *ad hoc* mode. As such networks lack centralised coordination and control; the communicating entities must coordinate amongst themselves as to how they access the available radio resources. Co-channel interference (CCI) resulting from the co-existence of two or more wireless links that share the same radio resource is the major bottleneck in improving the spectral efficiency, which has already been pointed out in Chapter 2.

In recent years, consumer devices that use the wireless interface for high data rate communications have been proliferating. An example is the Bluetooth interface that allows two or more devices to communicate with one another, such as the mobile phone with the headset or with another mobile phone. Likewise, recent initiatives include wireless home digital interface [39] that attempts to deliver high quality video from any source to any display device within a home using wireless interface. As the density of such devices within a spatial region increases, the system performance degrades because of CCI caused by one link to another. A characteristic feature of such links is that they are activated in an 'on demand' basis, which makes it difficult to realise any centralised control. To solve the problem of CCI, radio resource allocation in self-organising *ad hoc* networks in an indoor environment is addressed.

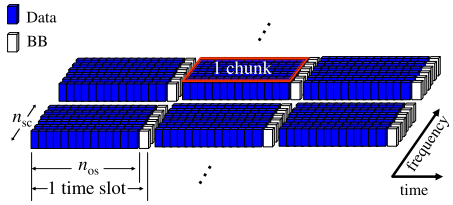

Figure 3.1: *Air interface in OFDMA–TDD*

3.2 Radio resource allocation in OFDMA–TDD *ad hoc* networks

An orthogonal frequency division multiple access (OFDMA)–TDD based air-interface is considered. A radio resource unit is a time-frequency slot referred to as a *chunk*, which comprises of n_{os} successive orthogonal frequency division multiplexing (OFDM) symbols and n_{sc} contiguous subcarriers as shown in Fig 3.1. A chunk is denoted as a pair (n, k), where $1 \leq n \leq N_{\mathrm{C}}$ denotes the frequency index and k represents the time slot index. N_{C} is the total number of chunks per time slot given by $N_{\mathrm{C}} = \lfloor \frac{B}{n_{\mathrm{sc}}\Delta_f} \rfloor$, where B is the signal bandwidth, Δ_f is the spacing between adjacent subcarriers and $\lfloor \cdot \rfloor$ is the floor-operator. Each time slot is divided into a 'data slot', which carries data from the transmitters to the receivers and a BB minislot, which is used to convey the BB signals (detailed out in Section 3.4). The duration of a time slot is, therefore, $n_{\mathrm{os}} + 1$ OFDM symbols, and it carries N_{C} chunks each paired with a busy burst of n_{sc} subcarriers spanning one OFDM symbol accommodated in a minislot.

3.3 System model

We consider an *ad hoc* network consisting of N_{L} end-to-end links. As discussed earlier in Section 2.7.4.3, a link is denoted as a pair (μ, α) where μ is the transmitter and α is the receiver as shown in Figure 3.2. The term $G_{\mu,\alpha}[n, k]$ is the channel gain between transmitter μ and receiver α of a frequency selective and time variant channel, modelled as discussed earlier in Section 2.3. For notational convenience, $\mathbf{x}$ represents a transmitter or a receiver of link (μ, α). Another link (ν, β), where $\mu \neq \nu$ and $\alpha \neq \beta$ is an interfering link, whose transmitter or receiver is designated $\mathbf{y}$. With this notation, the term $G_{\mathbf{x}}[n, k]$ represents the channel gains of an intended link and is equivalent to $G_{\mu,\alpha}[n, k]$. Likewise, the term $G_{\mathbf{y}}[n, k]$ represents the intended channel gains of a competing link and is equivalent to $G_{\nu,\beta}[n, k]$. The term $G_{\mathbf{xy}}[n, k]$ represents channel gains of the interfering link between transmitter $\mathbf{x}$ and receiver $\mathbf{y}$. $G_{\mathbf{xy}}[n, k]$ is equivalent to $G_{\mu,\beta}[n, k]$ if the interference caused by the transmitter of link (μ, α) to the

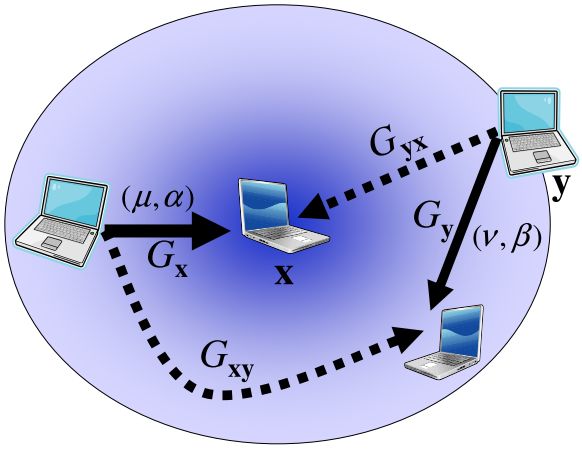

Figure 3.2: *2-link scenario in ad hoc networks. The intended links are shown as solid arrows whereas the interfering links are shown as dashed arrows. The oval represent the exclusion region that needs to be established around receiver* $\mathbf{x}$ *so as to meet the required signal to interference and noise ratio (SINR) target.*

receiver of link (ν, β) is modelled. All channel gain parameters are modelled using (2.18) with an appropriate substitution of relevant transmitter and receiver indices. The data transmit powers of the transmitters of $\mathbf{x}$ and $\mathbf{y}$ are denoted as $T^{\mathrm{d}}_{\mathbf{x}}[n,k]$ and $T^{\mathrm{d}}_{\mathbf{y}}[n,k]$ respectively. With the above notation, the intended signal power at receiver $\mathbf{x}$, $R^{\mathrm{d}}_{\mathbf{x}}$, is given by

$$R^{\mathrm{d}}_{\mathbf{x}} = T^{\mathrm{d}}_{\mathbf{x}}[n,k] G_{\mathbf{x}}[n,k]. \tag{3.1}$$

Likewise, the signal to interference and noise ratio (SINR) at the receiver of $\mathbf{x}$, $\gamma_{\mathbf{x}}[n,k]$, is expressed as

$$\gamma_{\mathbf{x}}[n,k] = \frac{T^{\mathrm{d}}_{\mathbf{x}}[n,k] G_{\mathbf{x}}[n,k]}{\underbrace{\sum_{\substack{\mathbf{y}\in\mathcal{T} \\ \mathbf{y}\neq\mathbf{x}}} T^{\mathrm{d}}_{\mathbf{y}}[n,k] G_{\mathbf{yx}}[n,k] + N}_{I^{\mathrm{d}}_{\mathbf{x}}[n,k]}}, \tag{3.2}$$

where $\mathcal{T}$ is the set of all active transmitters in the system and N is the thermal noise power.

3.4 Interference management using busy burst signalling

Interference management using busy burst (BB) signalling [25, 26] establishes an exclusion region around active receivers. An exclusion region defines an area around an active receiver, where no other transmitter is allowed to reuse the reserved radio resources. The exclusion regions are established individually for each chunk (n,k) [27]. It is assumed that the transmitter

$\mathbf{x}$ transmits data to its intended receiver using chunk (n, k). Provided that $\gamma_{\mathbf{x}}[n, k] \geq \Gamma_{\min}$, where $\Gamma_{\min}$ is the minimum SINR target required to continue reserving a chunk, the receiver broadcasts a BB in the associated BB minislot. The BB signal reserves the data slot of the n^{th} chunk for the next time slot $k+1$ for $\mathbf{x}$. Interference avoidance with BB-OFDMA can be described by the following protocol:

1. All potential transmitters must sense the BB associated to the data chunk (n, k) prior to transmission.
2. Transmitters are prohibited to access chunks where a BB is detected above a given threshold.

The co-channel interference (CCI) transmitter $\mathbf{y}$ causes to receiver $\mathbf{x}$ if it were to transmit is given by

$$I_{\mathbf{x}}^{\text{d}}[n, k] = T_{\mathbf{y}}^{\text{d}}[n, k] G_{\mathbf{yx}}[n, k]. \tag{3.3}$$

The BB power received at transmitter $\mathbf{y}$ originating from receiver $\mathbf{x}$ (*i.e.* BB transmitter) is

$$I_{\mathbf{y}}^{\text{b}}[n, k] = T_{\mathbf{x}}^{\text{b}}[n, k] G_{\mathbf{xy}}[n, k], \tag{3.4}$$

where $T_{\mathbf{x}}^{\text{b}}[n, k]$ is the The BB transmit power for receiver $\mathbf{x}$ (BB transmitter).

Exploiting the time division duplex (TDD) channel reciprocity,$G_{\mathbf{yx}}[n, k] = G_{\mathbf{xy}}[n, k]$, the transmitter $\mathbf{y}$ can ascertain $I_{\mathbf{x}}^{\text{d}}[n, k]$, the potential amount of interference it causes to a receiver $\mathbf{x}$ of a pre-established link, by measuring $I_{\mathbf{y}}^{\text{b}}[n, k]$ at the associated BB minislot [25], which is given by

$$I_{\mathbf{x}}^{\text{d}} n[n, k] = I_{\mathbf{y}}^{\text{b}}[n, k] \frac{T_{\mathbf{y}}^{\text{d}}[n, k]}{T_{\mathbf{x}}^{\text{b}}[n, k]}\,. \tag{3.5}$$

3.4.1 Fixed power BB

The maximum CCI $I_{\mathbf{x}}^{\text{d}} n[n, k]$ that a candidate transmitter $\mathbf{y}$ may cause to an active receiver $\mathbf{x}$ is given by the interference threshold I_{th}, which is constant and known to the entire network. Provided that both $T_{\mathbf{x}}^{\text{b}}[n, k]$ and $T_{\mathbf{y}}^{\text{d}}[n, k]$ are known to the candidate transmitter $\mathbf{y}$, (3.5) enables

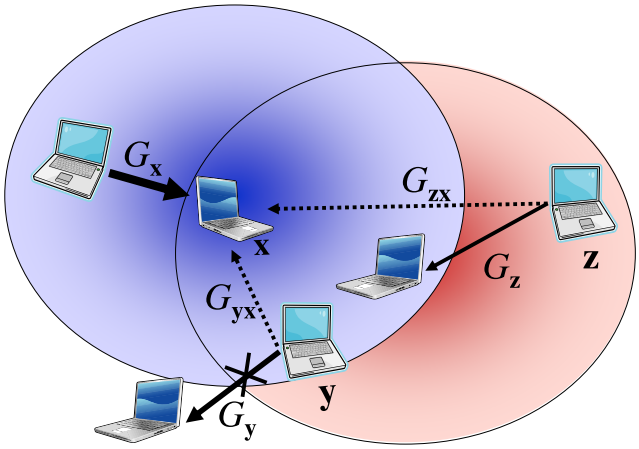

Figure 3.3: *Busy burst signalling using fixed BB power. The solid arrows represent the intended signals and the dotted arrows represent the CCI. Exclusion regions (represented as ovals around the active receivers) are established with the help of BB signalling.*

$\mathbf{y}$ to verify whether $I^{\mathrm{d}}_{\mathbf{x}}[n,k] < I_{\mathrm{th}}$, in which case $\mathbf{y}$ is outside the exclusion range of $\mathbf{x}$ [25, 26]:

$$I^{\mathrm{b}}_{\mathbf{y}}[n,k]\left(\frac{T^{\mathrm{d}}_{\mathbf{y}}[n,k]}{T^{\mathrm{b}}_{\mathbf{x}}[n,k]}\right) \leq I_{\mathrm{th}}\,. \tag{3.6}$$

In case $T^{\mathrm{d}}_{\mathbf{y}}[n,k]{=}T^{\mathrm{b}}_{\mathbf{x}}[n,k]$, condition (3.6) reduces to:

$$I^{\mathrm{b}}_{\mathbf{y}}[n,k] \leq I_{\mathrm{th}}\,. \tag{3.7}$$

An illustration of establishing exclusion region with fixed power BB is depicted in Figure 3.3. The receiver $\mathbf{x}$ has transmitted a BB signal to establish the exclusion region. The oval around the receiver $\mathbf{x}$ depicts the exclusion region established around the receiver $\mathbf{x}$. The trasmitter $\mathbf{y}$ lies within the exclusion region of $\mathbf{x}$ and therefore cannot reuse the chunks reserved by receiver $\mathbf{x}$. By contrast, the transmitter $\mathbf{z}$ lies outside the exclusion region of $\mathbf{x}$ and is allowed to reuse the resources reserved by $\mathbf{x}$.

By tuning I_{th}, the maximum CCI $I^{\mathrm{d}}_{\mathbf{x}}[n,k]$ in (3.2) is adjusted. A low I_{th} enables those links who have relatively low intended channel gains (hence lower $R^{\mathrm{d}}_{\mathbf{x}}[n,k]$) to meet their SINR target. However, this enforces a larger exclusion region around a vulnerable receiver through (3.7) because of which the reuse of the chunk decreases, leading to a decreased system throughput. By contrast, a high I_{th} increases the number of links that may reuse the given chunk, potentially

leading to enhanced system throughput. However, users with low intended channel gains are less likely to meet their SINR target, as interference protection is gradually eliminated. By tuning I_{th}, system throughput can be traded off for enhancing the link throughput for users with low intended channel gains.

3.4.2 Interference tolerance signalling via busy bursts

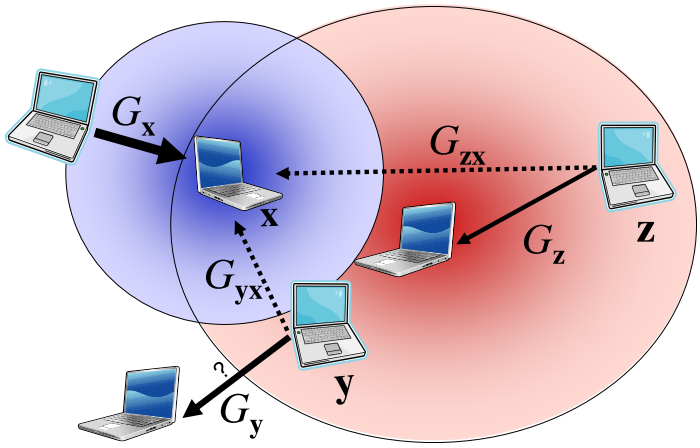

Figure 3.4: *Busy burst with interference tolerance signalling (BB-ITS) in ad hoc scenario. The solid arrows represent the intended signals and the dotted arrows represent the CCI. The ovals represent the exclusion region formed with BB-ITS.*

With fixed power BB signalling, the same level of interference protection is given to all links, disregarding the quality of the intended link. For illustration, two receivers $\mathbf{x}$ and $\mathbf{z}$ with respective channel gains $G_{\mathbf{x}}{>}G_{\mathbf{z}}$ are exposed to the same interferer $\mathbf{y}$ as illustrated in Figure 3.4. Provided that $\mathbf{y}$ causes the same amount of interference to $\mathbf{x}$ and $\mathbf{z}$, the SINR target Γ_m, corresponding to the chosen modulation format m is considered fixed systemwide, is more likely met for $\mathbf{x}$ than for $\mathbf{z}$. In such situation, $\mathbf{y}$ may reuse the chunk used by $\mathbf{x}$ but it must not reuse the chunk used by $\mathbf{z}$. To ensure that the SINR target is met and the chunk is reused whenever feasible, $\mathbf{x}$ and $\mathbf{z}$ to are allowed to transmit a BB with variable power signalling the individual amount of interference that each of the receiver $\mathbf{x}$ and $\mathbf{z}$ can tolerate to the candidate transmitter such as $\mathbf{y}$. For this, exclusion regions of different sizes are effectively formed around $\mathbf{x}$ and $\mathbf{z}$, as illustrated in Figure 3.4.

For busy burst with interference tolerance signalling (BB-ITS) [116] the objective is that a given SINR target, $\gamma_{\mathbf{x}}[n,k]{\geq}\Gamma_m$, is maintained for an active receiver $\mathbf{x}$. This means that the maximum allowable interference depends on the intended link quality $R^{\mathrm{d}}_{\mathbf{x}}[n,k]$. Let $I^{\mathrm{tol}}_{\mathbf{x}}[n,k]$

denote the interference limit, for which the SINR (3.2) approaches $\gamma_{\mathbf{x}}[n,k]{=}\Gamma_m$. Then the tolerable interference at receiver $\mathbf{x}$ is upper bounded by

$$I_{\mathbf{x}}^{\mathrm{d}}[n,k] \leq I_{\mathbf{x}}^{\mathrm{tol}}[n,k] = \frac{R_{\mathbf{x}}^{\mathrm{d}}[n,k]}{\Gamma_m} - N\,. \tag{3.8}$$

Adjusting the tolerable interference level (3.8) implies that larger exclusion regions are formed for links with weak desired signal levels $R_{\mathbf{x}}^{\mathrm{d}}[n,k]$ and vice versa.

To signal the variable interference tolerance level $I_{\mathbf{x}}^{\mathrm{tol}}[n,k]$ of a victim receiver $\mathbf{x}$ to candidate transmitters $\mathbf{y}$ intending to reuse the reserved chunk, the BB transmit power $T_{\mathbf{x}}^{\mathrm{b}}[n,k]$ is adjusted, such that the simple threshold test $I_{\mathbf{y}}^{\mathrm{b}}[n,k]{\leq}I_{\mathrm{th}}$ in (3.7) is retained. Hence no additional information for channel sensing is required for BB-ITS. The received BB power approaches a fixed threshold, $I_{\mathbf{y}}^{\mathrm{b}}[n,k]{=}I_{\mathrm{th}}$, if the CCI approaches $I_{\mathbf{x}}^{\mathrm{d}}[n,k]{=}I_{\mathbf{x}}^{\mathrm{tol}}[n,k]$. Inserting $I_{\mathbf{x}}^{\mathrm{d}}[n,k]{=}I_{\mathbf{x}}^{\mathrm{tol}}[n,k]$ and $I_{\mathbf{y}}^{\mathrm{b}}[n,k]{=}I_{\mathrm{th}}$ into (3.5) yields the variable BB power $T_{\mathbf{x}}^{\mathrm{b}}[n,k] = T_{\mathbf{y}}^{\mathrm{d}}[n,k]I_{\mathrm{th}}/I_{\mathbf{x}}^{\mathrm{tol}}[n,k]$. Assuming that $T_{\mathbf{y}}^{\mathrm{d}}[n,k]$ is fixed and denoted by T^{d}, the BB transmit power is adjusted as follows [116]

$$T_{\mathbf{x}}^{\mathrm{b}}[n,k] = \min\left(\frac{I_{\mathrm{th}}T^{\mathrm{d}}}{\frac{R_{\mathbf{x}}^{\mathrm{d}}[n,k]}{\Gamma_m} - N}, T_{\max}^{\mathrm{b}}\right) \tag{3.9}$$

where $T_{\max}^{\mathrm{b}}$ is the maximum BB transmit power. The $\min$ operator ensures that $T_{\mathbf{x}}^{\mathrm{b}}[n,k]{\leq}T_{\max}^{\mathrm{b}}$. Note that when $R_{\mathbf{x}}^{\mathrm{d}}[n,k]/\Gamma_m < N$, we get $\gamma_{\mathbf{x}}[n,k]{<}\Gamma_m$. In this situation, the chunk is released and no BB is transmitted. Therefore, it is ensured that $T_{\mathbf{x}}^{\mathrm{b}}[n,k]$ in (3.9) always has a positive value. We note that $I_{\mathbf{y}}^{\mathrm{b}}[n,k] = T_{\mathbf{x}}^{\mathrm{b}}[n,k]G_{\mathbf{xy}}[n,k]$ and $T_{\max}^{\mathrm{b}} = T_{\mathbf{y}}^{\mathrm{d}}[n,k]$. It can be checked by plugging (3.9) into (3.6) that the threshold test (3.6) effectively checks if $I_{\mathbf{x}}^{\mathrm{d}}[n,k] \leq I_{\mathbf{x}}^{\mathrm{tol}}[n,k]$, regardless of the threshold used, as long as the BB transmit power is not clipped. In this chapter, we choose $I_{\mathrm{th}} = -100$ dBm because the probability of BB transmit power being clipped was found to be lower than 0.05 for the given deployment scenario with $\Gamma_m = 2.2\,\mathrm{dB}$ and $m = 1$ used. Furthermore, with this threshold, the received BB at the intended transmitter (the lower bound of which is approximated by $I_{\mathrm{th}}\Gamma_m$) remains well above the noise floor ($-117.8\,\mathrm{dBm}$), such that it can be reliably detected.

3.4.3 Extension to multiple competing links

In a multi-cell scenario, signals from multiple links superimpose at the receiver. The total interference at data receiver $\mathbf{x}$ amounts to

$$I_{\mathbf{x}}^{\mathrm{d}}[n,k] = \sum_{\substack{\mathbf{z}\in\mathcal{T} \\ \mathbf{z}\neq\mathbf{x}}} T_{\mathbf{z}}^{\mathrm{d}}[n,k] G_{\mathbf{zx}}[n,k]\,, \tag{3.10}$$

where $\mathcal{T}$ is the set of simultaneously active transmitters. Likewise the received BB at the data transmitter (BB receiver) $\mathbf{y}$ yields

$$I_{\mathbf{y}}^{\mathrm{b}}[n,k] = \sum_{\substack{\mathbf{z}\in\mathcal{R} \\ \mathbf{z}\neq\mathbf{y}}} T_{\mathbf{z}}^{\mathrm{b}}[n,k] G_{\mathbf{zy}}[n,k]\,, \tag{3.11}$$

where $\mathcal{R}$ is the set active receivers (BB transmitters).

Unlike the case when two links compete for resources, $I_{\mathbf{y}}^{\mathrm{b}}[n,k]$ is no longer equivalent to $I_{\mathbf{x}}^{\mathrm{d}}[n,k]$ in the threshold test (3.7). This is because in (3.10) the interference powers from multiple transmitters $\mathcal{T}$ add up. Consequently, the total CCI at data receiver $\mathbf{x}$ may exceed the tolerable threshold such that $I_{\mathbf{x}}^{\mathrm{d}}[n,k] > I_{\mathrm{th}}$, although the BB power (3.11) observed by the individual interferers $\mathbf{y}\in\mathcal{T}$ is below the threshold, $I_{\mathbf{y}}^{\mathrm{b}}[n,k] \leq I_{\mathrm{th}}$. On the other hand, in (3.11) the interfering BB powers from multiple simultaneously active receivers observed at $\mathbf{x}\in\mathcal{R}$ add up. It is therefore possible that $I_{\mathbf{y}}^{\mathrm{b}}[n,k] > I_{\mathrm{th}}$, so that link $\mathbf{y}$ is prohibited from accessing chunk (n,k), although its individual CCI contribution, $T_{\mathbf{y}}^{\mathrm{d}}[n,k] G_{\mathbf{yx}}[n,k]$, would be below I_{th}. Note that the former effect partly compensates the latter. Moreover, in many cases the interference is dominated by one strong interfering source. Therefore, the threshold test (3.7) provides a good approximation to the level of interference potentially caused to the active receivers. In the rest of this section, the procedure for dynamic chunk allocation using BB signalling is detailed out.

3.4.4 Initial access in contention

CCI higher than a threshold value is avoided at the receivers on the reserved chunks via BB signalling mechanism discussed above. However, in the case of unreserved chunks, two or more transmitters may simultaneously transmit using such chunks provided (3.7) holds when such transmitters scan the BB minislot. This results in contention where the transmitters are not aware of the amount of interference they cause to the receiver of other links. Conse-

quently, several links may encounter a collision on chunk (n, k) where the SINR target may not be met. Hence, to reduce the occurrence of simultaneously accessed chunks in contention, a $p-$persistent chunk allocation procedure is applied to BB-OFDMA, where chunk (n, k) is accessed by transmitter $\mathbf{y}$ with probability p. Denoting the outcome of the $p-$persistent chunk allocation with the binary random variable $\chi_{\mathbf{y}}[n, k] \in \{0, 1\}$, the access probability is $\Pr(\chi_{\mathbf{y}}[n, k]{=}1) = p$. In this chapter, p is set to $1/N_{\mathrm{L}}$ such that on average the transmitter of only one link accesses a chunk in contention at any given time slot.

3.4.5 Dynamic chunk allocation with BB signalling

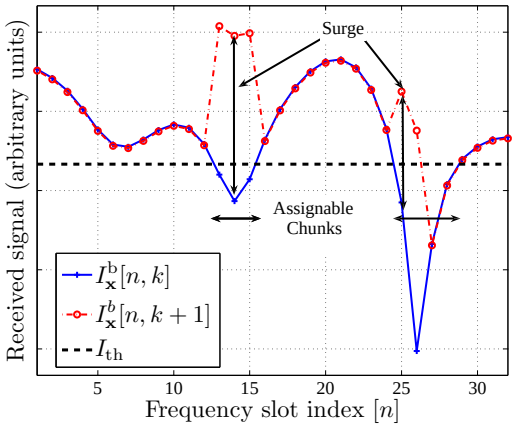

Figure 3.5: *Illustration of DCA using BB signalling. The receiver that intends to transmit using unreserved chunks is obliged to check if the received BB power is below the threshold.*

The dynamic chunk allocation (DCA) mechanism with BB signalling is explained with the help of Figure 3.3 and Figure 3.5. It is assumed that the receiver $\mathbf{x}$ in Figure 3.3 has transmitted BB on chunks it has reserved. Prior to transmission, the transmitter $\mathbf{y}$ must sense the BB minislot to ascertain the chunks it reuses are outside the exclusion region of existing transmitter(s). Provided (3.7) holds true, the transmitter $\mathbf{y}$ transmits data during the data slot. In the particular example depicted in Figure 3.5, the BB received on chunks 13–15 and 25–28 are below the threshold value and can be used for transmission. The set of chunks where the transmission is carried out belong to the set $\mathcal{A}$. The binary variable $a_{\nu}[n, k]$ [27] denotes whether or not

transmitter $\mathbf{y}$ used the chunk (n, k) for transmission[1]

$$a_\nu[n,k] = \begin{cases} 1\,, & \left(I^{\mathrm{b}}_{\mathbf{y}}[n,k] \leq I_{\mathrm{th}} \text{ and } \chi_{\mathbf{y}}[n,k] = 1\right) \text{ or } \Upsilon_\nu[n,k] = 1 \\ 0\,, & \text{otherwise}\,, \end{cases} \tag{3.12}$$

After chunk allocation, the transmitter of user ν uses the allocated chunk for transmission and the SINR achieved at the receiver ($\gamma_{\mathbf{y}}[n,k]$) is calculated. The chunks where $\gamma_{\mathbf{y}}[n,k] \geq \Gamma_m$ holds, where Γ_m is the minimum SINR target required to meet the QoS requirements for the modulation level m used for transmission, denote successfully accessed chunks and are denoted as

$$b_\nu[n,k] = \begin{cases} 1\,, & \gamma_{\mathbf{y}}[n,k] \geq \Gamma_m \text{ and } a_\nu[n,k] = 1 \\ 0\,, & \text{otherwise}\,. \end{cases} \tag{3.13}$$

With reservation based protocols such as the BB signalling mechanism, the chunks where $\gamma_\nu[n,k] \geq \Gamma_{\min}$, where $\Gamma_{\min}$ is the minimum SINR target corresponding to lowest order modulation scheme available in the system, are reserved for the next frame by setting the reservation indicator $\Upsilon_\nu[n,k+1]$ as follows

$$\Upsilon_\nu[n,k+1] = \begin{cases} 1\,, & \gamma_{\mathbf{y}}[n,k] \geq \Gamma_{\min} \text{ and } a_\nu[n,k] = 1 \\ 0\,, & \text{otherwise}\,. \end{cases} \tag{3.14}$$

By setting $\Upsilon_\nu[n,k+1] = 1$, the chunk $(n, k+1)$ is reserved for user ν in the next slot and the receiver transmits a BB during the time-multiplexed BB slot. The acknowledgement of successful transmission is implicitly conveyed to the transmitter via a surge in the received BB power levels [26]. In Figure 3.5, the surge in received power levels is detected in chunks with index 13–15 and 25–26, which signals to transmitter $\mathbf{y}$ that the transmission has been successful. By contrast, no surge in power level is detected in chunk with index 27 and 28 which signals the transmitter that the minimum SINR target in these chunks is not met. The chunks where the BB signal is not received from the intended receiver during the BB slot are released and may be allocated by other users in the system. It must be highlighted that if a fixed modulation scheme is used systemwide, $\Upsilon_\nu[n,k+1]$ and $b_{\mathbf{y}}[n,k]$ are identical. However, in

[1]For the purpose of DCA, the notation a_ν and b_ν is preferred over $a_{\mathbf{x}}$ and $b_{\mathbf{x}}$ notation, so as to have a consistent notation and avoid ambiguity in later chapters where a single transmitter (*e.g.* BS) serves multiple users.

the system where link adaptation is performed on a per-chunk basis, the bits may be received in error, *i.e.* $b_{\mathbf{y}}[n,k]=0$ but the minimum SINR target required to continue reserving may still be met, *i.e.* $\gamma_{\mathbf{y}} \geq \Gamma_{\min}$. In such case, $\Upsilon_{\nu}[n,k+1]=1$ and the chunk is retained for the same link but in the next slot, the transmitter is expected to lower the modulation order utilised as shall be discussed in Section 3.4.6.

3.4.6 Link adaptation

Let $\mathcal{M}=\{1,\ldots,M\}$ be the set of supported modulation schemes. Associated to each modulation scheme $m \in M$ is an SINR target $\Gamma=\Gamma_m$ that must be achieved to satisfy a given BER (bit error ratio). The objective is to select the modulation scheme $m_{\nu}[n,k]\in\mathcal{M}$ for chunk (n,k), which yields the highest spectral efficiency, for which $\gamma_{\nu}[n,k]\geq\Gamma_{m_{\nu}[n,k]}$ holds. Assuming that the channel does not change significantly between two consecutive time slots, the feedback of SINR observed in the preceding slot is used to select an appropriate modulation format for the next time slot. The steps of performing link adaptation are detailed as follows:

1. Determine the chunks (n,k) where (3.7) holds true.
2. Transmit using $m=1$, the modulation with lowest spectral efficiency.
3. Calculate the achieved SINR $\gamma_{\nu}[n,k]$ using (3.2).
4. Using lookup table, determine the modulation scheme $\hat{m}$ with highest spectral efficiency such that $\gamma_{\mathbf{x}}[n,k]\geq\Gamma_{\hat{m}}$ holds.
5. Adjust the modulation scheme as follows:

$$m_{\nu}[n,k+1]=\begin{cases}\bar{m}\ , & \gamma_{\nu}[n,k]\geq\Gamma_{m_{\nu}[n,k+1]}\\ 0\ , & \gamma_{\nu}<\Gamma_1\\ \hat{m}_{\nu}[n,k]\ , & \text{otherwise,}\end{cases} \tag{3.15}$$

   where $\bar{m}=\lceil(m_{\nu}[n,k]+\hat{m}[n,k])/2\rceil$, $\lceil\cdot\rceil$ is the ceiling operator and Γ_1 is the minimum SINR target corresponding to $m=1$.
6. If $m_{\nu}[n,k+1]$ = 0, or the chunk is no longer needed, release the chunk, else go to step 3.

The step 5 in the above algorithm allows the transmitter to choose the feasible modulation format in a fewer steps compared to using an incremental step of 1. After each time slot, the chosen modulation step is over a half way between currently utilised modulation scheme and the highest modulation step that could have been utilised under prevalent channel conditions at the receiver. This procedure is similar to the well known divide and conquer approach or the binary search algorithm which has an algorithmic complexity of $O(\log_2(n))$, unlike an incremental step of 1, which has an algorithmic complexity of $O(n)$. For example, assume that the highest modulation feasible for a link is 256-QAM, *i.e.* $m = 8$. If a unit step increment is used, the transmitter selects the feasible modulation format after 8 steps whereas with the proposed algorithm above, the transmitter selects 256-QAM modulation format within 4 steps.

3.5 Simulation setup

An *ad hoc* network deployed in an indoor office environment as defined in scenario A1 [28, 117] of wireless world initiative new radio (WINNER) is considered. The indoor office environment is modelled as a single floor in a building and consists of 40 rooms of size $10\mathrm{m} \times 10\mathrm{m} \times 3\mathrm{m}$ and two corridors of size $100\mathrm{m} \times 5\mathrm{m} \times 3\mathrm{m}$. The relevant parameters considered in simulation are presented in Table 3.1. The deployment scenario and the distribution of users are as shown in Figure 3.6.

Parameters	**Value**
MS transmit power	21 dBm
Center carrier frequency f_{c}	5.0 GHz
System bandwidth B	89.84 MHz
# subcarriers (SC)	1840
Subcarriers spacing Δf	48.8 kHz
OFDM symbols/time slot n_{os}	15
OFDM symbol duration T_{sym}	22.48 μs
# chunks/time slot N_{C}	230
Chunk size $n_{\mathrm{sc}} \times n_{\mathrm{os}}$	8 (freq.) $\times$ 15 (time) = 120
Protocol data unit (PDU) size	112 bits
Tx power/chunk T^{d}	-3.08 dBm
Antenna gain	0 dBi
Noise level/chunk N	-117.8 dBm
# Monte Carlo runs	500
Duration of each Monte Carlo run	75 ms

Table 3.1: *List of simulation parameters*

Modulation, # link PDUs per slot		Achieved SINR γ [dB]
no transmission	m=0	$-\infty < \gamma < 2.2$
BPSK	m=1	$2.2 \leq \gamma < 5.2$
QPSK	m=2	$5.2 \leq \gamma < 9.1$
cross 8-QAM	m=3	$9.1 \leq \gamma < 11.3$
16-QAM	m=4	$11.3 \leq \gamma < 14.4$
cross 32-QAM	m=5	$14.4 \leq \gamma < 16.6$
64-QAM	m=6	$16.6 \leq \gamma < 19.5$
cross 128-QAM	m=7	$19.5 \leq \gamma < 22.5$
256-QAM	m=8	$22.5 \leq \gamma < \infty$

Table 3.2: *Look up table for modulation scheme*

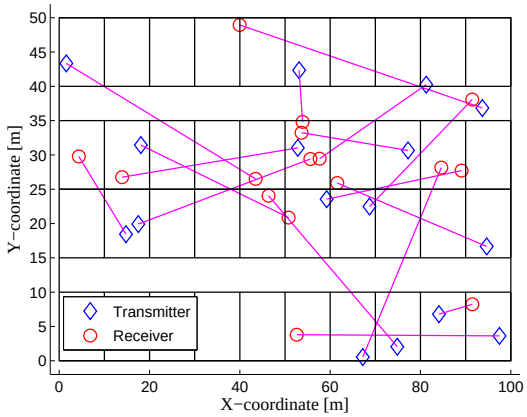

Figure 3.6: *Indoor scenario with its corresponding distribution of users. Each transmitter selects its receiver randomly from the initial distribution.*

A $3/4$-rate convolutional code and the SINR targets Γ_m for a given modulation scheme m are selected to attain a packet error ratio of 10^{-2} per PDU, given in Table 3.2 [118]. For non-adaptive modulation we consider a BPSK constellation with m=1 and a corresponding SINR target of Γ_1=2.2 dB. For link adaptation the modulation schemes $m \in \mathcal{M}$ are chosen based on the achieved SINR targets Γ_m.

The system is simulated as follows: $2N_{\mathrm{L}}$ mobile stations (MSs) are distributed uniformly in the space with a probability of 0.9 of lying inside the room and 0.1 of being in the corridor. Half of these MSs act as transmitters and the other half as receivers. Each transmitter selects a receiver randomly if the receiver is not already paired with another transmitter and the gain between them exceeds a minimum threshold value $G_{\min}$. In this chapter, $G_{\min}$ is set at 5 dB above the thermal noise level N because this avoids forming the links that would not meet the minimum

SINR target in a noise limited scenario. The channels are modelled according to the scenario A1 of WINNER [117], which models signal propagation in an indoor office environment. A line of sight (LoS) condition is considered when both the transmitter and receiver are located either in the same room or the same corridor. Otherwise, a non line of sight (NLoS) condition is considered. Both large scale and small scale fading are considered, as discussed earlier in Section 2.3. The path loss $(P^{\mathrm{ls}}_{\mu,\alpha})$ between a transmitter and receiver pair is given by using parameters from Table 3.3 in (2.13).

Scenario	A_{pl}	B_{pl}	C_{pl}	X_{pl}	σ
LoS	18.7	46.8	20	0	3.1
NLoS	36.8	38.8	20	$5\#\mathrm{walls}$	3.5

Table 3.3: *Parameters for modelling path loss in ad hoc scenario*

The fast fading parameters are modelled by considering a relative velocity of 5 km/h between the transmitter and the receiver, a central carrier frequency of 5.0 GHz With these parameters, the maximum Doppler spread f_{m} is found to be 23.15 Hz and the coherence time is 18.28 ms assuming a correlation of 0.9 using equations presented earlier in Section 2.3. Likewise, the coherence bandwidth is calculated to be approximately 1.55 MHz for LoS condition and 827.7 kHz for non-LoS conditions. In modelling the mobile fading channel, both time variance and frequency selectivity of the channel are taken into account as discussed earlier in Section 2.3. The performance statistics are collected using Monte Carlo method. At each Monte Carlo run, the MSs are distributed independently and uniformly as discussed earlier. A full buffer traffic is assumed, which means each user has enough data to occupy the entire bandwidth at each time slot. By this approach, the performance of scheduling and interference avoidance algorithms in a fully loaded network can be investigated. Each Monte Carlo run is of 100 ms duration, however statistics are collected only over the last 75 ms of the Monte Carlo run so as to avoid the transient effects at the start of the simulation. All assumption made in this paragraph apply to the results presented in the entire thesis.

3.6 Benchmark system

The benchmark system considered for performance evaluation is the state-of-the-art carrier sense multiple access with collision avoidance (CSMA/CA) mechanism. In the benchmark system, the transmitter senses the channel for any ongoing transmissions for the duration of a frame. If it detects no other transmissions, the transmitter allocates the chunk it sensed free

for transmission. To maintain a fair comparison with the BB protocol, a chunk is reserved and subsequently retained by the transmitter for transmission in the next frame provided that the minimum SINR target is met during the current transmission. Otherwise, the chunk is released. The exponential backoff part of CSMA/CA is not implemented in the system. However, the information about the achieved SINR at the receiver must be conveyed back to the transmitter via explicit signalling in this case, which would require additional bandwidth.

3.7 Results

In this section, the performance of the CCI mitigation approach with BB-signalling is compared against the CSMA/CA mechanism considered as the benchmark, as well as random chunk allocation algorithms. The performance metrics considered are as follows

1. Link throughput, defined as the number of bits successfully received. The transmitted bits are considered to be successfully received if the minimum SINR corresponding to the modulation format and coding considered (see Table 3.2) is met at the receiver. Mathematically, this is expressed as

$$T_\nu = \frac{n_{\mathrm{sc}}(n_{\mathrm{os}}-1)\left(\sum_{n=1}^{N_{\mathrm{C}}}\sum_{k=1}^{N_{\mathrm{k}}} m_\nu[n,k]b_\nu[n,k]\right)}{T_{\mathrm{s}}} \quad [\mathrm{Mbps}]\,, \tag{3.16}$$

   where N_{k} is the total number of frames transmitted during each Monte Carlo run duration T_{s}.

2. System throughput, defined as the sum of throughput of all users in the system, expressed as

$$T_{\mathrm{sys}} = \sum_{\nu\in\mathcal{U}} T_\nu \quad [\mathrm{Mbps}]\,, \tag{3.17}$$

   where $\mathcal{U}$ is the set of users in the system.

3. Energy consumption, defined as the energy required per bit for successful transmission. This is defined as

$$E_{\mathrm{eff}} = \frac{T^{\mathrm{d}}\left(\sum_{\nu\in\mathcal{U}}\sum_{n=1}^{N_{\mathrm{C}}}\sum_{k=1}^{N_{\mathrm{k}}} a_\nu[n,k]\right)}{T_{\mathrm{sys}}} \quad [\mathrm{J/bit}] \tag{3.18}$$

where T^{d} is expressed in milliwatts (mW), and T_{sys} is expressed in Mbps/cell and $a_{\nu}[n,k]$ is an integer that takes value 0 or 1, according to (3.12).

In the following sections, the number of links (N_{L}) in the network is arbitrarily set to 16. This translates to a link density of $1/300\,\mathrm{m}^2$ and would represent a moderately populated system. The performance of the considered *ad hoc* network with random chunk allocation scheme is considered first. The impact of detection threshold on CSMA/CA mechanism is considered next. The impact of BB specific threshold parameter on the system performance is considered next both for the system using binary phase shift keying (BPSK) modulation systemwide as well as the system performing adaptive modulation on a per chunk basis and the performance is compared against the CSMA/CA mechanism. Furthermore, the impact of varying the link density in the system is studied. Finally, the impact of threshold parameter on energy consumption per bit is addressed.

It should be noted that the main aim with dynamic chunk allocation algorithm is to improve spectral utilisation (measured by system throughput), reduce outage (number of users having 0 bps throughput) and increase guaranteed throughput. In this context, it is often necessary to determine metrics such as the average spectral utilisation, the average user throughput, the peak user throughput, the peak spectral utilisation and user throughput guaranteed at a certain percentile. These metrics can be easily obtained from the cumulative distribution function (cdf) plots. Therefore, cdfs are primarily used for performance evaluation. Other criteria such as satisfied user criteria, throughput as a function of distance and so on are also considered where necessary. In this context, a widely accepted measure of fairness in resource allocation is Jain's fairness index [119] which provides a quantitative measure of fairness. However, without additional information the fairness index cannot provide information on how efficiently the spectrum is utilised. As an example, when the performance is compared using Jain's fairness index, a system in which two users achieve 1 Mbps and 2 Mbps respectively attains a poorer fairness index compared to a system where both users achieve 0.5 Mbps, although each individual user experiences a better throughput in the former system than the latter. Moreover, the variation of distribution from the mean can be inferred qualitatively from the cdf plots. As an example, a fair distribution of resources can be inferred from the steepness of the graph, where a steep graph would correspond to a system where resources are fairly distributed and vice versa. For these reasons and due to space constraints, fairness indices is not considered further this thesis. Interested readers are referred to the accompanying paper [71] where fairness is analysed for

BB algorithm in Manhattan scenario using Jain's index.

3.7.1 Performance of random access techniques

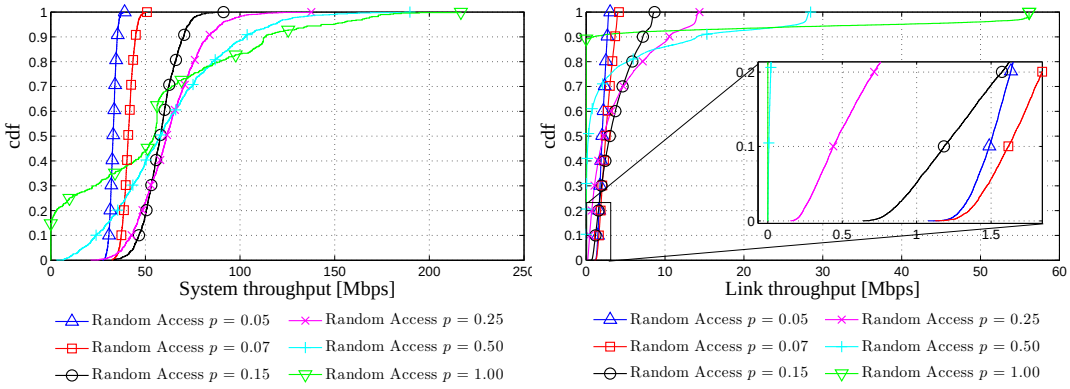

(a) System throughput (b) Link throughput

Figure 3.7: *Performance of random chunk allocation in ad hoc network.*

In a decentralized and self organizing network, the simplest chunk allocation technique is a technique that assigns a chunk with probability p to a link, provided that the transmitter has some data to transmit. With this technique, each link is allocated pN_{C} chunks on average. In a network where all of the transmitters are located within the exclusion region of the receivers of other links, this translates to a $p-$persistent slotted ALOHA.

Figure 3.7 depicts the impact of probability of accessing a chunk on system performance. The results demonstrate a trade-off between system throughput and lower 10^{th} percentile of link throughput. By increasing p, the number of chunks reused by a given link increases. On the one hand, the throughput potentially increases due to increase in bandwidth allocated to each link, whereas on the other hand, the CCI increases leading to decrease in the throughput. The users with a better channel gain are able to tolerate higher CCI whilst meeting the required signal to interference and noise ratio (SINR) target compared to those with lower channel gains. Therefore by increasing p, the users with better channel gains achieve a higher throughput at the cost of increase in outage (throughput of 0 bps) in the system. In particular, it can be noted that using $p = 1.0$, the outage is approximately 90%, whilst the maximum link throughput is approximately 56.2 Mbps. By reducing the access probability, the throughput of the users with lower channel gains is increased at the cost of throughput of users with higher channel gains. In particular, using $p = 0.07$, it is observed that a link throughput of 1.6 Mbps at the

lower 10^{th} percentile is achieved, while the peak link throughput reduces to 4 Mbps. For N_{L} links considered, using $p = 1/N_{\text{L}}$ ensures that the throughput is maximised in a worst case scenario where all transmitters are within the exclusion region of other receivers. For this reason, $p = 1/N_{\text{L}}$ is considered as an access probability for accessing unreserved chunks in this chapter. For 16 links considered in the system, $p = 1/16 = 0.0625$, therefore the access probability is rounded off to 0.07.

3.7.2 Performance of CSMA/CA

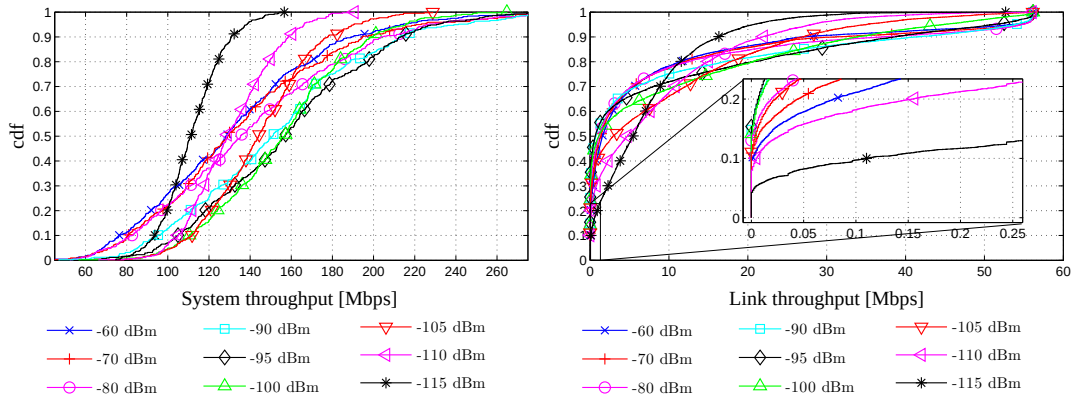

(a) System throughput (BPSK) (b) Link throughput (BPSK)

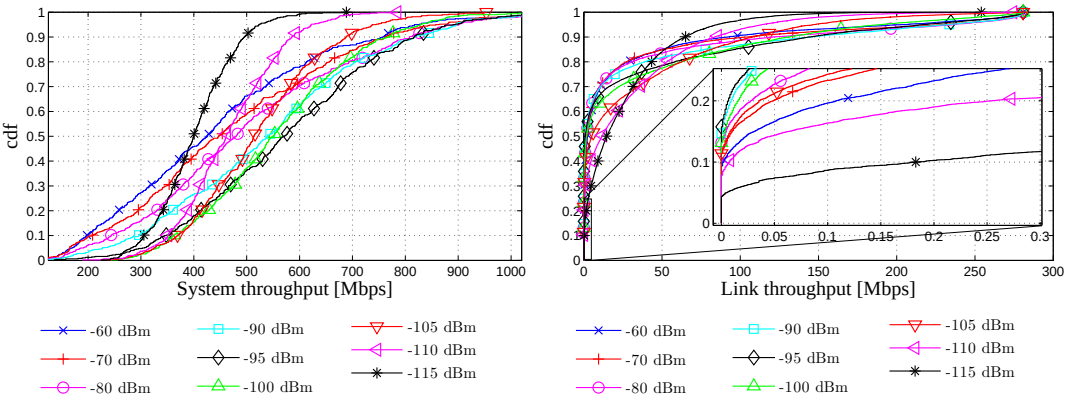

(c) System throughput (LA) (d) Link throughput (LA)

Figure 3.8: *Performance of CSMA/CA in ad hoc network.*

The impact of the threshold parameter which sets the size of the exclusion region on the performance of CSMA/CA is presented in Figure 3.8 for a system utilising fixed BPSK modulation (a-b) systemwide and for a system performing link adaptation (c-d) on a per chunk basis as discussed in Section 3.4.6. A link throughput of 110 kbps at the lower 10^{th} percentile and a median system throughput of 111 Mbps are achieved by setting the threshold to -115 dBm. At

this threshold, the system throughput is compromised because a low threshold used enforces a large exclusion region around the transmitter, which aggravates the exposed node problem with CSMA/CA. Likewise, when the threshold is increased; exposed node problem is mitigated but increases the likelihood of a hidden node. By setting the threshold to -95 dBm, the median system throughput with CSMA/CA system is enhanced but this results in an outage of 15% in the system. At this threshold, the links with better intended channel gains are served at the cost of the links with relatively lower intended channel gains.

By utilising CSMA/CA mechanism for CCI avoidance and by performing link adaptation, the median system throughput increases to 400 Mbps when the threshold is set to -115 dBm. The outage (links suffering from zero throughput) percent remains consistent with the figures obtained from the system utilising a BPSK modulation scheme system wide. This is expected because link adaptation improves the link throughput on those links that succeed in achieving SINRs better than the minimum SINR target in the system by allowing such links to utilise a more spectrally efficient modulation scheme. The improvement in lower 10^{th} percentile is due to the fact that on some of the chunks, the achieved SINR may be large enough to support a higher order modulation scheme.

A poor performance at the lower 10^{th} percentile is expected because with CSMA/CA approach, a potential transmitter sets an exclusion region around the active transmitter when in fact the exclusion region should have been set around the active receiver. CCI mitigation achieved by setting exclusion region around the transmitter is comparable to the CCI mitigation achieved by setting exclusion region around the receiver only if the transmitter and receiver are closely located. This means CSMA/CA benefits the links that already have higher channel gains for the intended signals and not the links whose channel gains are weaker, which are actually those links in the network that require most protection from CCI. As such, the CSMA/CA mechanism fails to mitigate CCI effectively. It is worth noting that an improvement in the lower 10^{th} percentile of link throughput is observed by setting a threshold of -115 dBm compared to those achieved by setting a higher threshold is attributed to the fact that the spatial reuse in the network is lowest as a result of which overall CCI at the receiver is also low.

When the threshold is increased to -95 dBm, a median system throughput of 580 Mbps is achieved but the system suffers from an outage close to 15%. Clearly, at such threshold the links with better channel gain benefit at the cost of starvation of approximately 15% of the user population. In this chapter, a threshold of -115 dBm is used with CSMA/CA approach because

this threshold is shown to enhance the link throughput at the lower 10^{th} percentile both in the system utilising fixed modulation format system wide as well as the system performing link adaptation. This allows us to compare the best case of CCI mitigation with a pre-emptive approach such as CSMA/CA with an interference aware BB protocol in a self organising network.

3.7.3 Performance of BB signalling

3.7.3.1 Impact of I_{th} on system performance

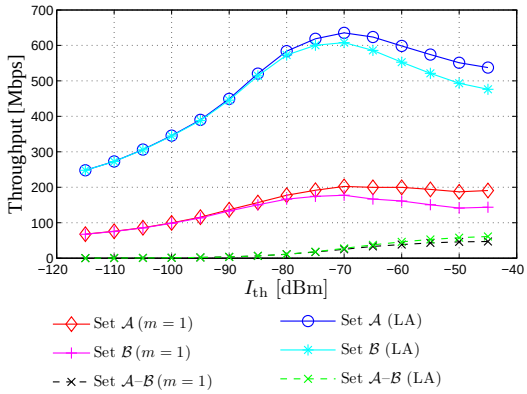

Figure 3.9: *Impact of interference threshold on mean system throughput using BPSK modulation scheme and adaptive modulation.*

The impact of adjusting the interference threshold parameter on the mean system throughput is depicted in Figure 3.9. The results are presented for the system utilising fixed BPSK modulation systemwide ($m = 1$) as well as the system performing adaptive modulation on a per-chunk basis by utilising the SINR feedback from the receiver. In the results presented, both data transmit power and busy burst transmit power are considered fixed systemwide. The result shown in Figure 3.9 depict that at a threshold of -115 dBm, closer to the noise floor ($N = 117.9$ dBm/chunk), the spatial reuse of chunk is minimum leading to lowest system throughput. However, at this threshold the system takes the most cautious approach to accepting additional link that reuses the reserved chunks. Therefore, all transmitted bits are received with the minimum SINR and the transmitted bits rejected by the receiver are close to 0. The system is *desensitised* by increasing the threshold, such that it accepts those link that cause larger amount of CCI to the pre-established links. On the one hand this increases the spatial reuse, potentially increasing the system throughput while on the other hand, the increase in CCI causes the SINR target not to be met in some of the links. The chunks where the SINR target is not met are released and reallocated to another link where the SINR target may *potentially*

be met. This leads to a trade-off between system throughput and guaranteed link throughput, which is discussed further in Section 3.7.3.2. Overall, the system throughput increases with an increase in threshold parameter until the system throughput is highest. For the considered *ad hoc* deployment scenario, this threshold is found to be at -70 dBm. At this threshold, the mean system throughput achieved is 177 Mbps is achieved using BPSK modulation and $3/4$ rate convolutional coding. With these parameters, the maximum throughput per link in an isolated (CCI free) scenario is 27.95 Mbps. This means with the BB mechanism, each chunk is reused an average of 6.3 times within the network. By performing link adaptation, the highest mean system throughput is also achieved by setting the threshold to -70 dBm. By setting this threshold, a median system throughput of 608 Mbps is achieved. In both systems, the system throughput decreases when the threshold is increased further. Particularly, with BPSK modulation utilised systemwide and when the CCI protection is voided by setting a threshold of -50 dBm and higher, the throughput decreases by almost 23% compared to the optimum. This is because increasing the threshold further compromises the protection from CCI and therefore decreases the number of links that are able to meet the SINR target. In such situation where protection from CCI is compromised, it is likely that the chunk that is reallocated after failing to meet the SINR target is allocated to another user that too fails to meet the SINR target. The transmitted bits that are received below the required SINR target at the receiver are discarded because of which the throughput decreases.

3.7.3.2 Trading off system throughput and fairness

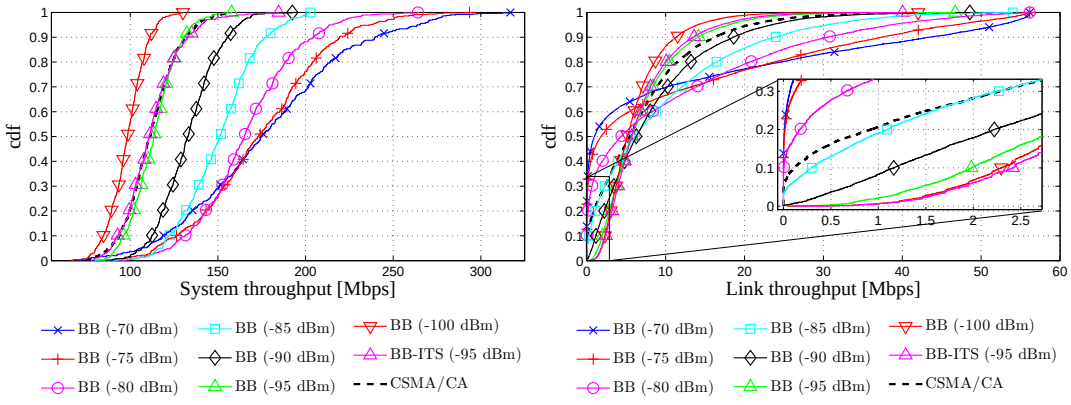

(a) System throughput (b) Link throughput

Figure 3.10: *Trading off system throughput and link throughput by adjusting the threshold.*

The impact of the threshold parameter on system throughput and link throughput on a system

utilising fixed BPSK modulation scheme systemwide is shown in Figure 3.10. The median system throughput is maximised by setting the threshold to -70 dBm (see Figure 3.10(a)) while the system suffers from 13% outage (see Figure 3.10(b). At this threshold, the median system throughput of 175 Mbps is achieved. By comparison, the state-of-the-art CSMA/CA achieves a median system throughput of 111 Mbps, approximately 4.5% outage and a link throughput of 110 kbps at the lower 10^{th} percentile. By lowering the threshold, the CCI protection rendered to active links is enhanced at the cost of spatial reuse of chunks. Consequently, this increases the number of users that are likely to meet the SINR target. As a result, the throughput at the lower 10^{th} percentile increases compared to that achieved using a threshold of -75 dBm. In particular, link throughput of 1.2 Mbps, 2.1 Mbps and 2.3 Mbps are achieved by setting the thresholds to -90 dBm, -95 dBm and -100 dBm respectively. At these thresholds, the median system throughputs achieved are 133 Mbps, 113.5 Mbps and 98.5 Mbps respectively. Moreover, by utilising the variable BB power to signal the interference tolerance of individual links, a link throughput of 2.4 Mbps at the lower 10^{th} percentile and a median system throughput of 111 Mbps are achieved. This represents a $20-$fold increase in link throughput at the lower 10^{th} percentile while achieving an approximately same median system throughput as the benchmark system.

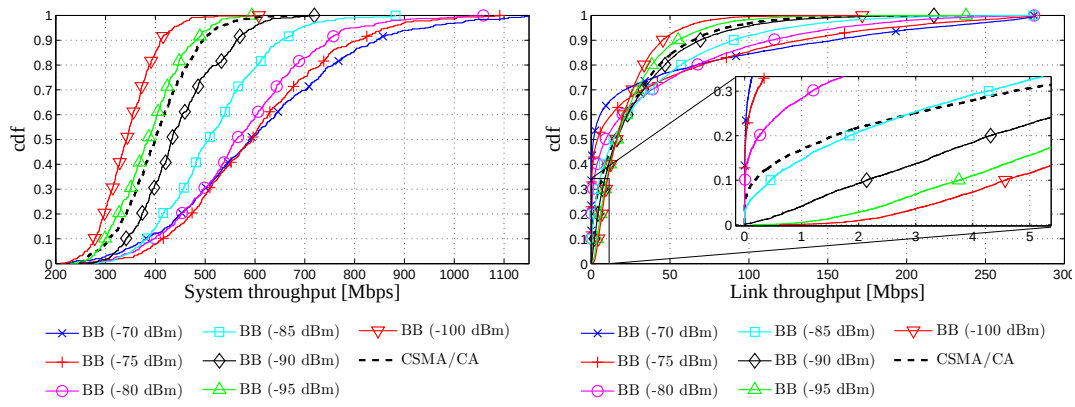

(a) System throughput (b) Link throughput

Figure 3.11: *Comparison of system performance with link adaptation.*

The impact of performing link adaptation on the system performance is depicted in Figure 3.11. In the results presented, three key findings are reported. First, the median system throughput and link throughput (except at the lower percentiles) increases by performing link adaptation compared to using a fixed BPSK modulation scheme, as expected. For those users that benefit from high channel gains and/or low CCI, the achieved SINR exceeds the minimum

SINR required for reserving the chunk. By performing link adaptation, higher order modulation schemes are selected which results in an increase in system throughput compared to the case when a fixed BPSK modulation format is used systemwide. Second, the threshold parameter can be used to trade-off system throughput for an enhanced link throughput at the lower 10^{th} percentile with LA performed. Third, the outage in the system when CCI protection is compromised is approximately 13% with BB scheme ($I_{\text{th}} = -70\,\text{dBm}$) and 4.5% with the benchmark, consistent with the number obtained when BPSK was used systemwide, as expected. The outage figures are consistent because in a system performing LA, outage occurs when the minimum SINR target of 2.2 dB is not met.

The results show that by setting low thresholds (*e.g.* $-100\,\text{dBm}$), the system throughput is the lowest because the transmitters become over-cautious in reusing reserved chunks. On the one hand, increasing the threshold improves the spatial reuse of chunks which potentially increases the system throughput, whereas on the other hand, the achieved SINR degrades due to an increase in CCI. This causes the transmitter to reduce the number of bits transmitted per chunk, reducing the system throughput. Overall, the median system throughput increases on increasing the threshold until an optimum threshold of about $-75\,\text{dBm}$ is reached, beyond which the median system throughput decreases. Using this threshold, a median system throughput of 592 Mbps is achieved, which is a 48% increase compared to the benchmark (see Figure 3.11(a)). However, at this threshold, the system suffers from approximately 13% outage (see Figure 3.11(b)). By lowering the threshold, the median system throughput is traded off for improving link throughput at the lower 10^{th} percentile. In particular, by setting the threshold to $-100\,\text{dBm}$, 250 Mbps of median system throughput is traded off to achieve 4.6 Mbps at the lower 10^{th} percentile of link throughput. However, using a threshold of $-100\,\text{dBm}$, the overall system throughput is 14% lower compared to the benchmark system due to compromised spatial reuse. If the spatial reuse is slightly enhanced by setting the threshold to $-90\,\text{dBm}$, a guaranteed link throughput of 2.1 Mbps together with a median system throughput of 433.5 Mbps can be achieved, which outperforms the benchmark in both metrics simultaneously. These results demonstrate that BB signalling approach allows a flexible network operation between maximising the sum rate in the network and maximising the guaranteed throughput of individual links or a trade-off between the two goals for self-organised operation. The above benefits achieved with BB technique are very important for the future generation wireless networks that are often envisioned to lack rigorous centralised control and infrastructure.

Provided that the quality-of-service (QoS) requirements stipulate that a certain data rate should be available at the lower 10^{th} percentile, an interesting question is to determine how many links can be accommodated in the system whilst satisfying the stated QoS constraints. This leads to determining the spectral efficiency that can be achieved whilst fulfilling the QoS constraints. These two issues are addressed next by varying the number of links in the system.

3.7.4 Impact of varying N_{L} in the system

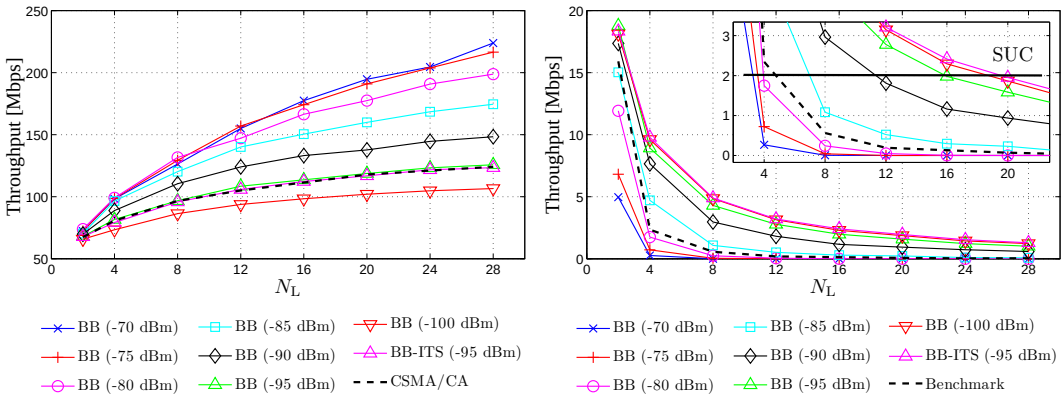

(a) System throughput (b) Link throughput

Figure 3.12: *Impact of varying N_{L} using fixed BPSK modulation for all links and on all chunks.*

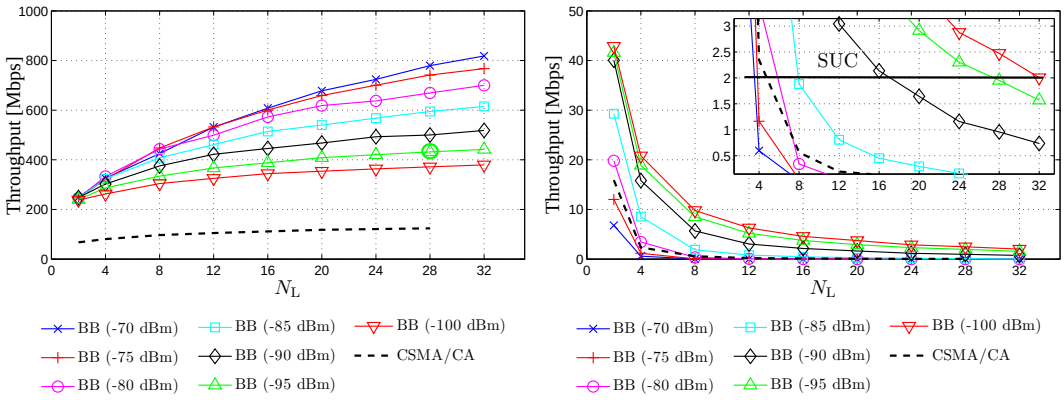

(a) System throughput (b) Link throughput

Figure 3.13: *Impact of varying N_{L} performing adaptive modulation*

The impact of varying the number of links in the system is examined in Figure 3.12 for the system utilising BPSK modulation system wide and in Figure 3.13 for the system performing link adaptation. In both cases, it is demonstrated that the system throughput increases with an increase in the number of links (see Figure 3.12(a) and Figure 3.13(a)), due to an increase

in spatial reuse of chunks. However, due to an increase in CCI, the link throughput at the lower 10^{th} percentile decreases with an increase in the number of links (see Figure 3.12(b) and Figure 3.12(b)). To evaluate the maximum number of feasible links in the considered system and its corresponding attainable spectral efficiency, we consider the *satisfied user criteria* (SUC). In this chapter, the SUC is considered to be fulfilled if 90 percentile of all links achieve a link throughput of 2 Mbps or more. With the benchmark system, the maximum number of links in the system for which the SUC is fulfilled is 5 both for the system using fixed BPSK modulation scheme systemwide as well as the system performing link adaptation. With BB scheme and using BPSK modulation scheme, the maximum number of links in the system such that the satisfied user criteria is met is 7, 11, 16 and 19 for -85 dBm, -90 dBm , -95 dBm and -100 dBm respectively. At these thresholds, the system throughputs are 114.25 Mbps, 120 Mbps, 113.6 Mbps and 187 Mbps respectively which translates to spectral efficiencies of 1.27 bps/Hz ,1.33 bps/Hz ,1.26 bps/Hz and 2.08 bps/Hz respectively. The highest spectral efficiency achieved with fixed power BB and BPSK modulation whilst satisfying the satisfied user criterion is 2.08bps/Hz and supports a maximum of 19 users. For comparison, using BB-ITS the satisfied user criterion is met for a maximum of 20 links and the corresponding spectral efficiency is 2.16bps/Hz. Therefore, it is demonstrated that the BB-ITS scheme allows a larger number of links to be supported in the given deployment area and simultaneously achieve a higher spectral efficiency.

By performing link adaptation with the BB approach, the results show that the SUC is fulfilled only when fewer than 4 links are present in the system (see Figure 3.13(b)) when a high threshold such as -70 dBm is set so as to maximise system throughput. By decreasing the threshold, the maximum number of links in the system such that the satisfied user criteria is met is 8, 16, 28 and 32 respectively if the thresholds are set to -85 dBm, -90 dBm, -95 dBm and -100 dBm respectively. The corresponding system throughputs obtained are 408 Mbps, 440 Mbps, 432 Mbps and 377 Mbps respectively. Using a signal bandwidth of 89.84 MHz, the achieved system throughput translates to spectral efficiencies of 4.5, 4.9, 4.8, and 4.2 bits/s/Hz respectively. The results demonstrate that using the BB approach, up to 32 links can be supported whilst fulfilling the satisfied user criterion. Moreover, it also shows that the spectral efficiency is highest with 16 links in the system. For comparison, the state-of-the-art CSMA mechanism only supports up to 5 users in the system whilst fulfilling the satisfied user criteria. This demonstrates that BB mechanism provides a flexible and scalable mechanism to CCI mitigation in self organising networks. This property can be particularly useful for radio resource

allocation in systems such as femtocell networks, where the access points are installed at the user's premises in an *ad hoc* manner or in avoiding interference with wireless LANs or even for the two systems co-existing on the industrial, scientific and medical (ISM) bands for spectrum access.

3.7.5 Energy consideration in *ad hoc* networks

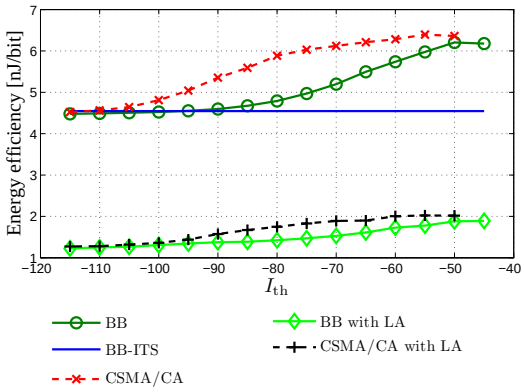

Figure 3.14: *Comparison of energy efficiency in ad hoc networks*

In mobile and *ad hoc* environments, the terminals are usually powered by a battery source and the energy source is often finite. One of the most important benefits of lowering the energy consumption is that the battery life of mobile terminals can be improved, which is especially important for most of the *ad hoc* networks. A considerable amount of research has been carried out in improving energy efficiency in the network [120–122]. Although the importance of reducing the transmit power in mobile terminal cannot be ignored, this section aims at demonstrating how the energy consumption per bit in the system can be adjusted using the BB protocol even in a system utilising a fixed transmit power.

The energy required per bit for successful transmission is depicted in Figure 3.14. For comparison, the energy consumption per bit at different thresholds for CSMA/CA system is also included. The result show that the energy required per bit increases with the threshold, with both the system using BB signalling mechanism as well as the system using CSMA/CA for chunk allocation. Moreover, at low thresholds such as -115 dBm, the energy consumption per bit is identical for BB scheme as well as CSMA/CA approach. However, it should be reiterated that the BB scheme results in a higher system and link throughput, despite the same energy consumption per bit.

In the system using fixed BPSK modulation systemwide, increasing the threshold increases the bit errors at the receiver due to an increase in the CCI. This means energy used for transmission on chunks where the corresponding SINR target is not met is wasted because the bits received in such chunks are discarded at the receiver. As the number of bit errors increase at the receiver, the energy consumption per bit successfully transmitted increases, which is why the energy consumption increases with the threshold.

By performing link adaptation, the average number of bits transmitted per chunk increases compared to using fixed BPSK modulation systemwide. Assuming a fixed transmit power and interference limited scenario, the total energy per bit for successful transmission decreases in a system performing LA on a per chunk basis compared to the system utilising fixed modulation scheme systemwide. In particular, by setting the threshold parameter to $-70\,\text{dBm}$ such that the system throughput is maximised, it is shown that by performing link adaptation the energy consumption per bit can be reduced by approximately 70% compared to using a fixed BPSK modulation systemwide. Furthermore, it is also demonstrated that the energy consumption per bit can be adjusted by adjusting the threshold, thereby tuning a required balance between link throughput, power consumption and system throughput. In this context, it is shown that by setting low thresholds (such as -115 dBm), the spatial reuse of the chunk is restricted. As a result, CCI is either very low or eliminated because of which high SINRs (closer to SNR) are achieved at the receiver. Utilising receiver feedback, the transmitter is able to utilise a more spectrally efficient scheme and thereby reduce energy consumption. By contrast, when the spatial reuse is increased by increasing the threshold, the average CCI caused to competing links also increases. As a result, the achieved SINRs decrease relative to those achieved by setting low thresholds. In such scenario, the transmitter would utilise a less spectrally efficient (such as QPSK or BPSK) modulation format for transmission, which would results in higher energy consumption per bit.

3.8 Chapter Summary

This chapter addressed decentralised CCI mitigation scheme using BB applied to self-organising *ad hoc* networks using parameters from the TDD mode of WINNER in an indoor deployment scenario. It was demonstrated that the system using BB-enabled CCI mitigation outperforms a system utilising CSMA/CA mechanism for chunk allocation considered as a benchmark system, by up to 48% in terms of system throughput. Moreover, it was demonstrated that the

threshold parameter can be used to trade-off the system throughput and the link throughput to aid links with weaker channel conditions. Specifically, it was demonstrated that with the BB approach and with link adaptation performed, up to 32 active links can be supported in an 89.84 MHz of system bandwidth whilst satisfying a QoS constraint that 90% of all users achieve a throughput of 2 Mbps or better. This demonstrates that the BB approach provides significantly better support for QoS provisioning compared to the benchmark system which only supports up to 5 links whilst satisfying the QoS constraint. Thus, the self-organising capability of BB protocol to provide either significantly improved QoS for link throughput or increased system throughput by controlling a single parameter, namely the BB interference threshold, has been demonstrated. This property is makes the BB protocol particularly suitable for radio resource allocation in femtocell networks which may be deployed in an *ad hoc* basis at user premises or in coordinating spectrum access among different co-existing systems within the ISM bands.

Chapter 4
Intercell Interference Coordination in Cellular OFDMA–TDD Networks

4.1 Introduction

Interference management is one of the major challenges for cellular wireless systems, as transmissions in a given cell cause co-channel interference (CCI) to the neighbouring cells. Full-frequency reuse where the transmitters are allowed an unrestricted access to all resources causes high CCI, which particularly impacts the cell-edge users [80, 81, 123]. Although CCI can be mitigated by traditional frequency planning, this potentially results in a loss in bandwidth efficiency due to insufficient spatial reuse of radio resources. Fractional frequency reuse (FFR) [79–82] addresses this issue by realising that in cellular networks, CCI predominantly affects users near the cell boundary. FFR typically involves a sub-band with full frequency reuse that is exempt from any slot assignment restrictions. The allocation of the remaining sub-bands is coordinated among neighbouring cells, in a way that the users in the given cell are denied access to sub-bands assigned to the cell-edge users in the adjacent cells. To this end, in [80] a user is classified as a cell-edge user based on the path loss to the desired base station (BS). This approach ignores the fact that the channel attenuation of the desired and the interfering signals are uncorrelated, and therefore fails to exploit the *interference diversity*. Therefore, CCI is not mitigated effectively, a problem which is exacerbated when the BSs are deployed in an uncoordinated manner. Moreover, frequency planning results in a hard spatial reuse of the available resources. As a result, it cannot cater for the dynamic traffic and load across different sites. Furthermore, in systems where BSs are dynamically added in an uncoordinated manner, such as home base stations [124], reconfigurable frequency reuse planning may prove to be increasingly cumbersome.

In this chapter, intercell interference coordination (ICIC) is addressed using busy burst (BB) signalling in cellular networks operating in a Manhattan deployment scenario as well as in a hexagonal cellular scenario.

4.2 System model

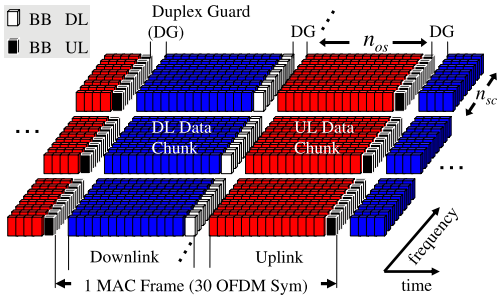

Figure 4.1: *Frame structure for OFDMA-TDD with BB signalling.*

The air interface for the cellular system considered in this chapter consists of a medium access control (MAC) frame divided into uplink (UL) and downlink (DL) sub-frames as illustrated in Figure 4.1. A multi-cellular scenario is considered where the allocation of radio resources are coordinated at the base station (BS). In an orthogonal frequency division multiple access (OFDMA) - time division duplexing (TDD) system, a chunk is a radio resource unit that can be allocated to one of the U_α users located within cell α, where cell α is defined as the spatial coverage region of BS α. No spatial multiplexing is considered, which means intra-cell interference is avoided. However, the same chunk can potentially be reused in adjacent cells, which results in CCI between entities in two different cells.

To model CCI between two cells, the following notation is used. An active link in a tagged cell is represented as a pair (μ, α), where μ is a mobile station (MS) which connects to BS α. An interfering link in an adjacent cell is defined as a pair (ν, β), where ν is a MS which connects to BS β. In the DL mode, the intended channel gain between MS μ and BS α on chunk (n, k) is designated $G_{\mu,\alpha}[n, k]$ and the interfering channel gain between MS μ and BS β on chunk (n, k) is designated $G_{\mu,\beta}[n, k]$. Both the intended and interfering channel gains takes into account the effects of signal propagation through the radio channel, such as the distance dependent path loss, log-normal shadowing, time variations due to Doppler shift and frequency-selective fading due to multipath propagation as described earlier in (2.18). Likewise, in the UL mode, the intended channel gain between MS μ and BS α is designated $G_{\alpha,\mu}[n, k]$ whilst the interfering gain between MS ν and BS α is designated $G_{\alpha,\nu}[n, k]$. Furthermore, due to channel reciprocity in TDD mode, $G_{\mu,\alpha} = G_{\alpha,\mu}$ holds for all BS and MS pairs, which may be either intended links or interfering links. The data transmit power, desired signal power and interference signal power of MS μ on chunk (n, k) are designated $T_\mu^{\mathrm{d}}[n, k]$, $R_\mu^{\mathrm{d}}[n, k]$ and $I_\mu^{\mathrm{d}}[n, k]$ respectively. Likewise, the data transmit power, desired signal power and interference signal power of BS

α on chunk (n,k) are designated $T_\alpha^{\mathrm{d}}[n,k]$, $R_\alpha^{\mathrm{d}}[n,k]$ and $I_\alpha^{\mathrm{d}}[n,k]$ respectively. The received signal power at the receiver of link (μ,α) is

$$\tilde{R}_\mu^{\mathrm{d}}[n,k] = R_\mu^{\mathrm{d}}[n,k] + I_\mu^{\mathrm{d}}[n,k] + N\,, \quad \text{(DL)} \tag{4.1}$$

$$\tilde{R}_\alpha^{\mathrm{d}}[n,k] = R_\alpha^{\mathrm{d}}[n,k] + I_\alpha^{\mathrm{d}}[n,k] + N\,, \quad \text{(UL)} \tag{4.2}$$

where N is the noise power/chunk.

To simplify notation and to have a common notation for both the UL and DL modes, let $\mathbf{x} = (\mu,\alpha)$ represent either a transmitter or receiver of an intended link (μ,α) and $\mathbf{y} = (\nu,\beta)$ represent a transmitter or a receiver of a link (ν,β) in cell β that interferes with transmission in cell α. With this notation, $G_{\mathbf{x}}[n,k]$ represents the channel gains of an intended link and $G_{\mathbf{xy}}[n,k] = G_{\mathbf{yx}}[n,k]$ represents the channel gains of an interfering link. The intended and interfering signals are expressed as

$$R_{\mathbf{x}}^{\mathrm{d}}[n,k] = T_{\mathbf{x}}^{\mathrm{d}}[n,k]G_{\mathbf{x}}[n,k] \tag{4.3}$$

$$I_{\mathbf{x}}^{\mathrm{d}}[n,k] = T_{\mathbf{y}}^{\mathrm{d}}[n,k]G_{\mathbf{xy}}[n,k]. \tag{4.4}$$

The signal to interference and noise ratio (SINR) achieved at receiver $\mathbf{x}$ can be expressed as

$$\gamma_{\mathbf{x}}[n,k] = \frac{R_{\mathbf{x}}^{\mathrm{d}}[n,k]}{I_{\mathbf{x}}^{\mathrm{d}}[n,k] + N}\,. \tag{4.5}$$

The aim is to coordinate the allocation of radio resources such that $\gamma_{\mathbf{x}}[n,k] \geq \Gamma_m$ holds, where Γ_m is the minimum SINR target that needs to be met for fulfilling the quality of service (QoS) constraints when a modulation level m is utilised. In this chapter, intercell interference coordination (ICIC) is carried out using BB signalling for OFDMA-TDD networks that was discussed earlier in Chapter 3. For comparison, ICIC performed using centralised frequency planning approaches - *viz.* static frequency planning and fractional frequency reuse mechanisms are also considered. With all of these ICIC mechanisms, users are scheduled using a modified score-based scheduler which is discussed in Section 4.3.

4.3 Multi user resource allocation

Provided that any given chunk is reused at most once per cell, the BS may flexibly assign the available chunks to its served users such that any intra-cell interference is avoided. The assumption of no intra-cell interference requires that the transmitters and receivers are perfectly synchronised in time and frequency and multiple access interference (MAI) caused due to Doppler's shift is negligible. A variant of the score-based scheduler [70] is proposed in this section, which distributes $1{\leq}n{\leq}N_{\mathrm{C}}$ chunks among $1{\leq}\nu{\leq}U_{\beta}$ users served by the BS in cell β. The score for user ν in cell β is computed as

$$s_{\nu,\beta}[n,k] = 1 + \epsilon_{\nu,\beta}[n,k] + \Psi_{\nu,\beta} + \sum_{\ell=1}^{N_{\mathrm{C}}} \mathbb{I}_{\{G_{\nu,\beta}[n,k] \leq G_{\nu,\beta}[\ell,k]\}} \,, \tag{4.6}$$

where the indicator function $\mathbb{I}_x \in \{0,1\}$ is set to 1 or 0 when the condition x is true or false, respectively. The last term containing the sum of indicator functions counts how many chunks within the system bandwidth have a channel gain higher than the considered chunk. In effect, this returns the position of the chunk when the chunks are sorted in the order of ascending channel gains. Therefore, if the chunk has the highest channel gain within the system bandwidth, the summation returns 1. By contrast, if the chunk has the lowest channel gain within the system bandwidth, it returns N_{C}. The $\epsilon_{\nu,\beta}[n,k]$ parameter controls whether or not user ν is granted access to chunk (n,k) in cell β. Especially with the interference aware and reservation-based MAC protocols such as BB-OFDMA (see Section 4.4), a user may be denied access to chunk (n,k) by setting $\epsilon_{\nu,\beta}[n,k]{\rightarrow}\infty$. This avoids radiation of CCI from cell β to any neighbouring cells that use the same chunk (n,k). Finally, the term $\Psi_{\nu,\beta}$ represents a 'priority penalty factor' for a user ν in cell β, which will be discussed shortly in this section.

In cell β, the chunk (n,k) is allocated to user $\zeta_{\beta}[n,k]$ if either a reservation indicator was set for user ν in the previous frame by setting $\Upsilon_{\nu}[n,k]{=}1$, or if the score (4.6) is minimized and no user in cell β has reserved the chunk, as follows

$$\zeta_{\beta}[n,k] = \begin{cases} \arg\min\limits_{\nu} s_{\nu,\beta}[n,k] \,, & \Upsilon_{\nu}[n,k] = 0 \,\forall\, \nu \in \{1 \,\ldots\, U_{\beta}\} \\ \nu \,, & \Upsilon_{\nu}[n,k] = 1 \,. \end{cases} \tag{4.7}$$

where U_{β} is the number of users served by BS β. For chunk allocation, (4.7) is evaluated individually for each chunk (n,k).

A binary variable $a_\nu[n,k]$ [27] defined as

$$a_\nu[n,k] = \begin{cases} 1\,, & \zeta_\beta[n,k] = \nu \\ 0\,, & \text{otherwise}\,, \end{cases} \tag{4.8}$$

denotes whether or not the chunk (n,k) is assigned to user ν for transmission. The chunks where $a_\nu[n,k] = 1$ belong to set $\mathcal{A}_\beta$, where set $\mathcal{A}_\beta$ represents a set of chunks used for transmission in cell β. We note that if $\epsilon_{\nu,\beta}[n,k] \rightarrow \infty$ for all users, all users in cell β are denied access to chunk (n,k) and the chunk (n,k) remains unallocated in cell β.

After chunk allocation, the transmitter of user ν uses the allocated chunk for transmission. The correctly received index $b_\nu[n,k+1] = 1$ and the reservation index $\Upsilon_\nu[n,k+1] = 1$ are set as done earlier in Section 3.4.5. The chunks where $b_\nu[n,k+1] = 1$ is set belong to set $\mathcal{B}_\beta$.

By setting $\Upsilon_\nu[n,k+1] = 1$, the chunk $(n,k+1)$ is reserved for user ν in the next slot and will subsequently be allocated to the same user by (4.7). However, the chunks where $\gamma_{\mathbf{y}}[n,k] < \Gamma_{\min}$ are released by setting $\epsilon_\nu[n,k+1] \rightarrow \infty$, so as to restrict the user ν from accessing the chunk in the next frame. It should be noted that (3.13) and (3.14) are identical if the same modulation format is used systemwide. However, when link adaptation is performed and if $\gamma_{\mathbf{y}}[n,k] < \Gamma_m$ and $\gamma_{\mathbf{y}}[n,k] \geq \Gamma_{\min}$, $\Upsilon_\nu[n,k+1]$ is set to 1 while $b_\nu[n,k]$ is set to 0.

The proposed score-based scheduler differs from the original score-based scheduler [70] in the following two respects. First, in the proposed method, the chunks are ranked along the frequency axis rather than along the time axis in [70] for calculating the scores. Consequently, the original method required a memory of $N_{\mathrm{W}}N_{\mathrm{C}}$, where N_{W} is the sliding window size (see Section 2.4.5) whereas the proposed method only requires a memory of N_{C}. Second, the allocation mechanism in the proposed variant allows chunk reservation, which makes it suitable for interference aware CCI mitigation approaches such as the BB approach. The price to be paid for reservation is that the channel variations cannot be exploited opportunistically to enhance system performance in a multi-user system.

In this thesis, two variants of the modified score-based scheduler are considered - blind and fair score based scheduler.

4.3.1 Blind score-based scheduler

The priority penalty factor $\Psi_{\nu,\beta}$ is set to 0 for all users in cell β. The scheduler is called blind score-based scheduler (BSBS) as it does not take into account the number of chunks reserved and/or already allocated to user ν in the k^{th} frame while allocating an additional chunk to user ν.

4.3.2 Fair score-based scheduler

The fair score-based scheduler (FSBS) takes into account the number of chunks already reserved and/or already allocated to user ν in the k^{th} frame by incrementing the priority penalty factor as

$$\Psi_{\nu,\beta} = \exp\left(\sum_{n=1}^{N_{\text{C}}} a_{\nu}[n,k]\right). \tag{4.9}$$

It is assumed that $\Psi_{\nu,\beta} = 1$ is set when the chunk allocation procedure starts for the k^{th} frame. The scheduler allocates the reserved chunks first to the respective users that reserved it in the preceeding frame. The priority penalty factor for each user is updated to

$$\Psi_{\nu,\beta} = \exp\left(\sum_{n=1}^{N_{\text{C}}} \Upsilon_{\nu}[n,k]\right). \tag{4.10}$$

The unallocated chunks are allocated using (4.7) one chunk at a time. After allocating a new chunk for transmission, the priority penalty factor is adjusted by evaluating (4.9) and the scores are recomputed using (4.6).

4.4 BB signalling for CCI avoidance in cellular networks

BB signalling provides a mechanism to inform the interfering transmitters in the adjacent cells about the amount of interference they would potentially cause to a receiver of an active link if they were to transmit. This knowledge enables the scheduler to exclude certain chunks for some or all users within the given cell such that potentially detrimental CCI caused towards the receiver in an adjacent cell is avoided.

To accomplish the above goal, the MAC frame is divided into data slots and BB mini-slots as illustrated in Figure 4.1. The BS transmits data in the ‘Data DL’ slot. Provided that the

minimum SINR target for an allocated chunk (n, k) is met, the intended MS transmits a BB in an associated mini-slot 'BB UL' on chunk (n, k) in the uplink mode. This reserves chunk n of 'Data DL' for the next frame $k+1$. Likewise, for uplink data transmitted by the MS in slot 'Data UL', the BB is transmitted by the intended BS in the downlink mini-slot 'BB DL'. The transmit BB power on chunk (n, k) for BB transmitter $\mathbf{x}$ is designated $T^{\mathrm{b}}_{\mathbf{x}}$ and received BB at the interfering transmitter on the BB mini slot on chunk (n, k) is designated $I^{\mathrm{b}}_{\mathbf{y}}[n, k]$. Provided that channel reciprocity holds, it was shown in Section 3.4 that $I^{\mathrm{d}}_{\mathbf{x}}$, the CCI that would be caused towards receiver $\mathbf{x}$ if $\mathbf{y}$ were to transmit is

$$I^{\mathrm{d}}_{\mathbf{x}}[n, k] = \left(\frac{T^{\mathrm{d}}_{\mathbf{y}}[n, k]}{T^{\mathrm{b}}_{\mathbf{x}}[n, k]} \right) I^{\mathrm{b}}_{\mathbf{y}}[n, k]. \tag{4.11}$$

Provided that the transmitter scans the BB slot and knows the BB transmit power used, the scheduler may either reuse all chunks but utilise a transmit power that is lower than the maximum transmit power, or avoid certain chunks for certain users whilst utilising the maximum transmit power on admitted links. This enables the scheduler to maintain $I^{\mathrm{d}}_{\mathbf{x}} < I_{\mathrm{th}}$ on all reserved chunks in the system. In this context, it was shown in [30, 125] that when two links compete for resources, the optimum system throughput is achieved when the maximum transmit power is used on either one or both links. For this reason, ICIC using power control approach is not considered in this thesis. If a constant data transmit power is utilised in all links, the condition for admitting a chunk for scheduling in the tagged cell is given by

$$I^{\mathrm{b}}_{\mathbf{y}}[n, k] \left(\frac{T^{\mathrm{d}}_{\mathbf{y}}[n, k]}{T^{\mathrm{b}}_{\mathbf{x}}[n, k]} \right) \leq I_{\mathrm{th}}. \tag{4.12}$$

In case $T^{\mathrm{d}}_{\mathbf{y}}[n, k]{=}T^{\mathrm{b}}_{\mathbf{x}}[n, k]$, condition (4.12) reduces to:

$$I^{\mathrm{b}}_{\mathbf{y}}[n, k] \leq I_{\mathrm{th}}\,. \tag{4.13}$$

By utilising (4.13), a transmitter can autonomously decide whether or not it may reuse the chunk. The decision whether to admit the chunk for scheduling or not is represented by the

access control indicator $\epsilon_{\nu,\beta}[n,k]$ in (4.6), given by

$$\epsilon_{\nu,\beta}[n,k] = \begin{cases} 0\ , & I^{\mathrm{b}}_{\mathbf{y}}[n,k] \leq I_{\mathrm{th}} \text{ and } \chi_{\beta}[n,k]{=}1 \\ \infty & a_{\nu}[n,k-1] = 0 \text{ and } \Upsilon_{\nu}[n,k] \neq 1 \\ \infty\ , & \text{otherwise,} \end{cases} \tag{4.14}$$

where $\mathbf{y}$ is the transmitter for link (ν,β), $\chi_{\beta}[n,k] \in \{0,1\}$ is a binary random variable where $\mathrm{E}[\chi_{\beta}]{=}p$ that denotes the outcome of $p-$persistent chunk allocation mechanism used for accessing unreserved chunks. A $p-$persistent mechanism (see Section 3.4.4) is used so as to reduce the likelihood of collisions due to simultaneous access of chunks in two cells that are located close enough to cause detrimental CCI.

If the chunk (n,k) in cell β is allocated to user ν by the scheduler (4.7), the transmitter $\mathbf{y}$ transmits data to its intended receiver. Provided that $\gamma_{\mathbf{y}} \geq \Gamma_{\mathrm{min}}$, a reservation indicator is set as shown in (3.14). The receiver $\mathbf{y}$ broadcasts a BB on those chunks where $\Upsilon_{\nu}[n,k+1]{=}1$ so as to reserve such chunks and protect the reserved chunks from detrimental CCI.

4.5 Balancing system throughput and fairness

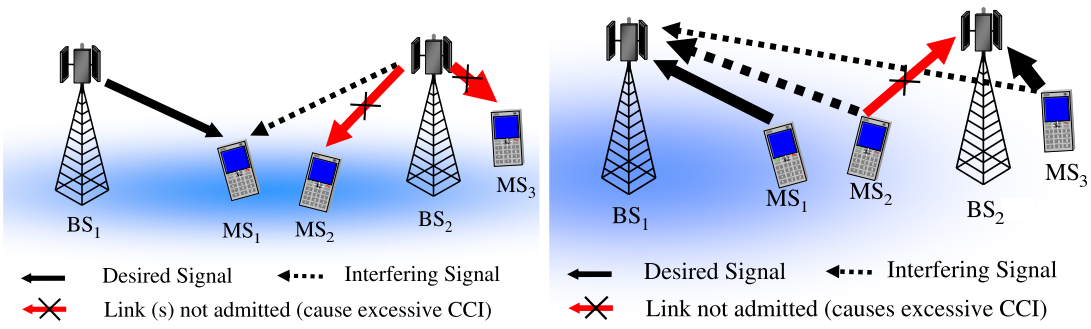

(a) DL (b) UL

Figure 4.2: *BB signalling applied to cellular system. The arrows depict the direction of desired and interfering signal and their relative strength is indicated by their width. The strength of BB signal is indicated by the darkness of the shade around the vulnerable receiver.*

To exemplify the principle of BB enabled interference avoidance, a typical interference scenario in a cellular system is illustrated in Figure 4.2(a) for the DL mode and Figure 4.2(b) for the UL

mode. In a cellular system, the cell-edge users are particularly affected by CCI for two reasons. First, the desired signal levels $R^{\mathrm{d}}_{\mathbf{x}}[n,k]$ for the cell-edge users are, on average, much weaker compared to the users located closer to the desired BS, due to relatively low channel gains on their intended links $G_{\mathbf{x}}[n,k]$. Second, the cell-edge users also suffer from high CCI in the downlink, or cause high CCI to the adjacent cells in the uplink.

By tuning the interference threshold I_{th} in (4.13), the amount of CCI $I^{\mathrm{d}}_{\mathbf{x}}[n,k]$ caused to the receiver $\mathbf{x}$ of a pre-established and co-existing link (μ,α) is adjusted. Lowering I_{th} enforces a larger exclusion region around the active receiver. This enables the cell-edge users to meet their SINR target Γ with a greater likelihood. On the other hand, by augmenting I_{th}, the number of simultaneously served links increases, giving rise to an enhanced system throughput. However, the cell-edge users are less likely to maintain their SINR target as interference protection is gradually eliminated. The chunks where the SINR target is not met are released, which means that these chunks are no longer reserved. The released chunk may be reallocated to other users within the cell. The cell-centre users are typically less exposed to CCI, compared to the cell-edge users assuming a full reuse of chunks. Therefore if the chunks released by the cell-edge users are allocated to the cell-centre users, such chunks are more likely to be retained by the cell-centre users. As the allocation of the resources is shifted from the cell-edge users towards the cell-centre users, fairness is compromised. Hence, by adjusting I_{th}, system throughput is traded-off for fairness in terms of enhanced cell-edge user throughput. However, it should be noted that if the released chunk is allocated to another user that fails to meet the SINR target, the chunk is again released, potentially resulting in *ping pong* effects, which reduces the overall spectral efficiency in the system.

4.5.1 Consequences for the downlink

In the downlink, MSs at the cell edge are exposed to high CCI from transmitters in adjacent cells (see Figure 4.2(a)). Note that the CCI observed at a given cell (cell 1, *i.e.* the area served by BS_1, in Figure 4.2(a)) is independent of the user distribution in adjacent cells (cell 2, *i.e.* the area served by BS_2, in Figure 4.2(a)), assuming a constant transmit power $T^{\mathrm{d}}_{\mathbf{x}}[n,k]$. This implies that if BS_2 lies within the exclusion region of MS_1, resources reserved by MS_1 cannot be spatially reused by *any* of the links in cell 2. However, if I_{th} is increased such that BS_2 is located outside the exclusion region of MS_1, *all* links in cell 2 qualify for a spatial reuse of the resources reserved by MS_1. However, the SINR target at MS_1 is less likely to be met. Should

the SINR target at MS_1 not be met, this would cause the chunk allocated to MS_1 to be released and reallocated to another user served by BS_1. Thus, by adjusting I_{th}, fairness in the system can be traded off for an enhanced system throughput in the downlink mode.

4.5.2 Consequences for the uplink

In the uplink, the transmitters (MSs) are distributed uniformly over the coverage area of the BS (see Figure 4.2(b)). Unlike the downlink, the CCI at the tagged BS depends on which MS transmits in the adjacent cell. To this end, the CCI observed at BS_1 in Figure 4.2(b) depends on whether MS_2 or MS_3 transmit to BS_2. Suppose that in cell 2 both MS_2 and MS_3 contend with MS_1 in cell 1 for chunks (n, k) and (n', k). In case MS_2 and MS_1 simultaneously access chunk (n, k), while MS_3 and MS_1 simultaneously access chunk (n', k), the SINR at BS_1 tends to be superior on chunk (n', k), due to the lower CCI caused by MS_3. While MS_2 causes excessive CCI to BS_1, MS_1 and MS_3 may share chunk (n', k), although both users might be located near the cell boundary. Thus the uplink benefits from *interference diversity*, due to the distributed location of mobile users. As a result, the degradation of performance at the cell-edge at high I_{th} in uplink mode is less severe compared to the downlink.

4.6 Benchmark system

A full chunk reuse system where users are scheduled using the score-based scheduler is considered as a benchmark for comparison. This means neither chunk reservation nor interference avoidance mechanism is considered. The chunks are assigned to user whose score (4.6) is minimised

$$\zeta_\beta[n, k] = \arg\min_{\nu} s_{\nu,\beta}[n, k]\,. \tag{4.15}$$

Chunk allocation for the benchmark system (4.15) corresponds to (4.7) when the reservation indicator is set as $\Upsilon_\nu[n, k] = 0$ in (4.7) and the access control indicator is set as $\epsilon_{\nu,\beta}[n, k]{=}0$ in (4.6) for all users.

4.7 Simulation environment

Cellular systems based on OFDMA-TDD are considered. The networks are assumed to be perfectly synchronized in time and frequency. Pedestrian mobile users are considered, that are moving with a velocity of 5 km/h. A full-buffer traffic model is assumed where the users are continuously attempting to transmit or receive data. Both the MSs and the BSs are assumed to be equipped with isotropic omnidirectional antennas. Except for the simulation parameters that are tabulated in Table 4.1, all other parameters are the same as those considered for *ad hoc* scenario (see Table 3.1).

Parameters		**Value**
Carrier centre frequency		3.95 GHz
System bandwidth	B	89.84 MHz
# subcarriers (SC)		1840
# sectors/cell		1
# users/cell	U	10
Tx power/chunk	T^{d}	16.4 dBm
Antenna gain		0 dBi
Noise level/chunk	N	-117.8 dBm
# Monte Carlo runs		500
Duration of each Monte Carlo run		75 ms

Table 4.1: *Additional simulation parameters for cellular scenario. All other parameters are same as those considered in Chapter 3.*

In this chapter, cellular systems deployed in Manhattan type scenarios and the cellular systems where the cells are modelled as hexagons are considered for investigation. Both of the these deployment scenarios are discussed below.

4.7.1 Manhattan grid deployment

An urban microcell deployment with a rectangular grid of streets (Manhattan grid) as defined in scenario B1 in WINNER [28] is considered where the antennas are mounted below the rooftop. The deployment scenario consists of building blocks of dimensions 200 m $\times$ 200 m, interlaced with streets of width 30 m, forming a regular structure called the Manhattan grid, as shown in Figure 4.3. The network consists of 11$\times$12 building blocks (72 BSs). However, the performance statistics are collected only over the central core of 3$\times$3 building blocks (6 BSs), so as to reduce the edge effects.

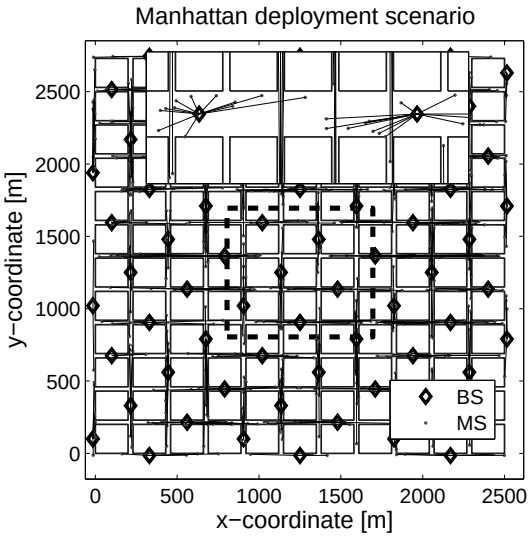

Figure 4.3: *Manhattan grid urban microcell deployment.*

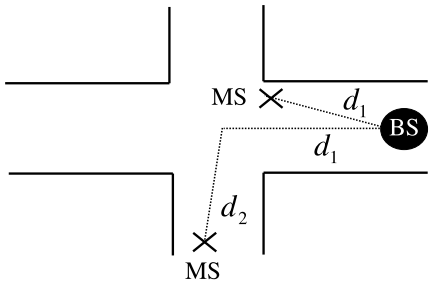

Figure 4.4: *Depiction of distances d_1 and d_2 used in path loss model.*

On average $U{=}10$ MSs are served by one cell, uniformly distributed in the streets and moving with a constant velocity of 5 km/h. BSs are placed in the middle of the street canyons with an inter-BS distance of 4 building blocks, as depicted in Figure 4.3. Distance dependent path loss, log-normal shadowing and frequency selective fading are taken into account, as specified in [126], channel model B1. While the effect of user mobility on the channel response due to the Doppler effect is taken into account, movement of users along the streets is not considered for the duration of one Monte Carlo run. Links where both the transmitter and the receiver are located on the same street are modelled as line of sight (LoS) channels, with significantly lower path loss attenuation than the non line of sight (NLoS) links [126].

The path losses in Manhattan scenario are modelled according to WINNER channel models B1-LOS and B1-NLOS [126] respectively. The MS are assumed to be connected to the BS on the basis of least path loss, unless both the MS and the BS are located within the same street. In the later case, they are connected to the closest BS. The actual height of BS (h_{BS}) and height of MS (h_{MS}) are assumed to be 10m and 1.5m respectively. The average height of surrounding objects in the environment is taken to be 1m in Manhattan scenario [126]. Therefore, the effective antenna height of BS ($h^{'}_{\mathrm{BS}}$) and the effective antenna height of MS ($h^{'}_{\mathrm{MS}}$) are calculated to be 9m and 0.5m respectively. Using the above parameters as well as a central carrier frequency (f_{c}) of 3.9 GHz and the velocity of electromagnetic waves (c = $3 \times 10^{8}\mathrm{m/s}$), the break point distance, *i.e.* the distance at which the path loss exponent changes from a lower exponent to a higher exponent, d_{BP}, given by

$$d_{\mathrm{BP}} = \frac{4h^{'}_{\mathrm{BS}}h^{'}_{\mathrm{MS}}f_{\mathrm{c}}}{c}, \tag{4.16}$$

is calculated to be 234m. The pathloss for the LoS scenario is obtained by plugging in the values from Table 4.2 into (2.13).

A_{pl}	B_{pl}	C_{pl}	X_{pl}	σ	Applicability Range
22.7	41.0	20	-	3.0	$10\mathrm{m} \leq d_1 \leq d_{\mathrm{BP}}$
40.0	9.45	2.7	$-17.3\log_{10}(h^{'}_{\mathrm{MS}})-$ $17.3\log_{10}(h^{'}_{\mathrm{MS}})$	3.0	$d_{\mathrm{BP}} \leq 5\mathrm{km}$

Table 4.2: *Parameters for modelling path loss in Manhattan scenario in LoS conditions*

In NLoS conditions, the path loss between MS ν and BS β is calculated by dividing the shortest path between the MS and BS into segments d_1 and d_2 as shown in Figure 4.4 and using the

following equation

$$P_{\nu,\beta}^{\mathrm{ls}} = \max(P_{\mathrm{L}}(d_1) + 20 - 12.5n_j + 10n_j \log_{10}(d_2) + \mathcal{N}(0,\sigma), P_{\nu,\beta}^{\mathrm{free}}) \tag{4.17}$$

where $n_j = \max((2.8 - 0.0024d_1), 1.84)$, $w = 20\,\mathrm{m}$ and $P_{\mathrm{L}}(d_1)$ is the path loss, calculated for LoS scenario based on the value of d_1, σ is the standard deviation of parameter modelling the log-normal shadowing and is 4 dB for NLoS scenario in Manhattan environment [126] and $P_{\nu,\beta}^{\mathrm{free}}$ is the free space path loss as discussed earlier in Section 2.3. The above model is valid for $10\,\mathrm{m} < d_1 < 5\,\mathrm{km}$ and $\frac{w}{2} < d_2 < 2\mathrm{km}$.

4.7.2 Hexagonal cellular deployment

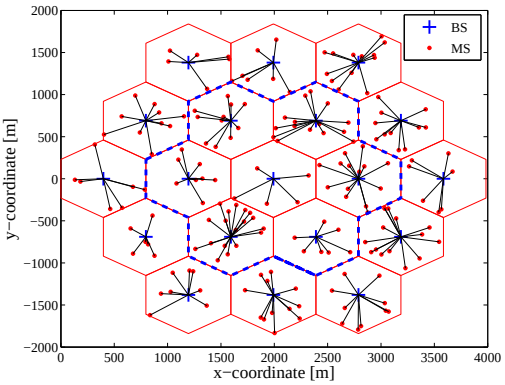

Figure 4.5: *Depiction of hexagonal cellular scenario considered for simulations. Note that in the figure, the MS are connected to the BS on the basis of least distance for clarity. In the simulated system, the MSs are handed over to the BS that provide the highest channel gain averaged over the system bandwidth.*

A cellular system modelled by non-overlapping hexagons of 19 cells is considered as depicted in Figure 4.5. A hexagonal cellular scenario typically models cellular deployment in sub-urban and rural settings, unlike the Manhattan cellular scenario which models cellular deployment in an urban setting. Each cell consists of a BS located at the centre of each cell and has a radius of 460 m. Performance statistics are collected over the central core of 7 cells indicated by a dashed line in Figure 4.5. Channels are modelled according to C1 scenario of WINNER [126]. In the considered model, a line of sight (LoS) condition between a transmitter and a receiver exists with probability p_{LOS} given by [126]

$$p_{\mathrm{LoS}} = \exp\left(-\frac{d}{200}\right). \tag{4.18}$$

where d is the separation distance between transmitter and receiver in meters. The path loss between the BS and MS is obtained by using parameters from Table 4.3 in (2.13).

A_{pl}	B_{pl}	C_{pl}	X_{pl}	σ	Applicability Range
LoS					
23.8	41.2	20	0	4	$10\mathrm{m} \leq d \leq d_{\mathrm{BP}}$
40.0	11.65	3.8	$-16.2\log_{10}(h_{\mathrm{BS}})$ $-16.2\log_{10}(h_{\mathrm{MS}})$	6	$d_{\mathrm{BP}} \leq d \leq 5\mathrm{km}$
NLoS					
$44.9 - 6.55\log_{10}$ (h_{BS})	31.46	23	$5.83\log_{10}(h_{\mathrm{BS}})$	8	$50 \leq d \leq 5\mathrm{km}$

Table 4.3: *Parameters for modelling path loss in hexagonal cellular scenario*

4.8 Results and discussions: Manhattan scenario

In this section, the performance of ICIC techniques in Manhattan scenario described in Section 4.7.1 are investigated both for the system utilising fixed modulation scheme systemwide as well as the system performing link adaptation.

4.8.1 ICIC on system utilising fixed modulation scheme

A fixed modulation of 16-QAM with $3/4$-rate convolutional coding is considered systemwide. The corresponding minimum SINR target required for fulfilling QoS requirements is 11.3 dB (see Table 3.2). Any chunks where the SINR target of 11.3 dB is not met are released.

4.8.1.1 Centralised frequency planning approach

The results obtained using centralised frequency allocation schemes for ICIC are presented in Figure 4.6. For comparison, the results obtained by performing a full reuse of chunks are also included. In the Manhattan scenario, CCI originating from the interferers located within the same street dominate the total CCI at the receiver. As there are 3 BSs per street in the considered Manhattan scenario (see Figure 4.3), it is reasonable to assume a cluster size of 3. For coordinating frequency allocation in the system, two schemes are considered. The first scheme, labelled 'frequency plan' in Figure 4.6 utilises a reuse factor of 3 for all available chunks in the system. The second scheme, called fractional frequency reuse (FFR) divides the available system bandwidth into two groups. The first group operates under a full reuse and

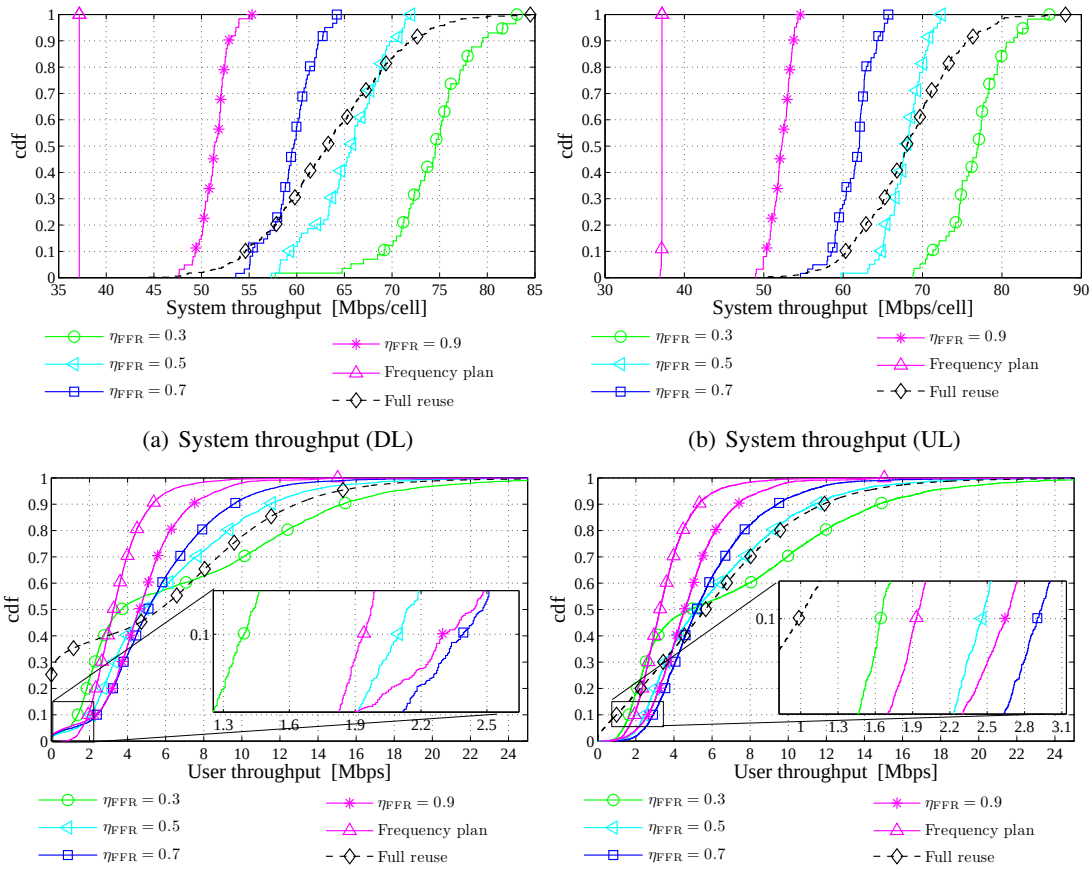

(a) System throughput (DL)

(b) System throughput (UL)

(c) User throughput (DL)

(d) User throughput (UL)

Figure 4.6: *Performance of frequency planning schemes using fixed modulation scheme of 16-QAM with an SINR target of 11.3 dB.*

is exclusively allocated to the cell-centre users. The second group, utilises a reuse factor of 3 and is allocated exclusively to cell-edge users. A user is classified as a cell-edge user if the path loss to its serving BS exceeds the median path loss of the user population connected to its serving BS. The term η_{FFR} represents the fraction of available bandwidth whose allocation is coordinated among the cell-edge users.

The results shown in Figure 4.6 demonstrate that operating the entire frequency bandwidth with a reuse factor of 3 improves the user throughput at the lower 10^{th} percentile compared to a full chunk reuse scheme; both in the DL and the UL mode. In particular, lower 10^{th} percentile user throughputs of 1.94 Mbps (DL) and 1.93 Mbps (UL) are achieved with frequency planning scheme using a reuse factor of 3 on the entire bandwidth. However, due to an overcautious reuse of chunks, a median system throughput of only 37.2 Mbps/cell is achieved both in the DL and the UL mode. This shortcoming is addressed by using FFR scheme and appropriately choosing the η_{FFR} parameter. The results show that using $\eta_{\mathrm{FFR}} = 0.5$, both the lower 10^{th} percentile of user throughput and median system throughput are enhanced simultaneously compared to both the full reuse system and the system operating with a reuse factor of 3 on the entire bandwidth. Using FFR and setting $\eta_{\mathrm{FFR}} = 0.5$, a median system throughput of 65.0 Mbps/cell (DL) and 68.2 Mbps/cell (UL) and a lower 10^{th} percentile of user throughput of 2.1 Mbps (DL) and 2.5 Mbps (UL) are achieved. The performance may be further optimised by adjusting the boundary between the cell-edge users and the cell-centre users as well as by adjusting the η_{FFR} parameter. Optimisation of FFR scheme is not further considered in this thesis but it is worth pointing out that fractional frequency reuse scheme is a preemptive approach for ICIC and does not completely solve the hidden and the exposed node problem. These shortcomings are addressed by utilising BB signalling so that the hidden and exposed node problem are solved.

4.8.1.2 Decentralised ICIC using BB signalling approach

The impact of the choice of interference threshold parameter on the mean system throughput in an OFDMA-TDD network operating in Manhattan scenario is depicted in Figure 4.7. It can be observed that the number of bits transmitted (corresponding to set $\mathcal{A}$) and those received above the SINR target (corresponding to set $\mathcal{B}$) are approximately equal for the lower values of I_{th}. In particular, by setting the threshold parameter to -115 dBm, a reserved chunk is only reused if the combined interference and noise power remains below -115 dBm. This requires that the contribution from the interference component remains below the noise floor, which is

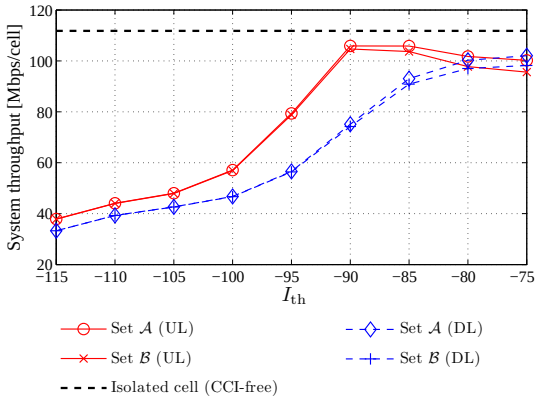

Figure 4.7: *Impact of I_{th} on mean system throughput using 16-QAM with SINR target of 11.3 dB in a Manhattan cellular scenario.*

at -117.4 dBm/chunk. Among the thresholds considered in Figure 4.7, using the threshold of -115 dBm results in the lowest mean system throughput because the size of the exclusion region enforced around the active receiver is the largest. By increasing the threshold, the system throughput gradually improves until the maximum is reached. The results in Figure 4.7 demonstrate that the mean system throughput is maximised by setting the thresholds to -75 dBm and -90 dBm in the DL and UL modes respectively. The maximum mean system throughputs achieved are 98.2 Mbps (88% of peak throughput in an isolated cell) and 104 Mbps (94% of peak throughput in isolated cell) in the DL and UL modes respectively. Due to interference diversity (discussed in Section 4.5.2) in the UL mode, the maximum system throughput achieved in the UL mode is larger than that achieved in the DL mode.

The impact of the threshold parameter on the system throughput and the user throughput is depicted in Figure 4.8. In the DL mode, the median system throughput is maximised by setting the threshold to -75 dBm (see Figure 4.8(a)). However, by setting the threshold to -75 dBm, 15% of all users in the system are in outage (see Figure 4.8(c)). In such scenario, the system throughput is maximised by serving higher data rates to the users located closer to their serving BS and starvation of users located at the cell-edge. By lowering the threshold, the CCI caused towards the cell-edge users is lowered at the cost of spatial reuse. As a result, the achieved SINR at the cell-edge is improved as a result of which the cell-edge user throughput (defined as the lower 10^{th} percentile of user throughput) increases. The results show that by setting the threshold to -90 dBm, the cell-edge user throughput is enhanced to 1.7 Mbps, which is achieved at a cost of 20% reduction in median system throughput compared to the median system throughput achieved by setting the threshold to -75 dBm in the DL mode. If the threshold

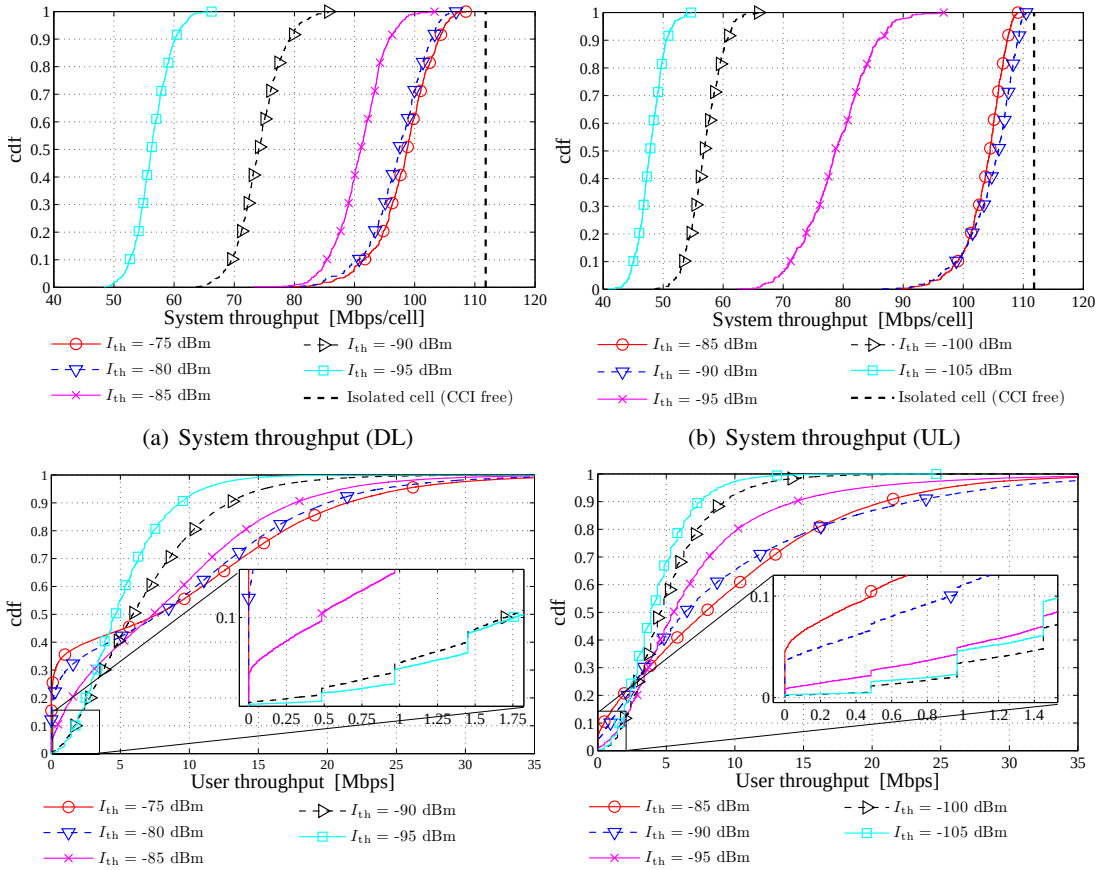

(a) System throughput (DL)

(b) System throughput (UL)

(c) User throughput (DL)

(d) User throughput (UL)

Figure 4.8: *Trading system throughput and user throughput by adjusting the interference threshold parameter in Manhattan cellular scenario.*

is lowered beyond -90 dBm, this decreases the overall number of chunks used at the BS and therefore significantly lowers the throughput for the cell-centre users whilst the throughput for the cell-edge users is improved very slightly. The results show that by setting the threshold to -95 dBm, the 90^{th} percentile of user throughput reduces by approximately 30% whilst the cell-edge user throughput improves only 3% (*i.e.* by 50 kbps). For this reason, a threshold of -90 dBm is chosen so as to enhance the cell-edge user throughput. Likewise, in the UL mode, the median system throughput is maximised by setting the threshold to -90 dBm (see Figure 4.8(b)). At this threshold, a median system throughput of 105.9 Mbps/cell and a cell-edge user throughput is 930 kbps is achieved. By adjusting the threshold to -100 dBm, the cell-edge user throughput is maximised, where a cell-edge user throughput of 1.93 Mbps is achieved at a cost of 50 Mbps (a reduction of 47%) in median system throughput. In light of these results, it can be concluded that the trade-off is more favourable in the DL mode rather than in the UL mode. This is because in the DL mode, the cell-edge users suffer from highest CCI as well as lowest intended channel gains. By reducing spatial reuse, SINR is improved which enables the cell-edge users to meet their SINR targets, which enhances the cell-edge user throughput in the DL mode. By contrast, in the UL mode the detrimental effects of CCI tend to be distributed among all users connected to the considered BS. In addition, the cell-edge users in the tagged cell are more likely that the cell-center users to be located within the exclusion region set in an adjacent cell than the cell-centre users when the threshold parameter is decreased. Therefore, the overall number of chunks available for the cell-edge users is reduced as the threshold is lowered, which potentially reduces the cell-edge user throughput. This effect is particularly observed when the threshold is reduced from -95 dBm to -100 dBm in the UL mode that the user throughput is only enhanced by 120 kbps whilst the system throughput degrades by 22 Mbps compared to the median system throughput achieved using a threshold of -95 dBm in the UL mode.

4.8.1.3 Comparison of results

The results obtained using the fixed power BB (discussed in Section 4.8.1.2) are compared against the system using variable BB power for interference tolerance signalling (labelled BB-ITS) and the system performing a full reuse of chunks. For the system utilising a fixed BB power, two thresholds each are chosen for both the UL and the DL modes. The first threshold is chosen such that it maximises the median system throughput whereas the second threshold chosen such that it enhances the cell-edge user throughput. To this end, the thresholds of

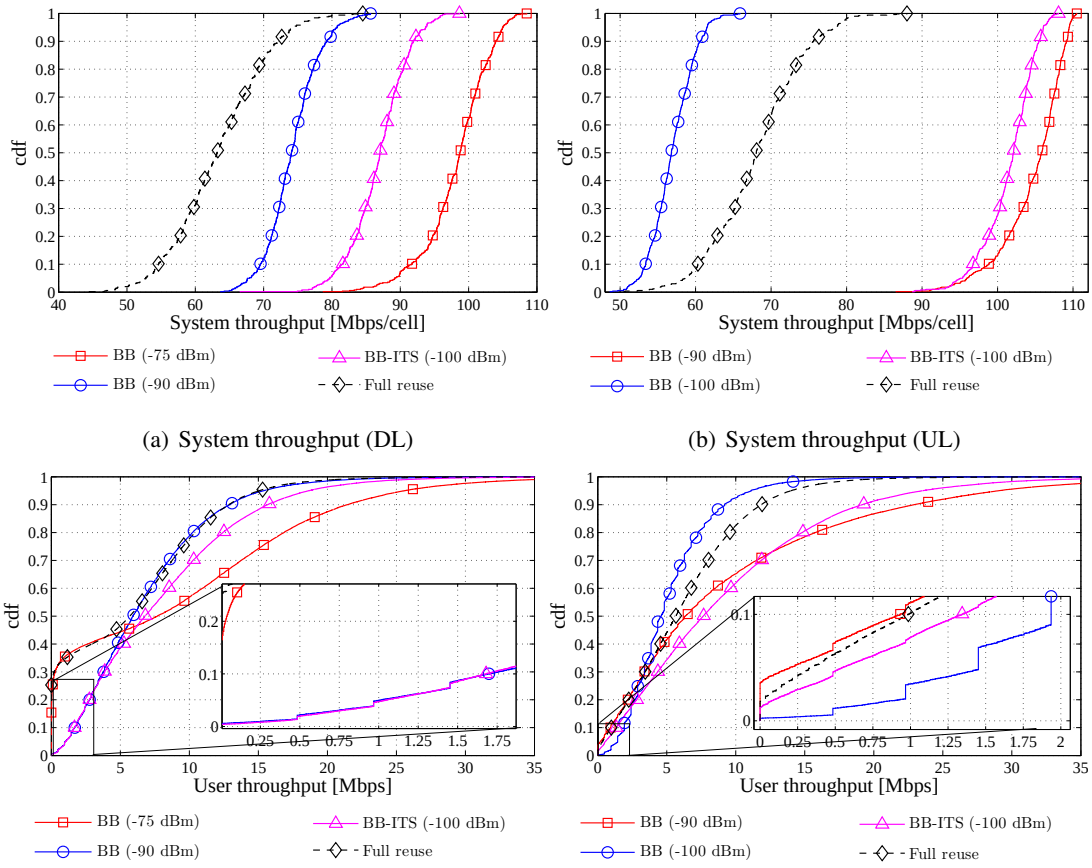

(a) System throughput (DL)

(b) System throughput (UL)

(c) User throughput (DL)

(d) User throughput (UL)

Figure 4.9: *Comparison of system throughput and user throughput with BB-enabled CCI mitigation approaches using fixed BB power and interference tolerance using variable BB power and benchmark system in a Manhattan cellular scenario.*

-75 dBm (DL) and -90 dBm (UL) are chosen so as to maximise the median system throughput whereas the thresholds of -90 dBm (DL) and -100 dBm (UL) are chosen so as to maximise the cell-edge user throughput. A threshold of -100 dBm is chosen for BB-ITS, such that the probability that the BB power clips to maximum power is kept below 5%.

Figure 4.9(a–d) depicts the cdf of user throughput and system throughput. The results demonstrate that the BB-enabled interference avoidance mechanism outperforms the system performing full reuse of chunks both in terms of median system throughput and cell-edge user throughput. The system performing full reuse of chunks achieves a median system throughput of 68 Mbps (UL) and 63 Mbps (DL) and a user throughput of 980 kbps (UL) and a 25 % outage in the DL. Compared to the full reuse system, the BB mechanism with the threshold set to maximise system throughput attains a 56% (UL) and 52% (DL) improvement in median system throughput. Likewise, when the threshold is set to maximise the user throughput, the BB-mechanism improves the cell-edge user throughput to 1.7 Mbps compared to a 25% outage with a full reuse system in the DL mode. Likewise, in the UL mode, the BB approach improves the cell-edge user throughput by 85%. These improvements are in addition to the 24 % (DL) and 33% (UL) in the median system throughput compared to the benchmark.

The results of utilising variable BB power to signal the interference tolerance of individual links, termed BB-ITS, are also included in Figure 4.9(a–d). The results demonstrate that BB-ITS achieves a median system throughput of 88 Mbps (DL) and 102 Mbps (UL) together with the cell-edge user throughput of 1.7 Mbps (DL) and 1.3 Mbps (UL) (see Figure 4.9(c-d)), at a modest degradation in system throughput (see Figure 4.9(a-b)) compared to the BB scheme where fixed power BB and a threshold to maximise the median system throughput are used. BB-ITS, therefore, not only avoids the need to tune the interference threshold so as to match a certain interference scenario (for example in UL or DL), but also achieves a preferable compromise between maximising system throughput and enhancing the cell-edge user throughput.

The distribution of user throughput as a function of distance from the serving BS is depicted in Figure 4.10. It can be observed that the cell-edge user throughput (measured beyond 400 m) is compromised both when the threshold is chosen so as to maximise the system throughput and when a full reuse of chunks is considered. Particularly in the DL mode, by setting a threshold of -75 dBm, the average user throughput is close to 0 Mbps for distance beyond 400 m. At such thresholds, the chunks are primarily used to serve the cell-centre users. By adjusting the threshold, the protection from CCI for these users is enhanced at the cost of throughput for

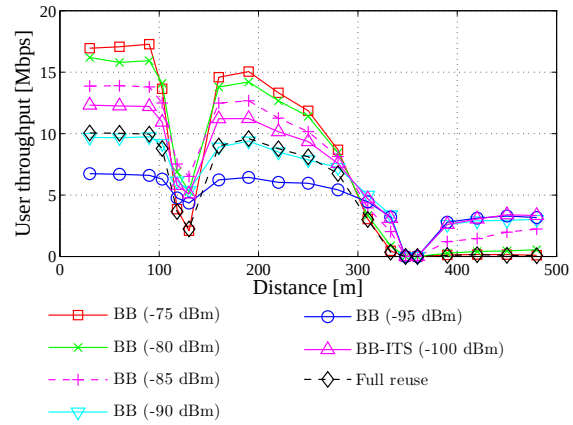

(a) DL

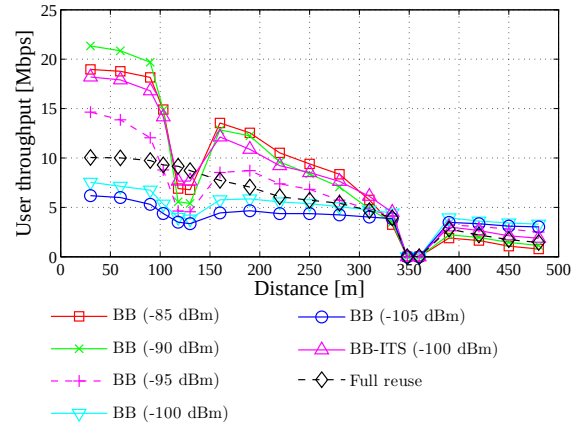

(b) UL

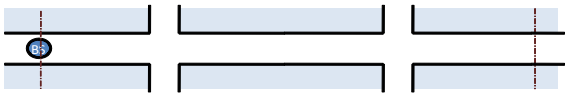

Figure 4.10: *Mean user throughput vs. distance from the serving BS, d, for BB-OFDMA with 16-QAM modulation for different interference thresholds I_{th}. For comparison results for full frequency reuse without interference protection are also included. Note that at d=115 m, links are exposed to strong LoS interference (data in DL, BB in UL) from cells in perpendicular streets, which compromises throughput, while at d=345 m, the MSs are connected to the BS in a perpendicular street due to better channel gains.*

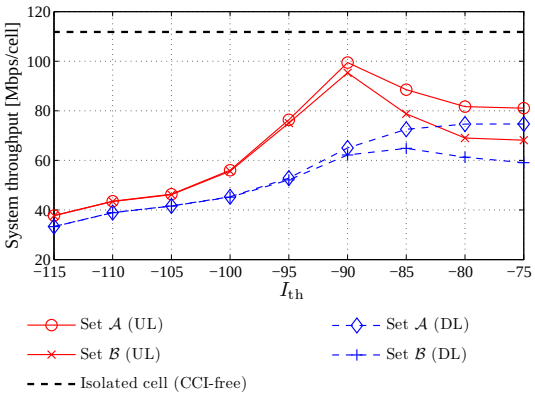

Figure 4.11: *Impact of varying I_{th} with a fair score-based scheduler (FSBS) in Manhattan scenario.*

cell-centre users.

The results presented demonstrate two notable differences between the UL mode and the DL mode. First, at the street crossing located between 100 m and 130 m, the user throughput drops as the threshold is increased. At this location, the user throughput is the minimum when the chunks are fully reused in the DL mode. By contrast, in the UL mode, the throughput is the highest when the chunks are fully reused. This is because the MSs at the first street crossings suffer from LoS interference from the BS located at the perpendicular street in the DL whereas these MS cause CCI towards the BS located at the perpendicular street in the UL mode. Second, a drop in the user throughput is more gradual in the UL mode whereas in DL mode the throughput drops more abruptly after crossing 220 m from the serving BS. This is because in the UL mode, the CCI caused due to chunk reuse in the neighbouring cell remains constant regardless of the MS location in the tagged BS whereas in the DL mode, the CCI is lower towards the centre and higher towards the cell-edge, assuming a full reuse. This results in a linear increase in SINR in the UL and a quadratic increase in SINR in the DL when the MS in the tagged cell moves from the cell-edge towards the cell-centre. In Figure 4.10, the average user throughput is shown to be 0 at the street crossing located at $d = 345$ m from the serving BS. This is because the MS located at the second street crossing are actually connected to the BS in the perpendicular street due to a lower path loss.

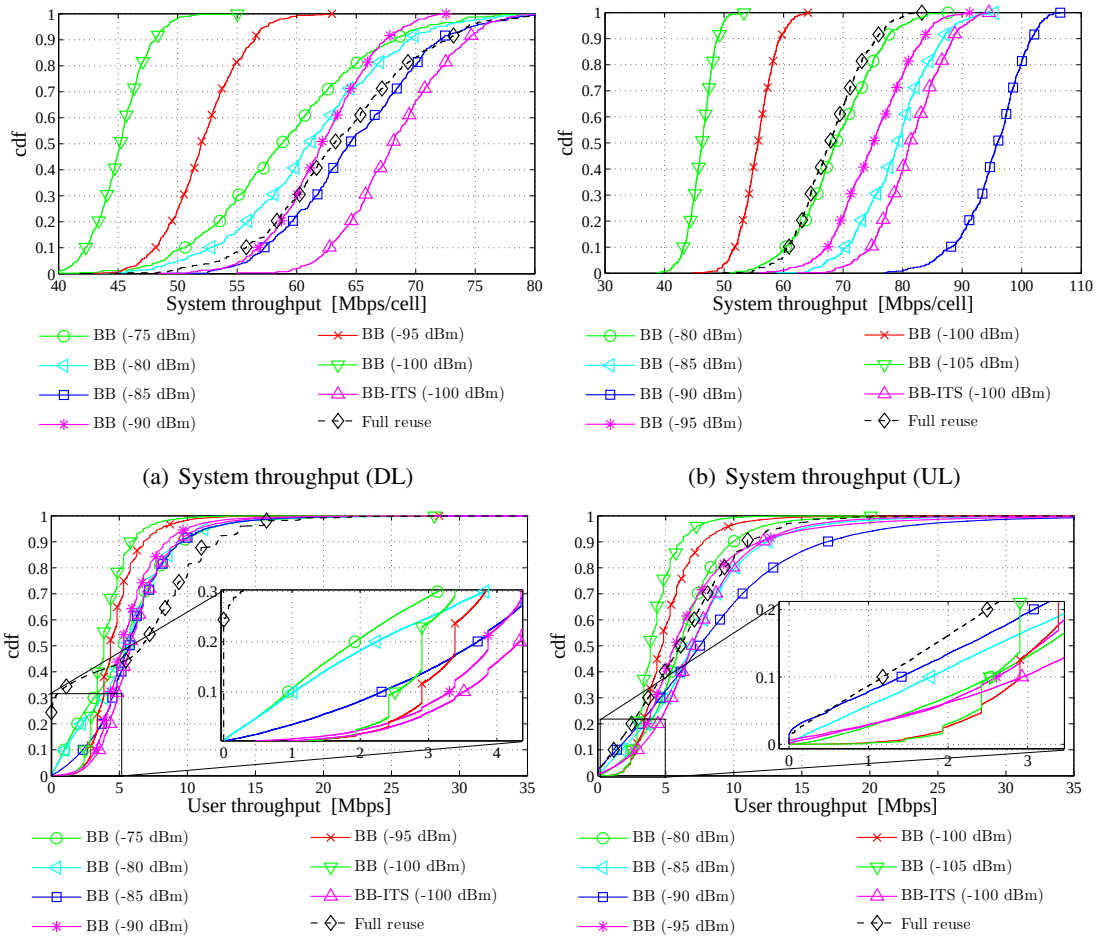

(a) System throughput (DL)

(b) System throughput (UL)

(c) User throughput (DL)

(d) User throughput (UL)

Figure 4.12: *Comparison of BB-enabled CCI mitigation approaches with full reuse using a fair score-based scheduler in Manhattan scenario.*

4.8.1.4 Performance of fair score-based scheduler

The results considered in Section 4.8.1.2 assumed a scheduler that assigned an unreserved chunk to a competing user solely based on the channel gains to the intended BS. The main problem associated with this scheduler is that (4.13) may not hold true for user ν where it has favourable scores and vice versa. This issue is addressed by adding a priority penalty factor to the score, such that the score grows exponentially with every additional chunk allocated to a given user. This prioritises user ν over another user $\mu \neq \nu$ where μ has a better rank on the channel gain but already has more chunks allocated to it than user ν.

The impact of interference threshold on mean system throughput is depicted in Figure 4.11. Comparing these results against those in Figure 4.7, it can be observed that the differences between set $\mathcal{A}$ and set $\mathcal{B}$ is larger when FSBS is used relative to the case when BSBS is used at higher thresholds (*e.g.* -75 dBm). This is because a larger value of I_{th} compromises protection from CCI and potentially allows a full reuse of chunks. However, due to high CCI, the SINR targets are not met and the chunks are released. As the scores are more favourable for users with fewer chunks already allocated, the released chunks are more likely to be allocated to another cell-edge user in the next frame. This results in a *ping-pong* effect where the chunks are allocated, fail to meet the SINR target and are released in succession, as a result of which the FSBS attains a lower throughput compared to the BSBS mechanism for allocating unreserved chunks. It is interesting to note that when a high threshold (*e.g.* -75 dBm) is used (see Figure 4.12(c)), the user throughput with FSBS mechanism is higher than that observed with the BSBS mechanism. This is because significantly fewer chunks are assigned on average in each cell (which can be inferred from Figure 4.11), which is due to the fact that once the chunks are released they are only allocated in a given cell with probability p. Furthermore, they are primarily allocated to cell-edge users. Therefore, the cell-edge users are able to meet the SINR target during those time slots when the transmitter in the adjacent cell has not accessed the chunks allocated to the cell-edge users in the tagged cell. This contributes to an increased system throughput at the cell-edge with the FSBS scheduler when a high threshold such as -75 dBm is set.

The results show that the cell-edge user throughput is maximised by setting thresholds to -90 dBm and -100 dBm in DL and UL modes respectively (see Figure 4.12(c-d)). By setting these thresholds, the cell-edge user throughputs are 3.3 Mbps (DL) and 2.9 Mbps (UL) respectively. By setting the same thresholds but with BSBS mechanism, user throughputs of 1.75 Mbps (DL) and 1.93 Mbps (UL) were achieved. Likewise, with BB-ITS mechanism, cell-

edge user throughput of 1.7 Mbps (DL) and 1.4 Mbps (UL) were achieved with BSBS scheduler and 3.5 Mbps (DL) and 2.9 Mbps (UL) with the FSBS scheduler. Clearly, when the thresholds are set so as to maximise the cell-edge user throughput, FSBS outperforms the BSBS scheduler in terms of the cell-edge user throughput. This difference is explained as follows - first of all, the unreserved chunks in a cell are allocated using a $p-$persistent approach. Moreover, only those chunks that meet the SINR target ($\Gamma_m = 11.3$ dB for $m = 4$) can be reserved with BB signalling to avoid detrimental CCI. Furthermore, when entities in two adjacent cells access an unreserved chunk simultaneously, it is more likely for a cell-centre user that a cell-edge user to meet the SINR target. Taking the aforesaid three points into account, on average the users closer to the cell-centre succeed in reserving a larger number of chunks than their cell edge counterparts, when unreserved chunks are accessed in two adjacent cells in contention. With the BSBS mechanism, an unreserved chunk is equally likely to be allocated to a cell-edge user as it is likely to be allocated to a cell-centre user depending on score. The FSBS mechanism attempts to balance the number of chunk allocated to the cell-edge users and the cell-centre users by incorporating the priority penalty factor. This ensures that the cell-centre users are allocated additional unreserved chunks with a lower priority than the cell-edge users in the subsequent frames. Consequently, the FSBS mechanism improves the cell-edge user throughput compared to the BSBS mechanism when threshold is chosen to maximise user throughput. Since FSBS mechanism allocates a larger number of chunks to the cell-edge than the BSBS mechanism, the spatial reuse is lower with the former. In particular, with FSBS mechanism median system throughputs of 62.15 Mbps/cell (DL) and 55.7 Mbps/cell (UL) are achieved by setting thresholds to -95 dBm and -100 dBm respectively and 68.1 Mbps/cell (DL) , 81.8 Mbps/cell (UL) is achieved with BB-ITS mechanism (see Figure 4.12(c)). This represents approximately 20% reduction in median system throughput compared to the BSBS mechanism.

4.8.2 ICIC on system performing link adaptation

The results presented in this section assume that link adaptation is performed on a per-chunk basis reflecting the prevalent channel conditions at the receiver. The modulation format utilised and their corresponding SINR targets are taken from Table 3.2.

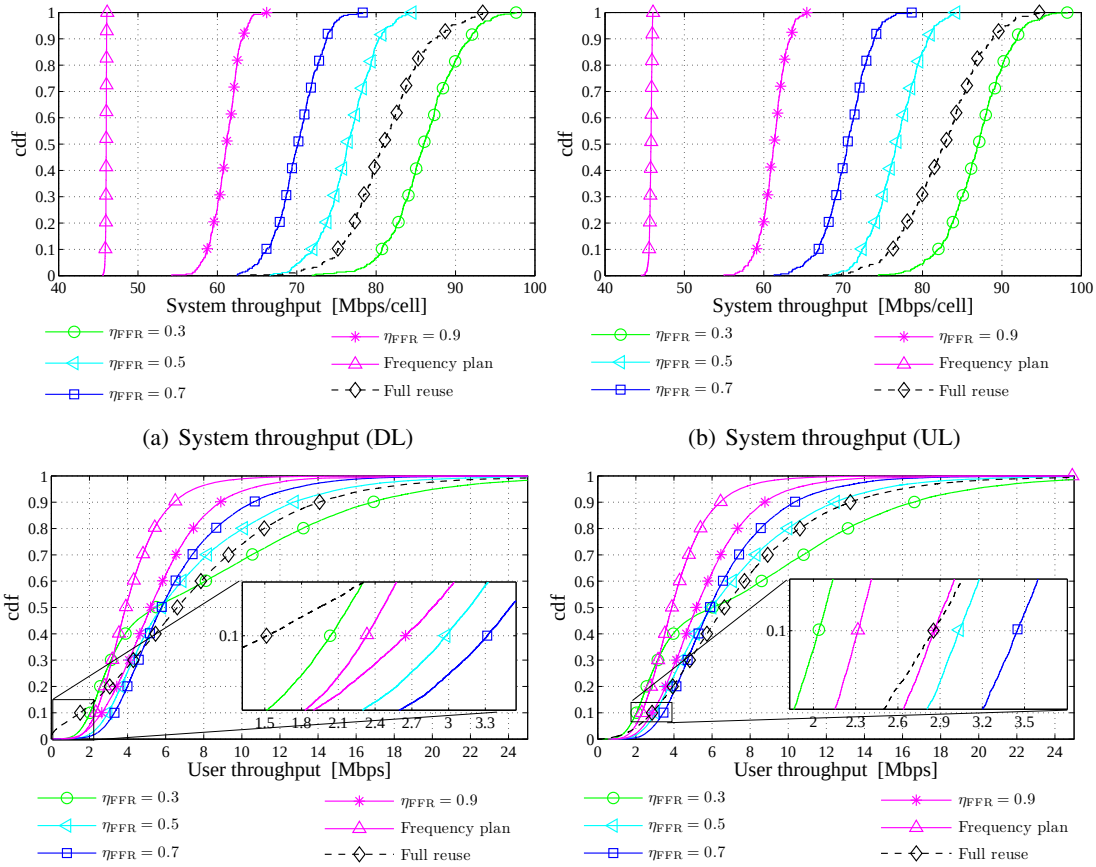

(a) System throughput (DL)

(b) System throughput (UL)

(c) User throughput (DL)

(d) User throughput (UL)

Figure 4.13: *Performance of frequency planning schemes by performing link adaptation on a per-chunk basis.*

4.8.2.1 Centralised frequency planning approach

Figure 4.13 investigates the use of centralised frequency allocation schemes in a system performing link adaptation on a per-chunk basis. All system parameters are identical to those considered for the system utilising a fixed modulation scheme of 16-QAM (see Section 4.8.1.1). The result demonstrate that coordination of the entire system bandwidth with a reuse factor of 3 performs worst in terms of system throughput both in the DL and the UL modes (see Figure 4.13(a-b)), as expected. Moreover, the system throughput is maximised when the resources are primarily allocated towards the cell-centre users. The cell-centre users benefit from high channel gains and/or lower CCI and are able to utilise higher order modulation formats even when the chunks are fully reused. Consequently, it is observed that the full reuse system and FFR system with $\eta_{\mathrm{FFR}} = 0.3$ perform best in terms of system throughput. In terms of user throughput in the lower 10^{th} percentile, the highest user throughput is observed when FFR with $\eta_{\mathrm{FFR}} = 0.7$ is set both in the UL and DL modes (see Figure 4.13(c-d)). In addition, frequency planning with reuse factor 3 performs better than full reuse in terms of lower 10^{th} percentile of user throughput in the DL whereas the system performing a full reuse of chunks outperforms frequency planning with reuse factor 3 in the UL. This is because of interference diversity in the UL mode because of which the achieved SINRs tend to be better in the UL mode rather than in the DL mode.

4.8.2.2 Decentralised ICIC using BB signalling approach

Figure 4.14 examines the impact of the threshold parameter on the system where link adaptation is performed on a per-chunk basis. Similar to the results obtained in the system where fixed modulation format was utilised systemwide, it is demonstrated that the threshold parameter can be adjusted to trade-off cell-edge user throughput and the median system throughput in a system performing link adaptation. The median system throughput can be maximised by setting the thresholds of -75 dBm (DL) and -90 dBm (UL). By setting the threshold to -75 dBm in the DL, the median system throughput is 129 Mbps and the cell-edge user throughput is 829 kbps. By adjusting the threshold to -90 dBm, a maximum cell-edge user throughput of 3.2 Mbps can be achieved at a cost of 50 Mbps/cell in median system throughput. Likewise, in the UL mode, setting the threshold to -90 dBm maximises the median system throughput. The corresponding median system throughput achieved is 147.4 Mbps/cell and the cell-edge user throughput achieved is 2.8 Mbps. By adjusting the threshold to -100 dBm, a cell-edge user throughput of

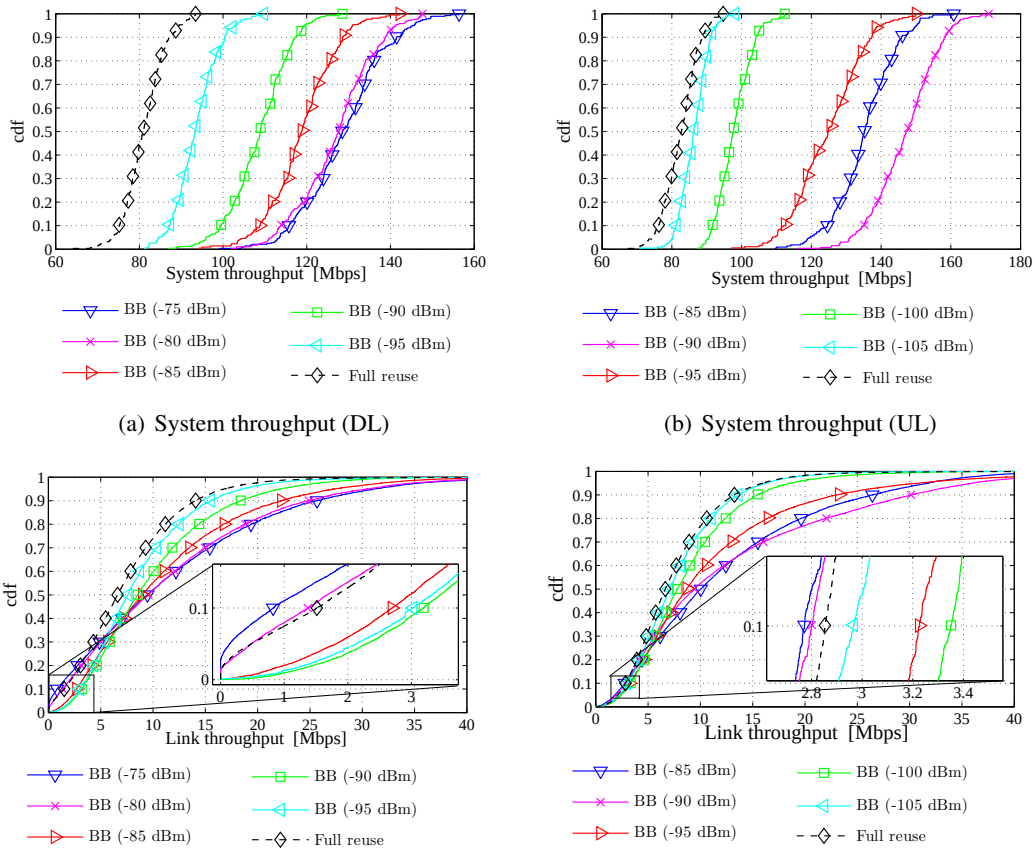

(a) System throughput (DL)

(b) System throughput (UL)

(c) User throughput (DL)

(d) User throughput (UL)

Figure 4.14: *Comparison of BB-enabled CCI mitigation and full chunk reuse system with link adaptation in a Manhattan cellular scenario.*

2.35 Mbps can be achieved at a cost of 20 Mbps/cell in median system throughput. Thus, the results demonstrate that the trade-off is more favourable in DL than in the UL mode, similar to the observations made with fixed modulation applied systemwide.

With link adaptation performed, spatial reuse increases with the threshold parameter as depicted in Figure 4.15(a-b). This results in an increased CCI due to which the achieved SINR degrades. By utilising receiver feedback, the transmitter then selects an appropriate modulation format corresponding to the SINR achieved at the receiver. This is depicted in Figure 4.15(c-d) that when the spatial reuse increases, the number of bits conveyed by each OFDM symbol decreases. In particular, the full reuse system that utilises all available 230 chunks only conveys approximately 3 bits/symbol on average. By contrast, with BB signalling up to 6.5 bits/symbol on average can be carried. Provided that a fixed transmit power per chunk is assumed and the links are interference limited rather than noise limited, an increase in the number of chunk increases the amount of energy used for transmission and vice versa. The results in Figure 4.15(e-f) demonstrate that the threshold parameter can be used to balance the energy consumption and system performance. In particular, the throughput at the cell-edge can be maximised and the energy consumption can be decreased simultaneously. In this context, by adjusting the threshold from -90 dBm to -95 dBm, a 10% saving in energy consumption together with a 10% enhancement in the cell-edge user throughput is achieved in the UL mode.

4.8.2.3 Performance of fair score-based scheduler

Criteria	Scheduler	UL			DL		
		I_{th}[dBm]		Full	I_{th}[dBm]		Full
		-90	-100	reuse	-75	-90	reuse
Median system throughput [Mbps/cell]	BSBS	147	98	83	129	109	81
	FSBS	134	96	76.5	114	104	73.7
10^{th}percentile user throughput [Mbps]	BSBS	2.8	3.4	2.9	0.83	3.2	1.6
	FSBS	4.0	4.7	3.1	1.7	4.4	1.7
Allocated chunks/cell	BSBS	229	135.5	230	228.5	162.5	230
	FSBS	228	180.6	135.0	214.4	158.8	230
Bits/symbol	BSBS	4.9	5.9	2.9	4.7	5.558	2.96
	FSBS	4.9	5.9	2.9	4.7	5.6	3.0
Energy consumption [nJ/bit]	BSBS	25.1	22.5	45.1	28.7	24.2	46.18
	FSBS	27.5	22.8	48.8	30.9	24.8	50.7

Table 4.4: *Comparison of fair score based scheduler and blind score based scheduler*

The performance of incorporating a FSBS mechanism with link adaptation in Manhattan sce-

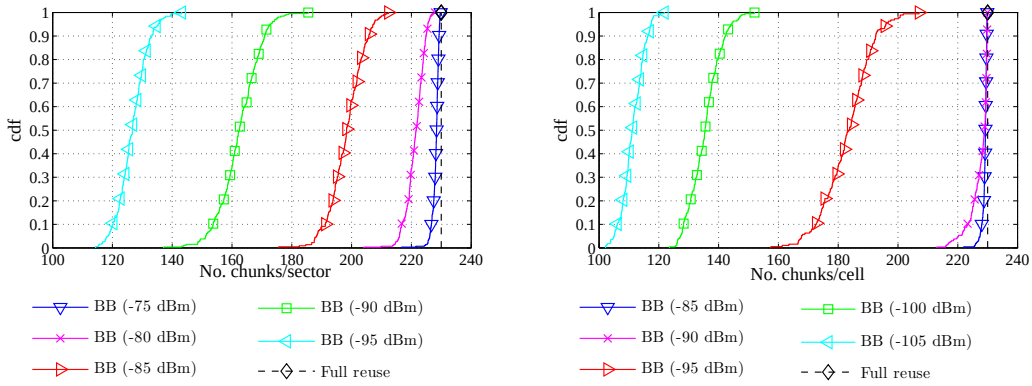

(a) Chunk reuse (DL)

(b) Chunk reuse (UL)

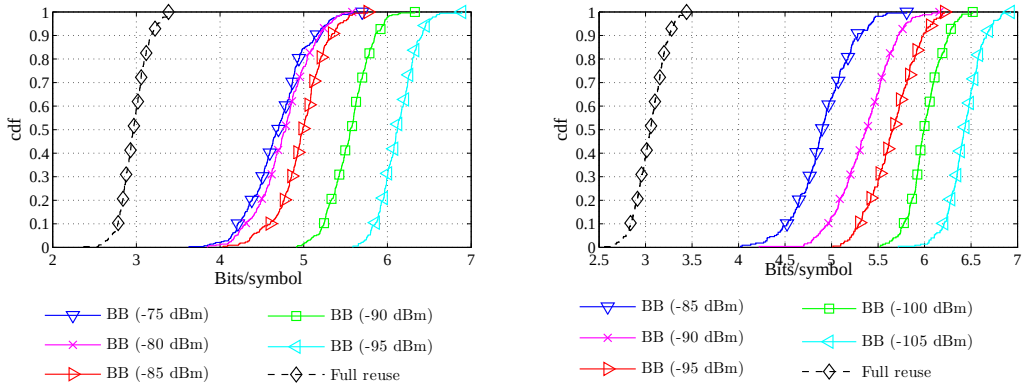

(c) Bits per symbol (DL)

(d) Bits per symbol (UL)

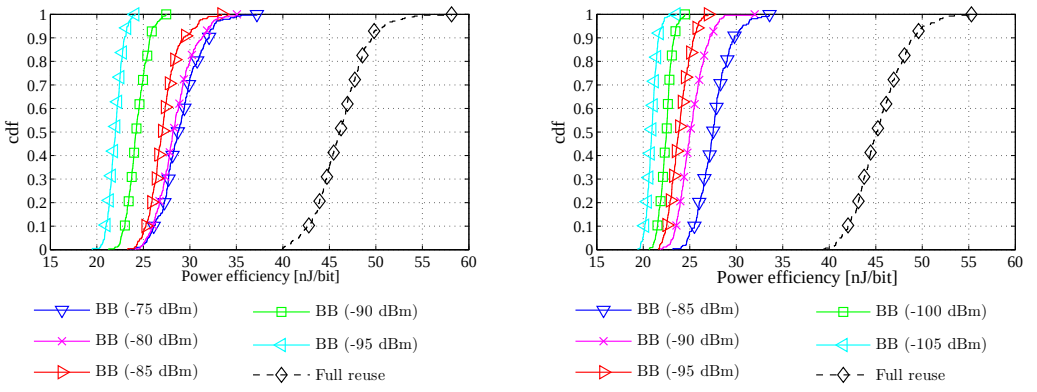

(e) Energy consumption (DL)

(f) Energy consumption (UL)

Figure 4.15: *Comparison of spatial reuse, used modulation scheme and energy consumption with BB-enabled CCI mitigation and full chunk reuse system with link adaptation in a Manhattan cellular scenario.*

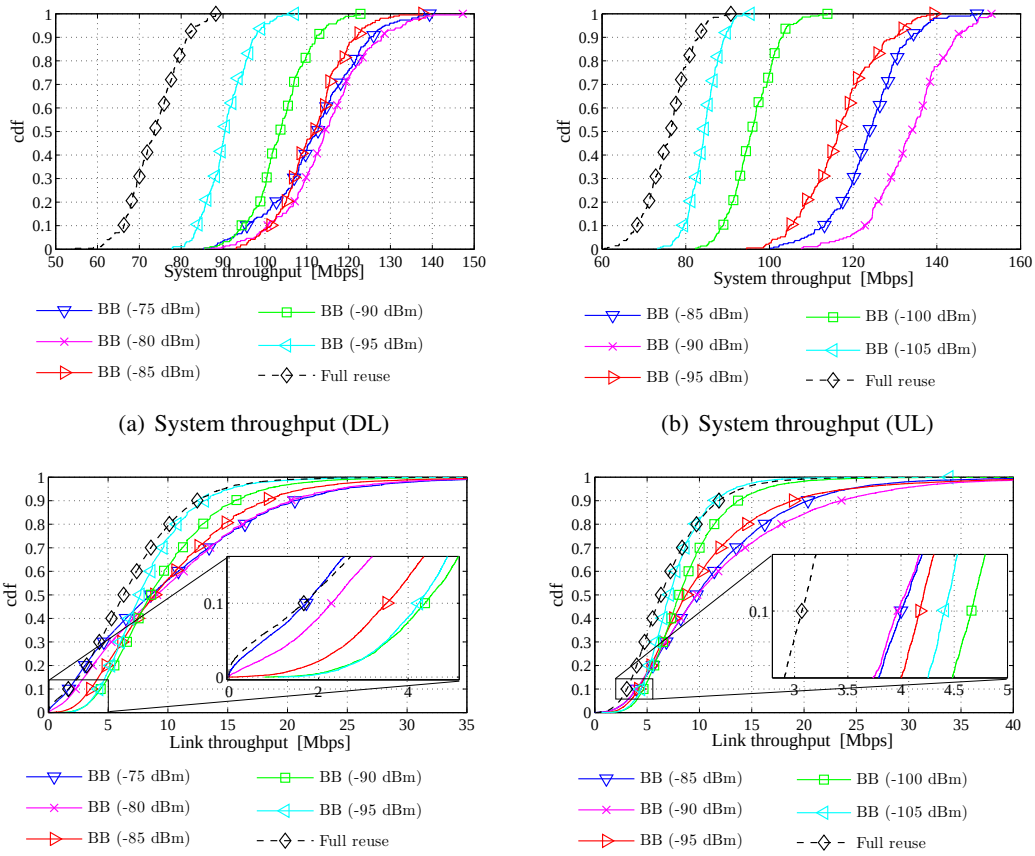

(a) System throughput (DL)

(b) System throughput (UL)

(c) User throughput (DL)

(d) User throughput (UL)

Figure 4.16: *Comparison of performance of fair score based scheduler with BB-enabled CCI mitigation and full chunk reuse system in a Manhattan cellular scenario.*

nario is presented in Figure 4.16. By applying fair scheduler, the cell-edge throughput is improved to 4.4 Mbps (DL) and 4.66 Mbps (UL) by setting the thresholds to -90 dBm and -100 dBm respectively. Likewise, median system throughputs of 114.4 Mbps/cell (DL) and 123.8 Mbps/cell (UL) are achieved by setting the thresholds to -75 dBm and -90 dBm respectively. The FSFS mechanism enhances the cell-edge user throughput by 36% (DL) and by 38% (UL) compared to the BSBS mechanism at a cost of less than 5% (DL) and less than 2% (UL) in terms of median system throughput, when the respective thresholds are set so as to maximise the cell-edge user throughput.

When the thresholds are set to maximise the respective median system throughputs, the FSBS mechanism enhances the cell-edge user throughput by 107% (DL) and 43% (UL) at a cost of 11% (DL) and 9% (UL) in terms of median system throughput (see Table 4.4). Due to an increase in threshold and consequently the spatial reuse, the overall CCI in the system increases. Consequently, some of the cell-edge users fail to meet the minimum SINR target (2.2 dB for BPSK modulation scheme). The chunks where the SINR target is not met are released. With FSBS mechanism unlike the BSBS mechanism, priority is given to the users that have fewer chunks already reserved. Such users are primarily cell-edge users and therefore only lower order modulation schemes can be supported for such users. By contrast, with the BSBS mechanism the likelihood of the cell-edge user accessing the released chunk is same as that of the cell-centre user. In the long term, the allocation of chunks is shifted from cell-edge users towards the cell-centre users. The cell-centre users are, on average, able to utilise higher order modulation schemes than the cell-edge users, which results in a higher system throughput with BSBS mechanism at the cost of cell-edge user throughput. Moreover, with the FSBS mechanism, the cell-edge users are favoured over the cell-centre users while allocating the released chunks. This can result in *ping pong* effects because of which the median system throughput reduces with the FSBS mechanism compared to the BSBS mechanism, when higher thresholds are utilised.

4.9 Results and Discussions: Hexagonal cellular scenario

In this section, ICIC is performed on the hexagonal cellular scenario as discussed earlier in Section 4.7.2.

4.9.1 ICIC on system utilising fixed modulation scheme

A fixed modulation scheme of 16-QAM with $3/4$-rate convolutional coding is considered systemwide. The corresponding minimum SINR target required for fulfilling QoS requirements is 11.3 dB (see Table 3.2).

4.9.1.1 Centralised frequency planning approach

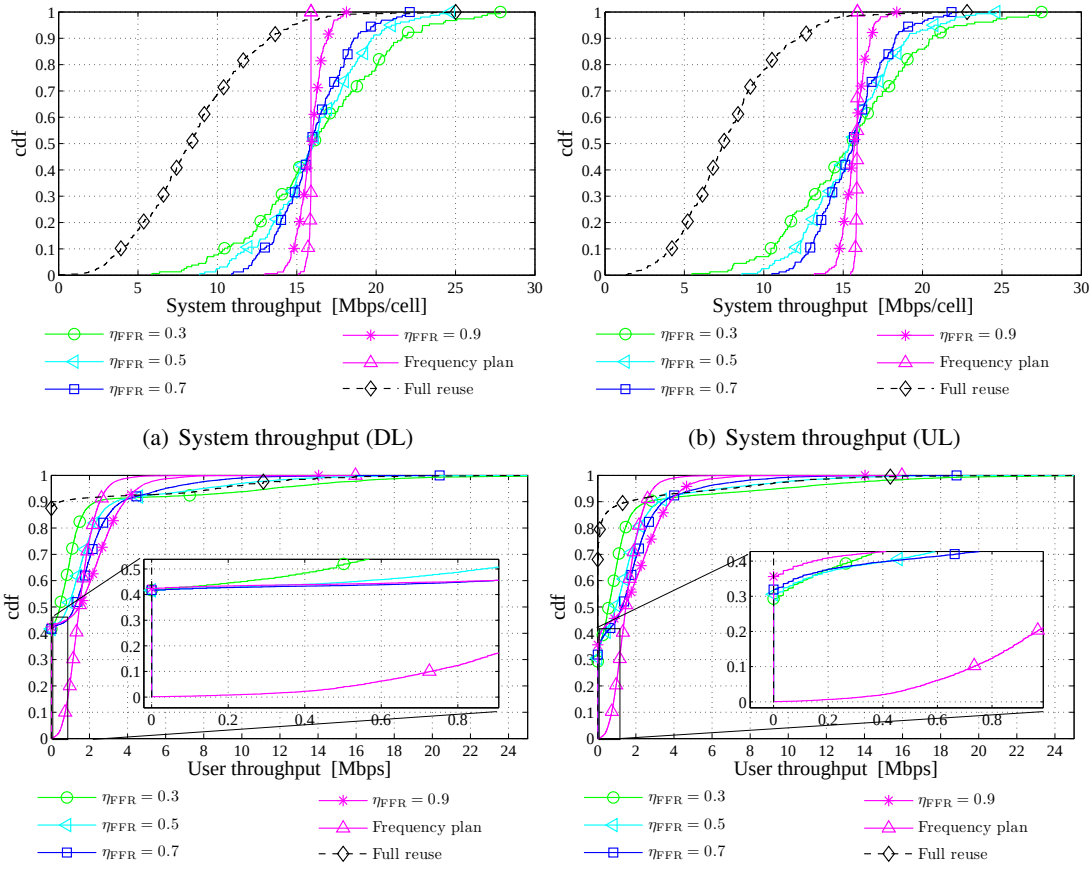

(a) System throughput (DL)

(b) System throughput (UL)

(c) User throughput (DL)

(d) User throughput (UL)

Figure 4.17: *Performance of frequency planning schemes using fixed modulation scheme of 16-QAM with an SINR target of 11.3 dB.*

The impact of using centralised frequency planning schemes for ICIC in hexagonal cellular scenario is depicted in Figure 4.17. The allocation of chunks is coordinated using a reuse factor of 7, such that no cell within the 1^{st} tier of the given cell reuses the chunks belonging to the coordinated frequency bandwidth. The results presented in Figure 4.17 show that a median system throughput of approximately 16 Mbps/cell is achieved both in the DL and the UL modes

in the systems performing fully coordinated frequency reuse with a reuse factor of 7, as well as the system performing fractional frequency reuse. The system with fully coordinated frequency reuse achieves a user throughput of 730 kbps (DL) and 740 kbps (UL). However, with FFR it is observed that the system suffers from an outage (zero throughput) of 40% (DL) and 30% (UL).

The spatial location of the users that are successfully served (non zero throughput) and the users in outage are plotted in Figure 4.18, where it can clearly be observed that outage occurs mainly at the boundary of the full reuse zone and the coordinated reuse zone. It was therefore identified that with an SINR target of 11.3 dBm, the borderline between the cell-centre users and the cell-edge users need to be made smaller than the median of the path loss of user population. To this end, the boundary was set up at $1/\Delta_{\mathrm{FFR}}$ of the median path loss of the user population. Likewise, the fraction of the resources allocated to the cell-centre user was also reduced reflecting the fact that there are now fewer users within the cell-centre region. With these adjustments, it was shown that using $\Delta_{\mathrm{FFR}} = 3$ with $\eta_{\mathrm{FFR}} = 0.9$ achieves outage less than 1.5% (see Figure 4.19(c-d)). Note that in order to completely avoid outage in the cell-centre region, allocation of chunks must be coordinated for the cell-centre as well as cell-edge users, which lowers the spatial reuse of chunks. For this reason, $\Delta_{\mathrm{FFR}} = 3$ with $\eta_{\mathrm{FFR}} = 0.9$ is chosen as suitable parameters for fractional frequency reuse when a fixed modulation format of 16-QAM is utilised systemwide. With these parameters, user throughputs of 645 kbps (DL) and 670 kbps (UL) at the lower 10^{th} percentile (see Figure 4.19(c-d)) and median system throughputs of 20.9 Mbps/cell (DL) and 21 Mbps/cell (UL) (see Figure 4.19(a-b)) are achieved.

4.9.1.2 Decentralised ICIC using BB signalling approach

The impact of threshold parameter on the mean system throughput in the hexagonal cellular scenario is depicted in Figure 4.20. The results demonstrate that the mean system throughput is maximised by setting the threshold parameter to -90 dBm both in the DL mode as well as the UL mode. The highest mean system throughput achieved is 22.5 Mbps/cell (DL) and 30 Mbps/cell (UL). This corresponds to 20% (DL) and 26% (UL) of peak throughput in an isolated cell. The overall system throughput is significantly lower in hexagonal cellular scenario compared to the Manhattan cellular scenario for two reasons. First, each cell is surrounded by six potentially interfering cells in hexagonal scenario within the first tier unlike two potentially interfering cells in Manhattan scenario. This results in an overall increased level of CCI in the hexagonal cellular scenario compared to the Manhattan scenario, provided that the chunks are

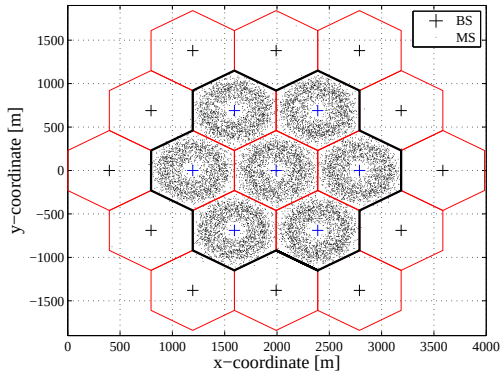

(a) Outage ($\Delta_{\mathrm{FFR}} = 1, \eta_{\mathrm{FFR}} = 0.7$)

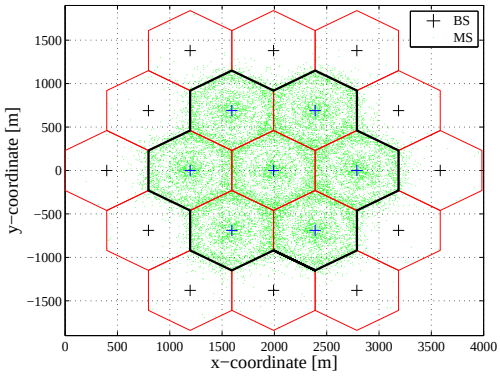

(b) Served ($\Delta_{\mathrm{FFR}} = 1, \eta_{\mathrm{FFR}} = 0.7$)

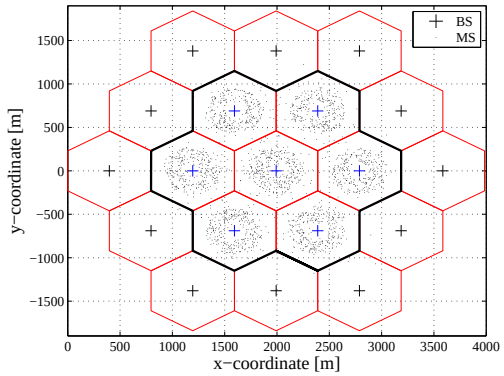

(c) Outage ($\Delta_{\mathrm{FFR}} = 2, \eta_{\mathrm{FFR}} = 0.8$)

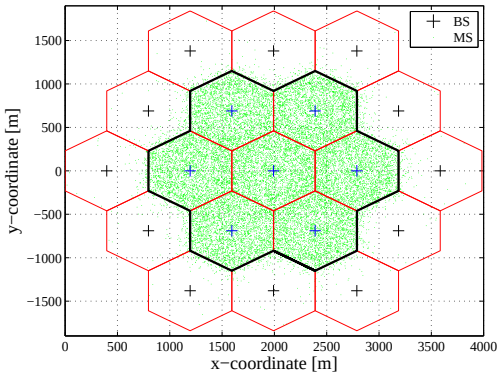

(d) Served ($\Delta_{\mathrm{FFR}} = 2, \eta_{\mathrm{FFR}} = 0.8$)

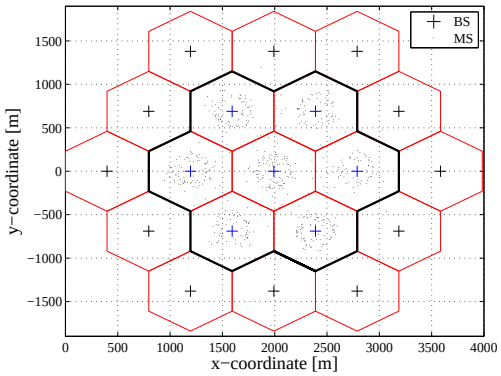

(e) Outage ($\Delta_{\mathrm{FFR}} = 3, \eta_{\mathrm{FFR}} = 0.9$)

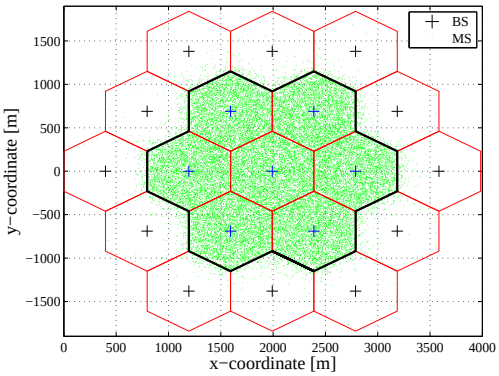

(f) Served ($\Delta_{\mathrm{FFR}} = 3, \eta_{\mathrm{FFR}} = 0.9$)

Figure 4.18: *Location of MSs in outage with fractional frequency ratio under different boundaries between cell-centre and cell-edge ($1/\Delta_{\mathrm{FFR}}$ of median path loss of user population) and fraction of resources allocated to cell-edge users (η_{FFR}).*

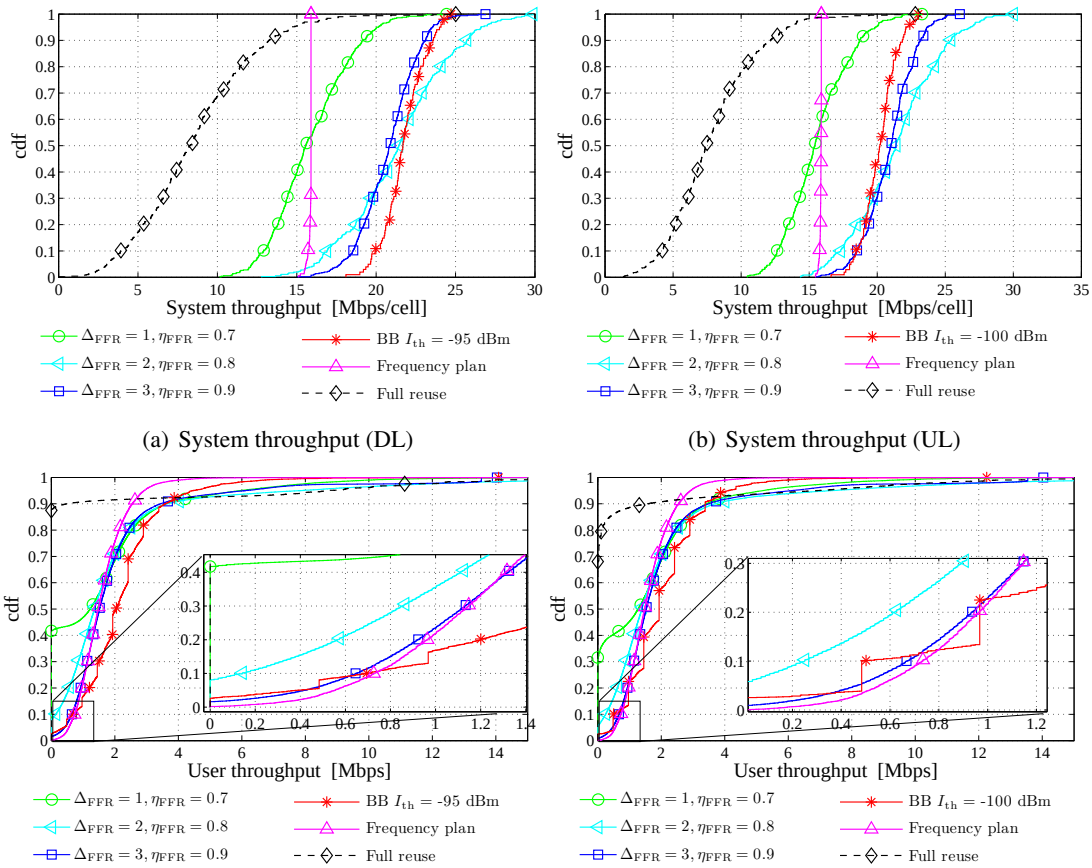

(a) System throughput (DL)

(b) System throughput (UL)

(c) User throughput (DL)

(d) User throughput (UL)

Figure 4.19: *Comparison of fractional frequency reuse with different size of full reuse region.*

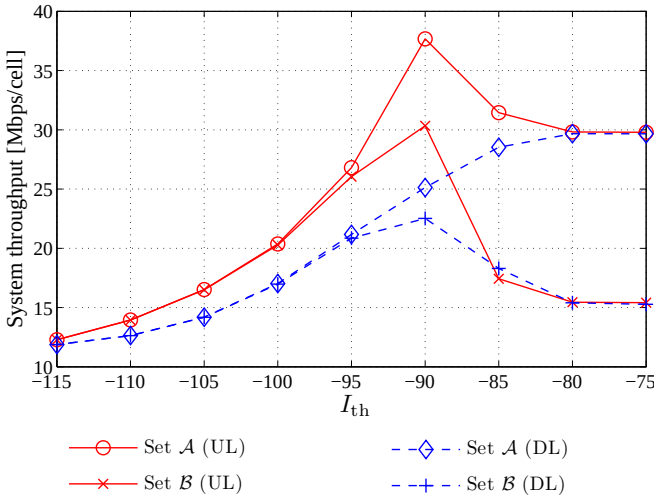

Figure 4.20: *Impact of I_{th} on mean system throughput using 16-QAM with SINR target of 11.3 dB in a hexagonal cellular scenario.*

fully reused in each cell. Second, assuming that the users are distributed uniformly in space, the users are more likely to be located towards the cell-edge than towards the cell-centre in the hexagonal cellular scenario. As a result, a chunk that is released by a cell-edge user after it fails to meet the SINR target is more likely to be allocated to another cell-edge user in the hexagonal scenario, unless appropriate backoff strategies are considered. As a result, *ping pong* effects are encountered more frequently which compromises the mean system throughput when CCI protection is lowered by utilising a high I_{th}.

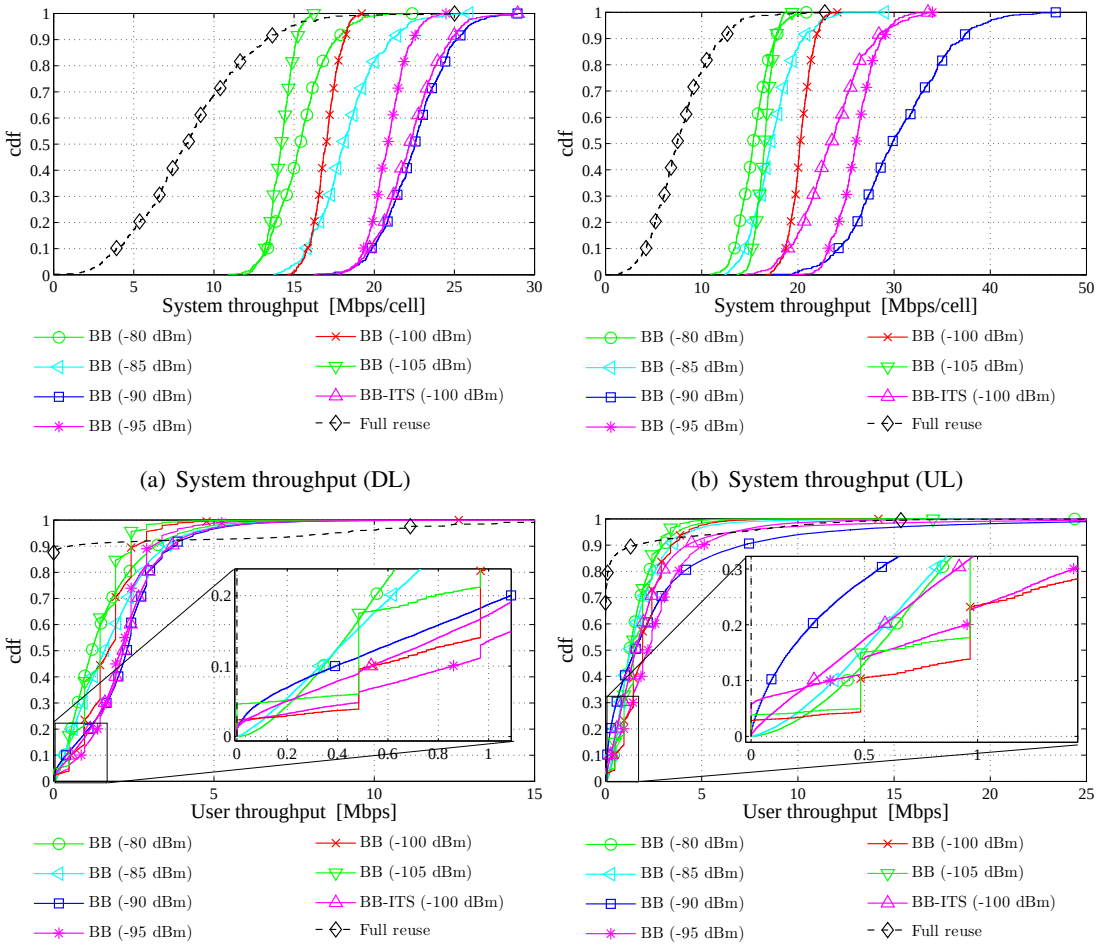

(a) System throughput (DL)

(b) System throughput (UL)

(c) User throughput (DL)

(d) User throughput (UL)

Figure 4.21: *Comparison of the threshold parameter on system throughput and user throughput with BB-enabled CCI mitigation approaches in a hexagonal cellular scenario using fixed BB power and interference tolerance using variable BB power (BB-ITS). For comparison, the full-frequency reuse system without interference protection is included.*

The impact of the threshold parameter on the system and user throughput is depicted in Fig-

ure 4.21 for BB-enabled CCI mitigation approach. For comparison, the results from the system performing full reuse of chunks are also included. With full reuse of chunks, the results show that the system suffers from 90% outage in DL and 80% outage in the UL. Likewise, the system throughput achieved is 8.43 Mbps/cell in the DL and 7.37 Mbps/cell in the UL, which demonstrates that with BB mechanism and without backoff strategies, a full reuse of chunks is not achievable in hexagonal cellular scenario with omnidirectional antennas at the BS. By lowering the thresholds to -95 dBm (DL) and -100 dBm (UL), the cell-edge user throughput can be enhanced to 860 kbps (DL) and 490 kbps (UL). By setting these thresholds, median system throughputs of 20.9 Mbps/cell (DL) and 20.3 Mbps/cell (UL) are achieved respectively. By adjusting the threshold to -90 dBm, a median system throughput can be increased to 22.5 Mbps/cell (DL) and 29.8 Mbps/cell (UL). The corresponding cell-edge user throughputs are 390 kbps (DL) and 100 kbps (UL). By using variable power BB to signal interference tolerance of individual links, a median system throughput of 22.2 Mbps/cell (DL) and 23.5 Mbps/cell (UL) are achieved together with a cell-edge user throughput of 530 kbps (DL) and 280 kbps (UL) respectively. In summary, in the hexagonal scenario, the BB-enabled CCI mitigation approaches significantly improve the performance for the cell-edge user as well as the system throughput. Likewise, the BB-ITS achieves a more preferable trade-off between system throughput and fairness as observed in the Manhattan scenario.

4.9.1.3 Performance of fair score-based scheduler

The results obtained using the FSBS mechanism (see Figure 4.22) are almost identical to those obtained with BSBS mechanism (see Figure 4.21). The highest median system throughput achieved with FSFS mechanism is 22.5 Mbps/cell (22.5 Mbps/cell achieved with BSBS) in the DL and 29.7 Mbps/cell (29.8 Mbps/cell achieved using BSBS) in the UL using a threshold of -90 dBm in both cases. Likewise, the maximum user throughput of 820 kbps (DL) and 480 kbps (UL) achieved using FSBS mechanism are similar to those achieved with BSBS mechanism.

It should be noted that when the protection from CCI is compromised to enable high spatial reuse, mainly the cell-edge users fail to meet the SINR target. Subsequently, the chunks would be released and reallocated. In a cellular system, the cell-centre users are more likely to meet the SINR target than the cell-edge users when CCI protection is compromised. Eventually, the chunks released by the cell-edge users would be allocated towards the cell-centre users.

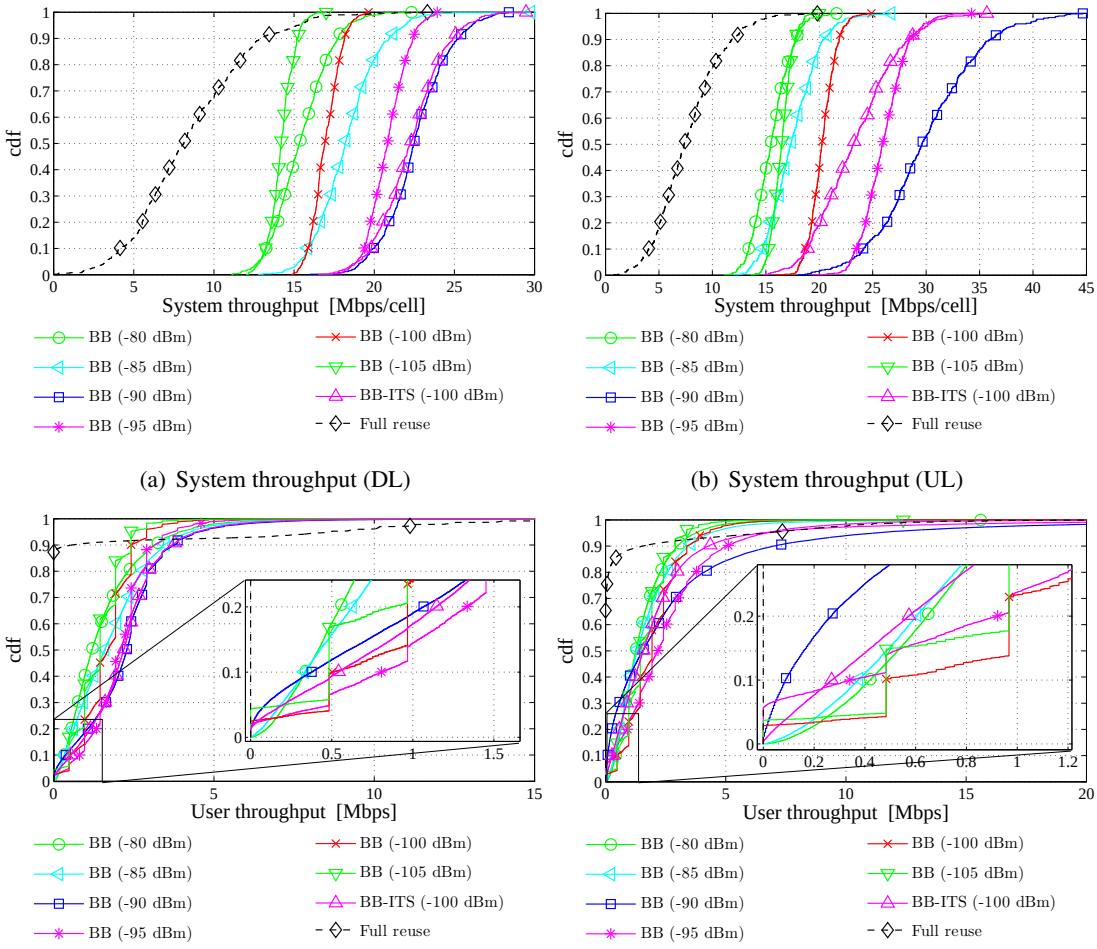

(a) System throughput (DL)

(b) System throughput (UL)

(c) User throughput (DL)

(d) User throughput (UL)

Figure 4.22: *Comparison of performance of fair score based scheduler with BB-enabled CCI mitigation and full chunk reuse system in a hexagonal cellular scenario.*

Provided that the chunk released by the cell-edge user was allocated to the cell-centre user, this would change the score in (4.6) in the favour of the cell-edge users. This was indeed the case in the Manhattan scenario because the chunks released by a cell-edge user were equally likely to be allocated to another cell-edge user or another cell-centre user. However, in the hexagonal cellular scenario, the released chunks are more likely to be allocated to another cell-edge user because the users are more likely to be located towards the cell-edge rather than towards the cell-centre. Therefore, utilising the FSBS mechanism results is a spatial distribution of chunks that is similar to that achieved with the BSBS mechanism. Thus, utilising the FSBS mechanism does not change the performance in hexagonal cellular scenario, when fixed modulation scheme of 16-QAM is utilised.

4.9.2 ICIC on system performing link adaptation

The results presented in this section assume that link adaptation is performed on a per-chunk basis reflecting the prevalent channel conditions at the receiver. The modulation format utilised and its corresponding SINR target is taken from Table 3.2.

4.9.2.1 Centralised frequency planning approach

The impact of link adaptation with centralised frequency planning schemes for ICIC is depicted in Figure 4.23. A reuse factor of 7 is considered for the allocation of chunks from the coordinated bandwidth. With frequency planning of entire system bandwidth, a median system throughput of 18.8 Mbps/cell both in DL and UL is achieved together with 840 kbps (DL) and 850 kbps (UL) at the lower 10^{th} percentile. Likewise, with the FFR scheme, the users are partitioned into cell-edge users or cell-centre users on the basis of median path loss of the user population served by given BS. The system is simulated for different fraction of bandwidth allocated for coordinated bandwidth allocation to the cell-edge users. The results demonstrate that the lower 10^{th} percentile of user throughput is maximised using $\eta_{\text{FFR}} = 0.7$. With these parameters, user throughput of 900 kbps (DL) and 1.03 Mbps (UL) at the lower 10^{th} percentile is achieved together with median system throughput of 23.7 Mbps/cell (DL) and 24.0 Mbps/cell (UL). The performance of FFR scheme with link adaptation may be fine tuned by adjusting the boundary between cell-edge and the cell-centre and changing the ratio of chunks allocated to the cell-edge users to the cell-centre users. However, as the scope of this work is not in optimising the FFR scheme, this issue is not considered any further.

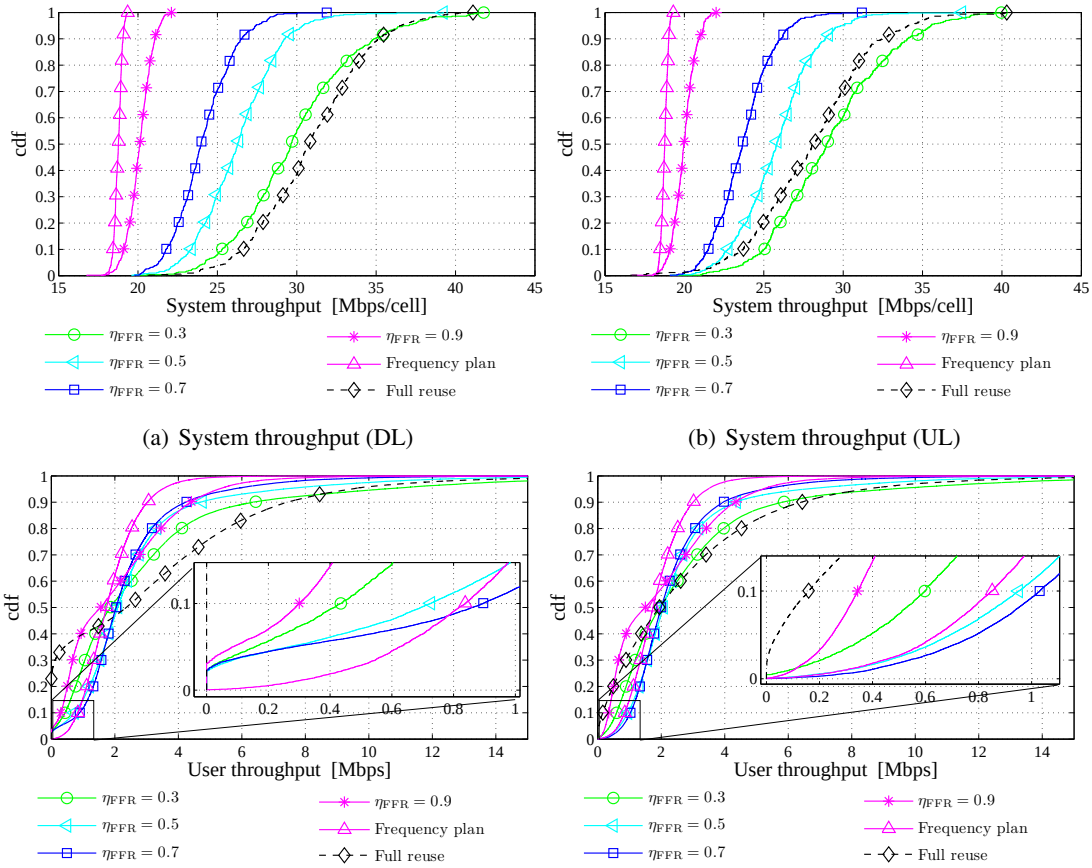

(a) System throughput (DL)

(b) System throughput (UL)

(c) User throughput (DL)

(d) User throughput (UL)

Figure 4.23: *Performance of frequency planning schemes by performing link adaptation on a per-chunk basis.*

4.9.2.2 Decentralised ICIC using BB signalling approach

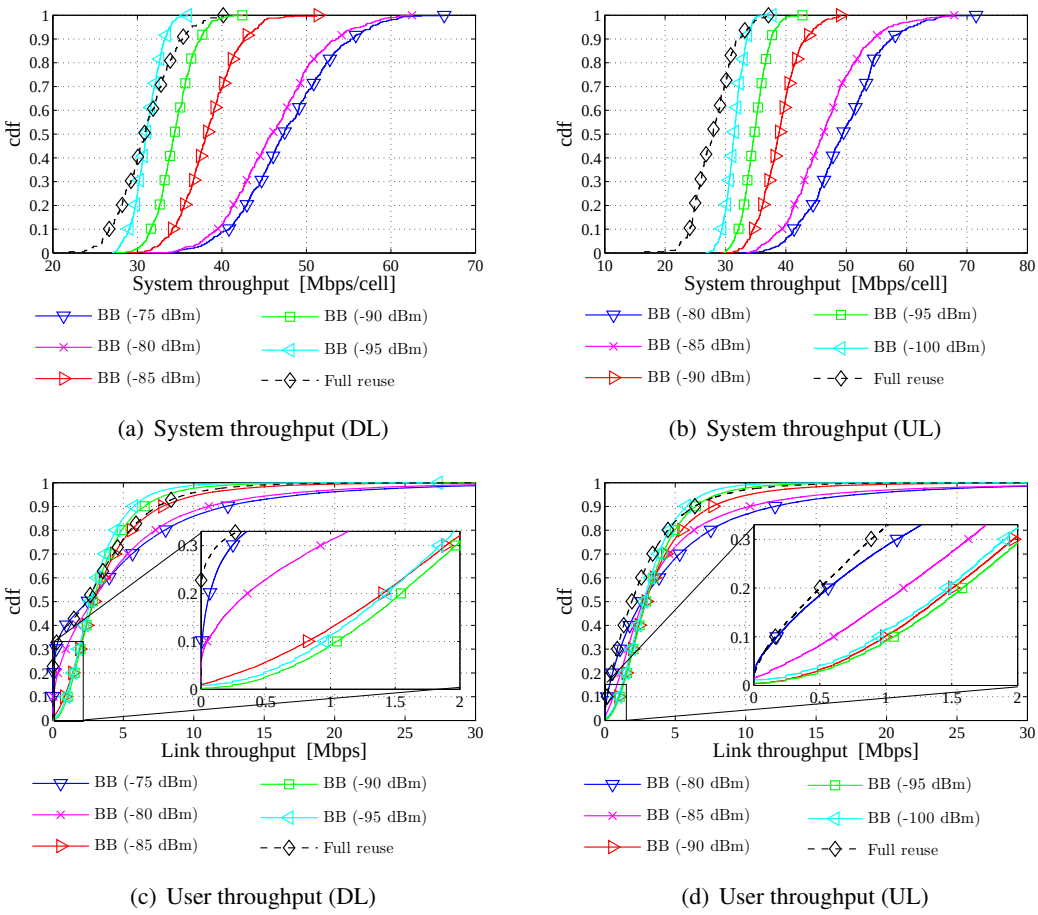

(a) System throughput (DL)

(b) System throughput (UL)

(c) User throughput (DL)

(d) User throughput (UL)

Figure 4.24: *Comparison of BB-enabled CCI mitigation and full chunk reuse system with link adaptation in hexagonal cellular scenario*

The impact of threshold parameter with an adaptive modulation performed on a per chunk basis in a hexagonal cellular scenario is depicted in Figure 4.24. With link adaptation performed, the system performing a full reuse of chunks results in an outage of 23% in the DL mode and a cell-edge user throughput of 169 kbps in the UL mode (see Figure 4.24(c-d)). Likewise, median system throughputs of 30.9 Mbps/cell and 28.0 Mbps/cell are achieved (see Figure 4.24(a-b)) in DL and UL respectively. The results tabulated in Table 4.5 demonstrate that a full spatial reuse of chunks results in a lower order modulation format chosen for each chunk. Moreover, by limiting the amount of CCI to a threshold value using BB signalling, it is demonstrated that both the system throughput and the user throughput at the cell-edge improve compared to the full reuse system.

Criteria	Mode	I_{th}[dBm]						Full reuse
		-75	-80	-85	-90	-95	-100	
Allocated chunks /cell	DL	194	184	124	82	58		230
	UL		201	166	111	77	57	230
Bits/symbol	DL	2.13	2.15	2.5	3.4	4.4		1.4
	UL		2.1	2.4	2.9	3.8	4.6	1.4
Energy consum–ption [nJ/bit]	DL	66.2	64.5	53.7	38.8	30.3		121
	UL		66.1	58.7	46.4	35.7	29.3	137

Table 4.5: *Comparison of chunk reuse, modulation format utilised and energy consumption in hexagonal cellular scenario.*

Using BB signalling, it is shown that the cell-edge user throughput is maximised by setting the thresholds to -90 dBm in the DL and -100 dBm in the UL. A maximum cell-edge user throughput of 1.05 Mbps and a median system throughput of 34.4 Mbps/cell are achieved in the DL. Likewise, a cell-edge user throughput of 1.07 Mbps and a median system throughput of 34.8 Mbps/cell are achieved in the UL. The median number of chunks allocated per BS is 82 and 77 in the DL and UL respectively, *i.e.* 1/3 of the system bandwidth is allocated on average on each cell. The CCI is mitigated due to lower spatial reuse (compared to full reuse system) and the cell-edge users succeed in meeting the SINR target of 2.2 dB or above that is required for reserving the chunk. Moreover, as the spatial reuse is only 1/3 per cell, some of the cell-edge users succeed is achieving the SINR target for higher order modulation schemes. The cell-edge user throughput is increased by utilising receiver feedback to select higher order modulation scheme.

The achieved SINR at the cell-edge degrades when the threshold parameters is increased to allow a larger spatial reuse. If the minimum SINR target is not met, the chunk is released. Otherwise, the order of the modulation format utilised is reduced. Both of these contribute towards lowering the cell-edge user throughput as can be seen in Figure 4.24(c-d). In particular, when the thresholds of -75 dBm (DL) and -80 dBm (UL) are used so as to maximise the system throughput, the lower 10^{th} percentile of user throughput is close to 0 (10 kbps) in the DL and 100 kbps in the UL. However, using the above thresholds, median system throughputs of 47 Mbps/cell (DL) and 49 Mbps/cell (UL) are achieved due to increased spatial reuse. The increase in system throughput is attributed to two reasons - first, the spatial reuse of the chunks in the system is enhanced and second, the chunks released by the cell-edge user are reallocated (potentially) to other users that may achieve higher SINRs. However, the possibility that the released chunks are not allocated to another user that would also fail to achieve the minimum

SINR target, thereby giving rise to *ping pong* effects, is not eliminated. When this occurs, the chunks repeatedly enter the backoff mode (enforced by $p-$persistence), get reallocated and released until they are allocated to the user that succeeds in meeting the SINR. For this reason, even when the high threshold is chosen the spatial reuse is not 100% with BB signalling mechanism as can be observed in Table 4.5.

4.9.2.3 Performance of fair score-based scheduler

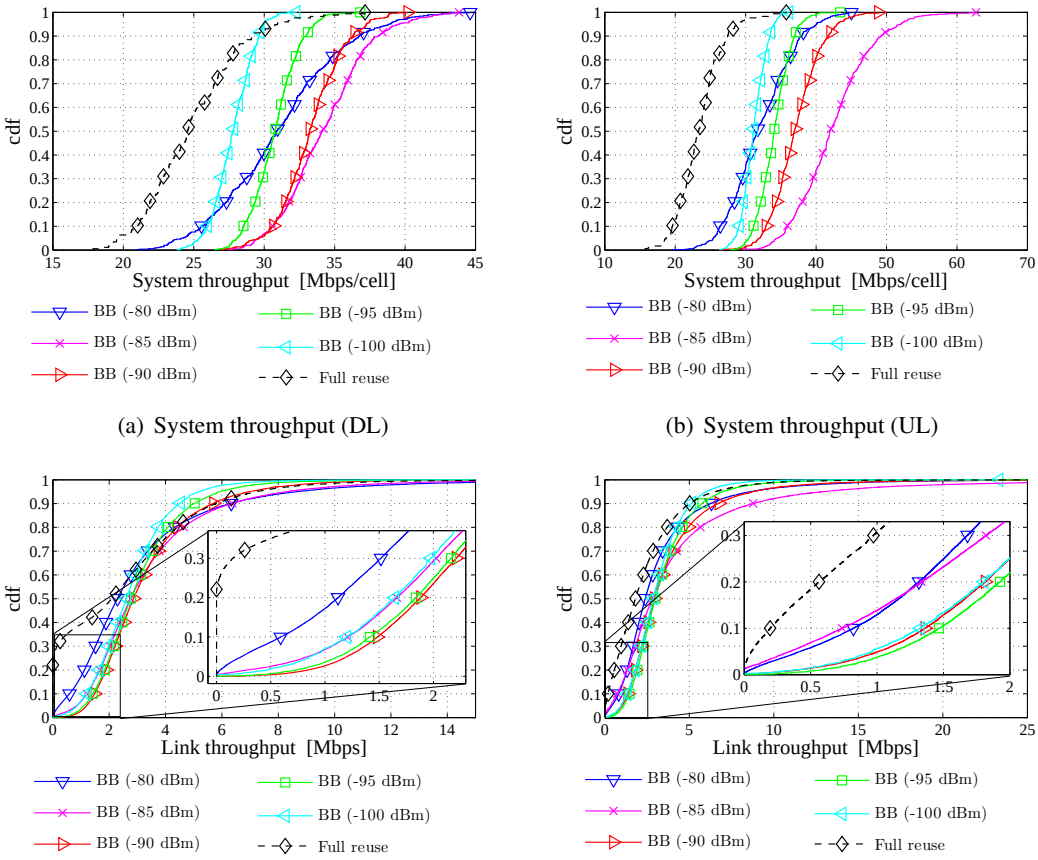

(a) System throughput (DL)

(b) System throughput (UL)

(c) User throughput (DL)

(d) User throughput (UL)

Figure 4.25: *Comparison of performance of fair score based scheduler with BB-enabled CCI mitigation and full chunk reuse system in a hexagonal cellular scenario.*

Figure 4.25 compares the system performance of full reuse system and BB-enabled chunk allocation with FSBS mechanism in a system performing link adaptation. A cell-edge user throughput of 1.48 Mbps and 1.66 Mbps and a median system throughput of 33.2 Mbps/cell and 34.1 Mbps/cell in the DL and UL respectively is achieved using FSBS mechanism, when

Criteria	Mode	I_{th}[dBm]					Full reuse
		-80	-85	-90	-95	-100	
Allocated chunks /cell	DL	136.8	115	81	58	45	230
	UL	162	150	109	76	56	230
Bits/symbol	DL	2.1	2.5	3.4	4.4	5.1	1.3
	UL	2.0	2.2	2.8	3.7	4.6	1.3
Energy consum–ption [nJ/bit]	DL	72	55	40	31	26	152
	UL	77	63	48	36	29	160

Table 4.6: *Comparison of fair score based scheduler and blind score based scheduler*

the thresholds are set respectively to $-90\,$dBm and $-95\,$dBm respectively. For comparison, the maximum cell-edge user throughput of $1.05\,$Mbps and $1.07\,$Mbps together with mean system throughput of $34.4\,$Mbps/cell and $34.8\,$Mbps/cell were achieved with BSBS mechanism. Therefore, the FSBS mechanism enhances the cell-edge user throughput by 40% and 55% in DL and UL respectively at a cost of less than 4%in terms of median system throughput in both cases.

By utilising the FSBS mechanism, a maximum median system throughput of 34.8 Mbps/cell (DL) and 42.1 Mbps/cell (UL) can be achieved. Furthermore, with the FSBS mechanism the threshold that maximises the median system throughput itself shifts closer towards the threshold that maximises the user throughput. This is because when the threshold is increased, the achieved SINR deteriorates and the number of chunks where the cell-edge users fail to meet the minimum SINR target increases. With the BSBS scheduler, some of the released chunks are allocated to the cell-centre users. These users achieve higher SINR and are able to sustain higher order modulation formats even when CCI is largely compromised. By contrast, the FSBS mechanism enforces a higher priority to the cell-edge users with fewer chunks already reserved. This increases the likelihood of *ping pong* effects with FSBS mechanism compared to the BSBS mechanism and results in a lower system throughput when the CCI protection is compromised.

4.10 Chapter Summary

This chapter addressed intercell interference coordination using BB signalling in cellular networks where the BS and MS are both equipped with omnidirectional antennas. Cellular networks deployed in Manhattan scenario (urban) as well as hexagonal cellular scenario (rural) were investigated. Comparison was made against a full frequency reuse system where at-

tempts to avoid interference are not made as well as the CCI mitigation approaches such as the frequency reuse coordination and fractional frequency reuse, where chunk allocation is coordinated in a centralised manner. The system where fixed modulation scheme is utilised systemwide as well as the system performing that performs link adaptation on a per chunk basis were considered.

The impact of BB-specific interference threshold parameter that limits the interference imposed pre-established and co-existing links was studied. It was demonstrated that the threshold parameter can be used to trade-off system throughput for the cell-edge user throughput, both in the system utilising a fixed modulation scheme systemwide and in the system performing link adaptation on a per chunk basis. In particular, in a system performing link adaptation, 17% (DL) and 50% (UL) of median system throughput was traded off to enhance the cell-edge user throughput by 3-fold (DL) and 20% (UL) in the Manhattan scenario. Likewise, in the hexagonal cellular scenario, the cell-edge user throughput was increased from 10 kbps (DL) and 100 kbps (UL) to approximately 1 Mbps in both cases by compromising 12 Mbps/cell (DL) and 10 Mbps/cell (UL). Furthermore, the impact of prioritising users with fewer chunks already reserved with BB signalling was investigated and it was shown that the scheduler that priorities the users with fewer chunk reserved boosts the cell-edge user throughput when the thresholds are set so as to maximise the cell-edge user throughput. However, it is demonstrated that such approach increase the *ping pong* effects and reduce the spectral efficiency when CCI protection is compromised.

In a system utilising a 16-QAM modulation scheme systemwide, a mean system throughput of up to 88% (DL) and 94% (UL) of the peak throughput in an isolated cell were achieved with BB signalling in a Manhattan scenario. By adjusting the threshold, it was demonstrated that the cell-edge user throughput was enhanced by 94% at a cost of 44% in median system throughput compared to the threshold that maximised the median system throughput. Likewise, in the DL mode, the cell-edge user throughput was enhanced to 1.7 Mbps from 15.4% outage at a cost of 25% in median system throughput. In summary, the trade-off was shown more favourable in the DL mode than in the UL mode. Furthermore, a variable BB approach to signal the interference tolerance of individual links was investigated and it was demonstrated that the variable BB approach leads to a more favourable trade-off between system throughput and fairness and relaxes the requirement to optimise the threshold parameter, both in Manhattan and hexagonal scenario.

With a 16-QAM modulation scheme utilised systemwide in a Hexagonal scenario, the performance was merely 26% and 20% of the peak throughput possible in an isolated cell. Furthermore, it was shown that increasing the threshold beyond the threshold that maximises user throughput does not significantly enhance the median system throughput due to an increase in *ping pong* effects. This was attributed to two effects - first, the assumption of omnidirectional transmitters increases the number of co-channel cells and second, the number of users in the cell that are at the cell-edge is higher than those closer towards the cell-centre in hexagonal cellular model. Therefore, even with link adaptation performed, the spectral efficiency remained below 1 bps/cell/Hz with hexagonal cellular deployments due to high CCI from up to 6 cells within the 1^{st} tier. Therefore, it is necessary to lower the overall amount of CCI to increase the overall spectral efficiency. This issue is addressed in the next chapter where CCI mitigation with beamforming is combined with BB signalling to obtain a hybrid CCI mitigation approach.

Chapter 5
BB Enabled CCI Mitigation and Avoidance with Switched Beam Approach

5.1 Introduction

In Chapter 4, it was demonstrated that the busy burst (BB) protocol effectively solves the hidden node problem. Moreover, in a hexagonal cellular scenario the use of omnidirectional antennas at the base station (BS) compromises spatial reuse due to excessive co-channel interference (CCI) caused towards the receivers in adjacent cells. It has been identified that the multiple antenna techniques at the BS such as a switched beam approach [15] or adaptive beamforming with opportunistic scheduling [14, 32] provide a powerful basic mechanism to mitigate CCI and enhance the reusability of radio resources, but these techniques generally suffer from the hidden node problem. Clearly, the BB protocol and beamforming techniques seem to perfectly complement each other enabling a high frequency reuse in the system while mitigating CCI. In this chapter, the BB protocol is combined with switched beam approach because of low signalling overhead accompanied as well as reduced complexity at the BS. To this end, pre-defined grid of beams (GoB) are generated at the BS and a user is served by switching on the closest beam.

The BB protocol ensures that the beams are only selected for a particular user in the cell if this transmission does not significantly interfere with any of the ongoing transmissions in the neighbouring cells. This *interference awareness* property of the BB protocol is achieved by a time-multiplexed busy signal transmitted omnidirectionally from the receiving mobile station (MS) by exploiting the TDD channel reciprocity and using that the overall gain is reciprocal if the precoding vector intended to be used for transmitting data in subsequent slots is used for scanning the BB minislot. In this chapter, the performance of the hybrid BB enabled switched beam approach is compared against the state-of-the-art switched beam approach.

5.2 Switched beam approach using antenna array

This section establishes the relationship between the spatial precoding vector and the effective channel gain. We start with a general consideration of an orthogonal frequency division multiple access (OFDMA) – time division duplexing (TDD) network where each of the BSs and MSs is equipped with N_{T} and N_{R} antennas respectively. Data transmission in the downlink is considered. The matrix $\mathbf{V} = [\mathbf{v}^{(1)}, \ldots, \mathbf{v}^{(N_{\mathrm{S}})}]$ is the spatial precoding matrix for N_{S} spatial layers available at the BS. The i^{th} column of the matrix $\mathbf{V}$, $\mathbf{v}^{(i)}$, contains the precoder of spatial layer i. The precoder is a vector $\mathbf{v}^{(i)} = [v_1^{(i)}, \ldots, v_{N_{\mathrm{T}}}^{(i)}]^T$, where $v_t^{(i)}$ is the complex coefficient applied to antenna element t.

The symbol transmitted at chunk (n, k) of spatial stream i is designated $x^{(i)}[n, k]$. The output of spatial precoding on the i^{th} stream is represented as

$$\mathbf{s}^{(i)}[n, k] = \mathbf{v}^{(i)} x^{(i)}[n, k]. \tag{5.1}$$

The output of spatial precoding is transmitted over a time-variant, frequency selective MIMO (multiple input multiple output) channel $\mathbf{H}_{\mu,\alpha}[n, k]$, where α and μ are BS and MS indices respectively. The MIMO channel is represented as a $N_{\mathrm{R}} \times N_{\mathrm{T}}$ matrix of the form

$$\mathbf{H}_{\mu,\alpha}[n, k] = \begin{pmatrix} h_{\mu,\alpha}^{1,1}[n, k] & \ldots & h_{\mu,\alpha}^{1,N_{\mathrm{T}}}[n, k] \\ \vdots & \ddots & \vdots \\ h_{\mu,\alpha}^{N_{\mathrm{R}},1}[n, k] & \ldots & h_{\mu,\alpha}^{N_{\mathrm{R}},N_{\mathrm{T}}}[n, k] \end{pmatrix}, \tag{5.2}$$

where $h_{\mu,\alpha}^{t,r}[n, k]$ represents the channel response between transmitting antenna t of BS α and receiving antenna r of MS μ observed at frequency and time index (n, k) assuming a rich scattering environment, which is given by [126]

$$h_{\mu,\alpha}^{t,r}[n, k] = \sqrt{\frac{G_{\mu,\alpha}^{\mathrm{ls}}}{L}} \sum_{\ell=1}^{L} \frac{1}{K_{\mathrm{D}}} \sum_{\kappa=1}^{K_{\mathrm{D}}} \rho_\ell \exp\left(j\theta_{\ell,\kappa} + j2\pi[f_{\ell,\kappa}^{\mathrm{D}} k n_{\mathrm{os}} T_{\mathrm{S}} - \tau_\ell(f_{\mathrm{l}} + n n_{\mathrm{sc}} \Delta_f)]\right) \exp\left(-j2\pi t \frac{\Delta_{\mathrm{T}}}{\lambda} \cos\phi_{\mathrm{T}}\right) \exp\left(-j2\pi r \frac{\Delta_{\mathrm{R}}}{\lambda} \cos\phi_{\mathrm{R}}\right) \tag{5.3}$$

where T_{S} and Δ_f denote the OFDM symbol duration and the subcarrier spacing, and λ is the carrier wavelength. The term $\sqrt{\frac{G_{\mu,\alpha}^{\mathrm{ls}}}{L}} \sum_{\ell=1}^{L} \frac{1}{K_{\mathrm{D}}} \sum_{\kappa=1}^{K_{\mathrm{D}}} \rho_\ell \exp\left(j\theta_{\ell,\kappa} + j2\pi[f_{\ell,\kappa}^{\mathrm{D}} k n_{\mathrm{os}} T_{\mathrm{S}} - \tau_\ell(f_{\mathrm{l}} + n n_{\mathrm{sc}} \Delta_f)]\right)$ models the time variant and frequency selective channel as done in (2.18). As dis-

cussed earlier in Section 2.6.4, the term $\exp\left(-j2\pi t\frac{\Delta_{\mathrm{T}}}{\lambda}\cos\phi_{\mathrm{T}}\right)$ models the phase of the signal at antenna t at the antenna array of the transmitter. Likewise, the term $\exp\left(-j2\pi r\frac{\Delta_{\mathrm{R}}}{\lambda}\cos\phi_{\mathrm{R}}\right)$ models the phase of the received signal at antenna r at the antenna array of the receiver. Δ_{T} and Δ_{R} are the separation of antenna elements. The channel response (5.3) is composed of $1{\leq}\ell{\leq}L$ local scatterers, with angles of departure (AoD) ϕ_{T} and angle of arrival (AoA) ϕ_{R}. The initial phase, Doppler shift and propagation delay of local scatterer ℓ are denoted by θ_ℓ, $f_{\mathrm{D},\ell}$ and τ_ℓ. The factor $G^{\mathrm{ls}}_{\mu,\alpha}$ represents the channel gain and incorporates distance dependent path loss and log-normal shadowing between MS μ and BS α.

To keep the notation consistent with those used in Chapter 3 and Chapter 4, the transmitter or receiver of link (μ,α) is denoted $\mathbf{x}$ and that of link (ν,β) is denoted $\mathbf{y}$. It is assumed that (μ,α) is an active link and (ν,β) is a link in adjacent cell that potentially reuses the resources used in cell α. The signal of the spatial stream i received at antenna array of receiver $\mathbf{x}$ is represented as

$$\mathbf{r}^{(i)}_{\mathbf{x}}[n,k] = \mathbf{H}_{\mathbf{x}}[n,k]\mathbf{s}^{(i)}[n,k] = \mathbf{H}_{\mathbf{x}}[n,k]\mathbf{v}^{(i)}x^{(i)}[n,k]. \tag{5.4}$$

$$\begin{aligned} y^{(i)}_{\mathbf{x}}[n,k] &= \left[\mathbf{u}^{(i)}\right]^T\mathbf{r}^{(i)}_{\mathbf{x}}[n,k] \\ &= \underbrace{\left[\mathbf{u}^{(i)}\right]^T\mathbf{H}_{\mathbf{x}}[n,k]\mathbf{v}^{(i)}}_{g^{(i)}_{\mathbf{x}}[n,k]}x^{(i)}[n,k]. \end{aligned} \tag{5.5}$$

The term $g^{(i)}_{\mathbf{x}}[n,k] = [\mathbf{u}^{(i)}]^T\mathbf{H}_{\mathbf{x}}[n,k]\,\mathbf{v}^{(i)}$ represents the effective channel between transmitter $\mathbf{x}$ and its intended receiver on spatial stream i. The channel gain, $G^{(i)}_{\mathbf{x}}[n,k]$, on spatial stream i from transmitter $\mathbf{x}$ towards its intended receiver is given by

$$G^{(i)}_{\mathbf{x}}[n,k] = \left|g^{(i)}_{\mathbf{x}}[n,k]\right|^2. \tag{5.6}$$

An important special case is when the BSs are equipped with multiple antennas and MSs are omnidirectional transceivers. This means N_{R} equals 1 and $u^{(i)}$ reduces to 1, for all spatial stream i chosen at the BS. The choice of omnidirectional antennas at the MSs reduces hardware and computational complexity at the subscriber units, which is important from size, portability and energy efficiency perspective. With omnidirectional antenna at the MS, the MIMO channel response $\mathbf{H}_{\mathbf{x}}[n,k]$ in (5.2) reduces to a row vector $\mathbf{h}_{\mathbf{x}}[n,k]$ of size $1{\times}N_{\mathrm{T}}$. Then the effective

channel between transmitter x and its intended receiver reduces to

$$g_{\mathbf{x}}^{(i)}[n,k] = \mathbf{h}_{\mathbf{x}}[n,k]\mathbf{v}^{(i)}\,. \tag{5.7}$$

A MS μ is served using the beam that provides the maximum channel gain, averaged over the system bandwidth. The term i_μ represents the serving beam for user μ, which is synonymous with $i_{\mathbf{x}}$,when $\mathbf{x}$ is used in the context of receiver. With these notations, the intended channel gains can be expressed as $G_{\mathbf{x}}^{(i_{\mathbf{x}})}[n,k]$ and the intended signal power received at MS μ is given by

$$R_{\mathbf{x}}^{\mathrm{d}}[n,k] = T_{\mathbf{x}}^{\mathrm{d}}[n,k]G_{\mathbf{x}}^{(i_{\mathbf{x}})}[n,k]. \tag{5.8}$$

Likewise, the interference caused by transmitter $\mathbf{y}$ to receiver $\mathbf{x}$ is

$$I_{\mathbf{x}}^{\mathrm{d}}[n,k] = T_{\mathbf{y}}^{\mathrm{d}}[n,k]G_{\mathbf{yx}}^{(i_{\mathbf{y}})}[n,k]\,. \tag{5.9}$$

5.3 Interference aware grid of beam selection in cellular networks using busy bursts

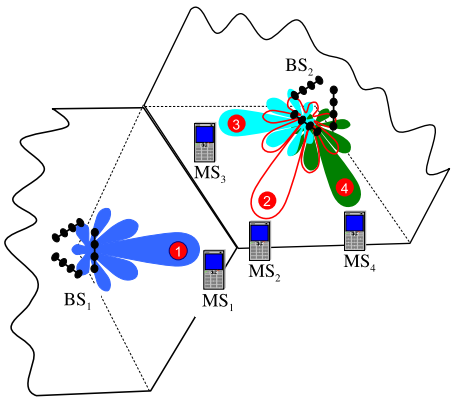

Figure 5.1: *Illustration of the use of hybrid BB+GoB scheme for interference aware chunk reuse.*

The combined use of interference mitigation achieved using switched beam approach and interference awareness using the BB protocol is explained using Figure 5.1. It is assumed that BS_1 activates beam 1 to serve MS_1 using chunk (n,k). Furthermore, it is assumed that BS_2 intends to reuse the chunk (n,k) on one of the beams generated using antenna array of the sector depicted in Figure 5.1. Since BS_2 is generally unaware of the positions of the user population

in cell 1, with full reuse beam switching, BS_2 might select to reuse the chunk (n, k) for MS_2 resulting in outage of both MS_1 and MS_2 on chunk (n, k). However, if MS_1 were to send a busy signal omnidirectionally on the same radio frequency carrier in a time-multiplexed mini slot following the data slot, BS_2 would sense a strong signal in beam 2, and a low signal in beam 3 and beam 4. Therefore, with the proposed BB-enabled switched beam approach, BS_2 would allocate the chunk either to MS_3 or MS_4, thereby avoiding outage in both cells.

This concept is mathematically formalized in the following paragraphs. It is assumed that the beam $i_{\mathbf{x}}$ is activated to transmit serve $\mathbf{x}$ using chunk (n, k). Provided that $\gamma_{\mathbf{x}}[n, k] \geq \Gamma_{\min}$, the receiver $\mathbf{x}$ transmits a BB signal omnidirectionally in the mini slot corresponding to its respective data transmission slot. This BB signal serves as a reservation indicator for the next slot which establishes exclusion region around the receiver where no other transmitters may reuse the chunk [26, 27]. Given x^{b} is the omnidirectional BB signal transmitted by receiver $\mathbf{x}$, the signal received at the antenna array of transmitter $\mathbf{y}$ is

$$\mathbf{r}_{\mathbf{y}}^{\mathrm{b}}[n, k] = \mathbf{h}_{\mathbf{yx}}^{\mathrm{T}}[n, k]\, x^{\mathrm{b}}[n, k]\,. \tag{5.10}$$

Given $\mathbf{v}^{(i)} \in \mathcal{V}$, where $\mathcal{V}$ is the set of precoding vectors available in the system. The output of applying precoding vector $\mathbf{v}^{(i)}$ to $\mathbf{r}_{\mathbf{y}}^{\mathrm{b}}[n, k]$ is

$$\begin{aligned} y_{\mathbf{y}}^{\mathrm{b},(i)}[n, k] &= \left[\mathbf{v}^{(i)}\right]^T \mathbf{r}_{\mathbf{y}} \\ &= \underbrace{\left[\mathbf{v}^{(i)}\right]^T \mathbf{h}_{\mathbf{yx}}^T[n, k]}_{g_{\mathbf{yx}}^{(i)}[n,k]}\, x^{\mathrm{b}}[n, k]. \end{aligned} \tag{5.11}$$

Thus, the effective channel transfer function between victim MS μ and transmitting antenna array in BS q that intends to reuse the chunk (n, k), $g_{\mathbf{x}}^{(i)}$, is given by $\mathbf{v}^{(i)^{\mathrm{T}}} \mathbf{h}_{\mathbf{y}}^{\mathrm{T}}$. Likewise, using transmitter y and receiver $\mathbf{x}$ on (5.7), the channel transfer function between transmitter $\mathbf{y}$ (*i.e.* BB receiver)and receiver $\mathbf{x}$ (*i.e.* BB transmitter) is given by

$$\begin{aligned} g_{\mathbf{y}}^{(i)} &= \mathbf{h}_{\mathbf{xy}} \mathbf{v}^{(i)} \\ &= \left[\left[\mathbf{v}^{(i)}\right]^T \mathbf{h}_{\mathbf{xy}}^T\right]^T. \end{aligned} \tag{5.12}$$

Applying (5.11) on (5.12) and using $\mathbf{h}_{\mathbf{xy}} = \mathbf{h}_{\mathbf{yx}}^T$ due to TDD channel reciprocity, $g_{\mathbf{yx}}^{(i)}$ can be

written as

$$g_{\mathbf{yx}}^{(i)} = \left[g_{\mathbf{xy}}^{(i)}\right]^T = g_{\mathbf{xy}}^{(i)}. \tag{5.13}$$

Thus it is demonstrated that the effective channel between the transmitter $\mathbf{y}$ and receiver $\mathbf{x}$ becomes reciprocal if the same precoding vector to be used for data transmission during the data slot of the frame is utilised to scan the BB mini slot. Therefore, using (5.6), it can be shown that $G_{\mathbf{yx}}^{(i)} = G_{\mathbf{xy}}^{(i)}$. As the effective channel is reciprocal, BB signalling mechanism [26, 27] can be used for interference aware resource allocation. To this end, given the power of BB signal emitted is $T_{\mathbf{x}}^{\mathrm{b}}[n,k]$, the received BB power on beam i can be written as

$$I_{\mathbf{y}}^{\mathrm{b},(i)}[n,k] = \left|y_{\mathbf{y}}^{\mathrm{b},(i)}[n,k]\right|^2 = T_{\mathbf{x}}^{\mathrm{b}}[n,k]G_{\mathbf{yx}}^{(i)}[n,k]\,. \tag{5.14}$$

Thus, by measuring the BB signal received on each of the beams, the transmitter becomes aware of the amount of interference it causes to the vulnerable receiver via exploitation of channel reciprocity [106, Chapter 12]. This enables the transmitter to select the beams that can *potentially* be activated to reuse the chunk (n,k) on BS q.

Combining (5.9) and (5.14) and using $G_{\mathbf{yx}}^{(i)}[n,k] = G_{\mathbf{xy}}^{(i)}[n,k]$ due to channel reciprocity, the relationship between BB power received on beam i and the interference potentially caused towards receiver $\mathbf{x}$ if beam i be activated at transmitter $\mathbf{y}$ is expressed as

$$I_{\mathbf{x}}^{\mathrm{d}}[n,k] = \left(\frac{T_{\mathbf{y}}^{d}[n,k]}{T_{\mathbf{x}}^{b}[n,k]}\right) I_{\mathbf{y}}^{\mathrm{b},(i)}[n,k]. \tag{5.15}$$

If (5.15) is compared against (4.12), it can be observed that both equation are same except that the interference in (5.15) is specific to the beam activated at the transmitter $\mathbf{y}$. In cellular system with omnidirectional antennas, the CCI caused to an active receiver could not be changed by altering the user scheduling. This means by activating a different beam at the BS, the CCI caused to active receiver is changed. This property enables the BS to enhance spatial reuse compared to the case with omnidirectional antennas whilst keeping the CCI below the threshold compared. By scanning the BB minislot using the corresponding precoder vector, $\mathbf{v}^{(i)}$, that the antenna array in BS q intends to use for data transmission during the subsequent data slot, the transmitter becomes aware of the amount of interference it potentially causes to MS μ if it were to activate beam i. In order to keep $I_{\mu,p}^{\mathrm{d}}[n,k] \leq I_{\mathrm{th}}$, where I_{th} is the maximum CCI that a newly admitted link may cause to the pre-established link, the BS q may reuse chunk (n,k) on

beam i if

$$\left(\frac{T_{\mathbf{y}}^{\mathrm{d}}[n,k]}{T_{\mathbf{x}}^{\mathrm{b}}[n,k]}\right) I_{\mathbf{y}}^{\mathrm{b},(i)}[n,k] \leq I_{\mathrm{th}}, \tag{5.16}$$

If $T_{\mathbf{x}}^{\mathrm{b}}[n,k] = T_{\mathbf{y}}^{\mathrm{d}}[n,k]$, which is easily accomplished by utilising fixed data and BB powers, (5.16) reduces to

$$I_{\mathbf{y}}^{\mathrm{b},(i)}[n,k] \leq I_{\mathrm{th}}, \tag{5.17}$$

5.3.1 Avoidance of collisions due to simultaneously activated links

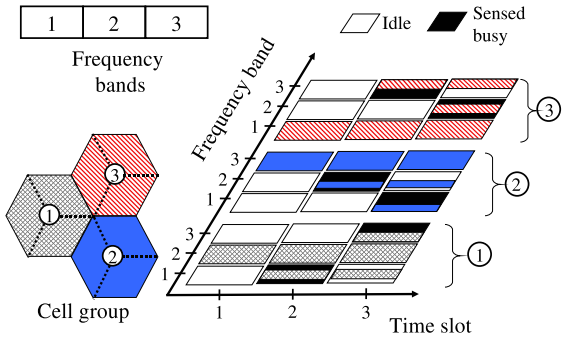

Figure 5.2: *Collision avoidance of unreserved chunks using CESAR mechanism: A simplified cellular scenario consisting of 3 cells is depicted. Each cell has a specific group number as shown in the left. Similarly, the available system bandwidth is partitioned into three blocks. A time evolution graph is depicted for all three cells (right). The unfilled slots depict the frequency block that has not yet been probed for possible allocation. The cell group that probes a particular frequency block at a given time slot is given by* (5.18)*. Using* (5.18)*, during the first time slot,* $(k = 1)$*, frequency block* $\eta = 1$ *is probed by cell group* 3*. Similarly, frequency blocks* $\eta = 2$ *and* $\eta = 3$ *are probed by cell group* 1 *and* 2 *respectively. Collisions are avoided because no two cells probe the same frequency block at the same time instant. Furthermore, all cells collectively probe the entire bandwidth in any given slot thereby avoiding any wastage. After transmission, the chunks where the SINR target is met are reserved for the subsequent time slots by transmitting BB. During the time slot* $k = 2$*, the frequency block 1,2 and 3 are probed by cell group 1, 2 and 3 respectively. In a portion of the probed frequency block, the transmitter will sense BB above the threshold and refrains from using such block to avoid CCI (shown as solid filled slots). Within* K *time slots, all chunks would have been probed for potential access by every cell in the network because of the cyclic shift pattern considered.*

Interference higher than the threshold value is avoided for the chunks that are reserved by transmitting BB signal. Using (5.16), competing transmitters are able to ascertain whether

they lie outside the exclusion region of the receiver that has reserved the chunk. Thus, the transmitters are able to decide whether or not to transmit so that the interference caused on the reserved chunk remains below the threshold. However, in the case of unreserved chunks, two or more transmitter fulfill (5.16) and therefore may be scheduled for transmission simultaneously in contention. During contention, the transmitters are not aware of the amount of interference they cause to the receiver of other links. As a result, one or several links may encounter a collision on chunk (n, k) where the SINR target may not be met.

To avoid collision, cellular slot allocation and reservation (CESAR) mechanism[1] proposed in [2] is considered in this chapter. The available N_{B} sectors in the system are grouped into K groups. The transmitter serving each sector has full functionality of a BS considered earlier in Chapter 4. The group to which BS β is associated is denoted $S_\beta \in \{1, \ldots, K\}$. The sectors within the same cell are associated to the same group. As the beams generated in one sector have side lobes towards another sector, CCI caused to a user served in an another sector within the same cell (intra-cell interference) is mitigated. Therefore, all sectors within the same cell are allowed to transmit simultaneously in contention. However, a preemptive approach is taken by utilising $p-$persistence mechanism in allocating unreserved chunks within different sectors within the cell. The inter-cell interference, however, may result due to the side beam as well as the main lobe alike. The impact of the latter is more severe than the former. Therefore, the access of chunks among two different cells has to be coordinated such that adjacent cells belong to different groups such that they do not transmit at the same time. To this end, the available N_{C} chunks in the system are divided into K blocks. The set $\mathcal{C}_\eta$ represents the set of chunks in block η where $1 \leq \eta \leq K$. Each block η contains $\lfloor N_{\mathrm{C}}/K \rfloor$ contiguous chunks except the K^{th} block which consists of $N_{\mathrm{C}} - \lfloor N_{\mathrm{C}}/K \rfloor$ chunks, where $\lfloor \cdot \rfloor$ is expresses rounding down to the nearest integer. In order to avoid contention, the access of unreserved chunks is regulated such that

1. At a given time, only one group of cell accesses a frequency band, and
2. Within K slots, all N_{C} available chunks would be accessed in each cell provided (5.16) holds.

The above requirements are fulfilled if a cyclically shifted reuse pattern is considered. To this

[1]The concept of allocating unreserved chunks in a cyclically shifted pattern to avoid contention is not a contribution of this thesis.

effect, at time slot k, the unreserved chunks belonging to the block η are allowed to be accessed by sectors where $s_{\eta,k} = S_\beta$ expressed as

$$s_{\eta,k} = ((\eta + k) \mod K) + 1 \quad 1 \leq \eta \leq K. \tag{5.18}$$

The binary variable $\chi_\beta[n,k] \in \{0,1\}$ determines whether or not a chunk (n,k) may be accessed in sector β given by

$$\chi_\beta[n,k] = \begin{cases} 0\ , & s_{\eta,k} = S_\beta \quad \forall n \in \mathcal{C}_\eta \\ 1\ , & \text{otherwise.} \end{cases} \tag{5.19}$$

An unreserved chunk (n,k) may be allocated to user ν only if (5.16) holds true for beam i_ν for transmitter $\mathbf{y}$ on sector β and (5.19) allows the unreserved chunk (n,k) to be accessed in sector β. As more than one user potentially satisfies the above criteria, scheduling and dynamic chunk allocation mechanism detailed out in section 4.3 is used to determine the user that is allocated the chunk (n,k) for transmission.

This principle is illustrated further in Figure 5.2 where the cells are divided into three groups so that $K = 3$. During 1^{st} time slot, the blocks $\eta = 1, 2$ and 3 are accessed by the transmitters located in the sectors with group $S_\beta = 3, 1$ and 2 respectively, thereby avoiding two cells from accessing the same frequency band simultaneously. These bands are reserved with BB and continue to be allocated in their respective cells in the subsequent time slots. During 2^{nd} time slot, the unreserved chunks in the blocks $\eta = 1, 2$ and 3 are accessed in sectors $S_\beta = 1, 2$ and 3 respectively. Note that (in Figure 5.2) the chunks reserved with BB in the previous slot are used for transmission in the current time slot as well. Furthermore, the slots where the BB is received above the threshold are avoided so as to limit the interference at the victim receivers below a threshold. Finally, within 3 time slots, given (5.16) holds, each chunk would have been probed for potential access in all cells.

5.3.2 Multi-User resource allocation in switched beam system

A sectorised cell where the chunks are potentially reused once per sector is considered, as discussed earlier. CCI due to simultaneous access of unreserved chunks is avoided with the strategy detailed out in Section 5.3.1. User scheduling is carried out using the fair score-

based scheduler discussed in Section 4.3.2. To limit the CCI to a threshold value, BB-enabled switched beam approach some users are excluded from being scheduled on certain chunks. This is accomplished by setting the access control indicator $\epsilon_{\nu,\beta}[n,k]\rightarrow\infty$ in (4.6) such that indicates that a user ν in BS β is denied access to chunk (n,k). With BB signalling, a user ν (*i.e.* transmitter $\mathbf{y}$) may be scheduled only if (5.17) holds true for beam i_ν. To this end, $\epsilon_{\nu,\beta}[n,k]$ is set as follows

$$\epsilon_{\nu,\beta}[n,k+1] \rightarrow \begin{cases} 0\ , & I_{\mathbf{y}}^{\mathrm{b},(i_{\mathbf{y}})}[n,k] \leq I_{\mathrm{th}} \text{ and } \chi_\beta[n,k]=1 \text{ and } \hat{\gamma}_{\mathbf{y}}[n,k] \geq \Gamma \\ \infty\ , & a_\nu[n,k-1]=1 \text{ and } b_\nu[n,k-1]=0 \\ \infty\ , & \text{otherwise,} \end{cases} \tag{5.20}$$

where $\mathbf{y}$ represents the transmitter for user ν, $i_{\mathbf{y}}$ is the serving beam for user ν and $\hat{\gamma}_{\mathbf{y}}$ is the estimated SINR of user ν on chunk (n,k) using feedback of interference observed in the previous slot, calculated as

$$\hat{\gamma}_{\mathbf{y}}[n,k] = \frac{T_{\mathbf{y}}^{\mathrm{d}}[n,k]G_{\mathbf{y}}^{(i_{\mathbf{y}})}[n,k]}{I_{\mathbf{y}}^{\mathrm{d}}[n,k-1]}. \tag{5.21}$$

Likewise, $a_\nu[n,k-1]$ and $b_\nu[n,k-1]$ are binary variables that indicate whether or not ν was allocated chunk $(n,k-1)$ and whether or not chunk (n,k) is reserved for user ν, as defined in Section 3.4.5.

The assumption of an *a priori* knowledge of SINR for user scheduling serves two purposes. First, given that the channel does not change abruptly between time instants k and $k+1$, the interference feedback gives an *a priori* estimate of the amount of interference that would actually be observed during the subsequent data slot. This avoids allocating chunks to a user ν where $I_\nu^{\mathrm{d}}[n,k-1]$ would be high such that $\hat{\gamma}_\nu[n,k] < \Gamma$. By allocating the chunks to users where $\hat{\gamma}_\nu[n,k] \geq \Gamma$, the likelihood of bit errors at the receiver is reduced. Note that in the system considered, we have assumed that the bits received below the minimum SINR required for fulfilling the QoS constraints are discarded. Second, the estimated SINR instead of channel gains can be utilised as a scheduling criteria for computing scores, which prioritises those chunks where the prevalent interference conditions are lower for transmission, potentially increasing the throughput. The price to be paid, however, is additional signalling overhead from MS to the BS which consumes bandwidth in the UL direction.

The precoding vector $\mathbf{v}^{(i_{\mathbf{y}})}$ is applied to the antenna array at sector q for transmission on the

chunks where $a_\nu[n,k]=1$, given by (4.8). This ensures that the beam $(i_{\mathbf{y}})$ is activated on the chunks allocated to user ν. The rest of the dynamic chunk allocation procedures are identical to those considered in Chapter 4.

5.4 Link Adaptation

Assuming that the channel does not change significantly between two consecutive time frames, feedback of SINR observed in the preceding frame is utilised to select appropriate modulation format for the next frame. Moreover, provided that an *a priori* estimate of SINR is available, this estimate can be utilised in selecting appropriate modulation scheme to be utilised during contention. This reduces the number of transient steps until the transmitter selects an appropriate modulation scheme corresponding to the prevalent channel conditions at the receiver. The steps of performing link adaptation is detailed as follows:

1. Estimate the SINR for the chunk (n,k) slot with (5.21) using interference power observed in the chunk $(n,k-1)$.
2. Using lookup table, select the largest order modulation scheme, $\hat{m}$, scheme that fulfills $\hat{\gamma_\nu}[n,k]\geq\Gamma_{\hat{m}[n,k]}$
3. Transmit using $m_\nu[n,k]=\hat{m}$, as calculated in the previous step.
4. Calculate the actual SINR achieved $\gamma_\nu[n,k]$ using (4.5).
5. Using lookup table, make a new estimate of $\hat{m}$, such that $\gamma_\nu[n,k]\geq\Gamma_{\hat{m}}[n,k]$
6. Adapt the modulation scheme according to the following rule:

$$m_\nu[n,k+1]=\begin{cases}\bar{m}\ , & \gamma_\nu[n,k]\geq\Gamma_{m_\nu[n,k]+1}\\ 0\ , & \gamma_\nu<\Gamma_{\min}\\ m_\nu[n,k]\ , & \text{otherwise,}\end{cases}\tag{5.22}$$

where $\bar{m}=\lceil(m_\nu[n,k]+\hat{m}[n,k])/2\rceil$ and $\lceil(\cdot)\rceil$ operator expresses rounding up to the nearest integer and $\Gamma_{\min}$ is the minimum SINR target required to continue reserving a chunk. In the considered system, this is the same as SINR target required for BPSK.

7. If $m_\nu[n, k+1] = 0$, or the chunk is no longer needed, release the chunk, else go to step 3.

It should be noted that with the link adaptation performed, the chunk is actually reserved for user ν as long as the minimum SINR target $\Gamma_{\min}$ continues to be met. The link adaptation algorithm proposed in this section is similar to that proposed in Section 3.4.6 except that the algorithm in Section 3.4.6 uses the lowest order modulation format available in the system when an unreserved chunk is accessed whereas the algorithm proposed in this section transmits using modulation level $\hat{m}$ (see step 1–2 above), estimated using the interference level prevalent at the receiver in the previous slot. There are two reasons why the above modification is made. First, the number of transient steps until the transmitter selects a modulation format matching the prevalent channel conditions at the receiver is reduced compared to the algorithm in Section 3.4.6. Second, using the CESAR mechanism, the interference signal observed in the $(k-1)^{\text{th}}$ slot is approximately equal to the interference signal observed in the k^{th} slot, provided that the BS$_\beta$ accesses an unreserved chunk (n, k). This is not true for BB utilising $p-$persistent mechanism for reducing collisions while accessing unreserved chunks because it is possible for two or more closely located BSs to access the same chunk in contention at the same time, which is why the above modification was not considered in Section 3.4.6.

5.5 Benchmark system

The benchmark systems uses a switched beam approach with full-frequency reuse. The users in this system compete for being scheduled in chunk $[n, k]$ if the *a priori* estimate of SINR given by (5.21) meets the minimum SINR target. The access control indicator $\epsilon_{\nu,\beta}[n, k]$ is set to $\epsilon_{\nu,\beta}[n, k] = 0$ for all users that are able to satisfy $\hat{\gamma}_\nu[n, k] \geq \Gamma_1$ and $\epsilon_{\nu,\beta}[n, k] \to \infty$ otherwise. The differences between the benchmark system and the proposed hybrid BB-enabled switched beam approach are that interference awareness and CESAR mechanism are not considered and that the chunks are not reserved (see (5.20) for access control with BB-enabled beam switching). However, the benchmark system uses the same fair scheduler [70] to allocate chunks to users. This system is a representative of a state-of-the-art implementation that lacks a feedback mechanism to avoid severe CCI caused to other co-existing links in neighbouring cells.

5.6 System model

A cellular system modeled by non-overlapping hexagons of 19 cells is considered. Each cell consists of a BS located at the centre of each cell with radius 460 m and contains three sectors. Each sector has an antenna array consisting of 4 antenna elements whose characteristics are given in Table 5.1. Five beams per sector are considered with main lobes at $[-\pi/3, -\pi/6, 0, \pi/6, -\pi/3]$ radians with respect to the normal of the antenna array. Uniformly distributed users equipped with omnidirectional antennas are considered. A full buffer traffic model and perfect time and frequency synchronisation of the network is assumed. Except for the parameters explicitly mentioned in Table 5.1, all other parameters considered in this chapter are same as those considered for the hexagonal cellular scenario in Chapter 4.

Parameters	**Value**
Number of sectors/cell	3
Number of antenna elements/sector	4
Elevation antenna gain A_{e}	14 dBi
Azimuth antenna element gain	$-\min\left[12\left(\frac{\theta}{\theta_{3\mathrm{dB}}}\right)^2, A_{\mathrm{m}}\right]$ [dB] where, $A_{\mathrm{m}} = 20$ and $\theta_{3\mathrm{dB}} = 70^\circ$
# Monte Carlo runs	1000
Duration of each Monte Carlo run	75 ms

Table 5.1: *Additional simulation parameters*

5.7 Results

The performance of BB-enabled beam switching algorithm proposed in this report is compared against the state-of-the-art beam switching algorithm chosen as a benchmark. The performance metrics of interest are considered are user throughput, system throughput and energy efficiency.

5.7.1 Impact of threshold on system performance

The results shown in Figure 5.3 compare the performance of the proposed BB-enabled switched beam approach with the benchmark system. In the results considered, a cluster size $K = 7$ is considered for BB-based system, so that at any time instant, an unreserved chunk is accessed only in 1 among the 7 closely located cells. The results demonstrate a trade-off between system throughput and cell-edge user throughput (measured at the lower 10^{th} percentile). It is demon-

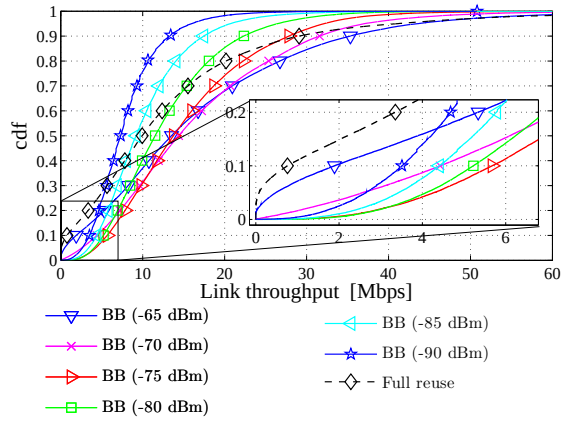

(a) User throughput

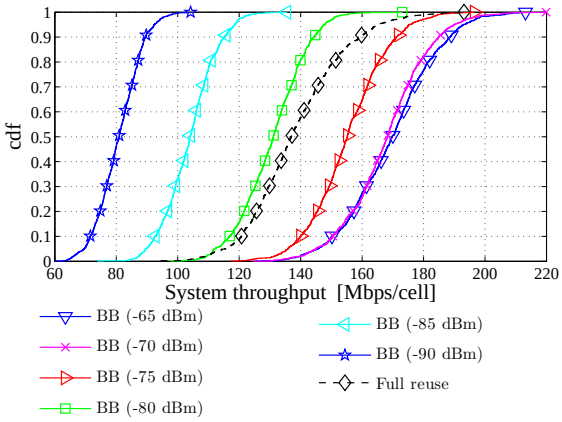

(b) System throughput

Figure 5.3: *Comparison of user throughput achieved with BB-enabled switched beam approach against a full-frequency reuse switched beam approach.*

strated that at low thresholds, (e.g. $I_{\text{th}} = -90\,\text{dBm}$), the system becomes over-cautious and restricts the spatial reuse of the chunks (see Figure 5.4(a)) . As a result, high SINRs are achieved at the receiver. By utilizing SINR feedback from the receiver, the transmitter selects higher order modulation schemes for transmission (see Figure 5.4(b)). As the threshold is increased, the spatial reuse of chunks in the system also increases (see Figure 5.4(a)). On the one hand, this increases number of chunks allocated to each user on average, as a fair scheduler is considered (see Section 4.3.2), while on the other hand, the achieved SINR in each of the chunks degrades due to an increase in CCI, as a result of which lower order modulation schemes are selected (see Figure 5.4(b)). As a result, both system throughput and cell-edge user throughput improve until an optimum cell-edge user throughput is reached using an $I_{\text{th}} = -75\,\text{dBm}$. Until the optimum point is reached, increasing the threshold increases the throughput because the gains in throughput achieved due to increase in bandwidth surpasses the loss in throughput due to degradation of SINR. At this threshold, BB-enabled switched beam approach achieves a median system throughput of 155.7 Mbps/cell together with 5.68 Mbps at the cell edge. Thus, the spectral efficiency using a signal bandwidth of 89.84 MHz during the downlink mode is 3.37 bps/Hz/cell. Compared to the benchmark, this is a 13% increase in median system throughput together with a 7.3-fold increase in lower 10percentile of user throughput compared to the benchmark. By increasing the threshold further to $I_{\text{th}} = -70\,\text{dBm}$, the users closer to the cell-centre benefit from an increased spatial reuse, due to which the overall system throughput increases, whereas the cell-edge users suffer due to an increased CCI. At this point, the median system throughput of 168.6 Mbps/cell (spectral efficiency of 3.75 bps/Hz/cell) and a cell-edge user throughput of 4.39 Mbps is achieved. This represents a 22% increase in median system throughput and a 5.8-fold increase in cell-edge user throughput compared to the benchmark.

On further increasing the threshold (beyond $I_{\text{th}} = -70\,\text{dBm}$), interference protection rendered to vulnerable links is gradually reduced. As a result, the number of chunks at the cell-edge where the lowest SINR target of 2.2 dB required for BPSK is met is reduced. The chunks where the achieved SINR is lower than the minimum SINR target are released, thereby reducing the number of chunks available to the cell-edge users. In such situation, the chunks are primarily allocated to the cell-centre users. However, despite an increased spatial reuse the median system throughput does not noticeably increase compared to using $I_{\text{th}} = -70\,\text{dBm}$ because fewer bits are transmitted per chunk as can be seen in Figure 5.4. It is observed that the BB-enabled switched beam approach performs better than the full reuse even when interference protection is largely compromised by setting a high threshold of $-65\,\text{dBm}$. This is because the released

chunks remain idle in the tagged cell until the time slot when the tagged cell can allocate unreserved resources, due to the CESAR mechanism discussed in section 5.3.1. As a result, CCI remains lower than that in a full reuse blind switched beam approach.

The trade-off between spatial reuse and spectrally efficient modulation scheme has significance in energy required per bit for transmission. The results shown in Figure 5.4 depict the energy consumption per bit for various thresholds and for the benchmark system. As the spatial reuse increases, the SINR decreases due to increase in CCI although the SNR (signal to noise ratio) is still high enough to meet higher order modulation schemes. A low achieved SINR causes the transmitter to select lower order modulation schemes and as such it requires a high amount of energy per bit for transmission. With BB-enabled switched beam approach, it is shown that by lowering the threshold, thus lowering the spatial reuse, the number of bits per symbol increases and the energy consumption per bit decreases. In particular, we show that by lowering the threshold from $-65\,\text{dBm}$ to $-70\,\text{dBm}$, the energy consumption is reduced by 18% in the latter compared to the former, whilst keeping the system throughput almost constant. Using $I_{\text{th}} = -70\,\text{dBm}$, so as to maximize the system throughput, we observe the energy consumption lower by approximately 40% while at the same time achieving a gain of 22% in system throughput (see Figure 5.3(b)) compared to the benchmark. Furthermore, it is shown that if the spatial reuse is reduced, by setting $I_{\text{th}} = -75\,\text{dBm}$, the energy consumption is lowered by more than half compared to the benchmark, whilst keeping the system throughput 13% higher than the benchmark. The significance of this finding is that the threshold allows the energy consumption of a network to be dynamically adjusted according to the traffic demands in the system, allowing network operators to lower their energy consumption.

5.7.2 Impact of number of antenna elements

Increasing the number of antenna elements at the transmit antenna array reduces the half power beamwidth of the beams used at the BS. Consequently, fewer links in adjacent cells suffer from CCI caused due to main lobe. Therefore, it is envisioned that CCI would be mitigated and system performance would improve. In such scenario, an important question is whether incorporating BB signalling on top of the state-of-the-art switched beam approach provides any additional gains. To address this question, the number of antenna elements at the transmitter is varied from 4 to 12 and the results are presented in Figure 5.5. The results for BB signalling shown in (a) and (b) are obtained using $I_{\text{th}} = -65\,\text{dBm}$ so that the system through-

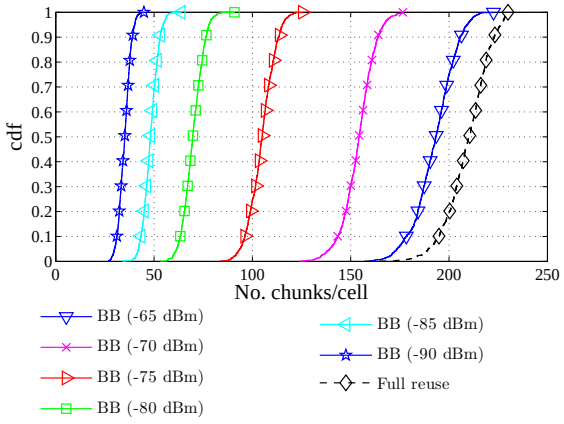

(a) Average number of chunks per sector

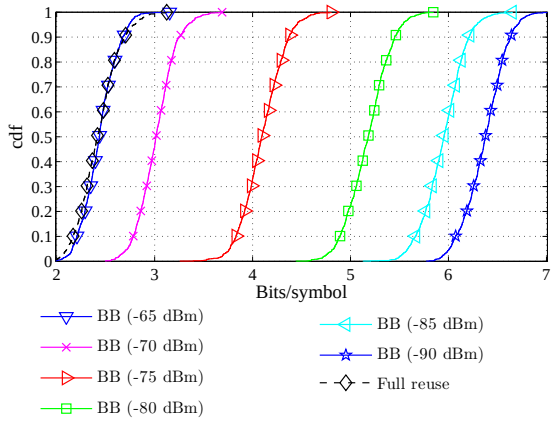

(b) Average number of bits per symbol

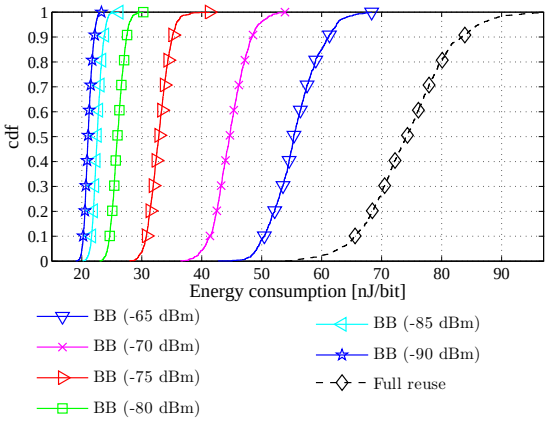

(c) Energy consumption per bit

Figure 5.4: *Comparison of spatial reuse, modulation format and energy consumption for a switched beam system.*

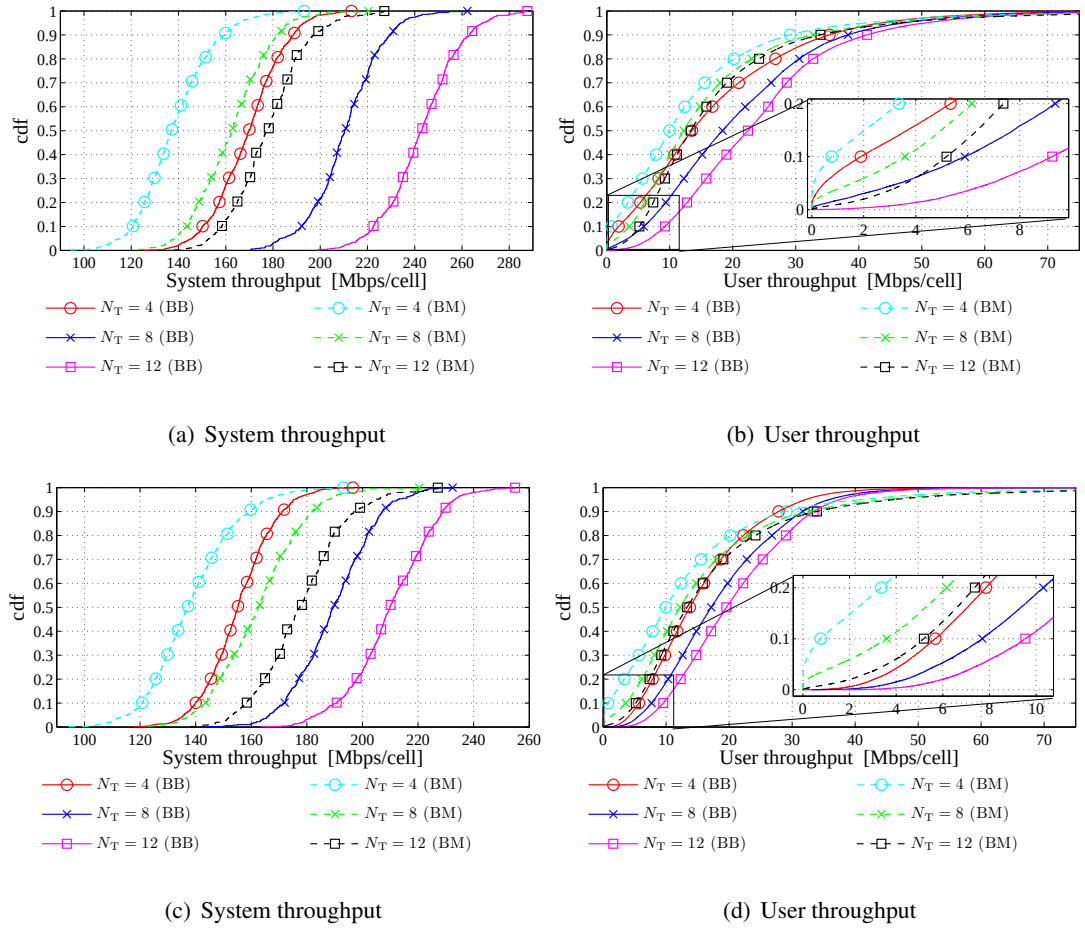

(a) System throughput

(b) User throughput

(c) System throughput

(d) User throughput

Figure 5.5: *Comparison of cdfs of system and user throughputs in the system with various number of antenna elements N_T at the BS antenna array. For BB enabled switched beam approach, a threshold of -65 dBm is used for (a) and (b) so as to maximize the system throughput. Likewise, a threshold of $I_{th} = -75$ dBm is used for (c) and (d) so as to maximize the user throughput.*

put is maximized, whereas those in (c) and (d) are obtained using $I_{\text{th}} = -75\,\text{dBm}$, so that the cell-edge user throughput is maximized. There are three important observations. First, the results demonstrate that increasing the number of antenna elements at the BS improve the system throughput and the user throughput, as expected, both in the benchmark system as well as with the proposed BB-enabled switched beam approach. Furthermore, increasing the number of antenna elements at the transmit array improves the performance of the users at the cell-edge as well as those closer to the BS (see Figure 5.5(b and d). The improvement is attributed to the decrease in CCI achieved by reducing the half power beamwidth. Second, the percentage improvement in the lower 10^{th}percentile user throughput achieved by lowering the threshold,

relative to using the threshold that maximises the system throughput decreases, as the number of antenna increases. Note that by adjusting the threshold from -65 dBm to -75 dBm the cell-edge user throughput improves from 1.65 Mbps to 5.6 Mbps (a 2.3 fold increase) using 4 antennas whereas it increases from 9.12 Mbps to 10.12 Mbps (a 10% increase) using 12 antennas. Finally, the results demonstrate that the BB-enabled switched beam approach outperform the benchmark system, regardless of the number of antennas used. These results therefore demonstrate that it is beneficial to add BB signalling to the system utilising a switched grid of beams and that incorporating BB signalling into the system is particularly desirable when a lower number of antenna elements at the transmit array are considered.

5.7.3 Impact of average number of users per BS

Figure 5.6 depicts the impact of varying the average number of users per cell on the system performance. In the results, 4 antenna elements at the BS are assumed[2]. A threshold of -75 dBm is chosen for the BB-enabled switched beam approach, so that the user throughput is maximized. The results demonstrate that with the BB-enabled switched beam approach, the system throughput increases with an increase in the average number of users per cell. In particular, by increasing the average number of user per BS from 10 to 40, the median system throughput increases from 153.8 Mbps to 168.8 Mbps (see Figure 5.6(a)), which is an approximately 10% increase. Furthermore, the lower 10^{th}percentile user throughput also increases with increase in average number of users per cell compared to the *scaled* user throughput. Provided that the user throughput is T_ν with U_1 users in the system, the scaled user throughput for U_2 users refers to the user throughput that would be achieved if U_2 users are present in the system. This is expressed as $\hat{T}_\nu = T_\nu U_1/U_2$. Note that the 10^{th} percentile user throughput depicted in Figure 5.6(b) are 5.61 Mbps and 1.7 Mbps with 10 and 40 users per BS respectively. Taking the former as a reference, the scaled throughput in the latter case would be 1.4 Mbps. The observed gains is attributed to multi-user diversity and may be explained as follows – using the BB-enabled switched beam approach, at a lower number of users in the system on average, such as $U = 10$, it is possible that none of the users lie in the beam where (5.17) is fulfilled. Thus, some of the chunks that could have been used for data transmission remain idle, resulting in a loss of system capacity. As the number of users per cell increases, the likelihood of chunks remaining idle is decreased and therefore the system throughput improves. By contrast, the benchmark

[2]Similar trends are obtained when a larger number of antenna elements are used. Therefore, these results are omitted for brevity.

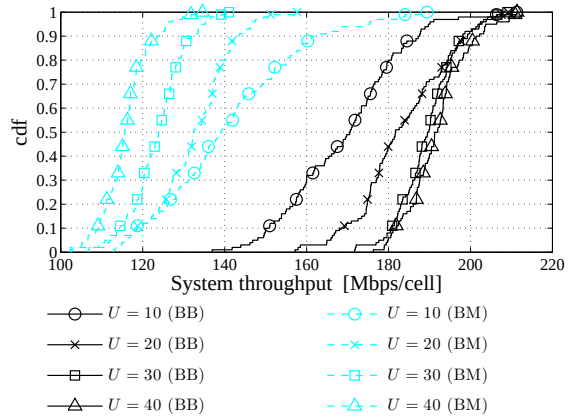

(a) System throughput

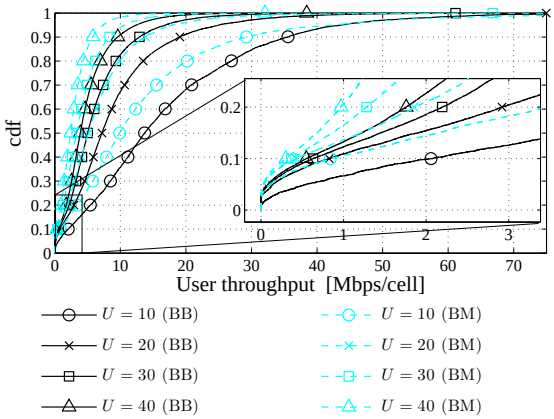

(b) User throughput

Figure 5.6: *Comparison of cdfs of system and user throughputs in the system with various number of users per BS U. A threshold of -75 dBm is used for BB enabled switched beam , so that the user throughput is maximised.*

system demonstrates that the system throughput decreases with an increase in the average number of users per cell. Note that the throughput decreases from 136.4 Mbps/cell with $U = 10$ to 115.4 Mbps/cell with $U = 40$. This is because the benchmark system reuses all chunks in the system *blindly* if there is a user in the sector where the *a priori* estimate of SINR exceeds the minimum SINR required for scheduling. While this can result that some chunks remain unused in some of the sectors at lower average number of users per cell, the likelihood of this decreases with increase in the number of users per BS. Consequently, the average amount of CCI caused to adjacent cell increases with the increase in the number of users per BS resulting in a decrease in the system throughput.

5.7.4 CESAR mechanism vs. $p-$persistence

In the results presented so far, CESAR mechanism described in Section 5.3.1 was used for allocating unreserved chunks. The performance of utilising $p-$persistence method for allocating unreserved chunks is compared against the CESAR mechanism in Figure 5.7. The results demonstrate that the CESAR mechanism improves the median system throughput by 5% and cell-edge user throughput by 16% compared to using $p-$persistence mechanism using $p = 0.3$. This is because with CESAR mechanism, collisions of transmission within a cluster of cells are eliminated. This enables the BB mechanism to reserve the chunks and avoid CCI higher than the threshold value. Although $p-$persistent mechanism reduces the likelihood of collisions, it does not completely eliminate them. As a result, fewer chunks remain reserved with $p-$persistent mechanism compared to the CESAR mechanism especially at the cell-edge. At the extreme, the results for $p = 1.0$ are presented, where an unreserved chunk is allocated simultaneously in contention in more than one cell. As two or more users allocate the same unreserved chunk simultaneously, they are not aware of the CCI they cause to the receiver(s) of the other links. As a result, the performance of the benchmark system and BB mechanism with $p = 1.0$ are approximately the same at the cell edge. However, with BB mechanism, the chunks where the SINR target is not met are released and reallocated. This causes the resources to be allocated primarily to the users that lie closer to the serving BS. Consequently, the system throughput is maximised due to high spatial reuse.

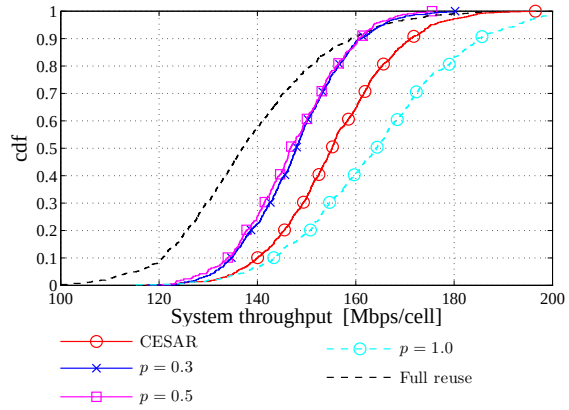

(a) System throughput

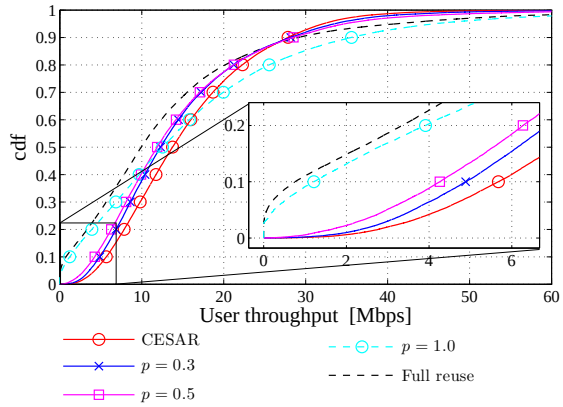

(b) User throughput

Figure 5.7: *Comparison of system performance with CESAR mechanism and $p-$persistence. A threshold of -75 dBm and $U = 10$ is used for BB enabled switched beam, so that the user throughput is maximised.*

5.7.5 Impact of interference feedback

BB mechanism enables the potential transmitter to avoid CCI higher than the threshold value towards the receiver of a pre-established link. Likewise, in the results presented so far, feedback of interference observed in chunk (n, k) was used to make an *a priori* estimate of SINR in chunk (n, k), which served two purposes - first, it avoided scheduling users on the chunks where the observed CCI was high enough to cause the SINR target not to be met and second, it allowed the transmitter to select an appropriate modulation format instantly without having to go through the transient phase if $m = 1$ was chosen as the initial modulation format. The *a priori* estimate of SINR target is valid because with CESAR mechanism, only one cell within the cluster allocates new chunk at a given instant. All other links avoid CCI higher than the threshold. However, such information needs to be explicitly conveyed back to the transmitter, which consumes bandwidth in the reverse direction. In particular, in the DL mode, each MS experiences a different amount of interference from the adjacent cells. Therefore, the assumption of SINR knowledge may not be feasible especially at higher number of users at the BS.

The impact of relaxing the knowledge of *a priori* estimate of SINR at the transmitter is compared against the system where interference feedback (IF) is utilised in Figure 5.8. The results demonstrate that when the threshold of -75 dBm is set such that the user throughput is maximised, both the system throughput Figure 5.8(a) and user throughput Figure 5.8(b) are practically the same, regardless of whether or not the interference feedback is utilised. In both cases, IF performs only slightly better. However, when the threshold is increased and CCI protection is compromised, IF significantly increases the system throughput because the chunks are allocated to the users that are able to meet the minimum SINR target. Consequently, the chunks are allocated predominantly towards the cell-centre and are reserved by the cell-centre users. As the number of chunks available for cell-edge users is lower with IF feedback, the cell-edge user throughput is compromised. Without IF, the performance of benchmark system is degraded by over 53% in terms of system throughput and 66% in terms of user throughput. Without IF applied for user scheduling, the BB mechanism enhances the system throughput by 70% and cell-edge user throughput by 20-fold compared to the benchmark system.

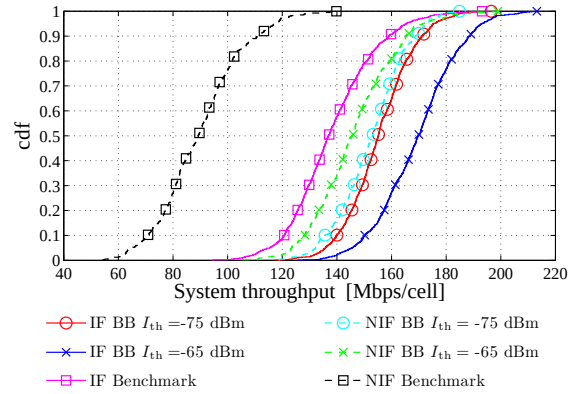

(a) System throughput

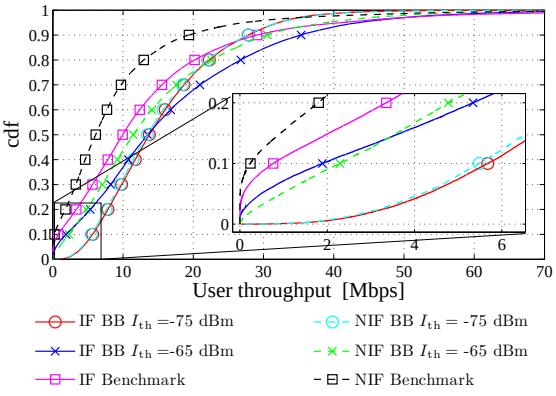

(b) User throughput

Figure 5.8: *Impact of utilising interference feedback (IF) from the preceding slot to estimate the SINR in current slot for user scheduling.*

5.8 Chapter summary

In this chapter, a new hybrid interference avoidance and mitigation technique has been proposed which combines two existing powerful techniques - interference mitigation using switched beam approach and interference avoidance using BB signalling. A comparison has been made against the state-of-the-art switched beam approach employing a full-frequency reuse, chosen as the benchmark. It was demonstrated that the proposed approach achieved a spectral efficiency of up to 3.75 bps/Hz/cell together with a cell-edge user throughput of 4.38 Mbps/user. This represents a 22% higher spectral efficiency and a 5.8-fold increase in cell-edge user throughput compared to the benchmark. It was further demonstrated that by adjusting the threshold parameter of the BB technique, the spectral efficiency can be traded off for an enhanced cell-edge user throughput. In particular, by adjusting the threshold, 0.38 bps/Hz/cell was sacrificed to achieve a 7.3-fold increase in cell-edge user throughput compared to the benchmark system. It was further demonstrated that the improvements of system as well as the user throughput attained through the hybrid BB enabled switched beam approach comes at a reduction of energy consumption by more than 40% on top. This is not a surprising result and highlights the importance of cooperative interference management techniques such as the hybrid BB enabled switched beam approach analysed in this chapter. Finally, it has been demonstrated that additional gains in system performance have been achieved with the proposed scheme compared to the benchmark even with an increase in the number of antenna elements at the transmit array and/or with the increase in the average number of users served by a BS. More importantly, it is shown that in the considered system, the BB mechanism does not compromise the performance even without explicit feedback of CCI whereas the performance of the benchmark system degrades by more than 50% without interference feedback for user scheduling. The performance enhancements are achieved by simply adding a computationally simple algorithm, and therefore easily implementable, to a system already implementing the switched beam approach. In the light of these results, the proposed scheme can be viewed as a natural complement to existing state-of-the-art switched beam approach.

Chapter 6
Conclusions

6.1 Summary and conclusions

Co-channel interference (CCI) is generally identified as the most dominant bottleneck in improving spectrum utilisation. In order to cater for a multitude of requirements prevalent in future wireless networks, the available spectrum needs to be utilised in the most efficient manner. To this end, CCI mitigation is often seen as a key.

In this thesis, CCI avoidance using the busy burst (BB) concept was investigated in *ad hoc* as well as cellular wireless networks. With BB protocol, after successful transmission of data, the receiver reserves the chunk for subsequent time slot by transmitting a BB signal on the associated time slot. Exploiting the channel reciprocity property of the time division duplexing (TDD) mode, the transmitter infers the potential amount of CCI it would cause to the receiver that has reserved the chunk if the transmitter were to transmit. The transmitter refrains from transmission if it receives BB power above a certain threshold which is constant systemwide. In this thesis, it was demonstrated that by adjusting this threshold parameter, the spectral efficiency can be traded off for enhancing the user throughput at the lower 10^{th} percentile, both in *ad hoc* as well as cellular networks. The lower 10^{th} percentile was chosen as a measure of the minimum data rate that can be guaranteed to individual links in the network in the long run. Moreover, by utilising variable BB power to signal the interference tolerance of individual links, it was demonstrated that a more preferable compromise between system throughput and link throughput can be made. Furthermore, it is demonstrated that a large spatial reuse corresponds to a poor achieved SINR and enables lower order modulation format to be used on each chunk. Assuming a fixed transmit power per chunk and interference limited scenario, it is demonstrated that a large spatial reuse results in high energy consumption per bit. By trading off spatial reuse for enhanced SINRs, it is demonstrated that the energy efficiency can be adjusted by varying the threshold.

In decentralised and self-organising *ad hoc* networks that lack dedicated centralised infrastructure and control, it was demonstrated that the BB protocol improves the performance both in

terms of spectral efficiency and fairness metrics compared to both random access techniques or prognostic approaches such as carrier sense multiple access (CSMA) approaches. In particular, the median system throughput was enhanced by 48% compared to the CSMA/CA (CSMA with collision avoidance) mechanism. Likewise, by adjusting the threshold it was demonstrated that the BB approach allows for a more flexible and scalable approach in chunk allocation. It particular, with the satisfied user criteria set at 2 Mbps, it was demonstrated that BB approach with link adaptation supports up to 32 links compared to 5 links supported by the CSMA/CA approach. The self organising property of BB protocol makes it particularly attractive for radio resource allocation in systems lacking centralised coordination such as femtocell networks or for spectrum sharing application on industrial, scientific and medical (ISM) bands.

Soft reuse of chunks using BB concept was investigated for cellular networks deployments in Manhattan and hexagonal cellular scenario. When a full reuse of chunks is considered, high CCI is coupled with low desired signal power in the downlink (DL) whereas in the uplink (UL) the detrimental effects of interference are distributed more equally among all users, giving rise to interference diversity. This results in poorer SINR achieved at the cell-edge in the DL compared to those in the UL. It is demonstrated that the trade off between system throughput and cell-edge user throughput is more favourable in the DL rather than in the UL. In particular, it was shown that with BB signalling and link adaptation, 17% (DL) and 50% (UL) of median system throughput was traded off to enhance the cell-edge user throughput by 3-fold (DL) and 20% (UL) in Manhattan scenario. The impact of prioritising users with fewer reserved chunks for new chunk allocation was studied and it was demonstrated that user prioritisation enhances the cell-edge user throughput. However, user prioritisation also increases collisions if the threshold is set such that level of CCI protection is compromised.

Finally, a new hybrid interference avoidance and mitigation technique has been proposed which combines two existing powerful techniques - interference mitigation using switched beam approach and interference avoidance using BB signalling. Compared to the state-of-the-art switched beam approach employing a full-frequency reuse, chosen as the benchmark, a 22% higher spectral efficiency together with a $5.8-$fold increase in cell-edge user throughput compared to the benchmark. It was shown that decreasing the beamwidth by increasing the number of transmit antennas increases both the system throughput and user throughput in the benchmark system. However, incorporating BB on top of switched beam approach increases the performance even further, regardless of the number of antennas used.

6.2 Limitations and future work

The key assumption made in this thesis is that the channel is reciprocal in TDD mode, *i.e.* the channel gain between transmitter to the receiver is the same as the channel gain between transmitter and receiver. This is true in a TDD air interface as long as the data slot and BB slot are separated by a small fraction of the coherence time. For a frequency division duplexing (FDD) air interface, due to high frequency separation between the frequency used for transmission and reception, the channel variations can be in order of tens of dB. While the log-normal shadowing and distance dependent fading is similar in the uplink and the downlink bandwidth and BB protocol can indeed be utilised for CCI mitigation, BB is envisioned to exhibit some degradation when used in an FDD system. This limitation also affects the TDD systems where the relative velocity between the transmitter and the receiver is very high, such as the velocities achieved by high velocity trains. In such systems, the coherence time decreases and the channel may not be reciprocal during the data slot and BB slot. Moreover, different OFDM symbols within a frame experience different amount of CCI, the assumption of constant CCI within a chunk may not be a realistic assumption in such scenario. One possible solution to improve the throughput on links that are subject to signal to interference and noise ratio (SINR) fluctuations within a chunk is to utilise a hybrid automatic repeat request (HARQ) and chase combining, which can be investigated further in future.

An important assumption made throughout this thesis is that the transmitters and receivers in the network are perfectly synchronised in time and frequency, which may not always be realisable in practice. Imperfect synchronisation causes additional interference at the receiver. Even if the transmitters and receivers are synchronised to a common clock, which may be achieved by using network time protocol or global positioning system (GPS) receivers, propagation delays can result in transceivers that are not synchronized to one another. In this context, an important limitation of this work is that multiple access interference (MAI) is not considered. Doppler shift and frequency offsets of local oscillators are responsible for MAI. The assumption of constant SINR among all subcarriers within a chunk is violated when MAI is present. In a system with MAI, the SINRs achieved in the subcarriers at the boundary between two chunks are typically worse than those in the middle of the chunk, provided that the two chunks are allocated to two different users.

A third limitation in this thesis is that the data transmit power was assumed constant in the network and CCI was avoided by refraining from transmitting on chunk observed not to be

free. Although BB mechanism allows power control, this has not been investigated in this thesis. In a cellular system, the power control algorithm must be jointly considered with user scheduling, which is a subject of further investigation.

Finally, the performance of BB signalling on a homogeneous network was investigated in this thesis. In realistic networks, different users have a different requirement in terms bandwidth demand, delay tolerance, bit error ratio (BER) and so on. In such network, low priority users may have to release their reserved chunks to serve high priority users. Alteration in chunk allocation in a tagged cell alters the CCI observed at the receiver, particularly in the DL mode. User scheduling concepts to mitigate CCI in the system with heterogeneous demands and priority is another topic that needs to be investigated in future.

Appendix A
Publications

A.1 Journal Papers

1. B. Ghimire, G. Auer, and H. Haas, "Busy Bursts for Trading off Throughput and Fairness in Cellular OFDMA–TDD" EURASIP Journal on Wireless Communications and Networking, vol. Volume 2009, Article ID 462396, 14 pages, 2009.

2. G. Auer, S. Videv, B. Ghimire and H. Haas, "Contention Free Inter-Cellular Slot Reservation", IEEE Communications Letters, vol. 13, pp. 318320, May 2009.

3. B. Ghimire, G. Auer and H. Haas, "Busy Burst Enabled Interference Coordination in Networked MIMO Systems", envisaged submission to IEEE transactions on Wireless Communications.

A.2 Conference Papers

1. B. Ghimire, S.Sinanović H. Haas, and G. Auer, "Self-organised Interference Mitigation in Wireless Networks Using Busy Bursts", in Proc. of the International Symposium on Applied Sciences in Biomedical and Communication Technologies (ISABEL), Bratislava, Slovakia, Nov. 24–27, 2009, pp. 6 pages on a CDROM *(Invited paper)*.

2. B. Ghimire, H. Haas, and G. Auer, "OFDMA–TDD Networks with Busy Burst Enabled Grid-of-Beam Selection", in Proc. of the International Conference on Communications (ICC), Dresden, Germany, Jun. 14–18, 2009, pp. 6 pages on a USB disk.

3. G. Auer, S. Videv, B. Ghimire and H. Haas, "Contention Free Slot Allocation and Reservation in Cellular Networks", in Proc. of the IEEE Sarnoff Symposium, Princeton, USA, Mar. 30 – Apr. 1, 2009, pp 5 pages on CDROM.

4. B. Ghimire, H. Haas, and G. Auer, "Balancing System Throughput and Fairness in Multi–User OFDMA–TDD using Busy Bursts" in Proc. of the International Symposium on

Personal, Indoor and Mobile Radio Communications (PIMRC), Cannes, France, Sep. 15–18, 2008, pp. 6 pages on CDROM.

5. B. Ghimire, H. Haas, and G. Auer, "Busy Burst Enabled Interference Avoidance in WINNER-TDD," in Proc. of the International Symposium on Personal, Indoor and Mobile Radio Communications (PIMRC), Athens, Greece, Sep. 3–7, 2007, pp. 5 pages on CDROM.

Hindawi Publishing Corporation
EURASIP Journal on Wireless Communications and Networking
Volume 2009, Article ID 462396, 14 pages
doi:10.1155/2009/462396

Research Article

Busy Bursts for Trading off Throughput and Fairness in Cellular OFDMA-TDD

Birendra Ghimire,[1] Gunther Auer,[2] and Harald Haas[1,3]

[1] *Institute for Digital Communications, Joint Research Institute for Signal and Image Processing, The University of Edinburgh, EH9 3JL, UK*
[2] *DOCOMO Euro-Labs, Landsberger Straße 312, 80687 Munich, Germany*
[3] *School of Engineering and Science, Jacobs University Bremen, 28759 Bremen, Germany*

Correspondence should be addressed to Harald Haas, h.haas@ed.ac.uk

Received 1 July 2008; Accepted 8 December 2008

Recommended by Mohamed Hossam Ahmed

Decentralised interference management for orthogonal frequency division multiple access (OFDMA) operating in time division duplex (TDD) cellular systems is addressed. Interference aware allocation of time-frequency slots is accomplished by letting receivers transmit a busy burst (BB) in a time-multiplexed minislot, upon successful reception of data. Exploiting TDD channel reciprocity, an exclusion region around a victim receiver is established, whose size is determined by a threshold parameter, known at the entire network. By adjusting this threshold parameter, the amount of cochannel interference (CCI) caused to active receivers in neighbouring cells is dynamically controlled. It is demonstrated that by tuning the interference threshold parameter, system throughput can be traded off for improving user throughput at the cell boundary, which in turn enhances fairness. Moreover, a variable BB power is proposed that allows an individual link to signal the maximum CCI it can tolerate whilst satisfying a certain quality-of-service constraint. The variable BB power variant not only alleviates the need to optimise the interference threshold parameter, but also achieves a favourable tradeoff between system throughput and fairness. Finally, link adaptation conveyed by BB signalling is proposed, where the transmission format is matched to the instantaneous channel conditions.

1. Introduction

Orthogonal frequency division multiplexing (OFDM) has been selected as a radio access technology for a number of wireless communication systems, for instance, the wireless local area network (WLAN) standard IEEE 802.11 [1], the European terrestrial video broadcasting standard DVB-T [2], and for beyond 3rd generation (B3G) mobile communication systems [3]. In OFDMA, the available resources are partitioned into time-frequency slots, also referred to as *chunks*, which can be flexibly distributed among a number of users who share the wireless medium. Provided that channel knowledge is available at the transmitter, resources can be assigned to users with favourable channel conditions, giving rise to multiuser diversity [4].

Interference management is one of the major challenges for cellular wireless systems, as transmissions in a given cell cause cochannel interference (CCI) to the neighbouring cells. Full-frequency reuse where the transmitters are allowed an unrestricted access to all resources causes high CCI, which particularly impacts the cell-edge users [5–7]. Although CCI can be mitigated by traditional frequency planning, this potentially results in a loss in bandwidth efficiency due to insufficient spatial reuse of radio resources. Fractional frequency reuse (FFR) [4–6, 8] addresses this issue by realising that in the cellular networks CCI predominantly affects users near the cell boundary. FFR typically involves a subband with full-frequency reuse that is exempt from any slot assignment restrictions. The allocation of the remaining subbands is coordinated among neighbouring cells, in a way that the users in the given cell are denied access to subbands assigned to the cell-edge users in the adjacent cells. To this end, in [5] a user is classified as a cell-edge user based on the path loss to the desired base station (BS). This approach ignores the fact that the channel attenuation of the desired and the interfering signals is uncorrelated, and therefore fails to

exploit interference diversity. Moreover, frequency planning results in a hard spatial reuse of the available resources. As a result, it cannot cater for the dynamic traffic and load across different sites. Furthermore, in systems where BSs are dynamically added in an uncoordinated manner, such as home base stations [9], reconfigurable frequency reuse planning may prove to be increasingly cumbersome.

The busy-signal concept [10–16] has been identified as an enabler for decentralised and interference aware slot assignment. Receiver feedback informs a potential transmitter about the instantaneous CCI it causes to the "victim" receivers, which enables the transmitter to take appropriate steps to avoid interference, such as deferring its own transmission to another chunk. Early works [10, 11] rely on dedicated frequency-multiplexed channels that carry narrowband busy tones for channel reservation. As the protocol requires the transceivers to listen to the out-of-band busy tones whilst transmitting, complex RF units are required due to additional filters and duplexers involved. This drawback is avoided in [12–14], where time-multiplexed busy bursts (BBs) serve as a reservation indicator for a reservation-based medium access control (MAC) protocol. By transmitting an in-band BB in an associated minislot following a successful transmission, two important goals are accomplished [13, 14]. First, the transmitter of its own link is informed whether or not the data is successfully received. Second, at the same time potential transmitters of the competing links are notified about ongoing transmissions, so that these transmitters can take appropriate steps to avoid interference. Therefore, both slot reservation and channel sensing tasks are accomplished. Furthermore, *interference diversity* is exploited, in the way that competing links may spatially reuse the same slot, given the interfering links are sufficiently attenuated.

None of the busy tone-based MAC protocols [11–14] allow for dynamic resource allocation where multiple users share a set of parallel frequency slots of a broadband frequency-selective radio channel, such as the 100 MHz channel of the WINNER (Wireless world Initiative New Radio, www.ist-winner.org) TDD mode [17].

By extending the BB concept to OFDMA [15, 16], the channel reciprocity of TDD [18] is exploited for decentralised interference management such that the chunks can be dynamically assigned on a short-term basis thereby ensuring a soft spatial reuse of chunks among cells. This concept termed BB-OFDMA works in a completely decentralised fashion and is therefore applicable to self-organising networks, which may consist of cellular as well as *ad hoc* network topologies.

The attainable system throughput of BB-OFDMA is sensitive to the selected interference threshold [15, 16]. In this paper, it is demonstrated how the interference threshold can be tuned to tradeoff system throughput to enhance cell-edge user throughput, thereby enhancing fairness. Moreover, by using a variable BB power that takes into account the quality of the intended link, a favourable tradeoff between system throughput and fairness is achieved. A variable BB power exhibits the further advantage that the sensitivity of the selected interference threshold on the performance is mitigated. Finally, BB-OFDMA with variable BB power is the basis for a novel receiver-driven link adaptation algorithm. System-level simulations demonstrate a significant improvement both in terms of fairness and total system throughput of BB-OFDMA, compared to the system with full-frequency reuse, where attempts to avoid interference are not made.

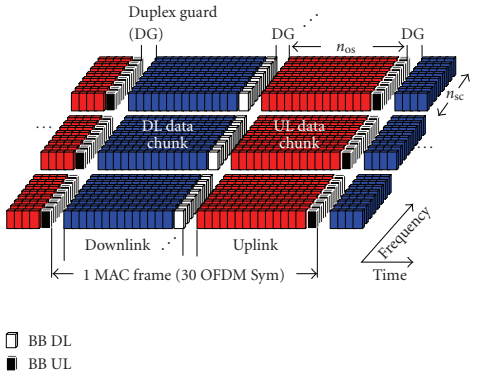

Figure 1: Frame structure for OFDMA-TDD with BB signalling.

The remainder of the paper is arranged as follows. Section 2 describes the air interface of WINNER-TDD. The allocation of radio resources among the competing user population is discussed in Section 3. Section 4 introduces the BB signalling mechanism and its variants as well as the proposed link adaptation algorithm. The considered Manhattan grid deployment scenario and the system level simulator are introduced in Section 5, and the simulation results are discussed in Section 6. Finally, the conclusions are drawn in Section 7.

2. System Model

A time-frequency slotted OFDMA-TDD air interface based on the WINNER-TDD mode [8] is implemented, as illustrated in Figure 1. A chunk comprises of n_{sc} subcarriers and n_{os} OFDM symbols and represents a resource unit that can be allocated to one out of U users located in cell q. Successive downlink (DL) and uplink (UL) slots, each of which contains N_C chunks, constitute a frame. A chunk with frequency index $1 \le n \le N_C$ at frame k is denoted by (n, k). The transmit power of user ν at chunk (n, k) is denoted by $T^{d}_{\nu,q}[n, k]$.

The transmitted signal of chunk (n, k) propagates through a mobile radio channel. The corresponding channel gain $G_{\nu,q}[n, k]$ comprises radio effects such as distance-dependent path loss, log-normal shadowing as well as channel variations due to frequency-selective fading and user mobility [19]. While channel variations of $G_{\nu,q}[n, k]$ between adjacent chunks in time and frequency are taken into account, fluctuations within a chunk are neglected. This approximation is justified as long as the chunk dimensions are significantly smaller than the coherence time and frequency [20].

The received signal power of user ν can be expressed as

$$\widetilde{R}^{\mathrm{d}}_{\nu,q}[n,k] = R^{\mathrm{d}}_{\nu,q}[n,k] + I^{\mathrm{d}}_{\nu,q}[n,k] + N, \tag{1}$$

where N is the thermal noise power. Both the received signal powers of the intended and the interfering links, denoted by $R^{\mathrm{d}}_{\nu,q}[n,k] = T^{\mathrm{d}}_{\nu,q}[n,k]G_{\nu,q}[n,k]$ and $I^{\mathrm{d}}_{\nu,q}[n,k]$, may vary significantly between different chunks, as elaborated in more detail in Section 4. The achieved signal-to-interference-plus-noise ratio (SINR) at chunk (n,k) is in the form

$$\gamma_{\nu,q}[n,k] = \frac{R^{\mathrm{d}}_{\nu,q}[n,k]}{I^{\mathrm{d}}_{\nu,q}[n,k] + N}. \tag{2}$$

3. Multiuser Resource Allocation

Provided that only one user per cell transmits on a given chunk, the base station (BS) may flexibly assign chunks to users, such that the intracell interference is avoided. However, as chunks may be simultaneously accessed by adjacent cells, CCI is encountered. Multiuser resource allocation is carried out by a score-based scheduler [21] variant, which distributes the $1 \le n \le N_{\mathrm{C}}$ chunks among $1 \le \nu \le U$ users served by the BS in cell q. Assuming that the channel gains $G_{\nu,q}[n,k]$ are available at BS_q, the score for user ν at chunk (n,k) is computed as

$$s_{\nu,q}[n,k] = 1 + \sum_{\ell=1}^{N_{\mathrm{C}}} \Upsilon_{\{G_{\nu,q}[n,k] \le G_{\nu,q}[\ell,k]\}} + \epsilon_{\nu,q}[n,k], \tag{3}$$

where the Boolean operator $\Upsilon_x \in \{0,1\}$ is set to 1 or 0 when the condition x is true or false, respectively. The parameter $\epsilon_{\nu,q}[n,k] \in \{0,\infty\}$ indicates whether or not user ν is granted access to chunk (n,k). For interference aware and reservation-based MAC protocols such as BB-OFDMA (see Section 4.4), setting $\epsilon_{\nu,q}[n,k] \to \infty$ ensures that user ν in cell q is denied access to chunk (n,k). This effectively avoids radiation of CCI from cell q to any neighbouring cells that use the same chunk (n,k).

Score based multiuser scheduling with reservation assigns chunk (n,k) to user ν if either a reservation indicator was set in the previous frame, $\beta_q[n,k-1] = \nu$, or the score given by (3) is minimised

$$a_q[n,k] = \begin{cases} \arg\min\limits_{\nu} s_{\nu,q}[n,k], & \beta_q[n,k-1] = 0, \\ \beta_{\nu,q}[n,k-1], & \text{otherwise.} \end{cases} \tag{4}$$

In case $\epsilon_{\nu,q}[n,k] \to \infty$ for all users, cell q leaves chunk (n,k) unassigned in (4). The user ν that is assigned chunk (n,k) transmits data to its intended receiver. The set of chunks $n \in \{1,\ldots,N_C\}$ at time k, for which $a_q[n,k] = \nu$ are denoted by $\mathcal{A}_{\nu,q}$. Allocated chunks $a_q[n,k] = \nu$ whose achieved SINR $\gamma_{\nu,q}[n,k]$ exceeds the target Γ, such that

$$b_q[n,k] = \begin{cases} \nu, & a_q[n,k] = \nu \text{ and } \gamma_{\nu,q}[n,k] \ge \Gamma, \\ 0, & \text{otherwise} \end{cases} \tag{5}$$

represent the set of successfully allocated chunks of user ν, denoted by $\mathcal{B}_{\nu,q} \subseteq \mathcal{A}_{\nu,q}$ [15].

For BB-OFDMA chunks with $b_q[n,k] \neq 0$ are reserved and protected from interference at the next frame $k+1$ by setting the reservation indicator to $\beta_q[n,k] = b_q[n,k]$ in (4). When the SINR target is not met, $\gamma_{\nu,q}[n,k] < \Gamma$, the reservation indicator is reset to $\beta_q[n,k] = b_q[n,k] = 0$. These chunks $\mathcal{A}_{\nu,q} \setminus \mathcal{B}_{\nu,q}$ are released in a way that user ν is prohibited access in the next slot $k+1$ by setting $\epsilon_{\nu,q}[n,k+1] \to \infty$. Subsequently, chunk $(n,k+1)$ is assigned to other users by (4).

In a cellular OFDMA system without interference protection, there is no restriction for accessing any chunks, so $\epsilon_{\nu,q}[n,k] = 0\ \forall n,k$ in (3) for all users in the cell. Moreover, no reservation indicator is set, $\beta_q[n,k] = 0\ \forall n,k$ in (4), irrespective of $b_q[n,k]$ in (5).

4. Busy Burst Signalling

Interference management using busy burst (BB) signalling [13, 14] establishes an exclusion region around active receivers. An exclusion region defines an area around an active receiver in cell q, where potential transmitters in adjacent cells $p \neq q$ must not transmit, so that excessive CCI by close-by interferers is mitigated. In the context of OFDMA, the exclusion regions are to be established individually for each chunk (n,k) [15]. In BB-OFDMA, an MAC frame is divided into data slots and BB minislots as illustrated in Figure 1. The BS transmits data in slot "Data DL." Provided that the SINR target for an allocated chunk (n,k) is met, the intended mobile station (MS) transmits a BB in the associated minislot "BB UL" at uplink chunk (n,k). This reserves chunk n of "Data DL" for the next frame $k+1$. Likewise, for uplink data transmitted by the MS in slot "Data UL," the BB is transmitted by the intended BS in the downlink minislot "BB DL." In summary, BB-OFDMA is described by the following protocol.

(1) All potential transmitters must sense the BB associated to the data chunk (n,k) prior to transmission.

(2) Transmitters are prohibited to access chunks where a BB is detected above a given threshold.

The resulting BB signalling overhead amounts to 6.7%, as 2 OFDM symbols out of 30 OFDM symbols per frame are used for BB signalling. However, instead of dismissing BB signalling as overhead, the BB minislots may be utilised to convey the feedback and control information. Hence, BB signalling may serve as an alternative control channel.

To exemplify the principle of BB-enabled interference avoidance in cellular system, a typical downlink and uplink interference scenario is illustrated in Figure 2. In the downlink shown in Figure 2(a), MS_1 has transmitted a BB after successful reception from BS_1. As BS_2 detects a strong BB from MS_1, BS_2 cannot spatially reuse this chunk with BS_1. In the uplink shown in Figure 2(b), BS_1 has transmitted a BB after successful reception from MS_1. While MS_2 is denied access to this chunk, as it detects a strong BB from BS_1, MS_3 is located outside the exclusion region of BS_1, and may therefore simultaneously access this chunk with MS_1.

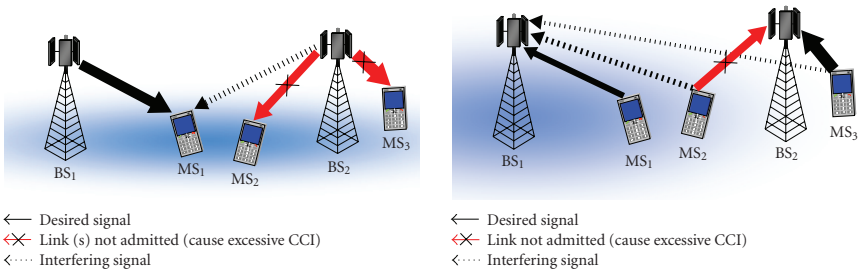

FIGURE 2: BB signalling applied to cellular system. The arrows depict the direction of desired and interfering signals and their relative strength is indicated by their width. The strength of BB signal is indicated by the darkness of the shade around the vulnerable receiver.

4.1. Two Competing Links. To mathematically describe BB-enabled interference avoidance, let $\mathbf{x} = (\nu, q)$ define a transmitter or receiver (either BS or MS) of user ν within cell q. With this notation, the channel gain of the intended link at chunk (n,k) becomes $G_{\mathbf{x}}[n,k] = G_{\nu,q}[n,k]$. The channel gain of an interfering link, between transmitter $\mathbf{y} = (\mu, p)$ of user μ located in an adjacent cell $p \neq q$ and receiver $\mathbf{x}$, is denoted by $G_{\mathbf{yx}}[n,k]$. In case two links compete for resources, the CCI between transmitter $\mathbf{y}$ and receiver $\mathbf{x}$ amounts to $I^{\mathrm{d}}_{\mathbf{x}}[n,k] = G_{\mathbf{yx}}[n,k]T^{\mathrm{d}}_{\mathbf{y}}[n,k]$. (The term $I^{\mathrm{d}}_{\mathbf{x}}[n,k]$ is equivalent to the CCI $I^{\mathrm{d}}_{\nu,q}[n,k]$ as defined in (1). While the notation $I^{\mathrm{d}}_{\mathbf{x}}[n,k]$ is preferred for intercellular interference management, the latter is used for intracell resource allocation. The same rule applies for related quantities that denote transmitted and received signal powers.) Likewise, $T^{\mathrm{b}}_{\mathbf{x}}[n,k]$ and $I^{\mathrm{b}}_{\mathbf{y}}[n,k] = G_{\mathbf{xy}}[n,k]T^{\mathrm{b}}_{\mathbf{x}}[n,k]$ are the transmit power of the BB transmitter $\mathbf{x}$ (data receiver) and the interfering BB power received at data transmitter $\mathbf{y}$ (BB receiver), respectively.

Exploiting TDD channel reciprocity [18], transmitter $\mathbf{y}$ can ascertain $I^{\mathrm{d}}_{\mathbf{x}}[n,k]$, the potential amount of interference it causes to an existing link $\mathbf{x}$, by measuring $I^{\mathrm{b}}_{\mathbf{y}}[n,k]$ at the associated BB minislot [13]. Applying the channel reciprocity property of TDD, $G_{\mathbf{yx}}[n,k] = G_{\mathbf{xy}}[n,k]$, yields

$$I^{\mathrm{d}}_{\mathbf{x}}[n,k] = I^{\mathrm{b}}_{\mathbf{y}}[n,k] \cdot \frac{T^{\mathrm{d}}_{\mathbf{y}}[n,k]}{T^{\mathrm{b}}_{\mathbf{x}}[n,k]}. \tag{6}$$

The maximum CCI $I^{\mathrm{d}}_{\mathbf{x}}[n,k]$ that a candidate transmitter $\mathbf{y}$ may cause to an active receiver $\mathbf{x}$ is determined by the interference threshold I_{th}, which is constant and known to the entire network. When $I^{\mathrm{d}}_{\mathbf{x}}[n,k] < I_{\mathrm{th}}$, transmitter $\mathbf{y}$ is located outside the exclusion range of $\mathbf{x}$. Provided that $T^{\mathrm{b}}_{\mathbf{x}}[n,k]$ is known to the candidate transmitter $\mathbf{y}$, (6) enables $\mathbf{y}$ to verify whether $I^{\mathrm{d}}_{\mathbf{x}}[n,k] < I_{\mathrm{th}}$ by invoking the threshold test [13, 14]

$$I^{\mathrm{b}}_{\mathbf{y}}[n,k] \cdot \frac{T^{\mathrm{d}}_{\mathbf{y}}[n,k]}{T^{\mathrm{b}}_{\mathbf{x}}[n,k]} \leq I_{\mathrm{th}}. \tag{7}$$

In case $T^{\mathrm{d}}_{\mathbf{y}}[n,k] = T^{\mathrm{b}}_{\mathbf{x}}[n,k]$, condition (7) reduces to

$$I^{\mathrm{b}}_{\mathbf{y}}[n,k] \leq I_{\mathrm{th}}. \tag{8}$$

By tuning I_{th}, the maximum CCI $I^{\mathrm{d}}_{\mathbf{x}}[n,k]$ in (2) is adjusted, which determines the size of the exclusion range around active receivers.

4.2. Extension to Multiple Cells. In a multicell scenario, signals from multiple links superimpose at the receiver. The total interference at data receiver $\mathbf{x}$ amounts to

$$I^{\mathrm{d}}_{\mathbf{x}}[n,k] = \sum_{\substack{\mathbf{z}\in\mathcal{T} \\ \mathbf{z}\neq\mathbf{x}}} T^{\mathrm{d}}_{\mathbf{z}}[n,k] \cdot G_{\mathbf{zx}}[n,k], \tag{9}$$

where $\mathcal{T}$ is the set of simultaneously active transmitters. Likewise, the received BB at the data transmitter (BB receiver) $\mathbf{y}$ yields

$$I^{\mathrm{b}}_{\mathbf{y}}[n,k] = \sum_{\substack{\mathbf{z}\in\mathcal{R} \\ \mathbf{z}\neq\mathbf{y}}} T^{\mathrm{b}}_{\mathbf{z}}[n,k] \cdot G_{\mathbf{zy}}[n,k], \tag{10}$$

where $\mathcal{R}$ is the set active receivers (BB transmitters).

Unlike the case when two links compete for resources, $I^{\mathrm{b}}_{\mathbf{y}}[n,k]$ is no longer equivalent to $I^{\mathrm{d}}_{\mathbf{x}}[n,k]$ in the threshold test (8). This is because in (9) the interference powers from multiple transmitters $\mathcal{T}$ add up. Consequently, the total CCI at data receiver $\mathbf{x}$ may exceed the tolerable threshold such that $I^{\mathrm{d}}_{\mathbf{x}}[n,k] > I_{\mathrm{th}}$, although the BB power (10) observed by the individual interferers $\mathbf{y} \in \mathcal{T}$ is below the threshold, $I^{\mathrm{b}}_{\mathbf{y}}[n,k] \leq I_{\mathrm{th}}$. On the other hand, in (10) the interfering BB powers from multiple simultaneously active receivers observed at $\mathbf{y} \in \mathcal{T}$ add up. It is, therefore, possible that $I^{\mathrm{b}}_{\mathbf{y}}[n,k] > I_{\mathrm{th}}$, so that link $\mathbf{y}$ is prohibited from accessing chunk (n,k), although its individual CCI contribution, $T^{\mathrm{d}}_{\mathbf{y}}[n,k] \cdot G_{\mathbf{yx}}[n,k]$ would be below I_{th}. Note that the former effect partly compensates the latter. Moreover, in many cases the interference is dominated by one strong interfering source. Therefore, the threshold test (8) provides a good approximation to the level of interference potentially caused to the active receivers.

4.3. Initial Access in Contention. Initial access of unreserved slots in BB-OFDMA is carried out in contention. During contention, two or more transmitters from adjacent cells may access chunk (n,k) simultaneously. As a result, one or several links may encounter a collision on chunk (n,k), where the SINR target is not met. To reduce the occurrence of simultaneously accessed chunks in contention, a p-persistent chunk allocation procedure is applied to BB-OFDMA, where chunk (n,k) in cell q is accessed with probability p. Denoting the outcome of the p-persistent chunk allocation with the binary random variable $\chi_q[n,k] \in \{0,1\}$, the access probability yields $\mathrm{P}(\chi_q[n,k]=1)=p$. The impact of p on the system performance is investigated in Section 6.1.

4.4. Decentralised Chunk Reservation with BB Signalling. The BB-OFDMA protocol enables a link $\mathbf{x}=(\nu,q)$ to contend for a chunk once it is ensured that the CCI caused to the coexisting links $\mathbf{y}$ in the neighbouring cells is below a given threshold (8). Prior to accessing chunk (n,k), transmitter $\mathbf{x}=(\nu,q)$ listens to the associated BB minislot. Whether a user ν within cell q may contend for chunk (n,k) in (4) is controlled by

$$\epsilon_{\nu,q}[n,k]=\begin{cases}0, & I^{\mathrm{b}}_{\nu,q}[n,k]\le I_{\mathrm{th}} \text{ and } \chi_q[n,k]=1,\\ \infty, & \text{otherwise.}\end{cases} \tag{11}$$

Chunks, where $a_q[n,k]=\nu$ in (4), are allocated to user ν. Those chunks where the achieved SINR is above a required SINR target, $\gamma_{\nu,q}[n,k]\ge\Gamma$, are reserved by setting the reservation indicator $\beta_q[n,k]=\nu$ in (4), and are subsequently protected from CCI by BB broadcast. The BB broadcast from the intended data receiver is observed as a *surge* in the received BB power [14], which effectively notifies the transmitter that the data of chunk (n,k) has been correctly received. User ν then reserves chunk n in the next frame $k+1$ by setting $b_q[n,k+1]=\nu$ in (5). On the other hand, if the transmitter does not detect a BB surge, it is understood that the SINR target was not met due to high CCI. These chunks are released by a reset of the reservation indicator to $\beta_q[n,k]=0$ and setting $\epsilon_{\nu,q}[n,k]\to\infty$, so that chunk $(n,k+1)$ may be assigned to other users.

4.5. Balancing System Throughput and Fairness. Cell-edge users are particularly affected by CCI for two reasons. First, the desired signal levels $R^{\mathrm{d}}_{\mathbf{x}}[n,k]$ are, on average, much weaker compared to users in close vicinity to the desired BS due to relatively low channel gains on their intended links $G_{\mathbf{x}}[n,k]$. Second, cell-edge users suffer from high CCI in the downlink, or cause high CCI to the adjacent cells in the uplink.

By tuning the interference threshold I_{th} in (8), the amount of CCI $I^{\mathrm{d}}_{\mathbf{x}}[n,k]$ caused to the receiver of a preestablished and coexisting link $\mathbf{x}=(\nu,q)$ is adjusted. Lowering I_{th} enforces a larger exclusion region around a vulnerable receiver. This enables cell-edge users to meet their SINR target Γ with a greater likelihood. On the other hand, by augmenting I_{th}, the number of simultaneously served links increases, giving rise to an enhanced system throughput. However, the cell-edge users are less likely to maintain their SINR target as interference protection is gradually eliminated. The chunks are released where the SINR target is not met, which means that these chunks are no longer reserved. Since the cell-centre users are less exposed to CCI, the chunks released by the cell-edge users are likely to be reallocated to the cell-centre users. As the allocation of the resources is shifted from the cell-edge users towards the cell-centre users, fairness is compromised. Hence, by adjusting I_{th}, system throughput is traded off for fairness.

A common measure to quantify fairness is Jain's fairness index [22], defined by

$$F=\frac{\left|\sum_{\nu=1}^{U}|\mathcal{B}_{\nu,q}|\right|^2}{U\sum_{\nu=1}^{U}|\mathcal{B}_{\nu,q}|^2}, \tag{12}$$

where U is the number of users in a given cell q. The user throughput $|\mathcal{B}_{\nu,q}|$ accounts for the number of successfully transmitted/received bits by user ν, as defined in (5). A fairness index of $F=1$ represents a perfectly fair system where all users achieve the same throughput. On the other extreme, a fairness index of $1/U$ represents an unfair system where one user is served while all other users starve. We note that the fairness definition (12) is a relative measure, which ignores the absolute achieved throughput per user. To this end, a good fairness index F may coincide with poor spectrum utilisation. For instance, a system where two users achieve 1 Mbps and 2 Mbps would result in a poorer fairness index than a system where both users achieve only 0.5 Mbps. When analysing fairness, the fairness definition (12) should therefore be considered jointly with user throughput results.

(1) Consequences for the Downlink. In the downlink, MSs at the cell edge are exposed to high CCI from transmitters in adjacent cells (see Figure 2(a)). Note that the CCI observed at a given cell (cell 1 in Figure 2(a)) is independent of the user distribution in adjacent cells (cell 2 in Figure 2(a)), assuming a constant transmit power $T^{\mathrm{d}}_{\mathbf{x}}[n,k]$. This implies that if BS_2 lies within the exclusion region of MS_1, resources reserved by MS_1 cannot be spatially reused by *any* of the links in cell 2. However, if I_{th} is increased such that BS_2 is located outside the exclusion region of MS_1, *all* links in cell 2 qualify for a spatial reuse of the resources reserved by MS_1. However, the SINR target at MS_1 is less likely to be met. Should the SINR target at MS_1 not be met, this would cause the chunk allocated to MS_1 to be released and reallocated to another user served by BS_1- possibly a user that is located closer to the the serving BS_1. Therefore, the cell-edge throughput would suffer.

(2) Consequences for the Uplink. In the uplink, the transmitters (MSs) are distributed uniformly over the coverage area of the BS (see Figure 2(b)). Unlike the downlink, the CCI at the tagged BS depends on which MS transmits in the adjacent cell. To this end, the CCI observed at BS_1 in Figure 2(b) depends on whether MS_2 or MS_3 transmits to BS_2. Suppose that in cell 2 both MS_2 and MS_3 contend with MS_1 in cell 1 for chunks (n,k) and (n',k). In case MS_2 and

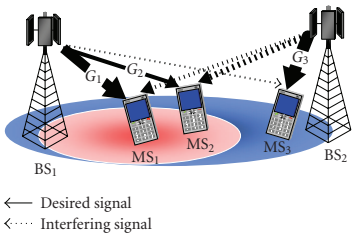

FIGURE 3: Busy burst with interference tolerance signalling (BB-ITS) in the downlink. The ovals represent the exclusion region formed with BB-ITS.

MS_1 simultaneously access chunk (n,k), while MS_3 and MS_1 simultaneously access chunk (n',k), the SINR at BS_1 tends to be superior on chunk (n',k) due to the lower CCI caused by MS_3. While MS_2 causes excessive CCI to BS_1, MS_1 and MS_3 may share chunk (n',k), although both users might be located near the cell boundary. Thus the uplink benefits from *interference diversity* due to the distributed location of mobile users. As a result, the degradation of performance at the cell edge at high I_{th} in uplink mode is less severe compared to the downlink.

4.6. Interference Tolerance Signalling via Busy Bursts. With fixed power BB signalling, the same level of interference protection is given to all links, disregarding the quality of the intended link. In case two receivers MS_1 and MS_2 with respective channel gains $G_1 > G_2$ are exposed to the same interference, as illustrated in Figure 3, the SINR target Γ is more likely met for MS_1 than for MS_2. By allowing MS_1 and MS_2 to transmit a BB with variable power, the individual amount of interference that can be tolerated by MS_1 and MS_2 is signalled to candidate transmitters in adjacent cells. Exclusion regions of different size are effectively formed around MS_1 and MS_2, as illustrated in Figure 3.

For busy burst with interference tolerance signalling (BB-ITS), the objective is that a given SINR target, $\gamma_{\mathbf{x}}[n,k] \geq \Gamma$, is maintained for an active receiver $\mathbf{x}$. This means that the maximum allowable interference depends on the intended link quality $R^{\text{d}}_{\mathbf{x}}[n,k]$. Let $I^{\text{tol}}_{\mathbf{x}}[n,k]$ denote the interference limit, for which the SINR (2) approaches $\gamma_{\mathbf{x}}[n,k] = \Gamma$. Then the tolerable interference at receiver $\mathbf{x}$ is upper bounded by

$$I^{\text{d}}_{\mathbf{x}}[n,k] \leq I^{\text{tol}}_{\mathbf{x}}[n,k] = \frac{R^{\text{d}}_{\mathbf{x}}[n,k]}{\Gamma} - N. \tag{13}$$

Adjusting the tolerable interference level (13) implies that larger exclusion regions are formed for links with weak desired signal levels $R^{\text{d}}_{\mathbf{x}}[n,k]$ and vice versa.

To signal the variable interference tolerance level $I^{\text{tol}}_{\mathbf{x}}[n,k]$ of a victim receiver $\mathbf{x}$ to candidate transmitters $\mathbf{y}$ in adjacent cells, the BB transmit power $T^{\text{b}}_{\mathbf{x}}[n,k]$ is adjusted, such that the simple threshold test $I^{\text{b}}_{\mathbf{y}}[n,k] \leq I_{\text{th}}$ in (8) is retained. Hence no additional information for channel sensing is required for BB-ITS. The received BB power approaches a fixed threshold, $I^{\text{b}}_{\mathbf{y}}[n,k] = I_{\text{th}}$, if the CCI approaches $I^{\text{d}}_{\mathbf{x}}[n,k] = I^{\text{tol}}_{\mathbf{x}}[n,k]$. Inserting $I^{\text{d}}_{\mathbf{x}}[n,k] = I^{\text{tol}}_{\mathbf{x}}[n,k]$ and $I^{\text{b}}_{\mathbf{y}}[n,k] = I_{\text{th}}$ into (6) yields the variable BB power $T^{\text{b}}_{\mathbf{x}}[n,k] = T^{\text{d}}_{\mathbf{y}}[n,k] \cdot I_{\text{th}}/I^{\text{tol}}_{\mathbf{x}}[n,k]$. Assuming that $T^{\text{d}}_{\mathbf{y}}[n,k]$ is fixed and denoted by T^{d}, the BB transmit power is adjusted as follows [23]:

$$T^{\text{b}}_{\mathbf{y}}[n,k] = \min\left(\frac{I_{\text{th}} \cdot T^{\text{d}}}{R^{\text{d}}_{\mathbf{x}}[n,k]/\Gamma - N}, T^{\text{b}}_{\max}\right), \tag{14}$$

where $T^{\text{b}}_{\max}$ is the maximum BB transmit power. The min operator ensures that $T^{\text{b}}_{\mathbf{x}}[n,k] \leq T^{\text{b}}_{\max}$. Note that when $R^{\text{d}}_{\mathbf{x}}[n,k]/\Gamma < N$, we get $\gamma_{\mathbf{x}}[n,k] < \Gamma$. In this situation, the chunk is released and no BB is transmitted. Therefore, it is ensured that $T^{\text{b}}_{\mathbf{x}}[n,k]$ in (14) always has a positive value. We note that $I^{\text{b}}_{\mathbf{x}}[n,k] = T^{\text{b}}_{\mathbf{y}}[n,k] \cdot G_{\mathbf{xy}}[n,k]$ and $T^{\text{b}}_{\max} = T^{\text{d}}_{\mathbf{y}}[n,k] = T^{\text{d}}_{\mathbf{x}}[n,k]$. It can be checked by plugging (14) into (8) that the threshold test (8) effectively checks if $I^{\text{d}}_{\mathbf{y}}[n,k] \leq I^{\text{tol}}_{\mathbf{y}}[n,k]$, regardless of the threshold used, as long as the BB transmit power is not clipped. In this paper, we choose $I_{\text{th}} = -90$ dBm because the probability of BB transmit power being clipped was found to be lower than 0.05 for the given deployment scenario with $\Gamma = 11.3$ dB used. Furthermore, with this threshold, the received BB at the intended transmitter (the lower bound of which is approximated by $I_{\text{th}} \cdot \Gamma$) remains well above the noise floor -117.8 dBm, such that it can be reliably detected.

4.7. Link Adaptation with BB Signalling. Receiver feedback based on BB-ITS (see Section 4.6) allows for receiver-driven link adaptation, where the chosen transmission rate is adapted to the instantaneous channel conditions. Let $\mathcal{M} = \{1,\ldots,M\}$ be the set of supported modulation schemes. Associated to each modulation scheme $m \in M$ is an SINR target $\Gamma = \Gamma_m$ that must be achieved to satisfy a given frame error rate (FER).

Provided that the channel response does not change between successive frames, changes in Γ_m may be signalled from receiver to transmitter through (14), since any fluctuation in received BB power $R^{\text{b}}_{\mathbf{x}}[n,k] = G_{\mathbf{x}}[n,k]\,T^{\text{b}}_{\mathbf{x}}[n,k]$ is due to a change of Γ_m in (14). In summary, BB-ITS serves two important objectives. First, by adjusting the SINR target Γ_m, the receiver implicitly signals to the transmitter through BB-ITS that the transmission format should be changed; second, by varying the BB power $T^{\text{b}}_{\mathbf{x}}[n,k]$ in (14), the size of the exclusion region around the active receiver is adjusted, so that the required SINR target Γ_m is met in successive frames.

Link adaptation with BB-ITS is carried out in two phases: the *contention phase,* where the link is established and the *link adaptation* (LA) phase, where the receiver adjusts its transmission format to the current channel conditions.

Contention Phase. In contention, multiuser chunk allocation is carried out as described in Section 4.3. To contend for an unreserved chunk (n,k), transmitter $\mathbf{x} = (\nu,q)$ initially uses the modulation scheme with the lowest spectral efficiency $m_{\mathbf{x}}[n,k] = 1$. Chunks that satisfy $\gamma_{\mathbf{x}}[n,k] \geq \Gamma_1$ are reserved in the next frame $k+1$ by BB signalling (see Section 4.4), where the transmit power $T^{\text{b}}_{\mathbf{x}}[n,k]$ in (14) is set using $\Gamma = \Gamma_1$. Then the transmission proceeds to the link adaptation phase.

Link Adaptation Phase. The objective of the link adaptation phase is to select the modulation scheme $m_{\mathbf{x}}[n,k] \in \mathcal{M}$ for chunk (n,k), which yields the highest spectral efficiency, for which $\gamma_{\mathbf{x}}[n,k] \geq \Gamma_{m_{\mathbf{x}}[n,k]}$ holds. By utilising BB-ITS link, adaptation is accomplished without any explicit feedback. The receiver executes the following algorithm.

(1) Calculate the achieved SINR $\gamma_{\mathbf{x}}[n,k]$ at chunk (n,k).

(2) Increment the number of bits per symbol based on $\gamma_{\mathbf{x}}[n,k]$

$$m_{\mathbf{x}}[n,k+1] = \begin{cases} m_{\mathbf{x}}[n,k]+1, & \gamma_{\mathbf{x}}[n,k] \geq \Gamma_{m_{\mathbf{x}}[n,k]+1}, \\ & m_{\mathbf{x}}[n,k] < M, \\ m_{\mathbf{x}}[n,k]-1, & \gamma_{\mathbf{x}}[n,k] < \Gamma_{m_{\mathbf{x}}[n,k]}, \\ m_{\mathbf{x}}[n,k], & \text{otherwise.} \end{cases} \quad (15)$$

(3) If $m_{\mathbf{x}}[n,k+1] \geq 1$, adjust the BB power (14) using the SINR target $\Gamma = \Gamma_{m_{\mathbf{x}}[n,k+1]}$ and transmit the BB.

(4) If $m_{\mathbf{x}}[n,k+1] < 1$, terminate the link adaptation phase and return to the contention phase.

The transmitter senses the BB minislot associated to chunk (n,k). In order to determine the modulation scheme $m_{\mathbf{x}}[n,k+1]$ requested by the receiver, the transmitter executes the following algorithm.

(1) Measure the busy signal power received from the intended data receiver $R^{\mathrm{b}}_{\mathbf{x}}[n,k]$ and compute the difference to the BB power received from intended data receiver in the preceding slot, $\Delta R = R^{\mathrm{b}}_{\mathbf{x}}[n,k] - R^{\mathrm{b}}_{\mathbf{x}}[n,k-1]$.

(2) The modulation format is adjusted based on ΔR as follows:

$$\hat{m}_{\mathbf{x}}[n,k+1] = \begin{cases} \hat{m}_{\mathbf{x}}[n,k]+1, & \Delta R \geq I_{\mathrm{th}}\Delta\Gamma_m - \varepsilon, \\ \hat{m}_{\mathbf{x}}[n,k]-1, & \Delta R < I_{\mathrm{th}}\Delta\Gamma_{m-1} + \varepsilon, \\ \hat{m}_{\mathbf{x}}[n,k], & \text{otherwise,} \end{cases} \quad (16)$$

where $\Delta\Gamma_m = \Gamma_m - \Gamma_{m+1}$, $m = \hat{m}_{\mathbf{x}}[n,k]$. The constant $\varepsilon > 0$ introduces a detection margin to enhance the robustness towards estimation errors in $\hat{R}^{\mathrm{b}}_{\mathbf{x}}[n,k]$ due to channel variations and noise.

(3) If $\hat{m}_{\mathbf{x}}[n,k+1] \geq 1$, transmit data on chunk $(n,k+1)$ using the new modulation scheme $\hat{m}_{\mathbf{x}}[n,k+1]$.

(4) If $\hat{m}_{\mathbf{x}}[n,k+1] < 1$, terminate the link adaptation phase and return to the contention phase.

Estimation errors due to channel variations and noise may cause detection errors, so that $\hat{m}_{\mathbf{x}}[n,k] \neq m_{\mathbf{x}}[n,k]$. Mismatch between the selected modulation schemes at transmitter and receiver can be mitigated if the transmitter announces $\hat{m}_{\mathbf{x}}[n,k]$ together with payload data on chunk (n,k).

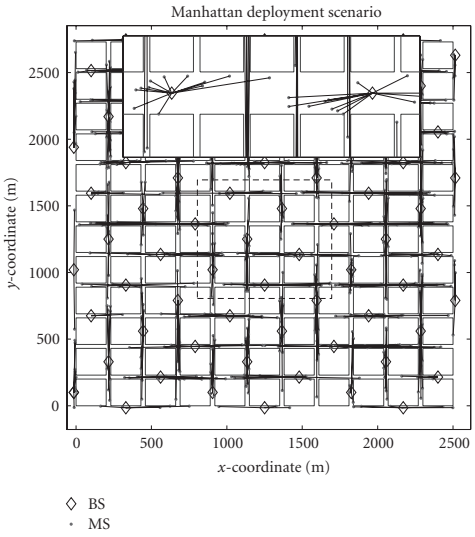

Figure 4: Manhattan grid urban microcell deployment.

4.8. Benchmark System. Full-frequency reuse with adaptive score-based chunk allocation (ASCA) is considered as the benchmark system. This means that neither chunk reservation nor interference avoidance mechanisms is in place. In order to maintain a fair comparison, the same fair scheduling algorithm (3) as in BB-OFDMA is applied. With ASCA, the score-based scheduler assigns chunk (n,k) to user ν whose score (3) is minimised

$$a_q[n,k] = \arg\min_{\nu} s_{\nu,q}[n,k]. \quad (17)$$

Chunk allocation for ASCA (17) corresponds to (4) by setting the reservation indicator to zero, $\beta_q[n,k] = 0$, and by allowing a cell to access all chunks, which is achieved by setting $\epsilon_{\nu,q}[n,k] = 0$ for all n,k in (3).

5. Manhattan Grid Deployment

An urban microcell deployment with a rectangular grid of streets (Manhattan grid) as defined in scenario B1 in WINNER [17] is considered, where antennas are mounted below the rooftop. The deployment scenario consists of building blocks of dimensions 200 m × 200 m, interlaced with the streets of width 30 m, forming a regular structure called the Manhattan grid, as shown in Figure 4. The network consists of 11 × 12 building blocks (72 BSs). However, the performance statistics are collected only over the central core of 3 × 3 building blocks (6 BSs), so as to reduce edge effects.

On average $U = 10$ MSs are served by one cell, uniformly distributed in the streets and moving with a constant velocity of 5 km/h. BSs are placed in the middle of the street canyons with an inter-BS distance of 4 building blocks, as

depicted in Figure 4. Distance dependent path loss, log-normal shadowing, and frequency selective fading are taken into account, as specified in [24], channel model B1. While the effect of user mobility on the channel response due to the Doppler effect is taken into account, movement of users along the streets is not considered during the duration of one snapshot. Links where transmitter and receiver are located on the same street are modelled as line-of-sight (LoS) channels, with significantly lower path loss attenuation than nonline-of-sight (NLoS) links [24]. WINNER channel models B1-LOS and B1-NLOS [24] are used to model the LoS and NLoS channels, respectively. MSs are connected to the BS with the least path loss. A network synchronised in time and frequency is assumed.

The traffic in the system is modeled as a burst of 100 protocol data units (PDUs) whose interarrival time is exponentially distributed. A PDU of 112 bit is assumed, which is the smallest unit of data that can be transmitted in one chunk. The average offered load per user L_u is adjusted by the interburst duration. It is considered that the arrival times for different users are independent. The maximum number of chunks that a user can be assigned in a given slot is the total number of available chunks in a frame. The simulation parameters are summarised in Table 1.

A 3/4-rate convolutional code and the SINR targets Γ_m for a given modulation scheme m are selected to attain a packet error ratio of 10^{-2} per PDU, given in Table 2. For non-adaptive modulation, we consider a 16-QAM constellation with $m = 4$ and a corresponding SINR target of $\Gamma_4 = 11.3$ dB. For link adaptation, the modulation schemes $m \in \mathcal{M}$ are chosen based on the achieved SINR targets Γ_m.

Table 1: Simulation parameters.

Parameters	Value
Carrier centre frequency	3.95 GHz
System bandwidth B	89.84 MHz
No. of subcarriers (SCs)	1840
Subcarriers spacing Δf	48.8 kHz
OFDM symbols/frame $2n_{os}$	30
OFDM symbol duration T_{sym}	22.48 μs
Frame duration	0.6912 ms
No. of chunks/frame N_C	230
Chunk size $n_{sc} \times n_{os}$	8 (freq.) $\times$ 15 (time) = 120
PDU size	112 bits
Access probability p	0.3
No. of sectors/cell	1
No. of users/cell U	10
Tx power/chunk T^d	16.4 dBm
Antenna gain	0 dBi
Noise level/chunk N	-117.8 dBm
No. of snapshots	500
Snapshot duration	75 ms
User load L_u	30 Mbps

Table 2: Look up table for modulation scheme.

Modulation, No. of link PDUs per slot	Achieved SINR γ (dB)
No transmission $m = 0$	$-\infty < \gamma < 2.2$
BPSK $m = 1$	$2.2 \leq \gamma < 5.2$
QPSK $m = 2$	$5.2 \leq \gamma < 9.1$
Cross 8-QAM $m = 3$	$9.1 \leq \gamma < 11.3$
16-QAM $m = 4$	$11.3 \leq \gamma < 14.4$
Cross 32-QAM $m = 5$	$14.4 \leq \gamma < 16.6$
64-QAM $m = 6$	$16.6 \leq \gamma < 19.5$
Cross 128-QAM $m = 7$	$19.5 \leq \gamma < 22.5$
256-QAM $m = 8$	$22.5 \leq \gamma < \infty$

6. Results and Discussion

The performance of BB-OFDMA and the benchmark system (ASCA) are evaluated in terms of user and system throughput. User throughput is defined as the number of successfully received bits per user per unit time. A transmission is considered successful if the SINR target Γ is met at the receiver. The system throughput is defined as the aggregate throughput of all users per cell.

6.1. Collisions Based on Access Probability. The likelihood of achieving the SINR target during the initial access in contention is depicted in Figure 5 for $m = 4$ with $\Gamma_4 = 11.3$ dB, where m is the number of bits per symbol. The cell-edge region suffers from collisions (SINR target not met) both in the uplink (Figure 5(a)) and the downlink (Figure 5(b)). Decreasing the access probability p substantially reduces the occurrence of collisions, since the probability of simultaneous access of chunks in contention reduces (see Section 4.3). In the downlink, cell-edge users suffer from weaker desired signal power and at the same time experience strong CCI. Furthermore, the users located at the street crossings at $d = 115$ m are exposed to strong LoS interference from BSs in the perpendicular streets. In the uplink, however, these users cause CCI to the neighbouring cells; which may impact either users at the cell-edge or users closer to the intended BS. Consequently, the SINR target is met with less likelihood at street crossings and the cell edge in the downlink mode compared to the uplink mode.

6.2. Setting the Threshold for Fixed Power BB Signalling. The impact of the choice of interference threshold on the mean system throughput is shown in Figure 6 for fixed 16-QAM modulation with $m = 4$. It is seen that for lower values of I_{th}, the amount of allocated resources (Set $\mathcal{A}$) and the achieved throughput (Set $\mathcal{B}$) are approximately equal. This is because at low I_{th}, larger exclusion regions around active receivers are enforced. Thus, CCI is mitigated at the expense of spatial reuse. By increasing I_{th}, the system throughput gradually improves until the maximum is reached. However, increasing I_{th} introduces additional links that cause more CCI to the existing links. As a result, some of the links (mainly cell-edge users) are less likely to meet the SINR target. Although it is desirable to maximise the spectral

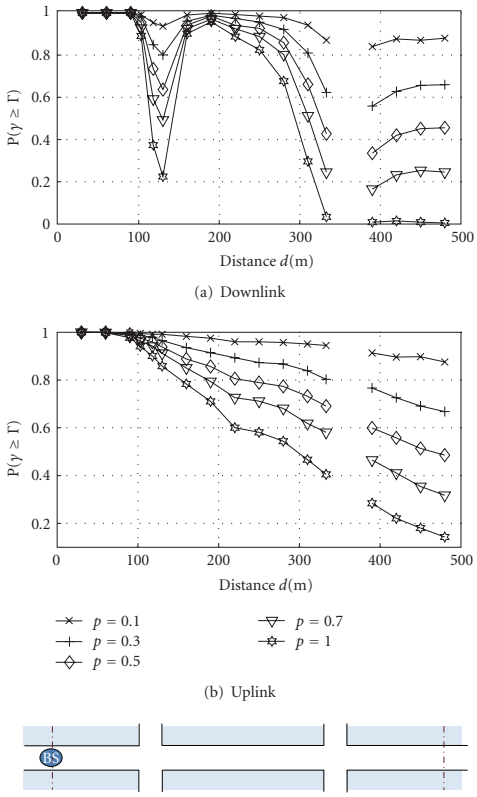

FIGURE 5: Probability of meeting the SINR target $\Gamma = 11.3$ dB in contention for different access probabilities p, as a function of the BS-MS distance d. At $d = 115$ m, links are exposed to strong LOS interference from cells in perpendicular streets, which causes collisions in the downlink, while at $d = 345$ m, the MSs are connected to BSs in a perpendicular street due to better channel gains.

efficiency, it may be necessary to maintain a fair distribution of resources to all users. Achieving a balance between maximising spectral efficiency and enhancing fairness is addressed in Section 6.3.

6.3. Impact of Interference Threshold on Fairness. Figure 7 shows the average user throughput versus distance d from the serving BS. It is observed that the performance of BB-OFDMA is sensitive to the chosen threshold I_{th}. The system throughput is maximised for $I_{\text{th}} = -75$ dBm in the downlink and for -85 dBm in the uplink (see Figure 6). However, these thresholds severely affect cell-edge user throughput. Increasing interference protection by lowering I_{th} enhances user throughput at the cell edge at the expense of system throughput. In the uplink (Figure 7(a)), the cell

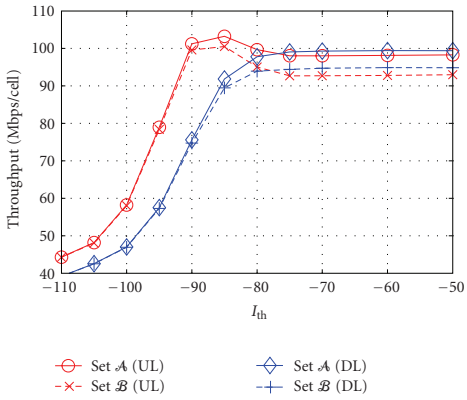

FIGURE 6: Mean system throughput versus I_{th} for BB-OFDMA with 16-QAM modulation using fixed BB transmit power. The mean system throughput is maximised for $I_{\text{th}} = -85$ dBm in the UL and $I_{\text{th}} = -75$ dBm in the DL.

edge throughput (measured at $d = 420$ m from the desired BS) improves from 1.5 Mbps ($I_{\text{th}} = -85$ dBm) to 3.08 Mbps ($I_{\text{th}} = -95$ dBm), an approximately onefold increase, whereas in the downlink (Figure 7(b)), user throughput increases from 267 kbps ($I_{\text{th}} = -75$ dBm) to 2.9 Mbps ($I_{\text{th}} = -90$ dBm), an approximately tenfold increase. At $d = 115$ m, MSs are exposed to LOS interference from BSs in perpendicular streets in the downlink. Consequently, high CCI compromises throughput for these users. In the uplink, MSs located at street crossings at $d = 115$ m transmit, so that these users are not exposed to LOS interference. Hence the uplink throughput of ASCA is not affected at $d = 115$ m. For BB-OFDMA, however, MSs located at street crossings are exposed to strong BB signals from BSs in perpendicular streets, which reduces the number of chunks such users can compete for, causing a drop of throughput for users located at street crossings.

Fairness is numerically quantified using Jain's fairness index (12). The cdf of the fairness distribution is presented in Figure 8(a) for the uplink and Figure 8(b) for the downlink. Applying the interference threshold that maximises system throughput, $I_{\text{th}} = -75$ dBm in the downlink and -85 dBm in the uplink, results in median fairness index of $F = 0.56$ and 0.66, respectively. Increasing the interference protection by lowering I_{th} improves fairness, as this enables cell-edge users to meet their SINR target. To this end, using $I_{\text{th}} = -95$ dBm in the uplink and -90 dBm in the downlink, approximately 22% of system throughput, is traded off for median fairness indices of $F \approx 0.72$. In the uplink, the median fairness index can be further improved to 0.78 by setting $I_{\text{th}} = -100$ dBm. However, the improved fairness significantly degrades system throughput (see Figure 6).

On the other hand, with BB-ITS, median fairness indices of $\approx$0.7 are achieved. The corresponding average uplink and downlink user throughputs at the cell edge amount to

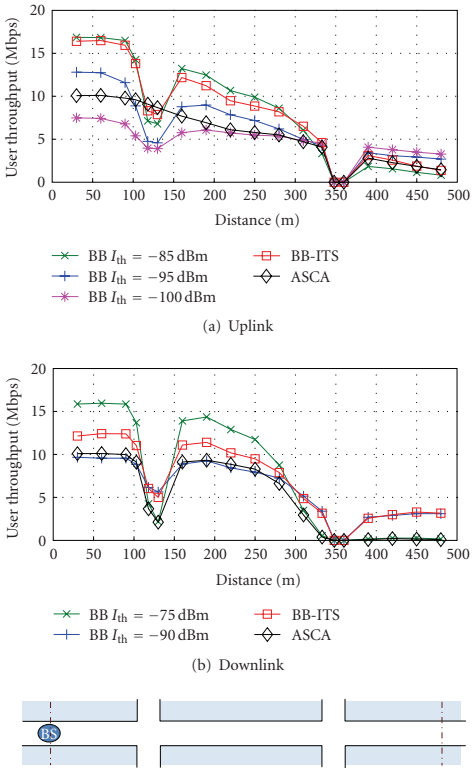

Figure 7: Mean user throughput versus distance from the serving BS, d, for BB-OFDMA with 16-QAM modulation for different interference thresholds I_{th}. For comparison, results for full-frequency reuse without interference protection termed ASCA are also included. Note that at $d = 115$ m, links are exposed to strong LOS interference (data in downlink, BB in uplink) from cells in perpendicular streets, which compromises throughput, while at $d = 345$ m, the MSs are connected to the BS in a perpendicular street due to better channel gains.

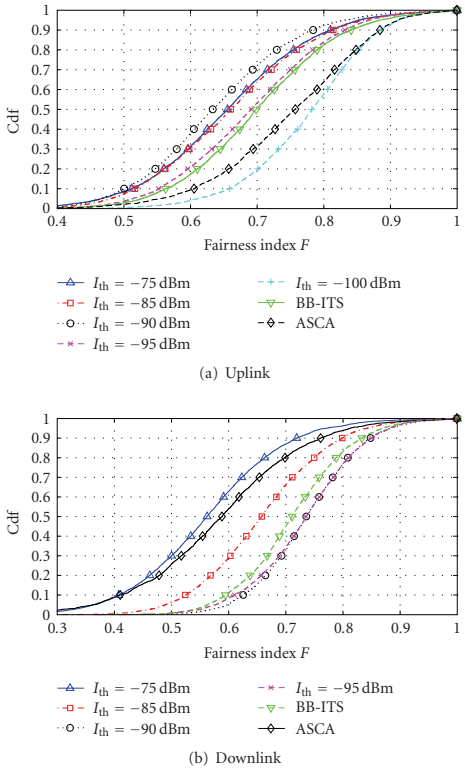

Figure 8: Cumulative distributive function (cdf) of Jain's fairness index (12) for BB-OFDMA compared to full-frequency reuse without interference avoidance (ASCA) both with 16-QAM modulation.

2.57 Mbps and 2.99 Mbps, respectively. The corresponding reduction in system throughput compared to the respective optimal thresholds with fixed power BB is only 1% in the uplink and 8% in the downlink. Note that BB-OFDMA with fixed BB power requires a 22% reduction in system throughput for a comparable performance at the cell edge. In light of this, BB-ITS results in a better tradeoff between system throughput and fairness.

For comparison, the median fairness resulting from ASCA is $F = 0.79$ in the uplink and 0.59 in the downlink. The corresponding average user throughputs at the cell edge are 2.278 Mbps and 208 kbps, respectively. This means that ASCA is more fair in the uplink compared to the downlink. The reason is that in the downlink cell-edge users are exposed to high CCI, while in the uplink cell-edge users cause high CCI to adjacent cells. Hence the detrimental effects of interference on the uplink tend to be more equally distributed among all users.

6.4. Comparison between BB-OFDMA and ASCA. Figures 9(a)–9(d) depict the cumulative distribution function (cdf) of the user throughput and the system throughput. The results shown in Figures 9(a)-9(b) demonstrate that BB-enabled interference avoidance exhibits a gain in median system throughput of up to 50% compared to ASCA, both in uplink and downlink. Using a modulation format of $m = 4$ bits per symbol and a 3/4-rate convolutional code, the upper bound on system throughput achieved in an isolated cell (CCI free system) is 111.8 Mbps. With $I_{th} = -85$ dBm in the uplink and -75 dBm in the downlink, a median system throughput of about 90% and 85% of the upper bound (CCI free system) is achieved.

Figures 9(c)-9(d) show the cdf of the user throughput for BB-OFDMA and ASCA. When fairness is the primary

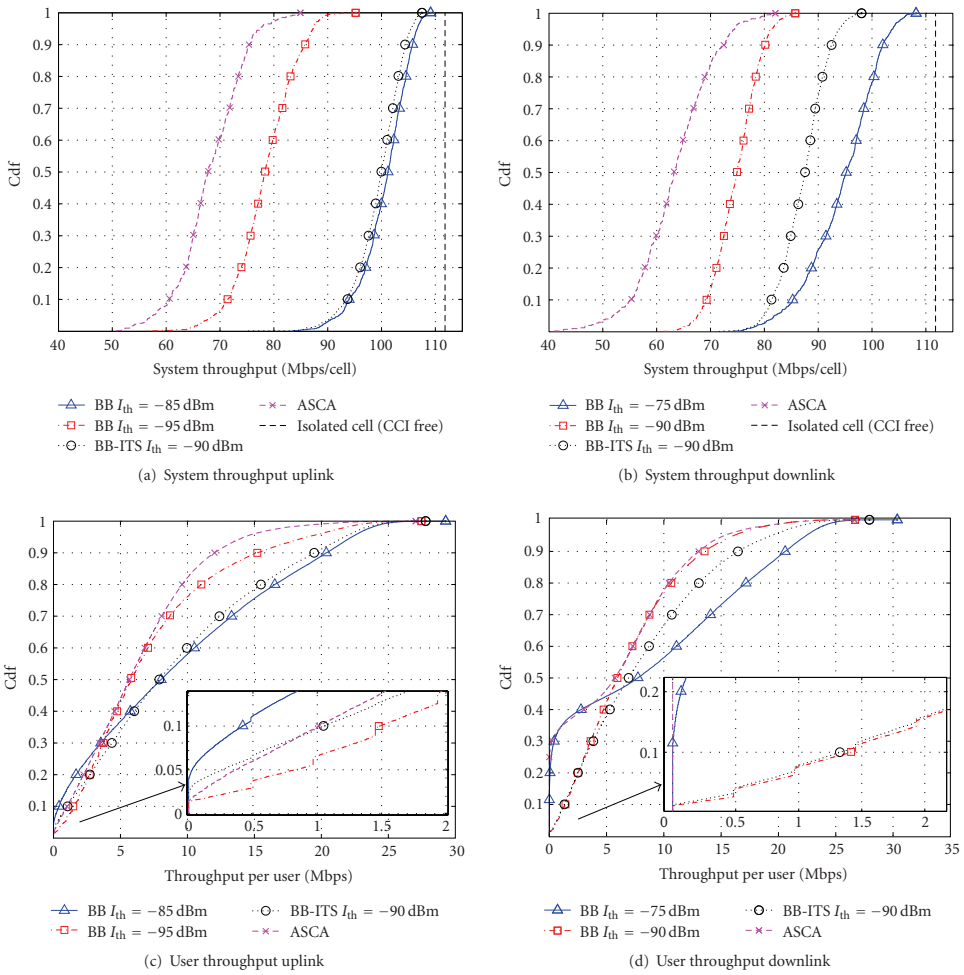

FIGURE 9: Cumulative distributive function (cdf) of system throughput and user throughput for BB-OFDMA with fixed BB power and BB-ITS. The performance for full-frequency reuse without interference protection termed ASCA is included for comparison. BB-ITS results in a favourable tradeoff between fairness and system throughput both in uplink and downlink.

concern, $I_{th} = -95$ dBm in the uplink and $I_{th} = -90$ dBm in the downlink are preferable. Then the 10%-ile of the achieved user throughput amounts to 1.48 Mbps in the uplink (see Figure 9(c)) and 1.42 Mbps in the downlink (see Figure 9(d)). In contrast, ASCA fails to deliver any downlink throughput to more than 20% of the users. In the uplink, the 10%-ile of the user throughput of BB-OFDMA is improved by 40% compared to ASCA. With these uplink and downlink thresholds of $I_{th} = -95$ dBm and -90 dBm, the median system throughput of BB-OFDMA is still 15% and 18% higher than that achieved with ASCA (see Figures 9(a)-9(b)).

The results of BB-OFDMA with variable BB power, termed BB-ITS, are also included in Figures 9(a)–9(d). With BB-ITS, the lower 10%-ile of user throughput achieved is 1.04 Mbps in uplink and 1.416 Mbps in downlink (see Figures 9(c)-9(d)), at a modest degradation in system throughput (see Figures 9(a)-9(b)) compared to BB-OFDMA with fixed threshold that maximises the respective system throughput. BB-ITS, therefore, not only avoids the need for tuning the interference threshold so as to match a certain interference scenario (e.g., in uplink or downlink), but

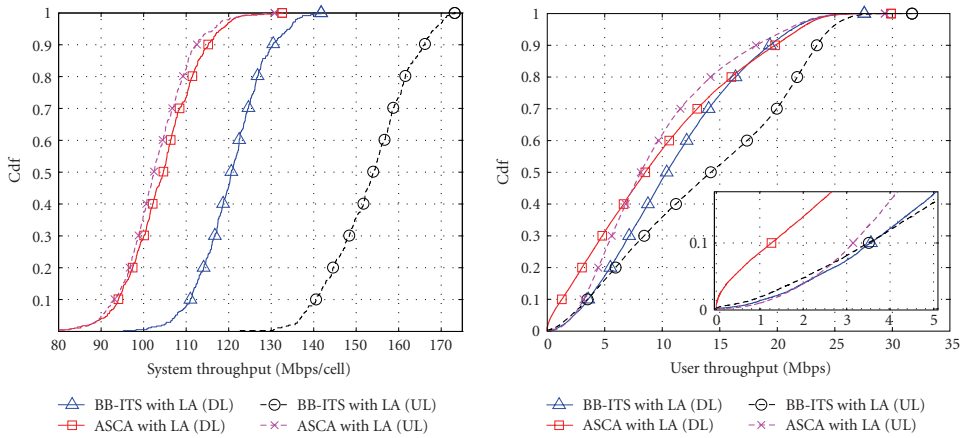

(a) System throughput (b) User throughput

FIGURE 10: Cdfs of system and user throughputs for BB-ITS and ASCA with LA. In the DL, the users that are located at the cell-edge benefit whereas in the UL the users that are located closer to their desired BS benefit.

also achieves a preferable compromise between maximising system throughput and maintaining fairness.

6.5. Link Adaptation with BB-Signalling. Figures 10(a)-10(b) compare the system and user throughput achieved by performing link adaptation (LA) with BB-ITS and ASCA. Both BB-ITS and ASCA utilise the same link adaptation algorithm presented in Section 4.7; the only difference is that for ASCA interference protection is omitted. The results shown in Figure 10(a) reveal that BB-ITS with link adaptation attains an improvement of 50% (uplink) and 13% (downlink) in median system throughput compared to ASCA with link adaptation. Furthermore, Figure 10(b) shows that the BB-ITS outperforms ASCA by a factor of 2.75 in terms of the lower 10%-ile of the downlink user throughput. On the other hand, the cell-edge user throughput of BB-ITS and ASCA in the UL is comparable, while significant improvements of up to 70% are observed for higher percentiles of the user throughput in Figure 10(b).

By performing link adaptation with BB-ITS, the cell-edge users benefit in the downlink, whereas the users that are closer to their desired BS benefit in the uplink. The reason for this opposite trend for the uplink and the downlink is elaborated in the following. Due to the specific point-to-multipoint structure in the downlink, the CCI observed by the cell-edge users is dominated by the interference originating from the closest BS. When a chunk is assigned to a cell-edge user in the downlink, interference tolerance signalling enforces that this chunk cannot be spatially reused by the closest BS in an adjacent cell. By ensuring that, this dominant interferer does not access this chunk, the achieved SINR is greatly improved, potentially enough to meet the higher SINR target(s), thus allowing for the higher-order modulation schemes. In the uplink, on the other hand, the chunks assigned to the cell-edge users are more likely to be reused in the adjacent cells due to the distributed location of the MSs transmitters (see Section 4.5). Consequently, it is less likely that a more spectrally efficient modulation scheme can be used by the cell-edge users. Furthermore, in the uplink, the distance between the MSs (transmitters) and the victim BSs (receivers) in neighbouring cells is larger for the cell-centre MSs than the cell-edge users. Hence the cell-centre users are more likely to be located outside the exclusion range of BSs receivers (BB transmitters). This results in a larger number of chunks that are available to be spatially reused for the cell-centre users. Lastly, the cell-centre users also benefit from higher SINRs as a result of which throughput is particularly boosted by performing link adaptation.

7. Conclusions

In this paper, the busy signal concept for decentralised and self-organised interference aware medium access has been applied to OFDMA-TDD systems operated in Manhattan grid deployment scenarios. An exclusion zone around victim receivers is established by means of receiver feedback in the form of time-multiplexed busy bursts (BBs), wherein no active transmitter from an adjacent cell may be located. BB enabled interference avoidance exhibits impressive gains in system and user throughputs compared to the benchmark system, with full-frequency reuse without interference avoidance, both in the uplink and the downlink. The impact of the BB specific threshold parameter that controls the interference imposed on coexisting links in neighbouring cells has been studied.

By adjusting this threshold parameter, the system benefits from flexible operation of either achieving high system throughput or enhanced fairness in terms of cell-edge

user throughput. A onefold (uplink) and tenfold (downlink) improvement in average cell-edge user throughput is achieved at a reduction in system throughput of about 22% (≈20 Mbps/cell) in both cases. BB-enabled interference avoidance is therefore particularly powerful in enhancing downlink cell-edge user throughput, since in the downlink high interference is coupled with low-desired signal levels, resulting in poor average SINRs at the cell edge. In the uplink, on the other hand, cell-edge users cause high CCI, so that the detrimental effects of uplink interference are distributed more equally among all users, giving rise to *interference diversity*.

By allowing each receiver to signal the amount of interference it can tolerate, by using a variable busy burst power, an even better tradeoff between system throughput and fairness is achieved. Especially in the downlink, a tenfold improvement has been achieved at the cost of only 8% reduction in maximum system throughput. Furthermore, this scheme also alleviates the need to adjust the BB threshold parameter. The latter property is particularly important for self-organising wireless networks, as the optimum choice of the BB threshold is sensitive to changes in the network topology, and may not be known *a priori*.

Finally, link adaptation has been combined with busy burst-enabled interference avoidance, where changes in the transmission format are implicitly signalled to the transmitter by virtue of a variable BB power. BB signalling with link adaptation attained a superior performance than the benchmark system with link adaptation, both in terms of system throughput and user throughput. Due to the particular interference scenario, the cell-edge users achieved larger gains in the downlink whereas the cell-centre users benefitted more in the uplink. Consequently, larger gains in system throughput in the uplink mode were achieved compared to the gains achieved in the downlink mode.

Acknowledgments

Initial parts of this work have been supported by DFG Grant HA 3570/1-2 within the program SPP-1163 (Techniken, Algorithmen und Konzepte für zukünftige COFDM Systeme-TakeOFDM) while some latter parts of this work have been performed within the framework of the IST Project IST-4-027756 WINNER, which is partly funded by the European Union. Harald Haas acknowledges the Scottish Funding Council support of his position within the Edinburgh Research Partnership in Engineering and Mathematics between the University of Edinburgh and Heriot Watt University. This work was presented in part at the IEEE International Symposium of Personal, Indoor and Mobile Radio Communications (PIMRC) 2008, Cannes, France.

References

[1] IEEE802.11a-1999, "Wireless LAN Medium Access Control (MAC) and Physical Layer (PHY) specifications; High-Speed Physical Layer in the 5 GHz Band," IEEE Standard Institution, Piscataway, NJ, USA, 1999.

[2] ETSI EN 300 744 v1.5.1 (2004-06), "Digital Video Broadcasting (DVB); Framing Structure, Channel Coding and Modulation for Digital Terrestrial Television," European Telecommunications Standards Institute (ETSI), June 2004.

[3] 3rd Generation Partnership Project (3GPP), "Evolved Universal Terrestrial Radio Access (E-UTRA); Physical Channels and Modulation (Release 8)," Technical Specification Group Radio Access Network, 3GPP TS 36.211 V8.2.0, 3GPP March 2008.

[4] M. Sternad, T. Svensson, T. Ottosson, A. Ahlen, A. Svensson, and A. Brunstrom, "Towards Systems Beyond 3G Based on Adaptive OFDMA Transmission," *Proceedings of the IEEE*, vol. 95, no. 12, pp. 2432–2455, 2007.

[5] S.-E. Elayoubi, O. Ben Haddada, and B. Fourestie, "Performance evaluation of frequency planning schemes in OFDMA-based networks," *IEEE Transactions on Wireless Communications*, vol. 7, no. 5, part 1, pp. 1623–1633, 2008.

[6] M. C. Necker, "Local interference coordination in cellular OFDMA networks," in *Proceedings of the 66th IEEE Vehicular Technology Conference (VTC '07)*, pp. 1741–1746, Baltimore, Md, USA, September-October 2007.

[7] S. M. Heikkinen, H. Haas, and G. J. R. Povey, "Investigation of adjacent channel interference in UTRA-TDD system," in *Proceedings of the IEE Colloquium on UMTS Terminals and Software Radio*, pp. 13/1–13/6, Glasgow, UK, April 1999.

[8] IST-4-027756 WINNER II, "D6.13.14 version 1.1 WINNER II System Concept Description," January 2008, http://www.ist-winner.org/WINNER2-Deliverables/D6.13.14 v1 .1.pdf.

[9] Z. Bharucha and H. Haas, "Application of the TDD underlay concept to home nodeB scenario," in *Proceedings of the 67th IEEE Vehicular Technology Conference (VTC '08)*, pp. 56–60, Singapore, May 2008.

[10] F. A. Tobagi and L. Kleinrock, "Packet switching in radio channels—part II: the hidden terminal problem in carrier sense multiple-access and the busy-tone solution," *IEEE Transactions on Communications*, vol. 23, no. 12, pp. 1417–1433, 1975.

[11] Z. J. Haas and J. Deng, "Dual busy tone multiple access (DBTMA)—a multiple access control scheme for ad hoc networks," *IEEE Transactions on Communications*, vol. 50, no. 6, pp. 975–985, 2002.

[12] R. Zhao, B. Walke, and M. Einhaus, "Constructing efficient multi-hop mesh networks," in *Proceedings of the 30th Anniversary IEEE Conference on Local Computer Networks (LCN '05)*, pp. 166–173, Sydney, Australia, November 2005.

[13] P. E. Omiyi and H. Haas, "Improving time-slot allocation in 4th generation OFDM/TDMA TDD radio access networks with innovative channel-sensing," in *Proceedings of the IEEE International Conference on Communications (ICC '04)*, vol. 6, pp. 3133–3137, Paris, France, June 2004.

[14] P. Omiyi, H. Haas, and G. Auer, "Analysis of TDD cellular interference mitigation using busy-bursts," *IEEE Transactions on Wireless Communications*, vol. 6, no. 7, pp. 2721–2731, 2007.

[15] H. Haas, V. D. Nguyen, P. Omiyi, N. Nedev, and G. Auer, "Interference aware medium access in cellular OFDMA/TDD networks," in *Proceedings of the IEEE International Conference on Communications (ICC '06)*, vol. 4, pp. 1778–1783, Istanbul, Turkey, July 2006.

[16] B. Ghimire, H. Haas, and G. Auer, "Busy burst enabled interference avoidance in winner-TDD," in *Proceedings of the 18th IEEE International Symposium on Personal, Indoor and Mobile Radio Communications (PIMRC '07)*, pp. 1–5, Athens, Greece, September 2007.

[17] IST-4-027756 WINNER II, "D6.13.7 v1.00, WINNER II Test Scenarios and Calibration Cases Issue 2," December 2006, http://www.ist-winner.org/WINNER2-Deliverables/D6.13.7.pdf.

[18] H. Haas and S. McLaughlin, Eds., *Next Generation Mobile Access Technologies: Implementing TDD*, Cambridge University Press, Cambridge, UK, 2008.

[19] T. S. Rappaport, *Wireless Communications: Principles and Practice*, Prentice Hall, Upper Saddle River, NJ, USA, 2nd edition, 2001.

[20] W. Wang, T. Ottosson, M. Sternad, A. Ahlén, and A. Svensson, "Impact of multiuser diversity and channel variability on adaptive OFDM," in *Proceedings of the 58th IEEE Vehicular Technology Conference (VTC '03)*, vol. 1, pp. 547–551, Orlando, Fla, USA, October 2003.

[21] T. Bonald, "A score-based opportunistic scheduler for fading radio channels," in *Proceedings of the European Wireless Conference (EWC '04)*, pp. 283–292, Barcelona, Spain, February 2004.

[22] R. Jain, D. Chiu, and W. Hawe, "A quantitative measure of fairness and discrimination for resource allocation in shared computer systems," Tech. Rep. TR-301, DEC, Maynard, Mass, USA, 1984.

[23] P. Agyapong, H. Haas, A. Tyrrell, and G. Auer, "Interference tolerance signaling using TDD busy tone concept," in *Proceedings of the 65th IEEE Vehicular Technology Conference (VTC '07)*, pp. 2850–2854, Dublin, Ireland, April 2007.

[24] IST-4-027756 WINNER II, "D1.1.2 v1.2 WINNER II Channel Models," November 2007, http://www.ist-winner.org/WINNER2-Deliverables/D1.1.2v1 .1.pdf.

Contention Free Inter-Cellular Slot Reservation

Gunther Auer, *Member, IEEE*, Stefan Videv, Birendra Ghimire, *Student Member, IEEE* and Harald Haas, *Member, IEEE*

***Abstract*—A distributed reservation protocol tailored for cellular wireless networks is presented that facilitates contention free inter-cellular slot allocation and reservation. While reserved slots are protected from inter-cell interference by a busy burst enabled reservation protocol, collisions due to simultaneously accessed unreserved slots by neighboring cells are mitigated by means of resource partitioning patterns. Shifting these partitioning patterns over time allows each cell to successively probe all slots. This ensures that full frequency reuse is maintained, in the way that all cells may utilize the entire frequency band. In effect a contention free inter-cellular slot allocation policy is established that in a distributed manner dynamically controls the spatial reuse, in terms of concurrently accessed radio resources by neighboring cells.**

***Index Terms*—Inter-cell interference coordination, resource partitioning, reservation ALOHA, PRMA, busy signal concept**

I. Introduction

When several users in a random access channel simultaneously attempt to access a given time-frequency slot, collisions due to co-channel interference (CCI) are encountered. Reservation protocols, such as reservation ALOHA (R-ALOHA) [1] and packet reservation multiple access (PRMA) [2], divide the available resources to idle and reserved slots. For R-ALOHA idle slots are allocated in contention and reserved slots are protected from CCI as follows [1]:

Contention: If the slot is sensed idle a packet is transmitted to contend with other users for an unreserved slot. In case of collision the packet is retransmitted in subsequent idle slots.

Reservation: Upon successful reception the receiver broadcasts an acknowledgment. This acknowledgment reserves the slot, in the way that all other users refrain from using that slot in future transmissions. R-ALOHA therefore limits the occurrence of collisions to the contention phase.

In wireless networks, slot reservation translates to an exclusion region around an active receiver [3]. A competing communication link is denied access to a reserved slot if its transmitter is located within the exclusion region; otherwise the slot may be concurrently accessed by both links. An efficient realization of R-ALOHA in decentralized wireless networks is provided by the busy signal concept, where the receiver acknowledges successful reception by means of a time-multiplexed busy burst [4, 5]. Sensing the busy burst prior to transmission controls the spatial reuse of reserved slots, in a way that potential transmitters of competing links are notified that they are located within the exclusion region of an active receiver. In [6] the busy signal concept is applied to orthogonal frequency division multiple access (OFDMA), enabling dynamic assignment of time-frequency slots to multiple users.

This paper targets the application of a distributed slot reservation protocol, such as R-ALOHA, to cellular wireless networks. While reserved slots are well protected from CCI, collisions in contention are encountered, caused by simultaneously accessed idle slots from neighboring cells. The proposed cellular slot allocation and reservation (CESAR) protocol completely avoids the contention phase, by virtue of specifically designed resource partitioning patterns: first, a frequency reuse of R ensures that at most one out of R neighboring cells may access an idle slot at a time; and second, cyclically shifting the proposed partitioning pattern allows each cell to successively contend for all slots. Hence, CESAR imposes no restrictions on the amount of resources one cell may allocate, and therefore overcomes the limitations of classical inter-cell resource partitioning based on static frequency reuse planning [7, 8]. We demonstrate through simulations that CESAR and a busy burst enabled reservation protocol [5] perfectly complement each other; the former mitigates collisions due to simultaneous access of idle slots, while the latter controls the spatial reuse of reserved slots.

II. Dynamic Inter-Cell Slot Allocation

A slotted multiple access scheme is considered where frames are divided into N_{s} slots, e.g. by means of OFDMA. The base station (BS) schedules one user per slot, so that interference within the cell is completely avoided, while a R-ALOHA based reservation protocol controls the slot allocation among neighboring cells. While reserved slots are well protected from CCI, simultaneous access of contention slots by entities in adjacent cells gives rise to collisions.

The objective of this work is to complement a distributed reservation protocol by a contention free allocation procedure for unreserved slots based on resource partitioning. For resource partitioning with frequency reuse factor R, cells are organized into R pre-defined cell groups, such that adjacent cells are in different cell groups G, $1 \leq G \leq R$, as illustrated in Fig. 1. Destructive interference from nodes located in nearby cells is mitigated by assigning mutually orthogonal slots to different cell groups, while cells that belong to the same cell group G spatially reuse resources. Associated to cell group G is one out of R resource partitioning patterns, which are constructed as follows:

1) all R patterns are mutually orthogonal
2) all patterns point to each slot once every R frames.

G. Auer is with DOCOMO Euro-Labs, Munich, Germany (e-mail: auer@docomolab-euro.com).
S. Videv is with Jacobs University Bremen, Germany (e-mail: s.videv@jacobs-alumni.de).
B. Ghimire and H. Haas are with The University of Edinburgh, UK (e-mail: {b.ghimire, h.haas}@ed.ac.uk).
This work has been performed within the framework of the CELTIC project CP5-026 WINNER+.

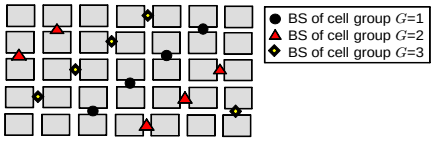

Fig. 1. Manhattan grid deployment: building blocks (gray) are interlaced by a rectangular grid of streets. Base station (BS) are organized to R=3 cell groups according to [9], in the way that direct line of sight interference between adjacent cells of the same group G is avoided.

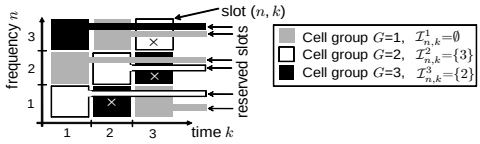

Fig. 2. CESAR working principle: slots are successively accessed by virtue of R=3 cyclically shifted resource partitioning patterns, under the condition that the interference induced to already reserved slots in adjacent cells is sufficiently low. In the illustrated example the transmitter in cell 1 is well separated from receivers in cells 2 and 3, so that $\mathcal{I}^1_{n,k}=\emptyset$. Hence, cell 1 may access all slots within R=3 frames. On the other hand, nodes in cells 2 and 3 mutually interfere, $\mathcal{I}^2_{n,k}=\{3\}$ and $\mathcal{I}^3_{n,k}=\{2\}$, so that resources reserved by cells 2 may not be accessed by cell 3 (marked by $\times$), and vice versa.

The first rule avoids collisions due to simultaneously accessed slots, provided that nodes associated to cells of the same group G experience low interference. The second rule ensures that all N_s slots are assigned to all R cell groups within R frames. These rules are satisfied by the cyclically shifted pattern

$$g_{n,k} = (n+k) \mod R\ , \quad 1 \le n \le N_\mathrm{s} \tag{1}$$

which associates slot n of frame k to cell group G=$g_{n,k}$. Unlike conventional resource partitioning in cellular networks based on static frequency planning [7, 8], the partitioning pattern (1) exclusively controls the contention free allocation of idle slots — reserved slots are governed by a distributed slot reservation protocol.

The proposed cellular slot allocation and reservation (CESAR) policy accomplishes two objectives: cell c retains all previously reserved slots, identified by the reservation indicator $\varrho^c_{n,k}$=1; in addition, nodes in cell c are granted contention free access to idle slots that satisfy (1). A transmitter in cell c may access slot (n,k) if the following condition is met

$$\Big(g_{n,k} = G \quad \text{and} \bigcup_{i \in \mathcal{I}^c_{n,k}} \varrho^i_{n,k} = 0\Big) \quad \text{or} \quad \varrho^c_{n,k} = 1 \tag{2}$$

where $\mathcal{I}^c_{n,k}$ comprises the set of active out-of-cell receivers at slot (n,k), which are vulnerable to interference from cell c. In (2) an unreserved slot (n,k) in cell c is sensed idle, if the transmitter in cell c is placed outside the exclusion range of any active out-of-cell receiver, such that $i \notin \mathcal{I}^c_{n,k}\ \forall\ \varrho^i_{n,k}$=1. Otherwise slot (n,k) is sensed busy, in which case $\varrho^i_{n,k}$=1 for at least one vulnerable out-of-cell receiver with $i \in \mathcal{I}^c_{n,k}$. Then the candidate transmitter in cell c is denied access for slot (n,k) in (2), regardless the outcome of (1).

The working principle of CESAR is illustrated in Fig. 2. Initially at frame k=1 all slots are idle, $\varrho^i_{n,1}$=0, $\forall\, n, i$, so that (2) allows each cell to initially allocate N_s/R slots. Provided the achieved signal to interference plus noise ratio (SINR) of slot (n,k) exceeds the target $\gamma_{n,k} \ge \Gamma$, cell i reserves slot n for the next frame k+1 by setting $\varrho^i_{n,k+1}$=1. In subsequent frames the cyclic shift of the partitioning pattern (1) allows nodes in adjacent cells to successively probe slot n. To this end, slot n previously reserved by cell i, may be accessed by cell c, if the interference induced to cell i is sufficiently low, such that $i \notin \mathcal{I}^c_{n,k}$ in (2), giving rise to spatially reused slots that are concurrently reserved by adjacent cells. After $k \ge R$ frames all slots are either reserved or busy so that CESAR converges to a steady state. The achieved spatial reuse in the steady state is determined by the distribution of out-of-cell receivers $\mathcal{I}^c_{n,k}$, and *not* by the reuse partitioning factor R.

Slots that satisfy (2) constitute the set of scheduled slots $\mathcal{S}$. The distribution of $\mathcal{S}$ among multiple users is carried out by a proportional fair type scheduling algorithm at the BS, as described in the companion paper [6]. Nodes are distributed in the cell and may therefore experience different interference conditions $\mathcal{I}^c_{n,k}$. Hence, the spatial reuse per slot varies over n, dependent on the scheduled users for slot (n,k).

Combination with the busy signal concept: A natural complement of CESAR is the combination with the busy signal concept [5]. Upon successful reception of a slot, the receiver emits a busy burst at a time-multiplexed mini-slot. Provided channel reciprocity holds, the interference that a transmitter in cell c imposes to a receiver in an adjacent cell i, is equivalent to the busy signal from cell i measured by the potential transmitter in cell c. Hence, a slot is identified as idle, if its received busy signal is below a certain threshold: $I^b_{n,k} \le I_\mathrm{th}$ [5]. The set of vulnerable receivers $\mathcal{I}^c_{n,k}$ in the vicinity of cell c coincides with the area where a strong busy signal is received, $I^b_{n,k} > I_\mathrm{th}$. In effect, the busy burst serves as the reservation indicator $\varrho^i_{n,k}$ for cells $i \in \mathcal{I}^c_{n,k}$, so that (2) is transformed to

$$\Big(g_{n,k} = G \text{ and } I^b_{n,k} \le I_\mathrm{th}\Big) \quad \text{or} \quad \varrho^c_{n,k} = 1 \tag{3}$$

The choice of the interference threshold I_th is important: as I_th increases, interference protection of reserved slots is sacrificed for enhanced spatial reuse [6].

III. Performance Evaluation

An OFDMA uplink (mobile to BS link) with N_s=230 frequency slots per frame is considered. A full buffer traffic model is assumed, where each user is trying to continuously send data. Perfect synchronization in time and frequency is assumed. The system parameters are summarized in Table I.

The micro-cellular deployment environment is simulated modeled by a Manhattan grid, consisting of 11×12 building blocks each of dimensions 200 m×200 m, interlaced by a rectangular grid of 30 m wide streets. In order to reduce edge effects, the performance metrics are collected only over the central core of 3×3 building blocks. On average U=10 outdoor users are served by one BS, uniformly distributed in the streets. The statistics are collected over 100 independent snapshots, each with a different user distribution. Users are

TABLE I
SIMULATION PARAMETERS

System bandwidth B	89.84 MHz
Frame length	337.2 μs
Number of frequency slots/frame N_s	230
SINR target Γ	10 dB
Average number of users/cell U	10
Transmit power per slot P	16.4 dBm
Busy signal threshold I_th	-90 dBm
Noise level	-117.8 dBm/slot

connected to the BS with the least path loss. BSs are mounted below rooftop and are deployed as depicted in Fig. 1. Distance dependent pathloss, log-normal shadowing and frequency selective fading are taken into account, with parameters taken from [10], channel model B1. Links where transmitter and receiver are located on the same street are modeled as line of sight (LoS) channels. Otherwise links are modeled as non line of sight (NLoS) channels, with significantly higher pathloss attenuation than LoS links [10]. Hence, interference between cells that belong to the same cell group G is minimized by avoiding a direct LoS connection. This is accomplished by organizing BSs into $R{=}3$ cell groups according to [9], as shown in Fig. 1.

CESAR is compared with a p-persistent variant of the busy signal concept [6], referred to as p-persistent slot allocation and reservation (p-PSAR). While CESAR controls access of idle slots by the resource partitioning pattern (1), p-PSAR transmits on idle slots with access probability $p{\in}(0,1]$. All other assumptions for CESAR and p-PSAR are identical, so to allow for a fair comparison.

The probability of outage over time in the uplink is plotted in Fig. 3. Outage occurs if the achieved SINR of slot (n,k) is below the target, $\gamma_{n,k}{<}10$ dB. Initially at $k{=}1$ all N_s slots are idle, and cells attempt to access slots dependent on the chosen slot allocation policy. While CESAR exhibits diminishing outage, p-PSAR initially suffers from a significant collision probability, especially when p is high, due to the random allocation of idle slots. The residual outage for CESAR is due to interference from distant cells that belong to the same cell group G.

The spatial reuse, in terms of normalized rate of successfully received slots whose achieved SINR exceeds the target $\gamma_{n,k}{\geq}10$ dB, is plotted in Fig. 4. A spatial reuse of 1 means that all cells can concurrently transmit on all $N_\mathrm{s}{=}230$ available slots; whereas a spatial reuse of $\frac{1}{R}{=}\frac{1}{3}$ resembles static frequency reuse of 3, where one cell transmits on $\frac{N_\mathrm{s}}{3}{=}76$ slots. Both CESAR and p-PSAR approach an spatial reuse of 95% in the steady state. The reason for this high spatial reuse is twofold: first, in Manhattan grid deployment multiple strong LoS interferers are only observed at street crossings; and second, on the uplink each user observes a different received busy signal power $I^b_{n,k}$ in (3), which provides a large degree of freedom for multi-user slot assignment [6]. CESAR reaches the steady state after only $R{=}3$ frames at diminishing outage. Hence, CESAR offers a favorable trade-off between avoiding outage and convergence to the steady state throughput. While lowering p significantly reduces outage for p-PSAR (see Fig. 3), the time to convergence to the steady state increases.

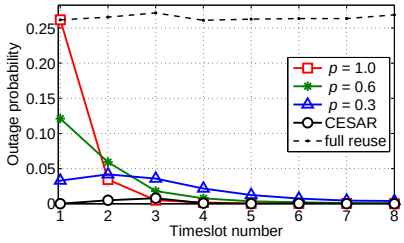

Fig. 3. Probability of outage over time k for slots that fail to achieve their SINR target $\gamma_{n,k}{<}10$ dB.

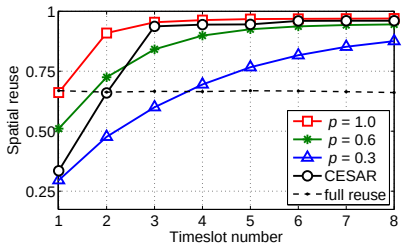

Fig. 4. Rate of successfully received slots with $\gamma_{n,k}{\geq}10$ dB over time k.

For comparison a system with full frequency reuse, where cells access all $N_\mathrm{s}{=}230$ available slots is also included in Fig. 3 and 4. As no attempts to avoid interference are made, outage and throughput do not change over time. CESAR exhibits superior performance in terms of both outage (see Fig. 3) and throughput (see Fig. 4).

REFERENCES

[1] W. Crowther, R. Rettberg, D. Walden, S. Ornstein, and F. Heart, "A System for Broadcast Communications: Reservation-ALOHA," in *Proc. 6th Hawaii Int. Conf. Sys. Sci.*, Jan. 1973, pp. 371–374.

[2] D. J. Goodman, R. A. Valenzuela, K. T. Gayliard, and B. Ramamurthi, "Packet Reservation Multiple Access for Local Wireless Communications," *IEEE Trans. Commun.*, vol. 37, no. 8, pp. 885–890, Aug. 1989.

[3] A. Hasan and J. Andrews, "The guard zone in wireless ad hoc networks," *IEEE Trans. Wireless Commun.*, vol. 6, no. 3, pp. 897–906, Mar. 2007.

[4] R. Zhao, B. Walke, and G. Hiertz, "An Efficient IEEE 802.11 ESS Mesh Network Supporting Quality-of-Service," *IEEE J. Sel. Areas Commun.*, vol. 24, no. 11, pp. 2005–2017, Nov. 2006.

[5] P. Omiyi, H. Haas, and G. Auer, "Analysis of TDD Cellular Interference Mitigation using Busy-Bursts," *IEEE Trans. Wireless Commun.*, vol. 6, pp. 2721–2731, July 2007.

[6] B. Ghimire, G. Auer, and H. Haas, "Busy Bursts for Trading off Throughput and Fairness in Cellular OFDMA-TDD," *EURASIP J. Wireless Commun. and Networking*, vol. 2009, Article ID 462396, 14 pages, 2009.

[7] S. Halpern, "Reuse partitioning in cellular systems," *Proc. IEEE Vehic. Technol. Conf. (VTC'83), Toronto, Canada*, vol. 33, pp. 322–327, May 1983.

[8] M. Sternad, T. Ottosson, A. Ahlen, and A. Svensson, "Attaining both Coverage and High Spectral Efficiency with Adaptive OFDM Downlinks," in *Proc. IEEE Vehic. Technol. Conf. 2003-Fall (VTC'F03), Orlando, USA*, Oct. 2003, pp. 2486–2490.

[9] IST-4-027756 WINNER II, "D6.13.14 WINNER II System Concept Description," Dec. 2007.

[10] ——, "D1.1.2 WINNER II Channel Models," Sept. 2007.

Self-Organised Interference Mitigation in Wireless Networks Using Busy Bursts

Birendra Ghimire, Sinan Sinanović, Harald Haas
Institute for Digital Communications
Joint Research Institute for Signal and Image Processing
The University of Edinburgh, EH9 3JL, Edinburgh, UK
E-mail: {b.ghimire, s.sinanovic, h.haas}@ed.ac.uk

Gunther Auer
DOCOMO Euro-Labs
80687 Munich, Germany
Email: auer@docomolab-euro.com

***Abstract*—In this paper, self-organised interference management in *ad hoc* networks that lack any centralised control, is addressed. Using time-multiplexed busy bursts (BB) in a minislot, the receivers actively broadcast a power signal on their reserved time-frequency slot. The potential new transmitters that intend to reuse the already reserved resources can infer from the received BB power the amount of co-channel interference (CCI) they would cause (prior to transmission) – especially if channel reciprocity can be guaranteed. This is vital information for the new transmitter to decide without any central supervision whether to transmit or defer the transmission to another time or frequency so as to limit CCI caused to the active link. Specifically, CCI is limited to a threshold value chosen system-wide. It is demonstrated that with the BB-enabled CCI mitigation approach, by setting the interference threshold parameter to an optimal value, a gain of up to 40% in sum throughput can be achieved compared to uncoordinated random medium access in such *ad hoc* networks. Moreover, it is demonstrated that by adjusting the system-wide threshold, the system throughput can be traded off to significantly enhance the link throughput in the lower percentiles.**

***Index terms*— CCI mitigation, self-organising networks, user cooperation, busy burst signalling, *ad hoc* networks.**

I. Introduction

Mobile communication faces a trend of ever increasing data rates while the available spectrum increases at a much slower pace. The only solution to the emerging bottleneck is a significant increase of system spectral efficiency (by factors). In general terms, this can be achieved by increasing the frequency reuse. On the physical layer, *e.g.* multiple-input-multiple-output (MIMO) transmissions achieve this goal via spatial multiplexing [1, 2] or beamforming [3]. On system/networking level, this goal is achieved by smaller cell radii through the introduction of femtocells [4] or *ad hoc* communication [5] and at the same time allowing all cells/links to access all frequency channels. Common to all these techniques is that they generate interference – in the case of MIMO, it is inter-channel interference (ICI) while in the case of increased system frequency reuse, it is CCI. In order to avoid increased interference, it is imperative that powerful interference mitigation techniques are employed. Smaller cell radii and random link deployments such as in femtocell and *ad hoc* networks render effective interference coordination techniques difficult since central control is not possible and the system, in fact, relies on self-organisation which requires the entities in the network to make own decisions based on local information. Also, when multiple links share the same time-frequency resources, the problems of collisions can be debilitating – especially since the vulnerable receiver cannot be 'sensed' by new transmitters entering the network - giving rise to the *hidden node* problems. In this paper, we show that the BB technique [6, 7] is a powerful interference management technique in *ad hoc* networks.

In an attempt to partially mitigate the hidden node problem, channel usage monitoring methods [8] have been proposed, where the transmitter and receiver monitor both the data and control channels and exchange the information to infer the free slots available at both ends. Protocols that solve these issues require separate dedicated channels where probe packets and extra reply packets [9] are transmitted. Dual busy tone multiple access [10] avoid collision of ready to send (RTS) and clear to send (CTS) packets by incorporating two narrowband channels. These approaches solve the hidden and exposed node problem at the expense of separate channels dedicated for out-of-band signalling. As a consequence, additional filters and duplexers are required which increase the complexity at the radio frequency (RF) unit. This issue is solved with the medium access control (MAC) protocol described in [11] in which busy-tones are used in a time-multiplexed fashion for solving the hidden node problem. However, none of these busy tone based MAC protocols exploit channel reciprocity for dynamic resource allocation in a broadband frequency selective radio frequency channel. These issues are addressed in [6, 7] where the channel reciprocity offered by the time division duplex (TDD) mode is exploited for interference aware subchannel allocation in a cellular environment. Time multiplexed power signals are used for this purpose. A key feature of this mechanism is that it is based on local information only (measured BB signal at the transmitter) which means it perfectly supports self-organisation.

BB-enabled CCI mitigation in an indoor *ad hoc* scenario was addressed in [12], where it was demonstrated that the system throughput can be maximised by an appropriate choice of the threshold parameter. In this paper, we demonstrate that system throughput can be traded off to enhance fairness among the competing user population in the system while using adaptive modulation as opposed to suboptimal systemwide fixed modulation scheme in [12].

The remainder of this paper is structured as follows - Section II discusses the air interface considered in this paper. The description of the *ad hoc* network considered is provided in Section III. Dynamic channel allocation using BB approach and the benchmark system are described in Section IV. The system model considered for study is discussed in Section V. Finally, the simulation results are provided in Section VI, and the conclusions are drawn in Section VII.

II. Radio Resource Allocation in OFDMA–TDD

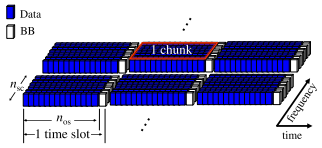

Fig. 1. Air interface in OFDMA–TDD

We consider an orthogonal frequency division multiple access (OFDMA)–TDD based air-interface. The basic resource unit is a time-frequency slot referred to as a *chunk*, which comprises of n_{os} successive orthogonal frequency division multiplexing (OFDM) symbols and n_{sc} contiguous subcarriers as shown in Fig 1. A chunk is denoted as a pair (n, k), where $1 \leq n \leq N_{\mathrm{C}}$ denotes the frequency index and k represents the time slot index. N_{C} is the total number of chunks per time slot given by $N_{\mathrm{C}} = \lfloor \frac{B}{n_{\mathrm{sc}} \Delta_f} \rfloor$, where B is the signal bandwidth, Δ_f is the spacing between adjacent subcarriers and $\lfloor \cdot \rfloor$ is the floor-operator. Each time slot is divided into a 'data slot', which carries data from the transmitters to the receivers and a BB minislot, which is used to convey the BB signals (detailed out in Section IV). The duration of a time slot is, therefore, $n_{\mathrm{os}}+1$ OFDM symbols, and it carries N_{C} chunks each paired with a busy burst of n_{sc} subcarriers spanning one OFDM symbol accommodated in a minislot.

III. System Description

We consider a generalised *ad hoc* network consisting of N_{L} end-to-end links. A link is denoted as a pair (μ, q) where μ is the transmitter and q is the receiver. Let $\mathbf{x}$ define a transmitter or a receiver of the link (μ, q). With this notation, the intended channel gain between transmitter μ and receiver q can be written as $G_{\mathbf{x}}[n,k] = G_{\mu,q}[n,k]$, which takes into account signal propagation effects such as distance dependent path loss, log-normal shadowing, as well as channel variations due to frequency-selective fading and user mobility. The channel gain between transmitter $\mathbf{y}$ of a interfering link (ν, r), where $\mu \neq \nu$ and $q \neq r$, and receiver $\mathbf{x}$ is denoted $G_{\mathbf{yx}}[n,k]$. The data transmit powers of the transmitters of $\mathbf{x}$ and $\mathbf{y}$ are denoted as $T^{\mathrm{d}}_{\mathbf{x}}[n,k]$ and $T^{\mathrm{d}}_{\mathbf{y}}[n,k]$ respectively. With the above notation, the signal to interference and noise ratio (SINR) at the receiver of $\mathbf{x}$, $\gamma_{\mathbf{x}}[n,k]$ is expressed as

$$\gamma_{\mathbf{x}}[n,k] = \frac{T^{\mathrm{d}}_{\mathbf{x}}[n,k] \cdot G_{\mathbf{x}}[n,k]}{\underbrace{\sum_{\substack{\mathbf{y} \in \mathcal{T} \\ \mathbf{y} \neq \mathbf{x}}} T^{\mathrm{d}}_{\mathbf{y}}[n,k] \cdot G_{\mathbf{yx}}[n,k] + \delta}_{I^{\mathrm{d}}_{\mathbf{x}}[n,k]}}, \tag{1}$$

where $\mathcal{T}$ is the set of all active transmitters in the system and δ is the thermal noise power.

IV. Interference Management using Busy Burst Signalling

Interference management using BB signalling [6, 7] establishes an exclusion region around active receivers. An exclusion region defines an area around an active receiver, where no other transmitter is allowed to reuse the reserved radio resources. The exclusion regions are established individually for each chunk (n,k) [13]. It is assumed that the transmitter $\mathbf{x}$ transmits data to its intended receiver using chunk (n,k). Provided that $\gamma_{\mathbf{x}}[n,k] \geq \Gamma$, where Γ is the minimum SINR target, the receiver broadcasts a BB in the associated BB minislot. The BB transmit power for receiver $\mathbf{x}$ (BB transmitter) is denoted $T^{\mathrm{b}}_{\mathbf{x}}[n,k]$. This reserves the data slot of the n^{th} chunk for the next time slot $k+1$ for $\mathbf{x}$. The BB-OFDMA can be described by the following protocol:

1) All potential transmitters must sense the BB associated to the data chunk (n,k) prior to transmission.
2) Transmitters are prohibited to access chunks where a BB is detected above a given threshold.

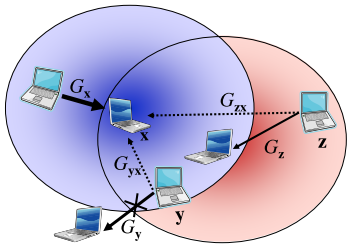

Fig. 2. Busy burst signalling using fixed BB power. The chunks reserved by the receiver $\mathbf{x}$ cannot be reused by transmitter $\mathbf{y}$ but it may be reused by transmitter $\mathbf{z}$ because the latter lies outside the exclusion region established around receiver $\mathbf{x}$.

Exploiting TDD channel reciprocity, transmitter $\mathbf{y}$ can ascertain $I^{\mathrm{d}}_{\mathbf{x}}[n,k]$, the potential amount of interference it causes to a receiver $\mathbf{x}$ of a pre-established link, by measuring $I^{\mathrm{b}}_{\mathbf{y}}[n,k]$ at the associated BB minislot [6], which is given by

$$I^{\mathrm{b}}_{\mathbf{y}}[n,k] = T^{\mathrm{b}}_{\mathbf{x}}[n,k] \cdot G_{\mathbf{xy}}[n,k]. \tag{2}$$

Applying the channel reciprocity property of TDD, $G_{\mathbf{yx}}[n,k] = G_{\mathbf{xy}}[n,k]$, yields

$$I^{\mathrm{d}}_{\mathbf{x}}[n,k] = I^{\mathrm{b}}_{\mathbf{y}}[n,k] \cdot \frac{T^{\mathrm{d}}_{\mathbf{y}}[n,k]}{T^{\mathrm{b}}_{\mathbf{x}}[n,k]}. \tag{3}$$

The maximum CCI $I^{\mathrm{d}}_{\mathbf{x}}[n,k]$ that a candidate transmitter $\mathbf{y}$ is allowed to cause to an active receiver $\mathbf{x}$ is defined by the interference threshold I_{th}, which is a network-wide constant and the same for all receivers. A key assumption is that the transmitter has knowledge of $T^{\mathrm{b}}_{\mathbf{x}}[n,k]$ used by the active receiver, which is easily accomplished by using constant transmit power. This limitation, however, is eliminated in a modified BB protocol in [14]. To ensure that the transmitter

$\mathbf{y}$ lies outside the exclusion region of receiver $\mathbf{x}$ on the chunk (n,k), $\mathbf{y}$ can either reduce its own transmit power $T^{\mathrm{d}}_{\mathbf{y}}[n,k]$ or refrain from transmitting on the chunk (n,k). The transmitter is outside the exclusion region of the receiver $\mathbf{x}$ when $I^{\mathrm{d}}_{\mathbf{x}}[n,k]<I_{\mathrm{th}}$. With the assumptions above, a candidate transmitter, $\mathbf{y}$, has full knowledge of all parameters of the right-hand side in (3). This enables $\mathbf{y}$ to verify whether $I^{\mathrm{d}}_{\mathbf{x}}[n,k]<I_{\mathrm{th}}$ by invoking the threshold test [6, 7]

$$I^{\mathrm{b}}_{\mathbf{y}}[n,k]\cdot\frac{T^{\mathrm{d}}_{\mathbf{y}}[n,k]}{T^{\mathrm{b}}_{\mathbf{x}}[n,k]}\leq I_{\mathrm{th}}\,. \tag{4}$$

In case $T^{\mathrm{d}}_{\mathbf{y}}[n,k]=T^{\mathrm{b}}_{\mathbf{x}}[n,k]$, condition (4) reduces to:

$$I^{\mathrm{b}}_{\mathbf{y}}[n,k]\leq I_{\mathrm{th}}\,. \tag{5}$$

By tuning I_{th}, the maximum CCI $I^{\mathrm{d}}_{\mathbf{x}}[n,k]$ in (1) is adjusted. It will be shown later in (Section VI) that the choice of I_{th} influences the sum throughput and user throughput of users with low desired channel gains. In the rest of this section, the procedure for dynamic chunk allocation using BB signalling is detailed out.

A. Initial access in contention

CCI higher than a threshold value is avoided at the receivers on the reserved chunks via BB signalling mechanism discussed above. However, in the case of unreserved chunks, two or more transmitters may simultaneously transmit using such chunks provided (5) holds when such transmitters scan the BB minislot. This results in contention where the transmitters are not aware of the amount of interference they cause to the receiver of other links. Consequently, several links may encounter a collision on chunk (n,k) where the SINR target may not be met. Hence, to reduce the occurrence of simultaneously accessed chunks in contention, a $p-$persistent chunk allocation procedure is applied to BB-OFDMA, where chunk (n,k) is accessed by transmitter $\mathbf{y}$ with probability p. Denoting the outcome of the $p-$persistent chunk allocation with the binary random variable $\chi_{\mathbf{y}}[n,k]\in\{0,1\}$, the access probability is $\Pr(\chi_{\mathbf{y}}[n,k]{=}1)=p$. In this paper, p is set to $1/N_{\mathrm{L}}$ such that on average the transmitter of only one link accesses a chunk in contention at any given time slot.

B. Dynamic chunk allocation with BB signalling

The dynamic chunk allocation (DCA) mechanism with BB signalling is explained with the help of Fig. 2 and Fig. 3. It is assumed that the receiver $\mathbf{x}$ in Fig. 2 has transmitted BB on chunks it has reserved. Prior to transmission, the transmitter $\mathbf{y}$ must sense the BB minislot to ascertain the chunks it reuses are outside the exclusion region of existing transmitter(s). Provided (5) holds true, the transmitter $\mathbf{y}$ transmits data during the data slot. In the particular example depicted in Fig. 3, the BB received on chunks 13–15 and 25–28 are below the threshold value and can be used for transmission. The set of chunks where the transmission is carried out belong to the set $\mathcal{A}_{\mathbf{y}}$. The binary variable $a_{\mathbf{y}}[n,k]$ denotes whether or not

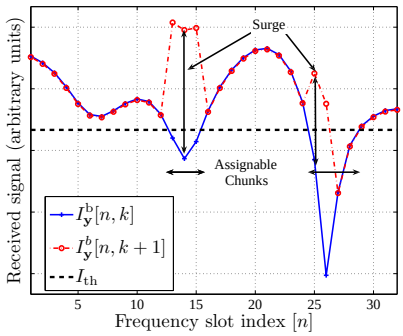

Fig. 3. Illustration of DCA using BB signalling. The receiver that intends to transmit using unreserved chunks is obliged to check if the received BB power is below the threshold.

transmitter $\mathbf{y}$ used the chunk (n,k) for transmission

$$a_{\mathbf{y}}[n,k]=\begin{cases}1\,, & \big(I^{\mathrm{b}}_{\mathbf{y}}[n,k]\leq I_{\mathrm{th}}\text{ and }\chi_{\mathbf{y}}[n,k]=1\big)\text{ or}\\ & b_{\mathbf{y}}[n,k]=1\\ 0\,, & \text{otherwise}\,,\end{cases} \tag{6}$$

where $b_{\mathbf{y}}[n,k]$ indicates whether or not the chunk (n,k) has been reserved by $\mathbf{y}$, defined as

$$b_{\mathbf{y}}[n,k+1]=\begin{cases}1\,, & a_{\mathbf{y}}[n,k]=1\text{ and }\gamma_{\mathbf{y}}[n,k]\geq\Gamma\\ 0\,, & \text{otherwise}\,.\end{cases} \tag{7}$$

Provided that $\gamma_{\mathbf{y}}[n,k]\geq\Gamma$ is maintained, the receiver transmits BB during the time-multiplexed BB. The acknowledgement of successful transmission is implicitly conveyed to the transmitter via a surge in the received BB power levels [7]. In Fig. 3, the surge in received power levels is detected in chunks with index 13–15 and 25–26, which signals to transmitter $\mathbf{y}$ that the transmission has been successful. By contrast, no surge in power level is detected in chunk with index 27 and 28 which signals the transmitter that the minimum SINR target in these chunks is not met. The chunks where the BB signal is not received from the intended receiver during the BB slot are released and may be allocated by other users in the system. The chunks where the acknowledgement of successful transmission is received belong to set $\mathcal{B}_{\mathbf{y}}\subset\mathcal{A}_{\mathbf{y}}$, where the binary variable $b_{\mathbf{y}}[n,k]=1$ indicates that the transmission is received above the minimum SINR target and that the chunk has been reserved for transmitter $\mathbf{y}$ for the k^{th} time slot.

C. Link adaptation

Let $\mathcal{M}{=}\{1,\cdots,M\}$ be the set of supported modulation schemes. Associated to each modulation scheme $m\in M$ is an SINR target $\Gamma{=}\Gamma_m$ that must be achieved to satisfy a given BER (bit error ratio). The objective is to select the modulation scheme $m_{\mathbf{x}}[n,k]\in\mathcal{M}$ for chunk (n,k), which yields the highest spectral efficiency, for which $\gamma_{\mathbf{x}}[n,k]\geq\Gamma_{m_{\mathbf{x}}[n,k]}$ holds. Assuming that the channel does not change significantly between two consecutive time slots, the feedback of SINR observed in

the preceding slot is used to select an appropriate modulation format for the next time slot. The steps of performing link adaptation is detailed as follows:

1) Determine the chunks (n, k) where (5) holds true.
2) Transmit using $m = 1$, the modulation with lowest spectral efficiency.
3) Calculate the achieved SINR $\gamma_{\mathbf{x}}[n, k]$ using (1).
4) Using lookup table, determine the modulation scheme $\hat{m}$ with highest spectral efficiency such that $\gamma_{\mathbf{x}}[n, k] \geq \Gamma_{\hat{m}}[n, k]$ holds.
5) Adjust the modulation scheme as follows:

$$m_{\mathbf{x}}[n, k+1] = \begin{cases} \bar{m}\,, & \gamma_{\mathbf{x}}[n, k] \geq \Gamma_{m_{\mathbf{x}}[n,k+1]} \\ 0\,, & \gamma_{\mathbf{x}} < \Gamma_1 \\ m_{\mathbf{x}}[n, k]\,, & \text{otherwise,} \end{cases} \tag{8}$$

where $\bar{m} = \lceil (m_{\mathbf{x}}[n, k] + \hat{m}[n, k])/2 \rceil$, $\lceil \cdot \rceil$ is the ceiling operator and Γ_1 is the minimum SINR target corresponding to $m = 1$.

6) If $m_{\mathbf{x}}[n, k+1] = 0$, or the chunk is no longer needed, release the chunk, else go to step 3.

D. Benchmark System

An interference blind chunk allocation scheme with reservation is chosen as a benchmark. The chunks are allocated in a decentralised fashion using $p-$persistent approach, where each link accesses a new chunk with probability $p = 1/N_{\mathrm{L}}$. The chunks where the minimum SINR target is met are retained for transmission in the next time slot, otherwise the chunks are released. The only difference between the BB-enabled CCI mitigation and the benchmark system is that interference avoidance is not considered in the benchmark system, which enables us to make fair comparisons between the two approaches.

V. Model and Methodology

An *ad hoc* network deployed in an indoor office environment as defined in scenario A1 [15, 16] of wireless world initiative new radio (WINNER) is considered. The indoor office environment is modelled as a single floor in a building and consists of 40 rooms of size $10\mathrm{m}\times10\mathrm{m}\times3\mathrm{m}$ and two corridors of size $100\mathrm{m}\times5\mathrm{m}\times3\mathrm{m}$. The relevant parameters considered in simulation are presented in Table I. The deployment scenario and the distribution of users is as shown in Fig. 4.

The system is simulated as follows: $2N_{\mathrm{L}}$ mobile stations (MSs) are distributed uniformly in the space with a probability of 0.9 of lying inside the room and 0.1 of being in the corridor. Half of these MSs act as transmitters and the other half as receivers. Each transmitter selects a receiver randomly if the receiver is not already paired with another transmitter and the gain between them exceeds a minimum threshold value $G_{\min}$. In this paper, $G_{\min}$ is set at 5 dB above the thermal noise level δ because this avoids forming the links that would not meet the minimum SINR target in a noise limited scenario. The channel between the transmitter(s) and receiver(s) are modelled according to the scenario A1 of WINNER [16]. A line of sight (LoS) condition is considered when both the transmitter and receiver are located either in the same room or the same corridor. Otherwise, a non line of sight (NLoS) condition is considered. Both large scale and small scale fading are considered. The path loss (P_{L}) between a transmitter and receiver pair is given by

$$\begin{aligned} P_{\mathrm{L}}[\mathrm{dB}] &= 38.8 + 36.8 \cdot \log_{10}(d) + \xi + 5\Omega \quad (\mathrm{NLoS}) \\ &= 48.6 + 18.7 \cdot \log_{10}(d) + \xi \quad (\mathrm{LoS})\,, \end{aligned} \tag{9}$$

where d is the separation distance between the transmitter and the receiver, ξ is a log-normal random variable that models shadowing between a transmitter and receiver pair, whose variance is 3.1 dB or 3.5 dB for LoS and NLoS scenarios respectively and Ω is the minimum number of walls between the transmitter and the receiver.

TABLE I
List of simulation parameters

Parameters	Value
MS transmit power	21 dBm
Center carrier frequency f_{c}	5.0 GHz
System bandwidth B	89.84 MHz
# subcarriers (SC)	1840
Subcarriers spacing Δf	48.8 kHz
OFDM symbols/time slot n_{os}	15
OFDM symbol duration T_{sym}	22.48 μs
# chunks/time slot N_{C}	230
Chunk size $n_{\mathrm{sc}}\times n_{\mathrm{os}}$	8 (freq.) $\times$ 15 (time) = 120
Modulation format	BPSK, QPSK, cross 8-QAM, 16-QAM, cross 32-QAM, 64-QAM, cross 128-QAM and 256-QAM
Coding	3/4-rate convolutional
SINR target Γ [dB]	2.2, 5.2, 9.1,11.3, 14.4,16.6, 19.5, 22.5
Protocol data unit (PDU) size	112 bits
Tx power/chunk T^{d}	-3.08 dBm
Antenna gain	0 dBi
Noise level/chunk δ	-117.8 dBm
# snapshots	500
Snapshot duration	75 ms

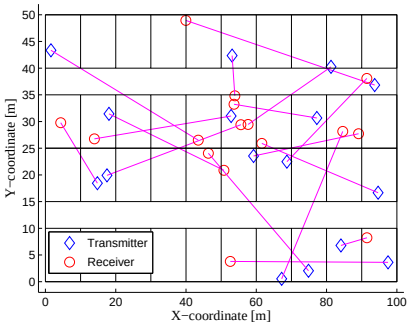

Fig. 4. Indoor scenario with its corresponding distribution of users. Each transmitter selects its receiver randomly from the initial distribution.

VI. Results

In this section, the performance of the CCI mitigation approach with BB-signalling is compared against the random chunk allocation with reservation mechanism, considered as

the benchmark. The performance metrics considered are link throughput and system throughput. Link throughput is the number of bits successfully received by the link. The system throughput is an aggregate of link throughput of all links in the system.

A. Trading off system throughput and fairness

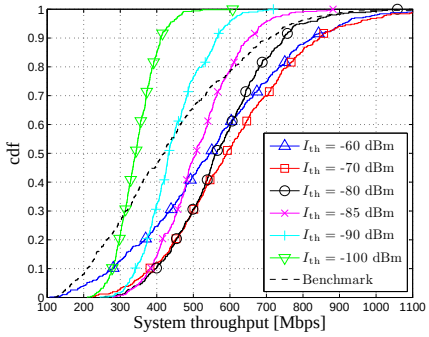

(a) System throughput

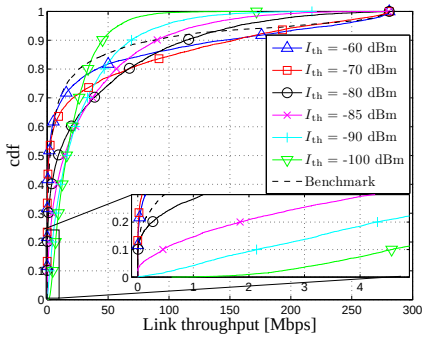

(b) Link throughput

Fig. 5. Comparison of system performance with link adaptation

The impact of the threshold parameter on system throughput and link throughput is shown in Fig. 5. In these results, N_{L} is arbitrarily set to 16, such that it represents a network with a moderate density of MSs. The results show that by setting low thresholds (*e.g.* -100 dBm), the system throughput is the lowest because the transmitters become over-cautious in reusing reserved chunks. On the one hand, increasing the threshold improves the spatial reuse of chunks which potentially increases the system throughput, whereas on the other hand, the achieved SINR degrades due to an increase in CCI. This causes the transmitter to reduce the number of bits transmitted per chunk, reducing the system throughput. Overall, the median system throughput increases on increasing the threshold until an optimum threshold of about -70 dBm is reached, beyond which the median system throughput decreases. Using this threshold, a median system throughput of 592 Mbps is achieved, which is a 40% increase compared to the benchmark (see Fig. 5(a)). However, at this threshold, the system suffers from approximately 13% outage (see Fig. 5(b)). By lowering the threshold, the median system throughput is traded off for improving link throughput at the lower 10^{th} percentile. In particular, by setting the threshold to -100 dBm, 250 Mbps of median system throughput is traded off to achieve 4.6 Mbps at the lower 10^{th} percentile of link throughput. However, using a threshold of -100 dBm, the overall system throughput is 20% lower compared to the benchmark system due to compromised spatial reuse. If the spatial reuse is slightly enhanced by setting the threshold to -90 dBm, a guaranteed link throughput of 2.1 Mbps together with a median system throughput of 433.5 Mbps can be achieved, which outperforms the benchmark in both metrics simultaneously. These results demonstrate that BB signalling approach allows a flexible network operation between maximising the sum rate in the network and maximising the guaranteed throughput of individual links or a trade off between the two goals for self-organised operation. The above benefits achieved with BB technique are very important for the future generation wireless networks that are often envisioned to lack rigorous centralised control and infrastructure.

Provided that the quality-of-service (QoS) requirements stipulate that a certain data rate should be available at the lower 10^{th} percentile, an interesting question is to determine how many links can be accommodated in the system whilst satisfying the stated QoS constraints. This leads to determining the spectral efficiency that can be achieved whilst fulfilling the QoS constraints. These two issues are addressed next by varying the number of links in the system.

B. Impact of varying number of links in the system

The impact of varying the number of links in the system is examined in Fig. 6. The results in Fig. 6(a) demonstrate that the system throughput increases with the increase in the number of links, due to an increase in spatial reuse of the chunks. However, due to an increase in CCI, the link throughput at the lower 10^{th} percentile decreases with an increase in the number of links as shown in Fig. 6(b). To evaluate the maximum number of feasible links in the considered system and its corresponding attainable spectral efficiency, we consider the *satisfied user criteria* (SUC). In this paper, the SUC is fulfilled if 90 %-ile of all links achieve a link throughput of 2 Mbps or more. The results demonstrate that in the benchmark system, the satisfied user criteria is not fulfilled in the presence of CCI for any number of links in the system. Likewise, with the BB approach, if a high threshold, such as -70 dBm is set, the SUC is fulfilled only when fewer than 4 links are present in the system (see Fig. 6(b)). By decreasing the threshold, the maximum number of links in the system such that the satisfied user criteria is met is 8, 16, 28 and 32 respectively if the thresholds are set to -85 dBm, -90 dBm, -95 dBm and -100 dBm respectively.

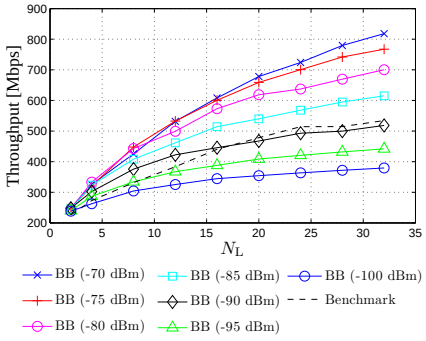

(a) System throughput

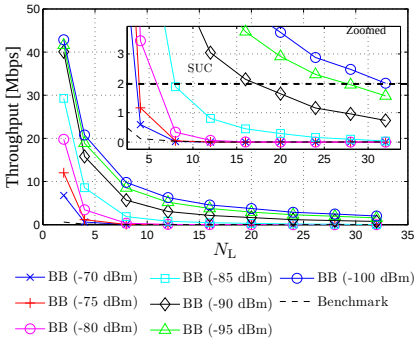

(b) Link throughput

Fig. 6. Impact of varying the number of links in the system.

The corresponding system throughputs obtained are 408 Mbps, 440 Mbps, 432 Mbps and 377 Mbps respectively. Using a signal bandwidth of 89.84 MHz, the achieved system throughput translates to a spectral efficiencies of 4.5, 4.9, 4.8, and 4.2 bits/s/Hz respectively. The results demonstrate that using the BB approach, up to 32 links can be supported whilst fulfilling the satisfied user criterion. Moreover, it also shows that the spectral efficiency is highest with 16 links in the system.

VII. Conclusions

This paper addressed decentralised CCI mitigation scheme using BB applied to self-organising *ad hoc* networks using parameters from the TDD mode of WINNER in an indoor deployment scenario. It was demonstrated that the system using BB-enabled CCI mitigation outperforms a benchmark system, performing random chunk allocation with reservation, by up to 40% in terms of system throughput. Moreover, it was demonstrated that the threshold parameter can be used to trade off the system throughput and the link throughput to aid links with weaker channel conditions. Specifically, it was demonstrated that with the BB approach, up to 32 active links can be supported in a 89.84 MHz of system bandwidth whilst satisfying a QoS constraint that 90% of all users achieve a throughput of 2 Mbps or better. This demonstrates that the BB approach provides significantly better support for QoS provisioning compared to the benchmark system which only provides less than 600 kbps of link throughput at the lower 10^{th} percentile even when the network contains only 2 competing links. We have therefore demonstrated self-organising capability of BB protocol to provide either significantly improved QoS for link throughput or increased system throughput by controlling a single parameter, namely the BB interference threshold.

References

[1] E. Telatar, "Capacity of Multi-Antenna Gaussian Channels," *European Transaction on Telecommunication*, vol. 10, no. 6, pp. 585–595, Nov. / Dec. 1999.

[2] R. Mesleh, H. Haas, S. Sinanović, C. W. Ahn, and S. Yun, "Spatial Modulation," *IEEE Transactions on Vehicular Technology*, vol. 57, no. 4, pp. 2228 – 2241, Jul. 2008.

[3] P. Viswanath, D. Tse, and R. Laroia, "Opportunistic Beamforming Using Dumb Antennas," in *Proc. of the International Symposium on Information Theory*. Lausanne , Switzerland: IEEE, 30 Jun.–5 Jul. 2002, p. 449.

[4] V. Chandrasekhar, J. Andrews, and A. Gatherer, "Femtocell Networks: A Survey," *IEEE Communcations Magazine*, vol. 46, no. 9, pp. 59–67, 2008.

[5] H. Wu, C. Qiao, S. De, and O. Tonguz, "Integrated Cellular and Ad Hoc Relaying Systems: iCAR," *IEEE Journal on Selected Areas in Communications*, vol. 19, no. 10, pp. 2105–2115, Oct. 2001.

[6] P. E. Omiyi and H. Haas, "Improving Time-Slot Allocation in 4th Generation OFDM/TDMA TDD Radio Access Networks with Innovative Channel-Sensing," in *Proc. of the International Conference on Communications (ICC)*, vol. 6. Paris, France: IEEE, Jun. 20–24 2004, pp. 3133–3137.

[7] P. Omiyi, H. Haas, and G. Auer, "Analysis of TDD Cellular Interference Mitigation Using Busy-Bursts," *IEEE Transactions on Wireless Communications*, vol. 6, no. 7, pp. 2721–2731, Jul. 2007.

[8] *A New Multi-channel MAC Protocol with On-demand Channel Assignment for Multi-hop Mobile ad hoc Networks*, Dallas, TX, USA, Dec.7-10, 2000.

[9] S. Singh and C. S. Raghavendra, "Power efficient MAC protocol for multihop radio networks," in *Proc. of the 9th IEEE International Symposium on Personal, Indoor and Mobile Radio Communications (PIMRC)*, vol. 1, Boston, MA, USA, Sep. 8–11, 1998, pp. 153–157.

[10] Z. J. Haas and J. Deng, "Dual Busy Tone Multiple Access (DBTMA)-A Multiple Access Control Scheme for ad hoc Networks," *IEEE Transactions on Communications*, vol. 50, no. 6, pp. 975–985, Jun. 2002.

[11] R. Zhao, B. Walke, and M. Einhaus, "Constructing Efficient Multihop Mesh Networks," in *Proc. of the Conference on Local Computer Networks (LCN)*. Sydney, Australia: IEEE, Nov. 15–17, 2005, pp. 166–173.

[12] B. Ghimire, H. Haas, and G. Auer, "Busy Burst Enabled Interference Avoidance in WINNER-TDD," in *Proc. of the International Symposium on Personal, Indoor and Mobile Radio Communications (PIMRC)*, Athens, Greece, Sep. 3–7, 2007, pp. 5 pages on CD–ROM.

[13] H. Haas, V. D. Nguyen, P. Omiyi, N. Nedev, and G. Auer, "Interference Aware Medium Access in Cellular OFDMA/TDD Networks," in *Proc. of the International Conference on Communications (ICC)*, vol. 4. Istanbul, Turkey: IEEE, Jun.11–15, 2006, pp. 1778–1783.

[14] B. Ghimire, G. Auer, and H. Haas, "Busy Bursts for Trading-off Throughput and Fairness in Cellular OFDMA-TDD," *Eurasip Journal on Wireless Communications and Networking*, vol. 2009, Article ID 462396, 14 pages, 2009.

[15] IST-4-027756 WINNER II, "D6.13.7, WINNER II Test Scenarios and Calibration Cases Issue 2," Retrieved Mar. 15, 2007, from https://www.ist-winner.org/WINNER2-Deliverables/.

[16] IST-2003-507581 WINNER, "D5.4 v1.0 Final Report on Link Level and System Level Channel Models," Retrieved Apr. 15, 2007, from https://www.ist-winner.org/DeliverableDocuments/, Nov. 2005.

OFDMA-TDD Networks with Busy Burst Enabled Grid-of-Beam Selection

Birendra Ghimire*, Gunther Auer† and Harald Haas*

*Institute for Digital Communications
The University of Edinburgh
EH9 3JL, Edinburgh, UK
{b.ghimire, h.haas}@ed.ac.uk

†DOCOMO Euro-Labs
80687 München, Germany
auer@docomolab-euro.com

***Abstract*—Interference aware user scheduling in fixed grid-of-beam (GoB) transmission is envisaged to significantly benefit from the receiver initiated busy burst (BB) protocol. Fixed GoB scheduling relies on the knowledge of the location of the intended users as well as the vulnerable users which effectively is provided by the BB protocol via exploitation of channel reciprocity. This paper studies the hybrid BB and GoB (BB+GoB) approach in a Manhattan environment. The new proposed hybrid interference avoidance scheme with an underlying score based scheduler is evaluated by means of system level simulations, and is compared against a pure GoB approach with the same scheduler as well as the BB based interference avoidance techniques applied to omnidirectional antennas. The results show an improvement in both system throughput and fairness (defined as cell edge user throughput). In particular, system throughput of up to 238.5 Mbps/cell or user throughput of up to 8.88 Mbps/user for the lower 10%-ile of users are shown to be feasible. In particular, the hybrid BB+GoB scheme exhibits a 16-fold improvement at the lower 10%-ile compared to pure GoB technique.**

I. Introduction

Current and future wireless networks are largely uncoordinated, random and hierarchical in nature. Consequently, these networks typically lack any static network, and frequency planning and co-channel interference (CCI) constitutes a major limiting factor for system performance. Therefore, powerful techniques are needed that avoid and/or eliminate CCI while ensuring high system spectral efficiency and user fairness (especially considering the cell edge users) [1–4]. In addition, these techniques need to take into account the heterogenous QoS (quality of service) and traffic demands prevalent in such systems. Moreover, the anticipated system performance must not be achieved at an expense of excessive signalling and computational complexity as this would significantly affect the power efficiency of the system.

One of the key issues that hinders effective interference avoidance in such networks is the hidden node problem. While a transmitter may infer the interference at its target receiver via SINR (signal-to-interference-plus-noise ratio) feedback and channel knowledge, it is generally unaware of the *receiver(s)* in its vicinity that receive at exactly the same time/frequency resource (hidden nodes), and which it would force into outage by causing very high CCI. This is a problem not only for cellular and *ad hoc* networks with specific radio frequency bands, but also a fundamental problem for all cognitive radio approaches.

This work has been performed in part within the framework of the CELTIC project CP5-026 WINNER+.

On the one hand, it has been demonstrated that BB protocol [5–9] effectively solves the hidden node problem. On the other hand, multiple antenna techniques at the base station (BS) such as a switched beam approach [10] or adaptive beamforming with opportunistic scheduling [11, 12] provide a powerful basic mechanism to enhance the reusability of radio resources, but these techniques generally suffer from the hidden node problem. The BB protocol and beamforming techniques seem to perfectly complement each other enabling a high frequency reuse in the system while mitigating CCI. In this paper, a switched beam approach is chosen because of low signalling overhead accompanied. Pre-defined beams are generated at the BS and a user is served by switching on the closest beam. The antenna gain in the direction of the side lobes is significantly lower than that of the main beam.

The BB protocol ensures that beams are only selected for a particular user in the cell if this transmission does not significantly interfere with any of the ongoing transmissions in the neighbouring cells. This *interference awareness* property of the BB protocol is achieved by a time-multiplexed busy signal transmitted omnidirectionally from the receiving mobile station (MS). Clearly, the TDD (time division duplex) mode is perfectly suited for this purpose. The performance of the hybrid BB+GoB scheme is compared against a 'blind' switched beam approach as well as pure BB approach with omnidirectional antennas at the BS.

The remainder of the paper is structured as follows: multi-user resource allocation is discussed in Section II. Section III describes the spatial processing of signals used. Section IV introduces the hybrid BB+GoB scheme considered in this paper. The considered Manhattan grid deployment scenario and the system level simulator are introduced in Section V, and the simulation results are discussed in Section VI. Finally, the conclusions are drawn in Section VII.

II. Multi-User Resource Allocation

The radio resource unit in OFDMA–TDD (orthogonal frequency division multiple access – time division duplex) air interface based on WINNER (wireless world initiative new radio) TDD mode [13] is a chunk, which comprises of successive n_c subcarriers and n_t OFDM (orthogonal frequency division multiplexing) symbols in a frame as shown in Fig. 1. A frame consists of a downlink (DL) and an uplink (UL) slot, each of which contains N_C chunks. A chunk with frequency index $1 \leq n \leq N_C$ at frame k is denoted by (n, k). Provided that

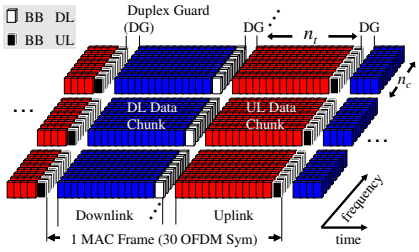

Fig. 1. Illustration of MAC frame in WINNER–TDD for BB signalling. Downlink (DL) data is transmitted during 'DL data chunk' and Uplink (UL) data during 'UL data chunk', BB corresponding to data in downlink is transmitted in 'BB UL' slot and vice versa.

channel knowledge is available at the transmitter, users can be assigned those chunks with favorable channel conditions, giving rise to multi-user diversity [14]. A variant of a score-based scheduler [15] is developed to distribute the $1{\leq}n{\leq}N_{\mathrm{C}}$ chunks among $1{\leq}\nu{\leq}U$ users served by BS q. The score at time instant k is computed as

$$s_{\nu,q}[n,k] = 1 + \sum_{\ell=1}^{N_{\mathrm{C}}} \mathbb{I}_{\{\hat{\gamma}_{\nu,q}[n,k] \leq \hat{\gamma}_{\nu,q}[\ell,k]\}} + \epsilon_{\nu,q}[n,k] + \Psi_{\nu,q}\,, \tag{1}$$

where $\hat{\gamma}_{\nu,q}[n,k]$ is the estimated SINR of user ν on chunk (n,k) using the amount of interference observed in the previous slot, $\epsilon_{\nu,q}[n,k] \in \{0,\infty\}$ defines whether or not user ν is granted access to chunk (n,k). The Boolean operator $\mathbb{I}_x \in \{0,1\}$ is set to 1 or 0 when the condition x is true or false, respectively. Furthermore, it is proposed here that the scores should be adjusted with a fairness parameter $\Psi_{\nu,q}$, which grows exponentially with every additional chunk allocated to ν so that when allocating a new chunk, priority is given to the users with fewer number of chunks already allocated.

User $\nu{=}\zeta_q[n,k]$ is assigned chunk (n,k) if either a reservation indicator was set in the previous frame $b_{\nu,q}[n,k{-}1]{=}1$, or the score (1) is minimized

$$\zeta_q[n,k] = \begin{cases} \arg\min\limits_{\nu} s_{\nu,q}[n,k]\,, & b_{\nu,q}[n,k{-}1] = 0\ \forall\,\nu \\ \nu\,, & b_{\nu,q}[n,k{-}1] = 1\,. \end{cases} \tag{2}$$

In the full frequency reuse OFDMA-TDD system with blind beam switching, considered as a benchmark, $\epsilon_{\nu,q}[n,k]{=}0$ for all users in the cell. As a result, all users compete for being scheduled in the chunk (n,k) using (2). However, for reservation based medium access control (MAC) protocols such as BB-OFDMA (see Section IV), some chunks are excluded for certain users. To this end, $\epsilon_{\nu,q}[n,k]{\rightarrow}\infty$ indicates that the user ν in cell q is denied access to chunk (n,k). We note that if $\epsilon_{\nu,q}[n,k]{\rightarrow}\infty$ for all users, cell q leaves chunk (n,k) unallocated, so that $\zeta_q[n,k]{=}\emptyset$.

III. Spatial Signal Processing

We start with a general consideration of an OFDMA–TDD network where each of the BSs and MSs is equipped with

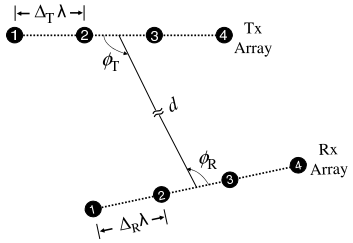

Fig. 2. Depiction of a transmitter and receiver pair equipped with multiple antennas. The LOS path is broken to show that the distances are not to scale.

N_{T} and N_{R} antennas respectively. Data transmission in the downlink is considered. The matrix $\mathbf{V} = [\mathbf{v}^{(1)}, \cdots, \mathbf{v}^{(N_{\mathrm{S}})}]$ is the spatial precoding matrix for N_{S} spatial layers available at the BS. The i^{th} column of the matrix $\mathbf{V}$, $\mathbf{v}^{(i)}$, contains the precoder of spatial layer i. The precoder is a vector $\mathbf{v}^{(i)} = [v_1, \cdots, v_{N_{\mathrm{T}}}]^T$, where v_t is the complex coefficient applied to antenna element t.

The transmitted sequence of spatial stream i is designated $x^{(i)}$. The output of spatial precoding on the i^{th} stream can be represented as

$$\mathbf{s}^{(i)} = \mathbf{v}^{(i)} x^{(i)}. \tag{3}$$

The output of spatial precoding is transmitted over a MIMO channel $\mathbf{H}_{p,\mu}$, where p and μ are BS and MS indices respectively. The MIMO channel is represented as a $N_{\mathrm{R}} \times N_{\mathrm{T}}$ matrix of the form

$$\mathbf{H}_{p,\mu} = \begin{pmatrix} h_{p,\mu}^{1,1} & \cdots & h_{p,\mu}^{1,N_{\mathrm{T}}} \\ \vdots & \ddots & \vdots \\ h_{p,\mu}^{N_{\mathrm{R}},1} & \cdots & h_{p,\mu}^{N_{\mathrm{R}},N_{\mathrm{T}}} \end{pmatrix}, \tag{4}$$

where $h_{p,\mu}^{t,r}$ represents the channel gain between transmitting antenna t of BS p and receiving antenna r of MS μ given by [16]

$$\begin{aligned} h_{p,\mu}^{t,r} \;=\; & a \exp\left(\frac{-j2\pi d}{\lambda}\right) \exp(-j2\pi(t-1)\Delta_{\mathrm{T}} \cos\phi_{\mathrm{T}}) \\ & \exp(-j2\pi(r-1)\Delta_{\mathrm{R}} \cos\phi_{\mathrm{R}}). \end{aligned} \tag{5}$$

In (5), d is the distance between the centers of the transmit and the receive antenna arrays and λ is the carrier wavelength. ϕ_{T} and ϕ_{R} are the angles of incidence of the line-of-sight (LOS) path with the planes of the transmit and receive antenna arrays respectively as depicted in Fig. 2. Δ_{T} and Δ_{R} are separation of antenna elements normalized to λ. The factor a represents the attenuation of the propagation path and incorporates distance dependent path loss, log–normal shadowing and small scale fading effects of the channel, given by the deployment scenario.

The signal of the spatial stream i received at antenna array of the MS μ is represented as

$$\mathbf{r}_{\mu}^{(i)} = \mathbf{H}_{p,\mu}\mathbf{s}_p = \mathbf{H}_{p,\mu}\mathbf{v}^{(i)} x^{(i)}. \tag{6}$$

The vector $\mathbf{r}_{\mu}^{(i)}$ is a $N_{\mathrm{R}} \times 1$ vector, where the k^{th} element of $\mathbf{r}_{\mu}^{(i)}$ represents the signal received at the k^{th} antenna of MS μ.

The received signal on the antenna array is spatially processed using vector $\mathbf{u}_{\mu}^{(i)} = [u_1, \cdots, u_{N_\mathrm{R}}]^T$, where u_k is the complex antenna weight applied to the antenna element k. The output of spatial processing at the receiver is

$$y_{\mu}^{(i)} = \left[\mathbf{u}^{(i)}\right]^T \mathbf{r}_{\mu}^{(i)} = \left[\mathbf{u}^{(i)}\right]^T \mathbf{H}_{p,\mu}\mathbf{v}^{(i)}x^{(i)}. \quad (7)$$

The scalar $y_{\mu}^{(i)}$ is the received signal at MS μ on the i^{th} spatial stream. The term $g_{p,\mu}^{(i)} = \left[\mathbf{u}^{(i)}\right]^T \mathbf{H}_{p,\mu}\mathbf{v}^{(i)}$ represents the effective channel between BS p and MS μ for spatial stream i. The term $G_{p,\mu}^{(i)} = E\left[|g_{p,\mu}^{(i)}|^2\right]$ represents the average channel gain of spatial stream i from transmitter (i.e. BS) p in the direction of the receiver (i.e. MS) μ.

In this paper, we concentrate on the system where BSs are equipped with multiple antennas and MSs are omnidirectional transceivers with $N_\mathrm{R} = 1$. The choice of omnidirectional antennas at the MSs eliminates spatial processing operations at the MS, thereby allowing less complex MS units to be used. With the above underlying assumptions, $\mathbf{H}_{p,\mu}$ from generalized MIMO description in (4) reduces to a row vector $\mathbf{h}_{p,\mu}$ of size $1 \times N_\mathrm{T}$ and $u^{(i)} = 1, \forall i$. Consequently, $\mathbf{r}_{\mu}^{(i)}$ in (6) reduces to a scalar $r_{\mu}^{(i)}$ and $y_{\mu}^{(i)} = r_{\mu}^{(i)}$ in (7). The overall channel gain between BS p and MS μ reduces to

$$\begin{aligned} G_{p,\mu}^{(i)} &= E\left[\left|\mathbf{h}_{p,\mu}\mathbf{v}^{(i)}\right|^2\right] \\ &= E\left[\left[\mathbf{v}^{(i)}\right]^H [\mathbf{h}_{p,\mu}]^H \mathbf{h}_{p,\mu}\mathbf{v}^{(i)}\right] \end{aligned} \quad (8)$$

where the operator $(\cdot)^H$ represents the Hermitian transpose of a vector. Note that by selecting a different precoding vector $\mathbf{v}^{(j)}$, where $j \neq i$, the channel gain in the direction of the observed receiver μ is adjusted. Provided that the BS is aware of the amount of CCI it potentially causes to an active receiver, it can apply appropriate precoding vector so as to attenuate the channel gains in the direction of such vulnerable receiver. To this end, in Section IV, a hybrid technique is proposed where the interference awareness property of BB signalling is exploited to enable the beam selection such that strong interference is avoided and the hidden node problem is solved.

IV. Hybrid BB+GoB Scheme

The basic principle of the combined use of fixed GoB approach and interference aware BB protocol[1] in the downlink is described with the help of Fig. 3. It is assumed that the chunk (n, k) is being used by BS_1 to serve MS_1. Since BS_2 is generally unaware of the positions of the user population in cell 1, with random beam switching, BS_2 might select to reuse the chunk (n, k) for MS_2 resulting in outage of both MS_1 and MS_2 on chunk (n, k). However, if MS_1 were to send a busy signal omnidirectionally on the same radio frequency carrier in a time-multiplexed mini slot (the BB), BS_2 would sense a strong signal in its 'beam 1', and a low signal its 'beam 2'. Therefore, with the proposed hybrid BB+GoB approach, BS_2 would reuse the same chunk to serve MS_3 using 'beam 2' resulting in no outage on chunk (n, k) both at BS_1 and BS_2.

[1]BB protocol for OFDMA–TDD system with omnidirectional antennas is covered in detail in our earlier paper [1].

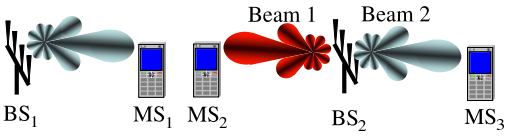

Fig. 3. Illustration of the use of hybrid BB+GoB scheme for interference aware chunk reuse.

This concept is mathematically formalized as follows: It is assumed that BS p transmits to MS μ using chunk (n, k) on spatial layer i. In this context, we shall use the terms 'spatial layer' and 'beam' interchangeably. It is considered that the user μ is served using the beam that provides maximum channel gain. The index of beam serving user μ is designated ω_μ. The received data power at MS μ on spatial layer i is given by

$$R_{\mu,p}^{\mathrm{d},(i)}[n,k] = T^{\mathrm{d}} G_{p,\mu}^{(i)}[n,k], \quad (9)$$

where T^{d} is the data transmit power. Similarly, the CCI caused at MS μ originating from BS q where $p \neq q$ is expressed as

$$I_{\mu,p}^{\mathrm{d},(i)}[n,k] = T^{\mathrm{d}} G_{q,\mu}^{(\xi_q)}[n,k], \quad (10)$$

where ξ_q is the index of the beam activated at BS q and $G_{q,\mu}^{(\xi_q)}$ represents the interfering gain between beam ξ_q of BS q towards the observed receiver μ.

The achieved SINR on chunk (n, k) on beam i, $\gamma_{\mu,p}^{(i)}[n,k]$, can be expressed as

$$\gamma_{\mu,p}^{(i)}[n,k] = \frac{R_{\mu,p}^{\mathrm{d},(i)}[n,k]}{I_{\mu,p}^{\mathrm{d},(i)}[n,k] + N}. \quad (11)$$

If $\gamma_{\mu,p}^{(i)} < \Gamma$, where Γ is the SINR target, such chunks are released by setting $\epsilon_{\mu,p}[n,k+1] \rightarrow \infty$, restricting the user μ from accessing the chunk in the next time slot. Otherwise, to ensure that the chunk $(n, k+1)$ is allocated to user μ, a reservation indicator is set as follows:

$$b_{\mu,p}[n,k] = \begin{cases} 1\,, & \gamma_{\mu,p}^{(i)}[n,k] \geq \Gamma \text{ and } \zeta_p[n,k] = \mu \\ 0\,, & \text{otherwise.} \end{cases} \quad (12)$$

The receiver μ transmits a BB on the reserved chunks where $b_{\mu,p}[n,k] = 1$ during its associated time multiplexed BB slot as shown in Fig. 1. Potential transmitters (BS in downlink mode), are obliged to sense the corresponding BB slot prior to transmission. Note that the effective channel gain between MS μ and BS q on the l^{th} beam is given by $\left[\mathbf{v}^{(l)}\right]^T \mathbf{h}_{q,\mu}^T = \left[\mathbf{h}_{q,\mu}\mathbf{v}^{(l)}\right]^T$. Thus, $G_{q,\mu}^{(l)}[n,k] = G_{\mu,q}^{(l)}[n,k]$. With this notation, the received BB power on beam l can be expressed as

$$I_{q}^{\mathrm{b},(l)}[n,k] = T^{\mathrm{b}} G_{q,\mu}^{(l)}[n,k], \quad (13)$$

where T^{b} represents the power of BB signal emitted. To keep $I_{\mu,p}^{\mathrm{d}}[n,k] \leq I_{\mathrm{th}}$, where I_{th} is the maximum CCI that a newly admitted link may cause to the pre-established link, the BS q may reuse chunk (n, k) on spatial layer l if

$$\left(\frac{T^{\mathrm{d}}}{T^{\mathrm{b}}}\right) I_{q}^{\mathrm{b},(l)}[n,k] \leq I_{\mathrm{th}}, \quad (14)$$

If $T^{\mathrm{b}} = T^{\mathrm{d}}$, (14) reduces to

$$I_q^{\mathrm{b},(l)}[n,k] \leq I_{\mathrm{th}}, \tag{15}$$

The CCI caused to active receiver is remains lower than the threshold if the chunk $(n, k+1)$ is reused on at most one of the beams that satisfy (15). The beam selected for chunk $(n, k+1)$ depends on the outcome of the scheduler discussed in Section II. To ensure that the chunk is allocated to one of the beams satisfying (15), the access control indicator is set as follows

$$\epsilon_{\nu,q}[n,k+1] \rightarrow \begin{cases} 0\,, & I_q^{\mathrm{b},(\omega_\nu)}[n,k] \leq I_{\mathrm{th}} \\ \infty\,, & \text{otherwise,} \end{cases} \tag{16}$$

where ω_ν refers to the the beam providing maximum channel gain to the user ν. The user that is scheduled on chunk $(n, k+1)$ is $\zeta_q[n, k+1]$, obtained using (2). The beam that is activated at BS q is given by

$$\xi_q[n,k] = \omega_{\zeta_q[n,k+1]}. \tag{17}$$

The BS q transmits to MS ν on chunk $(n, k+1)$ by activating the beam ξ_q during the $(k+1)^{\mathrm{th}}$ frame. The scheduled beam is activated by applying the precoding vector $\mathbf{v}^{(\xi_q)}$, to antenna array at the BS q.

In the following section, the performance of novel BB-based beam selection described above (referred to as 'BB+GoB') is compared to BB signaling assuming omnidirectional antennas. In addition, we consider a BB disabled beam selection algorithm that allocates chunk to users purely based on (2) with $b_{\nu,q}[n,k-1]$ and $\epsilon_{\nu,q}[n,k]$ both set to zero. This is simply referred to as 'GoB' technique in the following sections.

V. Manhattan Grid Deployment

An urban microcell deployment defined in scenario B1 in WINNER with a rectangular grid of streets (Manhattan grid) is considered where 72 BSs are distributed in streets as shown in Fig. 4. The performance statistics are collected only over the central core of 3×3 building blocks, so as to reduce the edge effects. The antennas are mounted below the rooftop and an effective antenna is a linear half wavelength array of 4-elements. The half power beamwidth of the array 32.3° in the broadside and the front-to-back ratio of antenna gain is 20 dB.

Outdoor MSs uniformly distributed in the streets and moving with a constant velocity of 5 km/h are considered. Two beams per BS, with the main lobes pointing towards the street direction with an angle of 180° between them are considered. Indoor MSs are not considered for the study because of high penetration losses due to the walls at high frequency as a result of which they are better suited to be served by femto-cell deployments, which is beyond the scope of this paper. Therefore, the beams pointing towards the buildings are ignored. On average U=10 MSs are served by one cell. The MSs are connected to the BS on the same street on the basis of least distance because of the favourable path loss in line-of-sight (LOS) condition in the street canyons.

B1-LOS and B1-NLOS models [17] are used to model the LOS and non-LOS (NLOS) channels respectively. A full buffer traffic model [18] and a network synchronised in time and frequency is assumed. No upper limit is placed on the number of available chunks that may be assigned to one user. The simulation parameters are summarised in Table I.

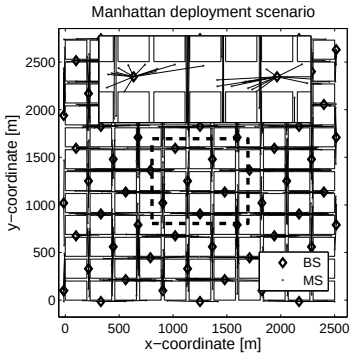

Fig. 4. Urban microcell deployment in a Manhattan grid.

TABLE I
Simulation Parameters

Parameters	**Value**
Total symbol length	22.48 μs
Carrier centre frequency	3.95 GHz
System bandwidth B	89.84 MHz
Number of subcarriers (SC)	1840
Frame duration	0.6912 ms
OFDM symbols/frame	30
Chunk size	15 (time) × 8 (frequency) = 120
Number of chunks/frame	2 (time) × 230 (frequency)
Access probability	0.3
Bits/symbol m	4 and 8
SINR target Γ	11.3 dB and 22.5 dB
Number of sectors/cell	2
Number of antenna elements/sector	4
Average number of users/cell U	10
Transmit power per chunk T^{d}	16.4 dBm
Elevation antenna gain A_{e}	14 dBi
Azimuth antenna element gain	$-\min\left[12\left(\frac{\theta}{\theta_{3\mathrm{dB}}}\right)^2, A_{\mathrm{m}}\right]$ [dB] where, $A_{\mathrm{m}} = 20$ and $\theta_{3\mathrm{dB}} = 70^\circ$
Noise level N	-117.8 dBm/chunk
Number of snapshots	50
Simulation duration per snapshot	50 ms

VI. Results and Discussions

The impact of the interference threshold, I_{th}, on mean user throughput as a function of distance from the intended BS is examined in Fig. 5(a-b) for the downlink. In Fig. 5(a), the SINR target is $\Gamma = 11.3$ dB which corresponds to 16-QAM (quadrature amplitude modulation) with rate 3/4 convolutional FEC (forward error correction) coding and a packet error ratio of 10^{-2} [19]. This plot demonstrates the interference awareness capabilities of the BB protocol. For example, for the lowest interference threshold of $I_{\mathrm{th}} = -100$ dBm, the system is most 'cautious'. A user would only be served, if no other MS in the network would suffer. As a consequence, the network exhibits a high level of fairness which is clearly illustrated

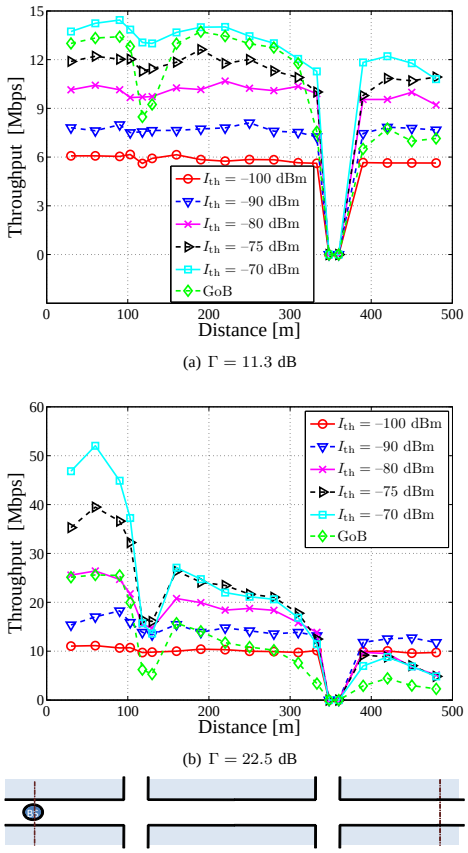

(a) $\Gamma = 11.3$ dB

(b) $\Gamma = 22.5$ dB

Fig. 5. Comparison of performance of the proposed hybrid BB+GoB scheme for different thresholds against the state-of-the-art GoB switching. Comparisons are made using 16-QAM with $\Gamma = 11.3$ dB and 64-QAM with $\Gamma = 22.5$ dB. At 115 m and 330 m are the street crossings of the Manhattan structure, due to which drop in throughput is observed.

in Fig. 5(a) where the user throughput for $I_{\rm th} = -100$ dBm is almost constant regardless of the location within the cell. Note, that a uniform user distribution is assumed. As the interference threshold is increased, the system is "desensitized" which generally results in a higher throughput close to the BS and a reduction in throughput closer to the cell edge. However, for all thresholds the throughput is improved at all locations relative to the case when $I_{\rm th} = -100$ dBm since the spatial reuse of resources is increased. The new BB+GoB techniques outperforms GoB at any location for a threshold of $I_{\rm th} = -70$ dBm. There are two more important observations: (a) for an interference threshold of $I_{\rm th} = -70$ dBm the BB+GoB approach achieves only slightly better throughput up to a distance of 300m, but the per user throughput at the cell edge (between around 330m and 480m) is improved by a factor of 2 or equivalently by 100%. The interference awareness property of the new BB+GoB approach clearly unfolds here, and (b) the robustness to interference is also demonstrated at the first street crossing at around 115 m where the state-of-the-art GoB faces a throughput drop of about 35% whereas the BB+GoB technique only experiences a drop of about 9%.

In Fig. 5(b), $\Gamma = 22.5$ dB corresponds to 256-QAM with rate 3/4 convolutional FEC coding and a packet error ratio of 10^{-2} [19]. It is recognized that the particular example is at the upper end of practical modulation orders for such systems, but it is chosen because it highlights a few more important properties of the new technique and it assists in the validation of the new approach since some of the expected behavior can indeed be observed. For instance, the spatial dependency of the throughput is increased – as expected. However, even for this modulation order and an interference threshold of $I_{\rm th} = -100$ dBm, a fair and constant throughput independent of location of about 10 Mbps can be seen. This is about 67% higher than than achieved with 16-QAM, i.e., the doubling of the spectrum utilization, from 4 bits/symbol to 8 bits/symbol, results in 67% improved throughput for $I_{\rm th} = -100$ dBm. User throughput achieved at the close vicinity of the serving BS is 50 Mbps/user and that at the cell-edge is 4.85 Mbps/user using $I_{\rm th} = -70$ dBm. This is in sharp contrast to GoB which only achieves approximately 26 Mbps/user close to the BS (only about 50% of what BB+GoB achieves), and about 2.3 Mbps/user at the cell edge (approx. 47% of BB+GoB).

Fig. 6(a–b) compare performance of BB+GoB against BB with omnidirectional antennas and pure GoB. An SINR target of $\Gamma = 22.5$ dB and 8 bits per symbol are assumed. Using omnidirectional antennas, a maximum median system throughput of 238 Mbps/cell (see Fig. 6(a)) is achieved in DL using $I_{\rm th} = -75$ dBm. However, fairness is compromised as more than 50% of all users in the system are in outage. The users having zero throughput are said to be in outage. By adjusting the threshold to -105 dBm, 5.16 Mbps for the 10 %-ile of user throughput is feasible (see Fig. 6(b)) at the cost of 59% reduction in median system throughput compared to using a threshold of -75 dBm. For comparison, the benchmark system (GoB) achieves a median system throughput of 129.0 Mbps/cell and a lower 10 %-ile of user throughput of 561.5 kbps. Using an interference threshold of $I_{\rm th} = -105$ dBm, BB with omnidirectional antennas provides an 9-fold increase in the lower 10%-ile of user throughput at the cost of 25% reduction in system throughput compared to the GoB.

Using BB+GoB, a median system throughput of 238.5 Mbps/cell is achieved using a threshold of -75 dBm (see Fig. 6(a)) and the corresponding 10 %-ile of user throughput is 4.36 Mbps (see Fig. 6(b)). This represents a 85% increase in median system throughput together with a 7.8-fold increase in the lower 10%-ile of user throughput compared to GoB. By adjusting $I_{\rm th}$ to -90 dBm, the 10 %-ile of user throughput improves to 8.88 Mbps. This is approximately a *16-fold* increase compared to GoB while at the same time the median system throughput is 20% higher

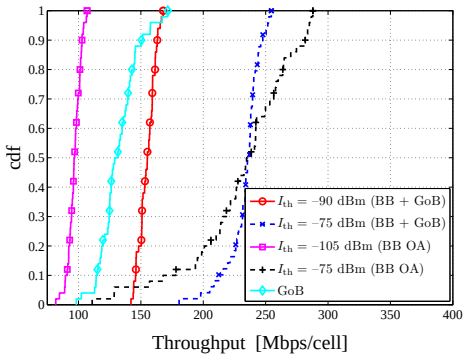

(a) CDF of system throughput

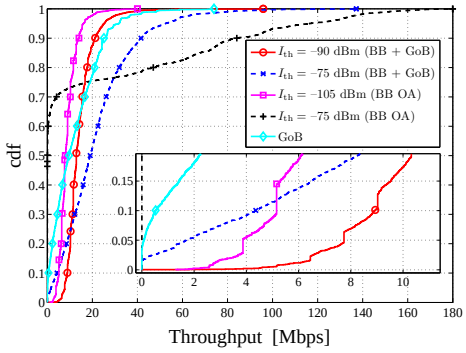

(b) CDF of throughput per user

Fig. 6. Comparison of performance of hybrid BB+GoB technology against BB with omnidirectional antennas ('BB OA') and GoB in the downlink mode.

than that achieved with GoB.

VII. Conclusions

A new hybrid interference avoidance technique has been proposed which combines two existing powerful techniques - GoB switching and interference aware concept using BB signalling. A comparison against CCI mitigation approaches: first, solely based on GoB switching, and second, solely based on BB signalling with omnidirectional antennas has been performed in a Manhattan environment. It has been shown that the BB interference threshold can be used to balance throughput and fairness in a cellular system. In particular, it was shown that by selecting a low interference threshold, which makes the system more cautious to CCI, a constant user throughput independent of distance from the BS can be accomplished. This comes at the expense of a reduced user throughput compared to GoB switching technique alone. However, by increasing the interference threshold, the average per user throughput at any location in the cell can clearly be improved compared to pure beam switching. In particular, the mean cell edge user throughput is increased by a factor of two. Moreover, it has been demonstrated that the throughput at the 10^{th} percentile, which is a measure for the minimum guaranteed throughput, can be improved by up to a factor of 16 for high SINR targets.

References

[1] B. Ghimire, G. Auer, and H. Haas, "Busy Bursts for Trading-off Throughput and Fairness in Cellular OFDMA-TDD," *EURASIP Journal on Wireless Communications and Networking*, vol. Volume 2009, Article ID 462396, 14 pages, 2009.

[2] S.-E. Elayoubi, O. B. Haddada, and B. Fourestie, "Performance Evaluation of Frequency Planning Schemes in OFDMA-Based Networks," *IEEE Transactions on Wireless Communications*, vol. 7, pp. 1623–1633, May 2008.

[3] M. C. Necker, "Local Interference Coordination in Cellular OFDMA Networks," in *Proc. of the Vehicular Technology Conference (VTC)*, Sep./Oct. 2007, pp. 1741–1746.

[4] S. M. Heikkinen, H. Haas, and G. J. R. Povey, "Adjacent Channel Interference on the UTRA-TDD Air Interface," in *Colloquium on UMTS Terminals and Software Radio*. Glasgow, Scotland: IEE, 26 Apr. 1999, pp. 13/1 – 13/5.

[5] Z. J. Haas and J. Deng, "Dual Busy Tone Multiple Access (DBTMA)-A Multiple Access Control Scheme for ad hoc Networks," *IEEE Transactions on Communications*, vol. 50, no. 6, pp. 975–985, Jun. 2002.

[6] R. Zhao, B. Walke, and M. Einhaus, "Constructing Efficient Multi-hop Mesh Networks," in *Proc. of the Conference on Local Computer Networks (LCN)*. Sydney, Australia: IEEE, Nov. 15–17, 2005, pp. 166–173.

[7] P. E. Omiyi and H. Haas, "Improving Time-Slot Allocation in 4th Generation OFDM/TDMA TDD Radio Access Networks with Innovative Channel-Sensing," in *Proc. of the International Conference on Communications (ICC)*, vol. 6. Paris, France: IEEE, Jun. 20–24 2004, pp. 3133–3137.

[8] P. Omiyi, H. Haas, and G. Auer, "Analysis of TDD Cellular Interference Mitigation Using Busy-Bursts," *IEEE Transactions on Wireless Communications*, vol. 6, no. 7, pp. 2721–2731, Jul. 2007.

[9] H. Haas, V. D. Nguyen, P. Omiyi, N. Nedev, and G. Auer, "Interference Aware Medium Access in Cellular OFDMA/TDD Networks," in *Proc. of the International Conference on Communications (ICC)*, vol. 4. Istanbul, Turkey: IEEE, Jun.11–15, 2006, pp. 1778–1783.

[10] R. Grünheid, H. Rohling, K. Brüninghaus, and U. Schwark, "Self-organised beamforming and opportunistic scheduling in an OFDM-based cellular network," in *Proc of Vehicular Technology Conference (VTC)*, vol. 2, May 2006, pp. 813–817.

[11] P. Viswanath, D. Tse, and R. Laroia, "Opportunistic Beamforming Using Dumb Antennas," in *Proc. of the International Symposium on Information Theory*. Lausanne , Switzerland: IEEE, 30 Jun.–5 Jul. 2002, p. 449.

[12] H. Dahrouj and W. Yu, "Coordinated Beamforming for the Multi-Cell Multi-Antenna Wireless System," in *Proc. of the Conference on Information Sciences and Systems CISS*, Mar. 2008, pp. 429–434.

[13] IST-4-027756 WINNER II, "D6.13.14 WINNER II System Concept Description," Retrieved Jun. 25, 2008, from https://www.ist-winner.org/deliverables.html, Dec. 2007.

[14] M. Sternad, T. Svensson, T. Ottosson, A. Ahlen, A. Svensson, and A. Brunstrom, "Towards Systems Beyond 3G Based on Adaptive OFDMA Transmission," *Proceedings of the IEEE*, vol. 95, no. 12, pp. 2432–2455, Dec. 2007.

[15] T. Bonald, "A Score-Based Opportunistic Scheduler for Fading Radio Channels," in *Proc. of the European Wireless Conference (EWC)*, Barcelona, Spain, Feb. 24–27, 2004.

[16] D. Tse and P. Viswanath, *Fundamentals of Wireless Communication*. Cambridge University Press, 2005.

[17] IST-4-027756 WINNER II, "D1.1.2 v1.2 WINNER II Channel Models," Retrieved Feb. 5, 2008, from https://www.ist-winner.org/WINNER2-Deliverables/.

[18] IST-4-027756 WINNER II, "D6.13.7, WINNER II Test Scenarios and Calibration Cases Issue 2," Retrieved Mar. 15, 2007, from https://www.ist-winner.org/WINNER2-Deliverables/.

[19] A. Persson, T. Ottosson, and G. Auer, "Inter-Sector Scheduling in Multi-User OFDM," in *IEEE International Conference on Communications (ICC)*, vol. 10, Istanbul, Jun. 2006, pp. 4415–4419.

Contention Free Dynamic Slot Allocation in Cellular Networks

Gunther Auer*, Stefan Videv†, Birendra Ghimire† and Harald Haas†
*DOCOMO Euro-Labs, 80687 Munich, Germany, Email: auer@docomolab-euro.com
†Institute for Digital Communications, The University of Edinburgh, Edinburgh EH9 3JL, UK, Email: h.haas@ed.ac.uk

***Abstract*—A distributed reservation protocol tailored for cellular wireless networks is presented that facilitates contention free inter-cellular slot allocation and reservation. While reserved slots are protected from inter-cell interference by a busy burst enabled reservation protocol, collisions due to simultaneously accessed unreserved slots by neighboring cells are mitigated by means of resource partitioning patterns. Cyclically shifting these partitioning patterns in time allows each cell to successively probe all slots within a fixed time interval. This establishes an inter-cellular slot contention policy that dynamically controls the initial spatial reuse, in terms of concurrently accessed radio resources by neighboring cells. Despite the controlled spatial reuse of resource during contention, the possibility of a cell to use all available radio resources, if the load and interference situation permits, remains unaffected. As a consequence, loss in spectrum efficiency as observed in frequency-planned cellular systems is avoided.**

***Index Terms*—Inter-cell interference coordination, resource partitioning, reservation ALOHA, PRMA, busy signal concept**

I. Introduction

When several users in a random access channel simultaneously attempt to access a given time-frequency slot, collisions due to co-channel interference (CCI) are encountered. Reservation protocols, such as reservation ALOHA (R-ALOHA) [1] and packet reservation multiple access (PRMA) [2], divide the available resources to idle and reserved slots. For R-ALOHA idle slots are allocated in contention and reserved slots are protected from CCI as follows [1]:

- **Contention**: Before transmission the channel is scanned. If the slot is sensed idle a packet is transmitted to contend with other users for an unreserved slot. Concurrently accessed contention slots by several users give rise to collisions. In case of collision the packet is retransmitted with probability p in subsequent idle slots, until the receiver acknowledges successful reception.
- **Reservation**: Upon successful reception the receiver broadcasts an acknowledgment. This acknowledgment reserves the slot, in the way that all other users refrain from using that slot in future transmissions.

R-ALOHA therefore limits the occurrence of collisions to the contention phase.

In wireless networks, slot reservation translates to an exclusion region around an active receiver. A competing communication link is denied access to a reserved slot if its transmitter is located within the exclusion region; otherwise the slot may be concurrently accessed by both links. An efficient realization of R-ALOHA in decentralized wireless networks is provided by the busy signal concept, where the receiver acknowledges successful reception by means of a time-multiplexed busy burst [3, 4]. The range where a strong busy burst is received notifies a potential transmitter that it is within the exclusion region of an active receiver. Sensing the busy burst prior to transmission accomplishes two objectives: first, reserved slots are protected from excessive CCI; and second, the spatial reuse, in terms of concurrently accessed slots by adjacent cells, is controlled. In [5] the busy signal concept is applied to orthogonal frequency division multiple access (OFDMA), enabling dynamic assignment of time-frequency slots to multiple users.

Unlike *ad hoc* networks, resource allocation in cellular networks is typically carried out in a centralized manner, in the way that the base station (BS) is in full control of assigning slots among multiple users. By doing so interference within a cell can be completely avoided. Interference coordination between neighboring cells is commonly achieved by resource partitioning, where adjacent cells are assigned different frequency bands. Fractional frequency reuse (FFR) is a static resource partitioning schemes that divides the cell coverage area into concentric zones with different frequency reuse factors [6]. FFR typically involves a sub-band with full frequency reuse that is exempt from any slot assignment restrictions, which is preferably allocated to users in close proximity to their desired BS. The allocation of the remaining sub-bands is coordinated among neighbouring cells, in a way that users in the given cell are denied access to sub-bands assigned to cell-edge users in adjacent cells [7–9].

While classical frequency reuse planning protects cell-edge users from excessive CCI from adjacent cells, the observed signal levels of the interfering signal are completely ignored. Furthermore, this static scheme is unable to adapt to changes in the traffic load and/or the distribution of users within cells. Consequently, it suffers from a significant loss in spectral efficiency.

This paper targets the application of a distributed slot reservation protocol, such as R-ALOHA, to cellular full frequency reuse wireless networks. While reserved slots are well protected from CCI, collisions in contention are encountered, caused by simultaneously accessed idle slots from neighboring cells. The proposed cellular slot allocation and reservation (CESAR) protocol completely avoids the contention phase, by virtue of specifically designed resource partitioning pat-

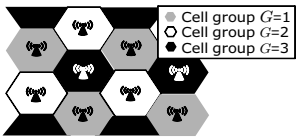

Fig. 1. Cellular system composed of hexagonal cells with frequency reuse 3. Cells that belong to the same cell group G spatially reuse resources, while cells associated to different groups are assigned mutually orthogonal resources.

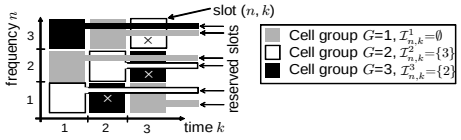

Fig. 2. CESAR working principle: slots are successively accessed by virtue of cyclically shifted resource partitioning patterns, provided the interference induced to already reserved slots in adjacent cells is sufficiently low. In the considered example the transmitter in cell 1 is well separated from receivers in cells 2 and 3, so that $\mathcal{I}^1_{n,k}=\emptyset$. Hence, cell 1 may spatially reuse all slots. On the other hand, cells 2 and 3 mutually interfere, $\mathcal{I}^2_{n,k}=\{3\}$ and $\mathcal{I}^3_{n,k}=\{2\}$, which means that resources reserved by cells 2 may not be accessed by cell 3 (marked by $\times$), and vice versa.

terns. CESAR imposes no restrictions on the amount of resources one cell may allocate, and therefore overcomes the limitations of classical inter-cell resource partitioning based on static frequency reuse planning [6–9]. We demonstrate through simulations that CESAR and a busy burst enabled reservation protocol [4] perfectly complement each other; the former mitigates collisions due to simultaneous access of idle slots, while the latter dynamically controls the spatial reuse of reserved slots.

II. Dynamic Inter-Cell Slot Allocation

A slotted multiple access scheme is considered where frames are divided into N_s slots, e.g. by means of OFDMA. The base station (BS) schedules one user per slot, so that interference within the cell is completely avoided, while a R-ALOHA based reservation protocol controls the slot allocation among neighboring cells. While reserved slots are well protected from CCI, simultaneous access of idle slots by adjacent cells cause an unpredictable drop in the received signal to interference plus noise ratio (SINR) of slot n at frame k, denoted by $\gamma_{n,k}$. In case $\gamma_{n,k}$ fails to achieve a certain target Γ, so that $\gamma_{n,k}<\Gamma$, slot (n,k) encounters a collision.

The contribution of this work is to combine a R-ALOHA based slot reservation protocol with inter-cell interference coordination by resource partitioning, so to facilitate contention free dynamic slot allocation and reservation in cellular networks. The key to avoid collisions in the contention phase is to prevent concurrent access of unreserved slots in neighboring cells. This is accomplished by the proposed CESAR protocol: resource partitioning is the enabler for contention free access of *unreserved slots*, while R-ALOHA ensures uncontested use of *reserved slots*. CESAR grants access to unreserved slots based on two conditions: (i) the slot is sensed idle, i.e. the interference caused to previously reserved slots in neighboring cells is sufficiently low, and (ii) a pre-defined resource partitioning pattern with frequency reuse factor R issues an access right to a given cell.

For resource partitioning with frequency reuse factor R, cells are organized into R pre-defined cell groups, such that adjacent cells are in different cell groups G, $1\leq G\leq R$, as illustrated in Fig. 1. Destructive interference from near-by cells is mitigated by assigning mutually orthogonal slots to different cell groups, while cells that belong to the same cell group G spatially reuse resources. Associated to cell group G is one out of R resource partitioning patterns, which are constructed according to the following rules:

1) all R patterns are mutually orthogonal,
2) all patterns point to each slot once every R frames.

The 1st rule avoids collisions due to simultaneously accessed slots, provided that cells within the same group G experience low interference. The 2nd rule ensures that all N_s slots may be assigned to all R cell groups within R frames. These rules are satisfied by the cyclically shifted pattern

$$g_{n,k} = (n+k) \mod R\,, \quad 1\leq n\leq N_\mathrm{s} \tag{1}$$

which associates slot n of frame k to cell group $G{=}g_{n,k}$. Unlike conventional resource partitioning in cellular networks based on static frequency planning, (1) exclusively controls the contention free allocation of idle slots — reserved slots are governed by a distributed slot reservation protocol, such as R-ALOHA.

The CESAR policy accomplishes two objectives: cell c retains all previously reserved slots, identified by the reservation indicator $\varrho^c_{n,k}{=}1$; in addition, cell c is granted contention free access to idle slots that satisfy (1). Cell c may access slot (n,k) if the following condition is met

$$\Big(g_{n,k}=G \quad \text{and} \bigcup_{i\in\mathcal{I}^c_{n,k}} \varrho^i_{n,k}=0\Big) \quad \text{or} \quad \varrho^c_{n,k}=1 \tag{2}$$

where $\mathcal{I}^c_{n,k}$ comprises the set of active out-of-cell receivers at slot (n,k), which are vulnerable to the interference caused by entities in cell c. In (2) an unreserved slot (n,k) of cell c is sensed idle, if the transmitter in cell c is outside the exclusion range of any active out-of-cell receiver, such that $i\notin I^c_{n,k}$ $\forall\,\varrho^i_{n,k}{=}1$. Otherwise slot (n,k) is sensed busy, in which case $\varrho^i_{n,k}{=}1$ for at least one vulnerable out-of-cell receiver $i\in\mathcal{I}^c_{n,k}$. Then cell c is denied access for slot (n,k) in (2), regardless the outcome of (1).

The working principle of CESAR is illustrated in Fig. 2. Initially at frame $k{=}1$ all slots are idle, $\varrho^i_{n,1}{=}0$, $\forall\,n,i$, so that (2) allows each cell to initially allocate N_s/R slots. Provided the achieved SINR exceeds the target $\gamma_{n,k}\geq\Gamma$, cell i reserves slot n for the next frame $k{+}1$ by setting $\varrho^i_{n,k+1}{=}1$. In subsequent frames the cyclic shift of the partitioning pattern (1) allows adjacent cells to successively probe slot n. To this end, slot n previously reserved by cell i, may be accessed by cell c, if the interference induced to entities in cell i is sufficiently

low, such that $i \notin \mathcal{I}^c_{n,k}$ in (2), giving rise to spatially reused slots that are concurrently reserved by adjacent cells. After $k \geq R$ frames all slots are either reserved or busy so that CESAR converges to a steady state. The achieved spatial reuse in the steady state is determined by the distribution of out-of-cell receivers $\mathcal{I}^c_{n,k}$, and *not* by the reuse partitioning factor R.

Slots that satisfy (2) constitute the set of scheduled slots $\mathcal{S}$. The distribution of $\mathcal{S}$ among multiple users is carried out by a proportional fair type scheduling algorithm at the BS, as described in the companion paper [5]. Mobile users are distributed in the cell and may therefore experience different interference conditions $\mathcal{I}^c_{n,k}$. Hence, the spatial reuse per slot varies over n, dependent on the scheduled users for slot (n,k).

A. Combination with the busy signal concept

A natural complement of CESAR is the combination with the busy signal concept [4]. Receiver feedback in the form of a time-multiplexed busy burst establishes an exclusion region around active receivers, which effectively implements the reservation indicator $\varrho^i_{n,k}$ in (2). An exclusion region defines an area around an active receiver in cell c, where potential transmitters in adjacent cells $i \neq c$ must not transmit, so that excessive CCI by close-by interferers is eliminated. In the context of a time-frequency slotted air interface, the exclusion regions are to be established individually for each slot (n,k) [5]. Associated to each data slot (n,k) is a time-multiplexed busy-slot dedicated for receiver feedback, as illustrated in Fig. 3. Upon successful reception of a slot and provided that more data is scheduled for transmission, the receiver emits a busy burst at a time-multiplexed mini-slot. This reserves chunk n for the next frame $k+1$. In summary, the busy signal concept is described by the following protocol:

1) All potential transmitters must sense the BB associated to the data chunk (n,k) prior to transmission.
2) Transmitters are prohibited to access chunks where a BB is detected above a given threshold.

The resulting signalling overhead for receiver feedback typicaly amounts to 5 to 10 %. However, instead of dismissing BB signalling as overhead, the BB mini-slots may be utilized to convey the feedback and control information. Hence, BB signalling may serve as an alternative control channel.

Provided channel reciprocity holds, the interference that a transmitter in cell c imposes on a particular receiver in an adjacent cell i is equivalent to the busy signal emitted from the receiver in cell cell i, and measured by the transmitter in cell c. Hence, a slot is identified as idle, if its received busy signal is below a certain threshold: $I^b_{n,k} \leq I_{\mathrm{th}}$ [4]. The set of vulnerable receivers $\mathcal{I}^c_{n,k}$ in the vicinity of cell c coincides with the area where a strong busy signal is received, $I^b_{n,k} > I_{\mathrm{th}}$. In effect, the busy burst serves as the reservation indicator $\varrho^i_{n,k}$ for cells $i \in I^c_{n,k}$, so that (2) is transformed to

$$\Big(g_{n,k} = G \text{ and } I^b_{n,k} \leq I_{\mathrm{th}}\Big) \quad \text{or} \quad \varrho^c_{n,k} = 1 \qquad (3)$$

The choice of the interference threshold I_{th} is important: as I_{th} increases, interference protection of reserved slots is sacrificed for enhanced spatial reuse [5].

B. Application to ad hoc networks

Although CESAR is most suited for cellular systems, application to *ad hoc* networks without network planning is also possible. Due to the lack of network planning the frequency reuse factor R needs to be somewhat larger than for cellular systems. In theory it is possible to group a map within any 2D area with only 4 colours so that no border exhibits the same colour, known as the four colour theorem [10]. On the other hand, to find appropriate colouring in a decentralized manner may be very complicated, so that in practice $R > 4$ may become necessary.

The problem of finding the appropriate group for a certain node also needs to be addressed. A node measures its local environment for a given time prior to transmission and selects a group that none of the nodes in its close vicinity are using. If no free groups can be found, either the group associated to the weakest received signal power may be selected, or alternatively the group with the least transmission activity. This ensures that the residual interference is kept to a minimum.

III. Performance Evaluation

An OFDMA air interface with $N_{\mathrm{s}} = 230$ frequency slots per frame is considered. A full buffer traffic model is assumed, where each user is trying to continuously send data. Perfect synchronization in time and frequency is assumed. The system parameters are summarized in Table I.

The micro-cellular deployment environment is simulated modeled by a Manhattan grid, consisting of 11×12 building blocks each of dimensions $200\,\mathrm{m} \times 200\,\mathrm{m}$, interlaced by a rectangular grid of $30\,\mathrm{m}$ wide streets. In order to reduce edge effects, the performance metrics are collected only over the central core of 3×3 building blocks. On average $U = 10$

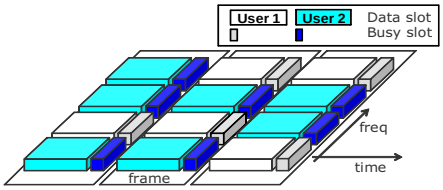

Fig. 3. Frame structure for busy-signal enabled interference management.

TABLE I
Simulation Parameters

Carrier centre frequency	4 GHz
System bandwidth B	89.84 MHz
Frame length	337.2 μs
Number of frequency slots/frame N_{s}	230
Bits/symbol	2
SINR target Γ	10 dB
Average number of users/cell U	10
User velocity	5 km/h
Transmit power per slot P	16.4 dBm
Busy signal threshold I_{th}	-90 dBm
Noise level	-117.8 dBm/slot

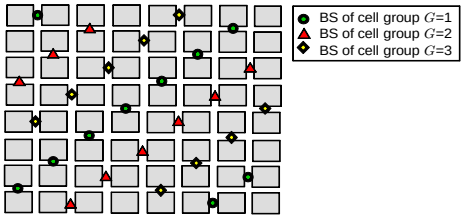

Fig. 4. Manhattan grid deployment: building blocks (gray) are interlaced by a rectangular grid of streets. Base station (BS) are organized to R=3 cell groups according to [11], in the way that direct line of sight interference between adjacent cells of the same group G is avoided.

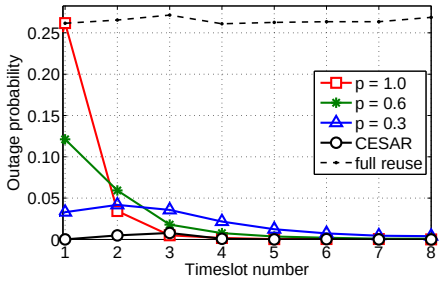

Fig. 5. Probability of outage over time k for slots that fail to achieve their SINR target $\gamma_{n,k}<10$ dB.

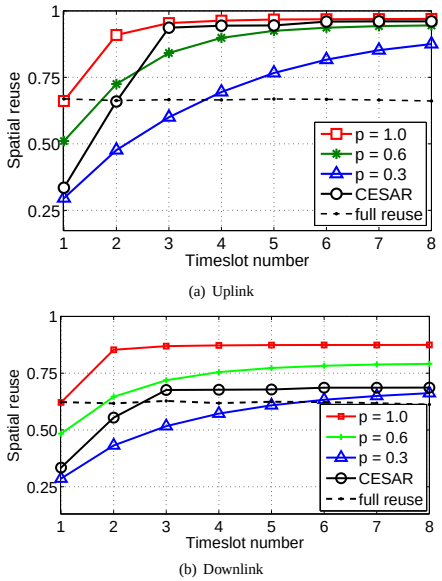

(a) Uplink

(b) Downlink

Fig. 6. Spatial reuse given by the normalized rate of successfully received slots with $\gamma_{n,k}\geq 10$ dB over time k.

outdoor users are served by one BS, uniformly distributed in the streets and moving with a constant velocity of 5 km/h. The statistics are collected over 100 independent snapshots, each with a different user distribution. Users are connected to the BS with the least path loss. BSs are mounted below rooftop and are deployed as depicted in Fig. 4. Distance dependent path loss, log-normal shadowing and frequency selective fading are taken into account, with parameters taken from [12], channel model B1. Links where transmitter and receiver are located on the same street are modeled as line of sight (LoS) channels. Otherwise links are modeled as non line of sight (NLoS) channels, with significantly higher pathloss attenuation than LoS links [12]. Hence, interference between cells that belong to the same cell group G is minimized by avoiding a direct LoS connection. This is accomplished by organizing BSs into R=3 cell groups according to [11], as shown in Fig. 4.

CESAR is compared with a p-persistent variant of the busy signal concept [5], referred to as p-persistent slot allocation and reservation (p-PSAR). While CESAR controls access of idle slots by the resource partitioning pattern (1), p-PSAR transmits on idle slots with access probability $p \in (0, 1]$. All other assumptions for CESAR and p-PSAR are identical, so to allow for a fair comparison.

The outage over time, given by the probability that slots fail to achieve their SINR target $\gamma_{n,k}<10$ dB, is plotted in Fig. 5. Initially at k=1 all N_s slots are idle, and cells attempt to access slots dependent on the chosen slot allocation policy. While CESAR exhibits diminishing outage, p-PSAR initially suffers from a significant collision probability, especially when p is high, due to the random allocation of idle slots. The residual outage for CESAR is due to interference from distant cells that belong to the same cell group G.

The spatial reuse, in terms of normalized rate of successfully received slots whose achieved SINR exceeds the target $\gamma_{n,k}\geq 10$ dB, is plotted in Fig. 6. A spatial reuse of 1 means that all cells can concurrently transmit on all N_s=230 available slots; whereas a spatial reuse of $\frac{1}{R}=\frac{1}{3}$ resembles static frequency reuse of 3, where one cell transmits on $\frac{N_s}{3}$=76 slots. CESAR reaches the steady state after only R=3 frames at diminishing outage. While lowering p significantly reduces outage for p-PSAR (see Fig. 5), the time to convergence to the steady state increases. For comparison a system with full frequency reuse, where cells access all N_s=230 available slots without attempting to avoid interference, is also included in Fig. 5 and 6. CESAR is seen to outperform the system with full frequency reuse both in terms of outage (see Fig. 5) and spatial reuse (see Fig. 6). In the uplink (Fig. 6(a)) both CESAR and p–PSAR approach a spatial reuse of 95% in the steady state, whereas in the downlink (Fig. 6(a)) the steady state spatial reuse of CESAR is considerably lower than p–PSAR with high access probability $p\geq 0.6$. The high spatial reuse is attributed

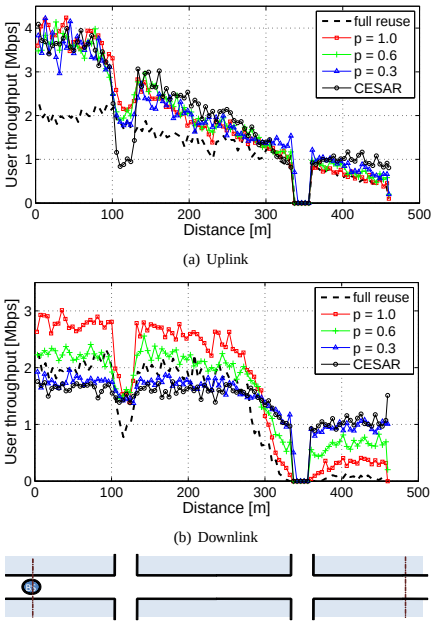

(a) Uplink

(b) Downlink

Fig. 7. Mean user throughput vs. distance from the serving BS, d, for CESAR and p–PSAR with various access probabilities p. At d=115 m, links are exposed to strong LoS interference from cells in perpendicular streets, which causes collisions in the downlink, while at d=345 m, the MSs are connected to BSs in a perpendicular street due to better channel gains.

to the Manhattan grid deployment, which exhibits more than one strong LoS interferer only at street crossings.

Fig. 7 further elaborates the different trend in uplink and downlink user throughput. The mean uplink and downlink user throughput vs. distance from its serving BS, d, is presented in Fig. 7(a) and Fig. 7(b). Interestingly, in the uplink the throughput-distance characteristic for CESAR and p–PSAR is similar, while the superior downlink user throughput of p–PSAR for high p is achieved at the expense of compromising throughput for users close to the cell boundary. The reason for this effect is twofold [5]: first, in the downlink cell-edge users are prone to interference, whereas in the uplink cell-edge users cause interference; second the uplink benefits from *interference diversity*, due to the distributed location of mobile users.

As a result, by increasing the access probability p for p–PSAR in the downlink, high CCI for cell-edge users provoke collisions particularly for cell-edge users, as an increasing number of users tend to access contention slots simultaneously. Lost contention slots by cell-edge users are likely to be reallocated to cell-centre users. Hence, by adjusting p, the allocation of resources for p–PSAR is shifted from cell-edge users towards cell-centre users, so that in the downlink p–PSAR trades system throughput for fairness. On the other hand, CESAR avoids collisions of contention slots and therefore accomplishes a fair distribution of resources to all users, while the convergence to the steady state (see Fig. 6(b)) is significantly better than p–PSAR with p=0.3.

In the uplink the detrimental effects of interference are more equally distributed among all users. Moreover, each user observes a different received busy signal power $I^b_{n,k}$ in (3), due to the distributed location of mobile users. This provides a large degree of freedom for multi-user slot assignment, giving rise to interference diversity, which benefits both CESAR and p–PSAR.

IV. Conclusions

The CESAR protocol utilizes the topology of wireless networks so to avoid collisions in reservation based protocols, caused by co-existing links when they simultaneously attempt to access idle slots. The collision avoidance is achieved through cyclically shifted resource partitioning patterns, which establishes a successive order on how neighboring cells access idle slots. The spatial reuse, in terms of concurrently accessed reserved slots by adjacent cells, is dynamically controlled by busy burst enabled interference protection. The protocol enables cellular systems to benefit from low outage and inherently introduces fairness in the sense that cell edge user throughput is not significantly compromised compared to p-persistent based protocols.

References

[1] W. Crowther, R. Rettberg, D. Walden, S. Ornstein, and F. Heart, "A System for Broadcast Communications: Reservation-ALOHA," in *Proc. 6th Hawaii Int. Conf. Sys. Sci.*, Jan. 1973, pp. 371–374.

[2] D. J. Goodman, R. A. Valenzuela, K. T. Gayliard, and B. Ramamurthi, "Packet Reservation Multiple Access for Local Wireless Communications," *IEEE Trans. Commun.*, vol. 37, no. 8, pp. 885–890, Aug. 1989.

[3] R. Zhao, B. Walke, and G. Hiertz, "An Efficient IEEE 802.11 ESS Mesh Network Supporting Quality-of-Service," *IEEE J. Sel. Areas Commun.*, vol. 24, no. 11, pp. 2005–2017, Nov. 2006.

[4] P. Omiyi, H. Haas, and G. Auer, "Analysis of TDD Cellular Interference Mitigation using Busy-Bursts," *IEEE Trans. Wireless Commun.*, vol. 6, pp. 2721–2731, July 2007.

[5] B. Ghimire, G. Auer, and H. Haas, "Busy Bursts for Trading off Throughput and Fairness in Cellular OFDMA-TDD," *EURASIP J. Wireless Commun. and Networking*, vol. 2009, Article ID 462396, 14 pages, 2009.

[6] S. Halpern, "Reuse partitioning in cellular systems," *Proc. IEEE Vehic. Technol. Conf. (VTC'83), Toronto, Canada*, vol. 33, pp. 322–327, May 1983.

[7] M. Sternad, T. Ottosson, A. Ahlen, and A. Svensson, "Attaining both Coverage and High Spectral Efficiency with Adaptive OFDM Downlinks," in *Proc. IEEE Vehic. Technol. Conf. 2003-Fall (VTC'F03), Orlando, USA*, Oct. 2003, pp. 2486–2490.

[8] S.-E. Elayoubi, O. B. Haddada, and B. Fourestie, "Performance Evaluation of Frequency Planning Schemes in OFDMA-Based Networks," *IEEE Transactions on Wireless Communications*, vol. 7, pp. 1623–1633, May 2008.

[9] M. C. Necker, "Local Interference Coordination in Cellular OFDMA Networks," in *Proc. of the Vehicular Technology Conference (VTC)*, Sept. 30 – Oct. 3, 2007, pp. 1741–1746.

[10] K. Appel and W. Haken, "Solution of the Four Color Map Problem," *Scientific American*, vol. 237, no. 4, pp. 108–121, Oct. 1977.

[11] IST-4-027756 WINNER II, "D6.13.14 WINNER II System Concept Description," Dec. 2007.

[12] ——, "D1.1.2 WINNER II Channel Models," Sept. 2007.

Balancing System Throughput and Fairness in Multi-User OFDMA-TDD using Busy Bursts

Birendra Ghimire*, Stefan Videv†, Gunther Auer‡ and Harald Haas*

*Institute for Digital Communications
The University of Edinburgh
EH9 3JL, Edinburgh, UK
{b.ghimire, h.haas}@ed.ac.uk

†School of Engineering and Science
Jacobs University Bremen
28759 Bremen, Germany
s.videv@jacobs-university.de

‡DoCoMo Euro-Labs
80687 München, Germany
auer@docomolab-euro.com

***Abstract*—This paper analyses busy burst (BB) enabled interference avoidance for multi-user orthogonal frequency division multiple access (OFDMA) in a Manhattan grid deployment scenario. Upon successful reception of data, the receiver transmits a BB in a time-multiplexed mini-slot. Exploiting the channel reciprocity of time division duplex (TDD), an exclusion region around a victim receiver is established, where potential transmitters are denied access to reserved resources. The size of the exclusion region is determined by a threshold parameter, known to the entire network. System level simulations compare the system and user throughput of BB enabled interference avoidance with greedy resource allocation that does not attempt to avoid interference. It is shown that by adjusting the BB threshold parameter, system throughput can be traded with fairness in terms of cell-edge user throughput. By tuning the BB threshold, either up to 45% increase in system throughput or up to 7-fold increase in cell-edge user throughput are feasible compared to greedy resource allocation. Moreover, by an appropriate adjustment of the BB power further gains in system throughput without compromising fairness are achieved.**

I. Introduction

The efficiency of dynamic channel allocation (DCA) algorithms is inevitably tied with their capability to deal with the hidden and exposed node problems. One means to provide the transmitter with the relevant information about the interference at the receiver has been identified by the busy signal concept [1–6]. Early works such as the dual busy tone multiple access [1] uses dedicated frequency multiplexed channels that carry narrow-band busy tones for channel reservation. As the protocol assumes that the transceivers listen to the out-of-band busy tones whilst transmitting, complex RF units are required, due to additional filters and duplexers involved. This drawback is avoided in [2–4], where time-multiplexed busy bursts (BBs) serve as a reservation indicator for a reservation based MAC (medium access control) protocol. By transmitting an in-band BB in an associated mini-slot following a successful transmission, two important goals are accomplished [3, 4]. First, the transmitter of the own link is informed whether or not the target signal to interference plus noise ratio (SINR) was met at the receiver. Second, at the same time potential transmitters of competing links are notified about ongoing transmissions, so that these transmitters can take appropriate steps to avoid interference. Therefore, both reservation and channel sensing tasks are accomplished, and the hidden and exposed node problems are effectively mitigated.

None of the busy tone based MAC protocols [1–4] allow for dynamic resource allocation where multiple users share a set of parallel frequency slots of a broadband frequency-selective radio channel, such as the 100 MHz channel of the WINNER[1] TDD mode [7]. By extending the BB concept to OFDMA [5, 6], the channel reciprocity of TDD [8] is exploited for decentralised interference management where time-frequency slots (chunks) can be dynamically assigned on a short-term basis. This concept termed BB-OFDMA works in a completely decentralised fashion and is therefore applicable to self-organising networks which may consist of cellular as well as *ad hoc* network topologies.

The attainable system throughput of BB-OFDMA is sensitive with respect to the selection of the interference threshold [5, 6]. In this paper, it is demonstrated how the interference threshold can be tuned to trade system throughput with fairness (defined as user throughput at the cell edge). Moreover, by using a variable BB power that takes into account the quality of the intended link, a further improvement in terms of both fairness and total system throughput is achieved. BB-OFDMA with variable BB power exhibits the further advantage that the sensitivity of the selected interference threshold on the performance is mitigated.

II. Multi-User Resource Allocation

The available bandwidth B is divided into N_{C} mutually orthogonal time-frequency resource units (chunks), each of which occupies a bandwidth B/N_{C}. Multi-user resource allocation at the base station (BS) involves the distribution of the N_{C} chunks to U mobile users. For OFDMA blocks of $n_{\mathrm{c}}{=}B/(N_{\mathrm{C}}\,\Delta f)$ subcarriers and n_{t} OFDM symbols constitute one chunk, as illustrated in Fig. 1, where Δf accounts for the subcarrier spacing. Provided that only one user per cell transmits on a given chunk, chunks can be flexibly assigned to users such that the intra-cell interference is avoided. However, as the same chunk may be reused in adjacent cells, co-channel interference (CCI) is encountered.

Provided that channel knowledge is available at the transmitter, users can be assigned those chunks with favourable channel conditions, giving rise to multi-user diversity [9]. A score-based scheduler [10] variant is used to distribute the $1{\leq}n{\leq}N_{\mathrm{C}}$ chunks among $1{\leq}\nu{\leq}U$ users served by BS q. The score at time instant k is computed as:

$$s_{\nu,q}[n,k] = 1 + \sum_{\ell=1}^{N_{\mathrm{C}}} \mathbb{I}_{\{g_{\nu,q}[n,k]\leq g_{\nu,q}[\ell,k]\}} + \epsilon_{\nu,q}[n,k]\,, \quad (1)$$

[1]Wireless World Initiative New Radio, URL: www.ist-winner.org

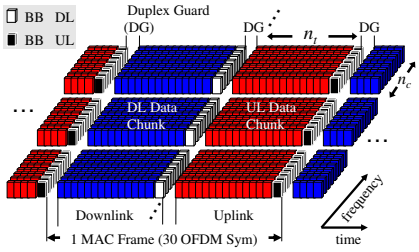

Fig. 1. Illustration of MAC frame in WINNER-TDD for BB signalling.

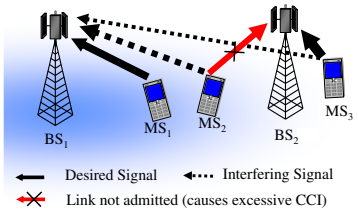

Fig. 2. BB signalling applied to cellular system. The arrows depict the direction of desired and interfering signal in UL mode and their relative strength. In DL mode, the direction of arrows reverse.

where $g_{\nu,q}[n,k]$ is the channel gain of user ν on chunk (n,k), and $\epsilon_{\nu,q}[n,k] \in \{0,\infty\}$ indicates whether or not user ν is granted access to chunk (n,k). The Boolean operator $\mathbb{I}_x \in \{0,1\}$ is set to 1 or 0 when the condition x is true or false, respectively.

User $\nu{=}\zeta_q[n,k]$ is assigned chunk (n,k) if either a reservation indicator was set in the previous frame $b_{\nu,q}[n,k{-}1]{=}1$, or the score (1) is minimised:

$$\zeta_q[n,k] = \begin{cases} \arg\min\limits_{\nu} s_{\nu,q}[n,k]\,, & b_{\nu,q}[n,k{-}1] = 0 \;\forall\, \nu \\ \nu\,, & b_{\nu,q}[n,k{-}1] = 1\,. \end{cases} \tag{2}$$

In an OFDMA-TDD system with full frequency reuse, CCI resulting from simultaneous access of chunks in adjacent cells is not avoided. In such system $\epsilon_{\nu,q}[n,k]{=}0$ for all users in the cell. Thus, all users compete for being scheduled in the chunk (n,k) using (2). However, for reservation based MAC protocols such as BB-OFDMA (see Section III), some chunks are excluded for certain users. To this end, $\epsilon_{\nu,q}[n,k]{\to}\infty$ indicates that user ν in cell q is denied access to chunk (n,k). We note that if $\epsilon_{\nu,q}[n,k]{\to}\infty$ for all users, cell q leaves chunk (n,k) unallocated, so that $\zeta_q[n,k]{=}\emptyset$.

III. Busy Burst Signalling

Resource allocation with full frequency reuse, where attempts to avoid the CCI are not made, in particular affects the cell-edge users for two reasons. First, the desired signal levels are, on average, much weaker compared to the users in close vicinity to the desired BS. Second, the cell-edge users either suffer from high CCI in the downlink (DL) or cause high CCI to adjacent cells in the uplink (UL). Therefore, it becomes imperative to reduce the CCI so to enable cell-edge users to meet a certain SINR target. A minimum SINR requirement is effectively enforced by an exclusion region around active receivers, which is established by BB signalling [3, 4]. An exclusion region defines an area around an active receiver in cell q, where potential transmitters in the adjacent cells $p{\neq}q$ must not transmit.

In the context of OFDMA, exclusion regions are to be established individually for each chunk (n,k) [5]. In BB-OFDMA, a MAC frame is divided into data slots and BB mini slots as illustrated in Fig. 1. The BS transmits data in 'Data DL' on chunk (n,k). Provided that the SINR target is met, and the BS intends to transmit more data, the intended mobile station (MS) transmits a BB in 'BB UL' slot. Thus, the 'Data DL' slot on chunk n is reserved for the given user in the next frame $k{+}1$. Likewise, for data transmitted by MS in 'Data UL' slot, the BB is transmitted by the intended BS in 'BB DL' slot. BB-OFDMA is summarised by the following protocol:

1) All potential transmitters must sense the BB slot corresponding to the data slot prior to transmission;
2) The transmitters are prohibited to use the chunk where a BB is detected above a given threshold.

To exemplify the principle of BB enabled interference avoidance, a typical interference scenario in a cellular system is illustrated in Fig. 2. In the considered example BS_1 has transmitted a BB after successful reception from MS_1. While MS_2 cannot access this chunk, as it detects a strong BB from BS_1, MS_3 may reuse this chunk, since MS_3 is located outside the exclusion region of BS_1.

To mathematically describe this concept, let $\mathbf{x}{=}(\nu,q)$ define a transmitter or receiver (either BS or MS) of user ν within cell q. With this notation the channel gain of the intended link at chunk (n,k) becomes $g_{\mathbf{x}}[n,k]{=}g_{\nu,q}[n,k]$. The channel gain of an interfering link, between transmitter $\mathbf{y}{=}(\mu,p)$ of user μ located in an adjacent cell $p{\neq}q$ and receiver $\mathbf{x}$, is denoted by $g_{\mathbf{yx}}[n,k]$. Then $T^{\mathrm{d}}_{\mathbf{x}}[n,k]$ and $R^{\mathrm{d}}_{\mathbf{x}}[n,k] = g_{\mathbf{x}}[n,k]\,T^{\mathrm{d}}_{\mathbf{x}}[n,k]$ define the data transmit power and the received data power of the intended link, while $I^{\mathrm{d}}_{\mathbf{x}}[n,k] = g_{\mathbf{yx}}[n,k]\,T^{\mathrm{d}}_{\mathbf{y}}[n,k]$ accounts for CCI between transmitter $\mathbf{y}{=}(\mu,p)$ and receiver $\mathbf{x}$ at chunk (n,k). Likewise, $T^{\mathrm{b}}_{\mathbf{y}}[n,k]$ is the BB transmit power of the BB transmitter $\mathbf{y}$ (i.e. data receiver) and $I^{\mathrm{b}}_{\mathbf{x}}[n,k] = g_{\mathbf{xy}}[n,k]\,T^{\mathrm{b}}_{\mathbf{y}}[n,k]$ is the interfering BB power from $\mathbf{y}$ received at data transmitter $\mathbf{x}$ (i.e. BB receiver). Thus, the SINR achieved at the receiver $\mathbf{x}$ at chunk (n,k) is in the form:

$$\gamma_{\mathbf{x}}[n,k] = \frac{R^{\mathrm{d}}_{\mathbf{x}}[n,k]}{I^{\mathrm{d}}_{\mathbf{x}}[n,k] + N} \tag{3}$$

where N is the thermal noise power. We assume that the data transmitted on chunk (n,k) is successfully received if (3) exceeds the target SINR Γ, that is $\gamma_{\mathbf{x}}[n,k]{\geq}\Gamma$.

Exploiting TDD channel reciprocity, the potential transmitter of link $\mathbf{y}$ can ascertain $I^{\mathrm{d}}_{\mathbf{x}}[n,k]$, the potential amount of interference it causes to the existing link $\mathbf{x}$, by listening to the BB mini-slot [3]. Applying the reciprocity property of TDD, $g_{\mathbf{yx}}[n,k] = g_{\mathbf{xy}}[n,k]$, results in the following relation

$$I^{\mathrm{d}}_{\mathbf{x}}[n,k] = I^{\mathrm{b}}_{\mathbf{y}}[n,k] \cdot \left(\frac{T^{\mathrm{d}}_{\mathbf{y}}[n,k]}{T^{\mathrm{b}}_{\mathbf{x}}[n,k]} \right) . \tag{4}$$

Two mechanisms that utilise (4) to enable the candidate transmitter $\mathbf{y}$ to decide whether or not it should transmit on chunk (n,k) are investigated.

A. Fixed power BB

In order to meet the SINR target, the maximum CCI $I^{\mathrm{d}}_{\mathbf{x}}[n,k]$ that a candidate transmitter $\mathbf{y}$ may cause to an active receiver $\mathbf{x}$ is given by the interference threshold I_{th}, which is constant and known to the entire network. Provided that both $T^{\mathrm{b}}_{\mathbf{x}}[n,k]$ and $T^{\mathrm{d}}_{\mathbf{y}}[n,k]$ are known to the candidate transmitter $\mathbf{y}$, (4) enables $\mathbf{y}$ to verify whether $I^{\mathrm{d}}_{\mathbf{x}}[n,k] < I_{\mathrm{th}}$, in which case $\mathbf{y}$ is outside the exclusion range of $\mathbf{x}$ [3, 4]:

$$I^{\mathrm{b}}_{\mathbf{y}}[n,k] \cdot \left(\frac{T^{\mathrm{d}}_{\mathbf{y}}[n,k]}{T^{\mathrm{b}}_{\mathbf{x}}[n,k]} \right) \leq I_{\mathrm{th}} \,. \tag{5}$$

In case $T^{\mathrm{d}}_{\mathbf{y}}[n,k]{=}T^{\mathrm{b}}_{\mathbf{x}}[n,k]$, condition (5) reduces to:

$$I^{\mathrm{b}}_{\mathbf{y}}[n,k] \leq I_{\mathrm{th}} \,. \tag{6}$$

By tuning I_{th}, the maximum CCI $I^{\mathrm{d}}_{\mathbf{x}}[n,k]$ in (3) is adjusted. A low I_{th} enables cell-edge users who typically observe relatively low channel gains to its BS (hence lower $R^{\mathrm{d}}_{\mathbf{x}}[n,k]$) to meet their SINR target. However, this enforces a larger exclusion region around a vulnerable receiver through (6). Thus, chunk (n,k) can be reused less likely in adjacent cells as I_{th} decreases, potentially leading to a lower system throughput. On the other hand, by increasing I_{th}, an increasing number of links are admitted, potentially leading to enhanced system throughput. However, cell-edge users are less likely to meet their SINR target, as interference protection is gradually eliminated. Thus, by tuning I_{th}, system throughput can be traded for fairness in terms of cell-edge user throughput.

B. BB with interference tolerance signalling

With fixed power BB signals, the same level of interference protection is given to all links, disregarding the quality of the intended link. The resulting problem is explained with the help of Fig. 3 where MS_1 and MS_2 are both connected to BS_1. It is assumed that $g_1{>}g_2$, thus MS_1 can tolerate more interference than MS_2 to meet a certain SINR target Γ. In case both MS_1 and MS_2 are exposed to the same interference, it is more likely that the SINR target is met for MS_1 than for MS_2. By allowing MS_1 and MS_2 to transmit a BB with variable power, the individual amount of interference that can tolerated by MS_1 and MS_2 is signalled to candidate transmitters in the adjacent cells. Thus, exclusion regions of different size are formed around MS_1 and MS_2, as illustrated in Fig. 3, which guarantees the same SINR target for receivers $\mathbf{x}$ with different link qualities $R^{\mathrm{d}}_{\mathbf{x}}[n,k]$. This maximum interference that the receiver $\mathbf{x}$ can tolerate whilst $\gamma_{\mathbf{x}}[n,k] \geq \Gamma$ is:

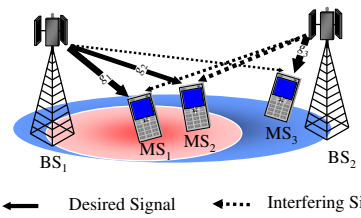

Fig. 3. BB signalling applied to cellular system in the DL mode. The ovals represent the exclusion region formed with BB-ITS.

$$I^{\mathrm{tol}}_{\mathbf{x}}[n,k] = \frac{R^{\mathrm{d}}_{\mathbf{x}}[n,k]}{\Gamma} - N \,. \tag{7}$$

To ensure that the interference caused to an active receiver $\mathbf{x}$ is kept below $I^{\mathrm{tol}}_{\mathbf{x}}[n,k]$, a chunk (n,k) may be accessed by $\mathbf{y}$ if (6) holds true. For this, the BB transmit power is set as follows [11]:

$$T^{\mathrm{b}}_{\mathbf{x}}[n,k] = \min \left(\frac{I_{\mathrm{th}} \cdot T^{\mathrm{d}}}{\left(\frac{R^{\mathrm{d}}_{\mathbf{x}}[n,k]}{\Gamma} - N \right)}, T^{\mathrm{b}}_{\mathrm{max}} \right) \tag{8}$$

where $T^{\mathrm{b}}_{\mathrm{max}}$ is the maximum BB transmit power and T^{d} is the fixed data transmit power for all links. This variant of BB-OFDMA is labelled BB with interference tolerance signalling (BB-ITS).

The $\min$ operator in (8) ensures that the BB transmit power is upper bounded by $T^{\mathrm{b}}_{\mathrm{max}}$. Note that when $\frac{R^{\mathrm{d}}_{\mathbf{x}}[n,k]}{\Gamma} < N$ or $\gamma_{\mathbf{x}}[n,k] < \Gamma$, the chunk is released, and thus no BB is transmitted. This ensures that the BB transmit powers (8) are always positive, $T^{\mathrm{b}}_{\mathbf{x}}[n,k]{>}0$. Moreover, increasing I_{th} for BB-ITS results in a proportional increase of $I^{\mathrm{b}}_{\mathbf{y}}[n,k] = g_{\mathbf{xy}}[n,k]\, T^{\mathrm{d}}_{\mathbf{y}}[n,k]$. Thus, the outcome of (6) does not depend on I_{th}, as long as (6) can be reliably detected. In this paper we choose $I_{\mathrm{th}}{=}{-}90\,\mathrm{dBm}$.

C. Dynamic channel allocation with BB Signalling

Initial access of unreserved slots in BB-OFDMA is carried out in contention. During contention, two or more transmitters from adjacent cells may access chunk (n,k) simultaneously. As the traffic load in the system increases, simultaneous access during contention becomes more likely. Due to this, cell-edge users are particularly affected, as they most likely do not meet their SINR target; hence no BB is transmitted and chunk (n,k) remains unreserved. As a result, outage especially at the cell-edge increases. To avoid this, simultaneous access in contention is reduced by using a $p-$persistent approach for accessing chunks in contention. The outcome of the $p-$persistent chunk allocation in a cell q is modelled with a binary random variable $\mathcal{X}_q[n,k] \in \{0,1\}$, such that $\mathrm{P}(\mathcal{X}_q[n,k]{=}1) = p$. Assuming Q cells that are close enough to interfere with one another, using $p{=}\frac{1}{Q}$ ensures that on average only one cell transmits in contention on a given chunk (n,k). In the considered Manhattan Grid deployment scenario (see Section IV), $Q{\leq}3$ in most cases and p is rounded off to 0.3.

Suppose that transmitter $\mathbf{x}{=}(\nu,q)$ intends to transmit data. Prior to accessing chunk (n,k), it listens to the associated BB mini-slot. Whether a user ν within cell q may contend to access chunk (n,k) in (1) is controlled by the parameter:

$$\epsilon_{\nu,q}[n,k] = \begin{cases} 0 \,, & I^{\mathrm{b}}_{\nu,q}[n,k] \leq I_{\mathrm{th}} \text{ and } \mathcal{X}_q[n,k]{=}1 \\ \infty \,, & \text{otherwise.} \end{cases} \tag{9}$$

The binary variable $a_{\nu,q}[n,k]$ indicates whether user ν in cell q transmits at chunk (n,k) and is defined as:

$$a_{\nu,q}[n,k] = \begin{cases} 1\,, & \zeta_q[n,k] = \nu \\ 0\,, & \text{otherwise.} \end{cases} \tag{10}$$

where $\zeta_q[n,k]$ is defined in (2). Denote $\mathcal{A}_{\nu,q}$, the set of chunks $n\in\{1,\cdots,N_C\}$ at time k, for which $a_{\nu,q}[n,k]=1$. Then the set of chunks used for transmission in a given cell amounts to set $\mathcal{A}_q$ with $\mathcal{A}_q = \cup_\nu \mathcal{A}_{\nu,q}$, where $\cup$ represents a set union. Furthermore, let $\mathcal{B}_q$ denote the subset of allocated chunks $\mathcal{B}_q \subseteq \mathcal{A}_q$ where the SINR target Γ at the intended receiver is met, specified by the reservation indicator [5]:

$$b_{\nu,q}[n,k] = \begin{cases} 1\,, & \gamma_{\nu,q}[n,k] \geq \Gamma \text{ and } a_\nu[n,k] = 1 \\ 0\,, & \text{otherwise} \end{cases} \tag{11}$$

where the SINR $\gamma_{\nu,q}[n,k]$ is defined in (3).

Chunks where $b_{\nu,q}[n,k]=1$ are subsequently reserved by BB broadcast. The BB broadcast from the intended data receiver is observed as a *surge* in the received BB signal [4], and effectively notifies the transmitter that the data of chunk (n,k) has been received correctly. In the next frame $k+1$, the chunk is reserved for user ν. On the other hand, if the transmitter does not detect a BB surge in the next frame $k+1$, it is understood that the SINR target was not met due to high CCI. These chunks are released by setting $b_{\nu,q}[n,k]=0$. Hence chunk $(n,k+1)$ may be assigned to other users.

IV. Manhattan Grid Deployment

An urban microcell deployment with a rectangular grid of streets (Manhattan grid) as defined in scenario B1 in WINNER [7] is considered where antennas are mounted below the rooftop. The deployment scenario consists of building blocks of dimensions 200 m × 200 m, interlaced with the streets of width 30 m, forming a regular structure called the Manhattan grid, as shown in Fig. 4. The network consists of 11×12 building blocks (72 BSs). However, the performance statistics are collected only over the central core of 3×3 building blocks (6 BSs), to reduce the edge effects.

On average $U=10$ MSs are served by one cell, uniformly distributed in the streets and moving with a constant velocity of 5 km/h. BSs are placed in the middle of the street canyons with an inter-BS distance of 4 building blocks, as depicted in Fig. 4. Distance dependent pathloss, log-normal shadowing and frequency selective fading are taken into account, as specified in [12], channel model B1. Links where transmitter and receiver are located on the same street are modelled as line of sight (LoS) channels, with significantly lower pathloss attenuation than non line of sight (NLoS) links [12]. The MSs are connected to the BS on the basis of least distance to the BS in the same street, due to the lower path loss in LOS conditions. A full buffer traffic model [7] and a network synchronised in time and frequency is assumed. No upper limit is placed on the number of chunks that can be assigned to one user. The simulation parameters are summarised in Table I.

TABLE I
Simulation Parameters

Parameters	Value
Total symbol length	22.48 μs
Carrier centre frequency	3.95 GHz
System bandwidth B	89.84 MHz
Number of subcarriers (SC)	1840
Frame duration	0.6912 ms
OFDM symbols/frame	30
Chunk size	15 (time) × 8 (frequency) = 120
Number of chunks/frame	2 (time) × 230 (frequency)
Access probability p	0.3
Bits/symbol	2
SINR target Γ	10 dB
Number of sectors/cell	1
Transmit power per chunk T^{d}	16.4 dBm
Antenna gain	0 dBi
Noise level N	-117.8 dBm/chunk
Number of snapshots	50
Simulation duration per snapshot	50 ms

V. Results and Discussion

Fig. 5 explores the impact of I_{th} on the system throughput of BB-OFDMA with fixed BB power, defined in Section III-A. The maximum system throughput (proportional to set $\mathcal{B}$) for the UL and the DL amounts to 67.2 Mbps/cell at $I_{\text{th}} = -90$ dBm and 62.2 Mbps/cell at $I_{\text{th}} = -75$ dBm, respectively. For comparison, the maximum cell throughput in an isolated cell (without CCI) is 74.5 Mbps.

Interestingly, the system throughput vs. I_{th} graph Fig. 5 attains a peak in the UL, while this effect is not observed in the DL. This effect is explained with the aid of the interference scenario in Fig. 2. In the UL, allocating a chunk to different

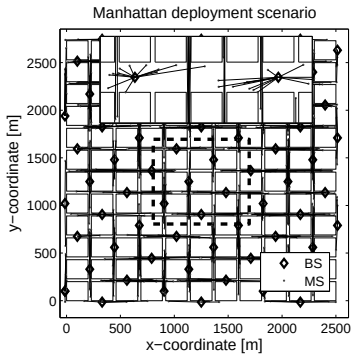

Fig. 4. Urban microcell deployment in a Manhattan grid.

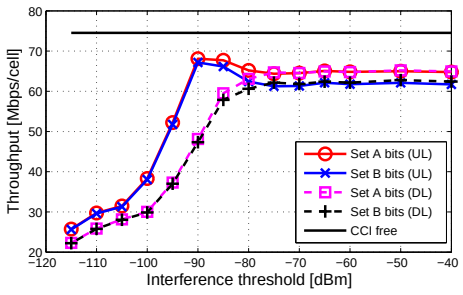

Fig. 5. Effect of I_{th} on system throughput. Uplink and DL behave differently due to the different spatial distribution of transmitters and receivers.

MSs causes different amounts of CCI at a BS in an adjacent cell (in Fig. 2, MS_2 causes higher CCI than MS_3 to BS_1), whereas in the DL, the same amount of CCI would be caused to the link in the adjacent cell, regardless of which MS is actually being served (in Fig. 2, interference at MS_1 from BS_2 is the same, no matter whether MS_2 or MS_3 is being served). Taking this into account, the impact of different I_{th} can be explained as follows: for $I_{\text{th}} = N$, $I^{\text{b}}_{\nu,q}[n,k] \geq I_{\text{th}}$ for all links. Consequently, neither in the UL nor in the DL are chunks (re)used. As I_{th} increases, in the UL $I^{\text{b}}_{\nu,q}[n,k] < I_{\text{th}}$ is met for some MSs that cause low CCI to existing links (such as MS_3 in Fig. 2). Admitting such links therefore enhances the system throughput, giving rise to the peak in Fig. 5. However, if I_{th} increases further, $I^{\text{b}}_{\nu,q}[n,k] < I_{\text{th}}$ also holds true for MSs that cause high CCI to existing links, (such as MS_2 in Fig. 2). In this case, the SINR target at BS_1 might no longer be met, compromising system throughput. On the other hand, in the DL, when I_{th} is increased, $I^{\text{b}}_{\nu,q}[n,k] < I_{\text{th}}$ holds true at a certain I_{th} for *all* users in cell q (as the BB is received at the BS, and the point-to-multipoint scenario in the DL). Hence, for the same chunk to be reused in a neighbouring cell $p \neq q$, the SINR target is only met if the MS in the adjacent cell p is close to its BS — regardless of which MS is being served in the tagged cell q. In Fig. 2, the SINR would not be met at MS_1 (at the cell edge) because the desired signal path and the interfering signal path are approximately the same, regardless of which MS is served by BS_2. Thus, *in the DL, CCI cannot be reduced by selecting one link instead of another*, unlike the UL which benefits from *interference diversity*, due to the distributed location of mobile users. The difference between UL and DL is responsible for the fact that in the DL no peak in the throughput plot of Fig. 5 is observed. The monotonic increase of the system throughput in the DL with increasing I_{th} is due to the fact that the interference protection is gradually eliminated, and only a few MSs in close vicinity to their BS are served. This means that throughput is maximised at the expense of fairness toward cell-edge users.

The throughput comparison between UL and DL is further elaborated in Fig. 6, where the average user throughput is plotted against the distance d to the serving BS. In the UL, shown in Fig. 6.(a), increasing I_{th} from -95 dBm to -90 dBm hardly compromises the cell-edge user throughput in terms of Set $\mathcal{B}$ ($d \geq 400$ m), but significantly improves the cell-centre user throughput ($d \leq 100$ m). In the DL, on the other hand, the user throughput is shifted from cell-edge users to cell-centre users as I_{th} increases, as shown in Fig. 6.(b). To this end, as I_{th} is increased from -90 dBm to -75 dBm, the cell-edge user throughput decreases from 1.9 Mbps to 0.25 Mbps (distance $d \geq 400$ m), whereas the cell-centre user throughput ($d \leq 100$ m) increases from 6 Mbps to 10 Mbps.

In Fig. 6 the throughput of BB-OFDMA is compared to greedy resource allocation which does not attempt to avoid CCI, termed adaptive score-based chunk allocation (ASCA). For ASCA, the chunk allocation is carried out by setting $\epsilon_{\nu,q}[n,k]=0$ in (1) for all users. While on the DL a 7-fold gain (from 240 kbps to 1.9 Mbps) in cell-edge user throughput of BB-OFDMA over ASCA is observed by lowering I_{th}, the corresponding UL gain is only 25% (from 1.5 Mbps to 2.1 Mbps). Of note is the significant data rejection with ASCA (in terms of Set $\mathcal{A}$ minus Set $\mathcal{B}$) for cell-edge users ($d \geq 400$ m).

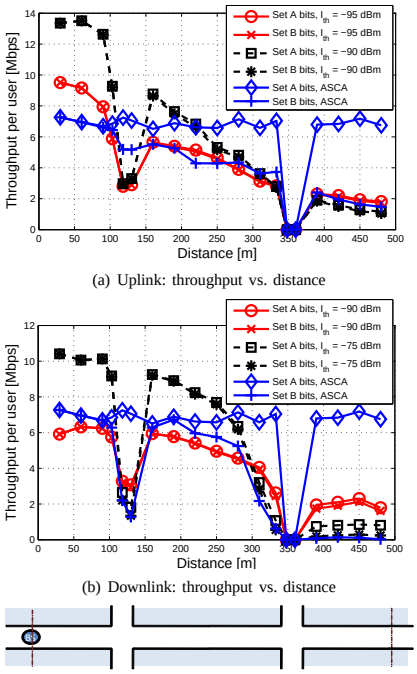

(a) Uplink: throughput vs. distance

(b) Downlink: throughput vs. distance

Fig. 6. Throughput per user over distance for different thresholds I_{th}. Cell-edge users experience improved throughput by lowering I_{th}. Street crossings are at 130 m and 360 m, leading to a dip in throughput at these locations.

Fig. 7 shows the cumulative distribution function (CDF) of the two BB-OFDMA variants and ASCA in terms of system and user throughput. Fig. 7.(a–b) show that BB-OFDMA with fixed BB power outperforms ASCA both in UL and DL in terms of system throughput. With $I_{\text{th}}=-90$ dBm in the UL and $I_{\text{th}}=-75$ dBm in the DL, the system throughput is maximised (see Fig. 5), and its median approaches $\approx$90% and 83% of the attainable system throughput in an isolated cell (CCI free system).

On the other hand, when the throughput of users at the cell boundary is the primary concern, $I_{\text{th}}=-95$ dBm in the UL and $I_{\text{th}}=-90$ dBm in the DL are preferable. Then, the 10%-ile of user throughput achieved amounts to 1.18 Mbps (UL) and 1.15 Mbps (DL), as shown in Fig. 7.(c-d). However, the improvement in cell-edge user throughput by lowering I_{th} is traded with a decrease in system throughput by 25%. Nevertheless, the median system throughput of BB-OFDMA is still 5% higher compared to ASCA both in UL and DL.

BB-OFDMA with variable BB power (8), termed BB-ITS discussed in Section III-B, provides a further gain of 19% and 7.5% in median UL and DL system throughput, together with 21% and 17% increase in the lower 10%-ile UL and DL user throughput, compared to BB-OFDMA with fixed BB power ($I_{\text{th}} = -95$ dBm in the UL and $I_{\text{th}} = -90$ dBm in

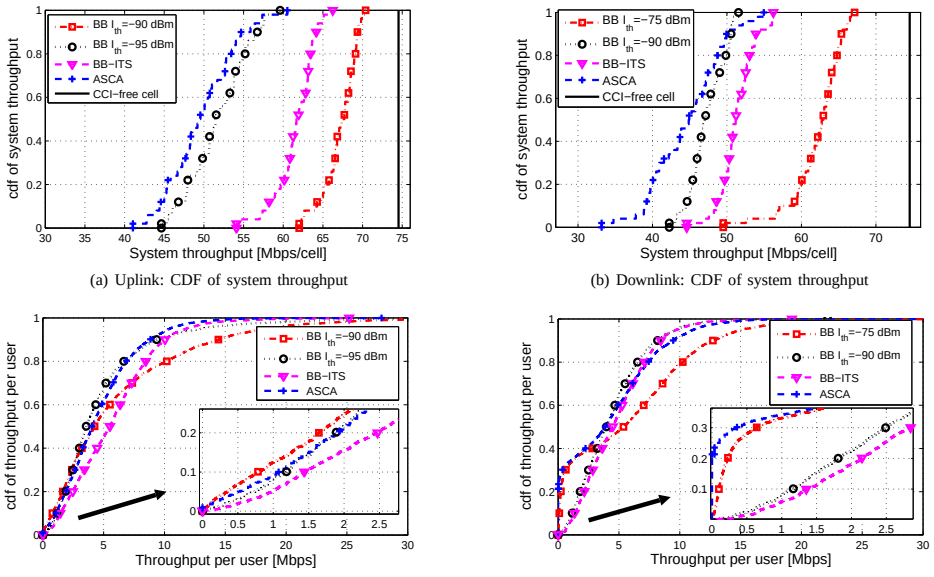

(a) Uplink: CDF of system throughput

(b) Downlink: CDF of system throughput

(c) Uplink: CDF of throughput per user

(d) Downlink: CDF of throughput per user

Fig. 7. Performance of the two BB signalling variants compared to the benchmark system.

the DL). Compared to ASCA, the gains in median system throughput with BB-ITS are 25% and 14% respectively in UL and DL. The lower 10%-ile throughput improves from 0 kbps in to 1.4 Mbps in the DL and from 1.1 Mbps to 1.4 Mbps in the UL.

VI. Conclusions

In this paper, busy signal concept for decentralised and self-organising interference avoidance was applied to OFMDA-TDD systems operating in Manhattan type environments. Busy burst (BB) enabled interference avoidance was shown to achieve 40% higher system throughput compared to greedy resource allocation without interference avoidance. It was found that system throughput can be traded with fairness by tuning the BB interference threshold parameter. To this end, a cell-edge user throughput exceeding 1 Mbps can be maintained by BB-OFDMA. Allowing for a variable BB power not only achieves a favorable trade-off between system throughput and fairness, but also alleviates the need to adjust the BB threshold parameter. The latter property is particularly important for self-organizing wireless networks, as the optimum choice of the BB threshold is sensitive to changes in the network topology.

References

[1] Z. J. Haas and J. Deng, "Dual Busy Tone Multiple Access (DBTMA)-A Multiple Access Control Scheme for ad hoc Networks," *IEEE Transactions on Communications*, vol. 50, no. 6, pp. 975–985, June 2002.

[2] R. Zhao, B. Walke, and M. Einhaus, "Constructing Efficient Multi-hop Mesh Networks," in *The IEEE Conference on Local Computer Networks (LCN)*, Sydney, Australia, Nov. 15–17, 2005, pp. 166–173.

[3] P. E. Omiyi and H. Haas, "Improving Time-Slot Allocation in 4th Generation OFDM/TDMA TDD Radio Access Networks with Innovative Channel-Sensing," in *Proc. of the International Conference on Communications (ICC)*, vol. 6, Paris, France, June 20–24 2004, pp. 3133–3137.

[4] P. Omiyi, H. Haas, and G. Auer, "Analysis of TDD Cellular Interference Mitigation Using Busy-Bursts," *IEEE Transactions on Wireless Communications*, vol. 6, no. 7, pp. 2721–2731, July 2007.

[5] H. Haas, V. D. Nguyen, P. Omiyi, N. Nedev, and G. Auer, "Interference Aware Medium Access in Cellular OFDMA/TDD Networks," in *Proc. of the International Conference on Communications (ICC)*, vol. 4, Istanbul, Turkey, June11–15 2006, pp. 1778–1783.

[6] B. Ghimire, H. Haas, and G. Auer, "Busy Burst Enabled Interference Avoidance in WINNER-TDD," in *Proc. of the International Symposium on Personal, Indoor and Mobile Radio Communications (PIMRC)*, Athens, Greece, Sept. 3–7 2007.

[7] IST-4-027756 WINNER II, "D6.13.7, WINNER II Test Scenarios and Calibration Cases Issue 2," Retrieved Mar. 15, 2007, from https://www.ist-winner.org/WINNER2-Deliverables/.

[8] H. Haas and S. McLaughlin, Eds., *Next Generation Mobile Access Technologies: Implementing TDD*. Cambridge University Press, ISBN: 13:9780521826228, Jan. 2008, 420 pages.

[9] M. Sternad, T. Svensson, T. Ottosson, A. Ahlen, A. Svensson, and A. Brunstrom, "Towards Systems Beyond 3G Based on Adaptive OFDMA Transmission," *Proceedings of the IEEE*, vol. 95, no. 12, pp. 2432–2455, Dec. 2007.

[10] T. Bonald, "A Score-Based Opportunistic Scheduler for Fading Radio Channels," in *Proc. of the European Wireless Conference (EWC)*, Barcelona, Spain, Feb. 24–27, 2004.

[11] P. Agyapong, H. Haas, A. Tyrrell, and G. Auer, "Interference Tolerance Signaling Using TDD Busy Tone Concept," in *Proc. of the Vehicular Technology Conference (VTC)*, Dublin, Ireland, Apr. 22–25 2007, pp. 2850–2854.

[12] IST-4-027756 WINNER II, "D1.1.2 v1.2 WINNER II Channel Models," Retrieved Feb. 5, 2008, from https://www.ist-winner.org/WINNER2-Deliverables/.

The 18th Annual IEEE International Symposium on Personal, Indoor and Mobile Radio Communications (PIMRC'07)

BUSY BURST ENABLED INTERFERENCE AVOIDANCE IN WINNER–TDD

Birendra Ghimire Harald Haas
Institute for Digital Communications
The University of Edinburgh, EH9 3JL, Edinburgh, UK
E-mail: {b.ghimire, h.haas}@ed.ac.uk

Gunther Auer
DoCoMo Euro-Labs
Landsberger Str. 312, 80687 Munich, Germany
Email: auer@docomolab-euro.com

ABSTRACT

This paper[1] analyses the busy burst (BB) enabled interference avoidance mechanism applied to an *ad hoc* indoor scenario with time division duplex (TDD) mode of WINNER parameters. The BB algorithm exploits the channel reciprocity of the TDD mode. Upon successful data reception, a receiver broadcasts a busy signal. A potential interfering transmitter can directly infer the level of interference it would cause to the vulnerable receiver from the received BB signal power. The new transmitter can, thus, autonomously decide whether to transmit, or to refrain from transmission so that interference at the vulnerable receiver is below a given threshold. As a consequence, significant co-channel interference is avoided and the system performance is ameliorated. The results show that using the BB protocol, approximately a three fold increase in throughput and a significant reduction in packet delay and packet expiration rate is achieved compared to uncoordinated random medium access in such *ad hoc* networks.

Index terms— Interference mitigation, WINNER–TDD, *ad hoc*, busy tone signalling

I. INTRODUCTION

Future wireless networks will see a plethora of wireless services each with different requirements in terms of data rate, delay, bit error rate performance and service type. The data rates are anticipated to range from few kilobits per second (kbps) to 50 megabits per second (Mbps) per user depending on applications [4]. With a multitude of such requirements, it becomes increasingly difficult to manage the bandwidth in a spectrally efficient manner. Co-channel interference (CCI) is by far the most significant bottleneck in achieving better spectral efficiency. Hence, mitigation of CCI is the key to achieve better spectral efficiency.

The assumptions of fully centralized control of radio resources as made in [1] or semi-decentralized such as in [8] would suffer from the requirement of significant signalling overheads in cellular systems. In *ad hoc* networks, it would be almost impossible to realize any centralized control. In addition, the above protocols suffer from the classical hidden and exposed node problems. Those protocols that solve these issues require separate dedicated channel where probe packets and extra reply packets [10] are transmitted. Dual busy tone multiple access [3] and its variants [11] avoid collision of ready to send (RTS) and clear to send (CTS) packets by incorporating two narrowband channels. This solves the hidden and exposed node problem at the expense of separate channels dedicated for out-of-band signalling. As a consequence, additional filters and duplexers are required which increase the complexity at the RF (radio frequency) unit. This issue is solved with the MAC (medium access control) protocol described in [12, 13] in which busy-tones are used in a time-multiplexed fashion for solving the hidden node problem. None of these busy tone based MAC protocols exploit channel reciprocity for active and dynamic resource allocation in a broadband frequency selective radio frequency channel such as the 100 MHz channel in WINNER-TDD. These issues are addressed in [2, 9] where the channel reciprocity offered by the TDD mode is exploited for interference aware subchannel allocation in a cellular environment. Time multiplexed busy-tone power signals are used for this purpose.

This paper builds on the concept presented in [2, 9] and presents the empirical results of using busy tone signalling in an *ad hoc* scenario applied to the WINNER–TDD indoor scenario. For this purpose a class III system level simulator [6] is developed. In this study, simulation is carried out for randomly selected transmitter and receiver pairs, instead of applying the classical least pathloss approach. The random link establishment does not *a priori* minimize interference and should rather reflect a more realistic user scenario. Results show a significant gain in performance using busy burst approach as opposed to random resource allocation schemes chosen as benchmark systems.

The remainder of the paper is arranged as follows: In Section II, the relevant WINNER–TDD physical layer details are outlined. Then the algorithm and the benchmark system are described in Section III. The system model considered for study is discussed in Section IV. Finally, the simulation results are provided in Section V, and the conclusions are drawn in Section VI.

II. RADIO RESOURCE ALLOCATION IN WINNER–TDD

The physical layer of WINNER–TDD [7] consists of 2048 subcarriers spanning a bandwidth of 100 MHz. Out of these 2048 subcarriers, only 1664 are used for data transmission. A MAC–frame in WINNER–TDD is 691.2μs and consists of 2 time-slots. Each of these two time-slots contains 15 OFDM (orthogonal frequency division multiplexing) symbols. A radio resource allocation unit (or time-frequency slot) in WINNER–TDD is known as a *chunk* which consists of a group of 8 adjacent subcarriers and spans one time-slot in the MAC frame.

III. ALGORITHM AND BENCHMARK SYSTEM

The busy tone algorithm [2, 9] studied in this paper uses an implicit feedback mechanism to mitigate CCI and to select channels for transmission. Channel reciprocity inherent to TDD systems is exploited such that the transmitter is aware of the level of interference it potentially causes to other co-existing links.

[1]This work has been performed in the framework of the IST project IST-4-027756 WINNER (World Wireless Initiative New Radio), which is partly funded by the European Union.

The 18th Annual IEEE International Symposium on Personal, Indoor and Mobile Radio Communications (PIMRC'07)

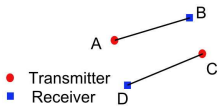

Figure 1: Two links in *ad hoc* scenario

In order to explain the working mechanism of the algorithm, let us assume that node A and node B in Figure 1 are the transmitter and the receiver respectively in an already established link. While the communication between A and B is underway, node C wants to transmit data to node D as shown in Figure 1. After receiving data during the data slot as shown in Figure 2, B broadcasts a busy tone signal during the busy tone minislot to signal back to A that the transmission was successful and that it can continue to transmit on this channel during the next time-slot, if there are still packets to be transmitted. From the level of busy tone power received at C during the busy tone minislot, node C can determine the potential amount of interference it would cause to node B.

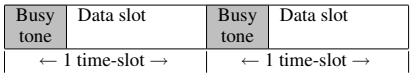

Figure 2: General MAC frame divided into data and busy tone minislots.

This behavior can be mathematically modeled as follows: T_{d} represent the data transmit power for all transmitters and T_{b} represent the busy transmit power for all receivers. $G^k_{(x,y)}$ represents the channel gain for the link between nodes x and y on chunk k which takes into account both fast fading and log-normal shadowing. The potential amount of interference caused at B due to transmission from C, I^k_d on the k^{th} chunk is given by

$$I^k_{\mathrm{d}} = G^k_{(C,B)} \cdot T_{\mathrm{d}} \,. \tag{1}$$

The received busy tone signal from receiving node B on k^{th} chunk, I^k_{b} during the busy tone slot can be written as

$$I^k_{\mathrm{b}} = G^k_{(B,C)} \cdot T_{\mathrm{b}} \,. \tag{2}$$

Due to channel reciprocity conditions, it holds that: $G^k_{(B,C)} = G^k_{(C,B)}$. Solving for $G^k_{(B,C)}$ in eqn. (2) and substituting into eqn. (1), we obtain

$$\frac{T_{\mathrm{d}}}{T_{\mathrm{b}}} \cdot I^k_{\mathrm{b}} = I^k_{\mathrm{d}} \,. \tag{3}$$

From eqn. (3), it can be found that if busy tone power and data power are known, it is possible for the transmitter to be aware of the level of interference I^k_{d} it can potentially cause. Note that I^b_k is received prior to transmission, and the busy tone power and data power are assumed to be known constants.

The signal to interference plus noise ratio (SINR) at the receiver for chunk k, γ^k, can be expressed as follows:

$$\gamma^k = \frac{T_{\mathrm{d}} \cdot G^k}{I^k_d + N} \,, \tag{4}$$

where, G represents the gain on the desired link and N represents the thermal noise per chunk.

For meeting the quality of service (QoS) requirements, it is necessary to achieve a particular SINR target, γ^{t}. As T_{d} and N are all fixed, and as G depends on the actual scenario, it is essential that I^k_d does not exceed a certain threshold I_{thres}. On rephrasing eqn. (3) to reflect this condition, we obtain the condition that must be fulfilled in order for the channel to be selected.

$$\frac{T_{\mathrm{d}}}{T_{\mathrm{b}}} \cdot I^k_{\mathrm{b}} \leq I_{\mathrm{thres}} \tag{5}$$

If $T_{\mathrm{d}} = T_{\mathrm{b}}$, eqn. (5) can be written as

$$I^k_{\mathrm{b}} \leq I_{\mathrm{thres}} \,. \tag{6}$$

This means that if the received busy signal power at any new transmitter is above the given threshold, I_{thres}, interference would prevent the ongoing link from maintaining the SINR target if a transmission were carried out. In order to avoid this to happen, the new transmitter may decide to refrain from transmission at this time-slot. In the sequel, this concept is modeled in the form of a MAC protocol for WINNER–TDD system that jointly takes care of chunk allocation and interference avoidance. Out of 15 OFDM symbols per time-slot in WINNER–TDD MAC frame, 14 OFDM symbols are used for data transmission and the remaining symbol serves as minislot for busy signal transmission.

It is assumed that the traffic arrives in the network in the form of packets. If a transmitter has a data packet queued for transmission, it listens to all chunks in the busy tone slot corresponding to the data transmission in the preceding time-slot. The available bandwidth in WINNER–TDD system is 100 MHz which is highly frequency selective. Therefore, some of the chunks can be used for transmission and others may not be used. Chunk k is used for transmission only if it is not in back–off state and eqn. (6) is fulfilled. This is illustrated in Figure 3 where it can be seen that the chunks 13–15 and 25–28 fulfill this condition and therefore are selected for transmission in the following time-slot. The interference threshold level is chosen based on empirical results as will be presented later in this paper. If the SINR achieved at the receiver meets the SINR target, the transmission is considered successful. If the transmission is not successful, the chunk where the transmission was scheduled goes into a back–off state for randomly selected number of time-slots for the given link. In a back-off state, a chunk cannot be used for transmission even when eqn. (6) is satisfied.

If the packet requires more time-slots to be completely transmitted, the receiving node transmits a busy tone on the chunks where the SINR target was met in the next busy tone slot. The transmitting node detects busy tone signal as a surge in the received level of power. This can be seen in Figure 3 in chunks 13–15 and 25–26. The surge explicitly signals the transmitter that the transmission has been successful. If the data transmitter receives no surge in the next busy tone slot, it implicitly understands that the transmission has not been successful. In the illustration in Figure 3, it is clear that the chunks 27–28 do not meet the SINR target as there is no surge in the received power levels. This establishes an implicit feedback mechanism which does not require any extra radio resource and it does not require channel knowledge.

The 18th Annual IEEE International Symposium on Personal, Indoor and Mobile Radio Communications (PIMRC'07)

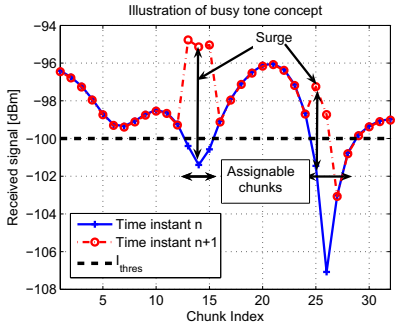

Figure 3: Demonstration of busy tone concept.

It should be obvious that the algorithm does not require any centralized control as the decision of whether or not to allocate any given chunks depends solely on the amount of interference signal received during the busy tone. This property makes the algorithm very suitable for *ad hoc* deployments.

The performance of the above algorithm is compared against the random allocation scheme as a benchmark system. The random allocation scheme schedules transmission on any chunk with probability p if there is data to be transmitted. In random allocation scheme, the selection of chunk for transmission does not depend on the selection of other chunks and whether or not this chunk was selected in previous time-slots.

IV. System Model

An indoor deployment environment as defined as scenario A1 in WINNER [5, 7] is simulated. It consists of one floor of a building consisting of 40 rooms of size $10\text{m} \times 10\text{m} \times 3\text{m}$ and two corridors of size $100\text{m} \times 5\text{m} \times 3\text{m}$. The users are assumed to be distributed uniformly inside the rooms and the corridors with a probability of 90% and 10% respectively. The relevant parameters considered in simulation are presented in Table 1. The deployment scenario and the distribution of users is as shown in Figure 4.

If N_L is the targeted number of links in the system, $2N_L$ mobiles are distributed in the indoor environment. For forming the links, two mobiles A and B are randomly selected from the mobiles distributed in the system. They form an *ad hoc* link if both of them are not already assigned to the links formed beforehand and the link gain (G) is larger than the minimum path gain $(G_{\min})$ required for the link to be selected. $G_{\min}$ is 10 dB above the receiver sensitivity level which is assumed to be at thermal noise level given by $N = kBT$ where k is the Boltzmann constant, B is the system bandwidth and T is the ambient temperature.

A quasi-static scenario is employed where the link gains between the transmitter and receivers remain static through the snapshot duration. Both time variance and frequency selectivity of the channel are taken into account. The channel models are taken from A1 scenario [5]. The coherence time is calculated to be approximately 18.28 ms for a velocity of 5 km/h. Similarly, the coherence bandwidth is approximately 1.55 MHz for line of sight (LOS) conditions and approximately 827.7 kHz for no LOS conditions assuming a correlation of 0.9. Perfect synchronization between transmitters and receivers in time and frequency is assumed.

Parameters	**Value**
MS transmit power	21 dBm
MS height	1.5m
Number of links	15
Symbol length	20.48 μs
Guard interval	1.28 μs
Total symbol length	21.76 μs
Center carrier frequency	5.0 GHz
Total bandwidth	100 MHz
Total number of subcarriers (SCs)	2048
Number of SCs used for data transmission	1664
Frame duration	691.2 μs
OFDM symbols per frame	30
Chunk size	15 (time)$\times$ 8 (frequency)
Number of chunks/frame	2 (time) $\times$ 208 (frequency)
Duplex guard	19.2 μs
Packet size	12208 bits
Bits per subcarrier	1
SINR target	4.8 dB

Table 1: List of simulation parameters

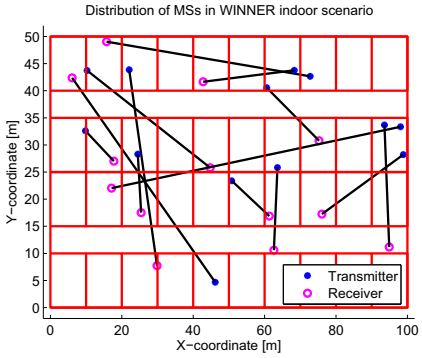

Figure 4: Indoor scenario with its corresponding distribution of users. Each transmitter selects its receiver randomly from the initial distribution.

At the beginning of a snapshot, each transmitter has a buffer which queues a fixed number of packets (N_{P}) of constant length as shown in Figure 5. The offered load to the system is changed by changing the packet arrival rate which is assumed to be the same for all users within a particular snapshot. The packets in the buffer are characterized by linearly increasing expiration time ($k\Delta t$, where k is the position of the packet in the queue) corresponding to the equidistant inter-packet arrival rate. Δt represents the interval between the expiration of k^{th}

The 18th Annual IEEE International Symposium on Personal, Indoor and Mobile Radio Communications (PIMRC'07)

packet and $(k+1)^{\text{th}}$ packet and is equal to $\frac{T_S}{N_P}$, where T_S is the snapshot duration. From such queue, the packets are taken out in a FIFO (first in first out) basis and are scheduled for transmission in portion of the total available bandwidth called a *pipeline*. A pipeline contains $\frac{1}{n}$ of total available chunks for each link and resembles a frequency division multiplex (FDM) system. A packet is thus multiplexed into one of these *pipelines*. The chunks actually used for transmission of a given packet are determined by the busy tone scheme or the benchmark system under consideration.

1	2	3	$\cdots$	N_P
Δt	$2\Delta t$	$3\Delta t$	$\cdots$	$N_P \Delta t$

Figure 5: Example of a traffic queue.

V. Results

The performance of the dynamic chunk allocation algorithms is evaluated on the basis of four metrics - throughput, data rejection rate, delay and packet expiration rate. Throughput is the number of bits that are transmitted successfully. A transmission is considered successful if the received SINR is greater than or equal to the SINR target. The data rejection rate corresponds to the average number of bits transmitted per unit time but fail to meet the SINR target, γ^t. Delay is the time elapsed between the beginning of the snapshot to the time the packet is completely received. The packets that expire before being fully transmitted are assumed to have infinite delay, which for simulation purposes is made equal to the snapshot duration (100 ms). The packets are assumed to expire if the transmission of the entire packet is not completed before the expiration deadline.

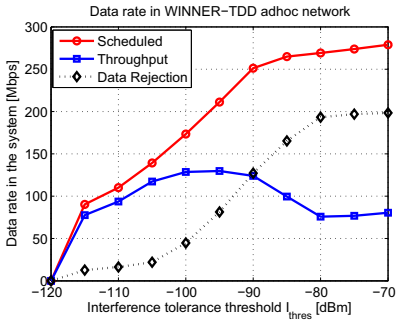

Figure 6: Determination of optimal interference tolerance threshold in WINNER-TDD *ad hoc* network

It should be noted that the choice of the interference threshold is critical as this determines how the system performs, as can be seen from Figure 6. It should be noted that thermal noise, N, is taken into account which is -117.9 dBm/chunk. Therefore, if the threshold is set below this value, eqn. (6) is not satisfied, as such no link can be selected. Increasing the threshold makes the system less sensitive to accepting interference and therefore selects more chunks for transmission. At a certain optimal value of I_{thres} (which is approximately -100 dBm for the system under consideration), it can be observed in Figure 6 that the system attains the highest throughput. If the threshold is increased beyond this point,chunks are more likely being used for simultaneous transmission, and, therefore, this results in greater amount of interference. As such, many links fail to meet their minimum SINR requirements thereby resulting in a drop in the amount of throughput. If the threshold is further increased and if no backoff mechanism is in place to reduce collisions, the performance approaches the random allocation scheme. For the rest of the results, the system is simulated at $I_{\text{thres}} = -100$ dBm.

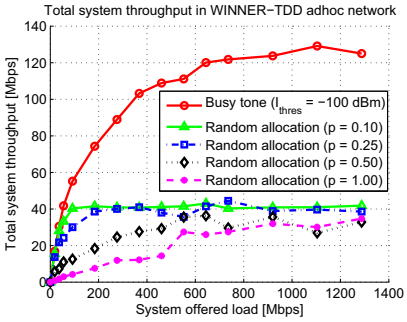

Figure 7: Comparison of total system throughput in WINNER–TDD *ad hoc* network.

The throughput results in Figure 7 show that the busy tone algorithm performs approximately three times better compared to the best among the benchmark systems. In the results, the offered load refers to the total number of bits queued at the beginning of the snapshot in the entire network divided by the snapshot duration. A maximum throughput of approximately 130 Mbps is achieved with busy tone scheme whereas the random allocation scheme with $p = 0.1$ and $p = 0.25$ give a maximum throughput of 40 Mbps. For low value of offered load to the system, the network is practically underused and therefore the random allocation is able to achieve a performance comparable to the busy tone algorithm. Using the fixed allocation scheme without frequency reuse in which the total number of chunks per time-slot are divided by the number of links in the system, the maximum system throughput that can be obtained is 67.4 Mbps. In this case, the system is free of CCI as no chunk is reused. From this it can be found that the BB algorithm approximately achieves an effective reuse of two as the maximum throughput is about 130 Mbps.

The busy tone algorithm performs better than the benchmark systems also in terms of delay and packet success rate as can be seen from Figure 9 and Figure 10. It should also be noted that the rate of successful packet transmission falls down more drastically in the random allocation scheme in comparison to busy tone algorithm. The lower delay and packet expiration rate is of paramount importance for time sensitive traffic and therefore establishes the busy tone as a preferred choice among the methods studied here. It can be seen that the packet de-

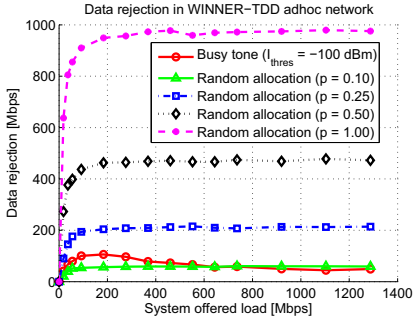

Figure 8: Comparison of data rejection in WINNER–TDD *ad hoc* network.

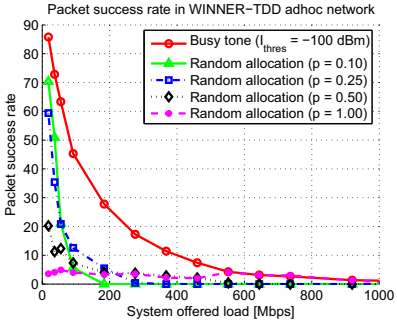

Figure 10: Comparison of packet success rate in WINNER–TDD *ad hoc* network.

lay approaches infinity (considered to be equal to the snapshot duration for the study) and the packet expiration reaches close to 1 for higher packet arrival rates. This results from the fact that with higher number of packets, the inter-packet expiration (Δt) time diminishes. As such, the packets hit the expiration deadline more likely than in the case with lower offered loads.

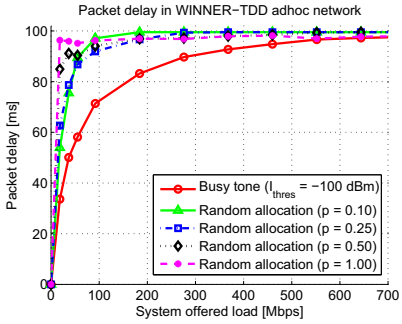

Figure 9: Comparison of delay in WINNER–TDD *ad hoc* network.

VI. Conclusion

In this paper, the BB mechanism for decentralised and self-organizing interference avoidance was investigated for *ad hoc* networks using WINNER–TDD parameters and the indoor test scenario. The performance gain in terms of throughput was found to be approximately three times higher than the highest throughput achieved with the random chunk selection approach. Moreover, it was demonstrated that the BB algorithm is able to double the reuse efficiency of the available spectrum compared to a pure FDM approach. The delay and packet expiration rates were also observed to be significantly lower compared to blind and random chunk selection approaches.

References

[1] J. Gross, I. Paoluzzi, H. Karl, and A. Wolisz. Throughput study for a dynamic OFDM-FDMA system with inband signaling. In *IEEE Vehicular Technology Conference (VTC 2004-spring)*, volume 3, pages 1787–1791, Milan, Italy, May 17–19, 2004.

[2] H. Haas, V. D. Nguyen, P. Omiyi, N. Nedev, and G. Auer. Interference Aware Medium Access in Cellular OFDMA/TDD Networks. In *IEEE International Conference on Communications (ICC 2006)*, volume 4, pages 1778–1783, Istanbul, Turkey, June 11–15, 2006.

[3] Z. J. Haas and J. Deng. Dual busy tone multiple access (DBTMA)-a multiple access control scheme for ad hoc networks. *IEEE Transactions on Communications*, 50(6):975–985, June 2002.

[4] IST-2003-507581 WINNER. D1.4 v1.0 Final requirements per scenario. Retrieved March 15, 2007, from https://www.ist-winner.org/DeliverableDocuments/, October 2005.

[5] IST-2003-507581 WINNER. D5.4 v1.0 Final Report on Link Level and System Level Channel Models. Retrieved April 15, 2007, from https://www.ist-winner.org/DeliverableDocuments/, November 2005.

[6] IST-4-027756 WINNER II. D6.13.1, WINNER II Test Scenarios and Calibration Cases issue 1. Retrieved March 15, 2007, from https://www.ist-winner.org/WINNER2-Deliverables/, June 2006.

[7] IST-4-027756 WINNER II. D6.13.7, WINNER II Test Scenarios and Calibration Cases issue 2. Retrieved March 15, 2007, from https://www.ist-winner.org/WINNER2-Deliverables/, December 2006.

[8] G. Li and H. Liu. Downlink dynamic resource allocation for multi-cell OFDMA system. In *IEEE Vehicular Technology Conference (VTC 2003-fall)*, pages 1698–1702, Florida, USA, October 4–9, 2003.

[9] P. Omiyi, H. Haas, and G. Auer. Analysis of TDD Cellular Interference Mitigation Using Busy-Bursts. *IEEE Transactions on Wireless Communications*, to appear.

[10] S. Singh and C. S. Raghavendra. Power efficient MAC protocol for multihop radio networks. In *IEEE International Symposium on Personal, Indoor and Mobile Radio Communications (PIMRC 1998).*, volume 1, pages 153–157, Boston, MA, USA, September 8–11, 1998.

[11] S. Wu, Y. Tseng, and J. Sheu. Intelligent medium access for mobile ad hoc networks with busytones and power control. In *Proceedings of International Conference on Computer Communications and Networks (ICCCN 1999)*, pages 71–76, Boston, MA, USA, October 11-13, 1999.

[12] R. Zhao, B. Walke, and M. Einhaus. Constructing efficient multi-hop mesh networks. In *The IEEE Conference on Local Computer Networks (LCN 2005)*, pages 166–173, Sydney, Australia, November 15–17, 2005.

[13] R .Zhao, B. Walke, and G. R. Hiertz. An Efficient IEEE 802.11 ESS Mesh Network Supporting Quality-of-Service. *IEEE Journal on Selected Areas in Communications*, 24(11):2005–2017, November 2006.

References

[1] B. Ghimire, S.Videv, G. Auer, and H. Haas, "Balancing System Throughput and Fairness in Multi-User OFDMA-TDD using Busy Bursts," in *Proc. of the International Symposium on Personal, Indoor and Mobile Radio Communications (PIMRC)*, (Cannes, France), pp. 6 pages on CD–ROM, IEEE, Sept. 15–18, 2008.

[2] G. Auer, S. Videv, B. Ghimire, and H. Haas, "Contention Free Inter-Cellular Slot Reservation," *IEEE Communications Letters*, vol. 13, pp. 318–320, May 2009.

[3] G.Auer, S.Videv, B. Ghimire, and H. Haas, "Contention Free Dynamic Slot Allocation in Cellular Networks ," in *Proc. of the IEEE Sarnoff Symposium*, (Princeton, USA), pp. 5 pages on CD–ROM, IEEE, Mar. 30–Apr. 1 2009.

[4] OFCOM, "The communications market 2008," Tech. Rep. 4 Telecoms, OFCOM, August 2009.

[5] E. Dahlman, S. Parkvall, J. Sköld, and P. Beming, *3G Evolution: HSPA and LTE for Mobile Broadband*. Academic Press, 2 ed., 2008.

[6] 3rd Generation Partnership Project (3GPP), Technical Specification Group Radio Access Network;, "High Speed Downlink Packet Access (HSDPA) – Overall Description, Stage 2 (Release 6)." 3GPP TS 25.308 V6.2.0 (2004-09), Sept. 2004.

[7] Ericsson, "HSPA, The Undisputed Choice for Mobile Broadband," white paper 284 23-3119 Uen Rev B, Ericsson, Retrieved Feb. 02, 2010, from www.ericsson.com/technology/whitepapers/hspa_Rev_b.pdf,Oct. 2009.

[8] Motorola Inc., "Long Term Evolution (LTE): A Technical Overview," white paper, Motorola Inc., Retrieved Jan. 12, 2009, from business.motorola.com/experiencelte/pdf/LTETechnicalOverview.pdf, 2007.

[9] Ericsson, "Long Term Evolution (LTE): An Introduction," white paper 284 23-3124 Uen, Ericsson, Retrieved Feb. 19, 2009, from www.ericsson.com/technology/whitepapers,Oct. 2007.

[10] OFCOM, "Public Fixed Wireless Access - 3.4 GHz Auction ," Retrieved Oct. 30, 2009 from http://www.ofcom.org.uk/static/archive/ra/topics/pfwa/3-4ghz/3-4-index.htm 2009.

[11] G. J. Foschini, "Layered Space-Time Architecture for Wireless Communication in a Fading Environment when Using Multi-Element Antennas," *Bell Labs Technical Journal*, vol. 1, pp. 41–59, Sept. 1996.

[12] E. Telatar, "Capacity of Multi-Antenna Gaussian Channels," *European Transaction on Telecommunication*, vol. 10, pp. 585–595, Nov. / Dec. 1999.

[13] R. Mesleh, H. Haas, S. Sinanović, C. W. Ahn, and S. Yun, "Spatial Modulation," *IEEE Transactions on Vehicular Technology*, vol. 57, pp. 2228 – 2241, July 2008.

[14] P. Viswanath, D. Tse, and R. Laroia, "Opportunistic Beamforming Using Dumb Antennas," in *Proc. of the International Symposium on Information Theory*, (Lausanne , Switzerland), p. 449, IEEE, June 30–July 5 2002.

[15] R. Grünheid, H. Rohling, K. Brüninghaus, and U. Schwark, "Self-Organised Beamforming and Opportunistic Scheduling in an OFDM-based Cellular Network," in *Proc of Vehicular Technology Conference (VTC)*, vol. 2, (Melbourne, Canada), pp. 813–817, IEEE, May 7–10, 2006.

[16] V. Chandrasekhar, J. Andrews, and A. Gatherer, "Femtocell Networks: A Survey," *IEEE Communications Magazine*, vol. 46, no. 9, pp. 59–67, 2008.

[17] H. Claussen, L. Ho, and L. Samuel, "Self-Optimization of Coverage for Femtocell Deployments," in *Proc. of the Wireless Telecommunications Symposium (WTS)*, (California, USA), pp. 278–285, Apr. 24–26 2008.

[18] H. Wu, C. Qiao, S. De, and O. Tonguz, "Integrated Cellular and Ad Hoc Relaying Systems: iCAR," *IEEE Journal on Selected Areas in Communications*, vol. 19, pp. 2105–2115, Oct. 2001.

[19] H. yu Wei, S. Ganguly, and R. Izmailov, "Ad hoc Relay Network Planning for Improving Cellular Data Coverage," vol. 2, pp. 769–773, Sept.5–8, 2004.

[20] R. Menon, R. Buehrer, and J. Reed, "On the Impact of Dynamic Spectrum Sharing Techniques on Legacy Radio Systems," *IEEE Transactions on Wireless Communications*, vol. 7, pp. 4198–4207, November 2008.

[21] J. G. Proakis, *Digital Communications*. McGraw–Hill, 1995.

[22] I. A. Glover and P. M. Grant, *Digital Communications*. Pearson Prentice Hall, 2 ed., 2004. ISBN 0 130 89399 4.

[23] P. K. Tang, Y. H. Chew, L. C. Ong, and M. K. Haldar, "Performance of Secondary Radios in Spectrum Sharing with Prioritized Primary Access," in *Military Communications Conference (MILCOM)*, (Washington D.C, USA), pp. 1–7, IEEE, Oct. 23–25, 2006.

[24] P. Popovski, H. Yomo, and R. Prasad, "Strategies for Adaptive Frequency Hopping in the Unlicensed Bands," *IEEE Wireless Communications*, vol. 13, pp. 60–67, Dec. 2006.

[25] P. E. Omiyi and H. Haas, "Improving Time-Slot Allocation in 4th Generation OFDM/TDMA TDD Radio Access Networks with Innovative Channel-Sensing," in *Proc. of the International Conference on Communications (ICC)*, vol. 6, (Paris, France), pp. 3133–3137, IEEE, June 20–24 2004.

[26] P. Omiyi, H. Haas, and G. Auer, "Analysis of TDD Cellular Interference Mitigation Using Busy-Bursts," *IEEE Transactions on Wireless Communications*, vol. 6, pp. 2721–2731, July 2007.

[27] H. Haas, V. D. Nguyen, P. Omiyi, N. Nedev, and G. Auer, "Interference Aware Medium Access in Cellular OFDMA/TDD Networks," in *Proc. of the IEEE International Conference on Communications (ICC)*, vol. 4, (Istanbul, Turkey), pp. 1778–1783, June 11–15, 2006.

[28] IST-4-027756 WINNER II, "D6.13.7, WINNER II Test Scenarios and Calibration Cases Issue 2." Retrieved Mar. 15, 2007, from https://www.ist-winner.org/WINNER2-Deliverables/.

[29] M. Chiang, C. W. Tan, D. P. Palomar, D. O'Neill, and D. Julian, "Power Control By Geometric Programming," *IEEE Transactions on Wireless Communications*, vol. 6, pp. 2640–2651, July 2007.

[30] A. Gjendemsj, D. Gesbert, G. E. Oien, and S. G. Kiani, "Binary Power Control for Sum Rate Maximization Over Multiple Interfering Links," *IEEE Transactions on Wireless Communications*, vol. 7, pp. 3164–3173, Aug. 2008.

[31] N. Ksairi, P. Bianchi, P. Ciblat, and W. Hachem, "Resource Allocation for the Downlink of OFDMA Cellular Networks and Optimization of the Reuse Factor," in *Proc. of the InternationalInformation Theory and Its Applications (ISITA)*, (Auckland), pp. 1–6, Dec. 7–10, 2008.

[32] H. Dahrouj and W. Yu, "Coordinated Beamforming for the Multi-Cell Multi-Antenna Wireless System," in *Proc. of the Conference on Information Sciences and Systems CISS*, (Princeton, USA), pp. 429–434, Mar. 19-21, 2008.

[33] ITU-R, "Framework and Overall Objectives of the Future Development of IMT-2000 and Systems Beyond IMT-2000," Tech. Rep. ITU-R M.1645, ITU, Retrieved Jan. 12, 2009 from http://www.itu.int/rec/R-REC-M.1645/e, 2003.

[34] ITU-R, "Requirements Related to Technical Performance for IMT-Advanced Radio Interface(s)," Tech. Rep. ITU-R M.2134, ITU, Retrieved Jan. 22, 2010 from http://www.itu.int/dms_pub/itu-r/opb/rep/R-REP-M.2134-2008-PDF-E.pdf, 2008.

[35] IST-2003-507581 WINNER, "D1.4 v1.0 Final requirements per scenario." Retrieved Mar. 15, 2007, from https://www.ist-winner.org/DeliverableDocuments/, Oct. 2005.

[36] Y.-J. Choi, C. S. Kim, and S. Bahk, "Flexible Design of Frequency Reuse Factor in OFDMA Cellular Networks," in *Proc. of the International Conference on Communications (ICC)*, vol. 4, (Istanbul, Turkey), pp. 1784–1788, IEEE, June 11-15 2006.

[37] S. Sesia, I. Toufik, and M. Baker, *LTE - The UMTS Long Term Evolution: From Theory to Practice*. Wiley, 1 ed., 2009.

[38] IEEE802.11a-1999, "Wireless LAN Medium Access Control (MAC) and Physical Layer (PHY) specifications; High-Speed Physical Layer in the 5 GHz Band," 1999.

[39] WHDI. Retrieved from http://www.whdi.org/, Jan. 2010.

[40] T. S. Rappaport, *Wireless Communications: Principles and Practice*. Prentice Hall PTR, 2 ed., 2002.

[41] D. J. Love, R. W. Heath Jr., W. Santipach, M. L. Honig, "What is the Value of Limited Feedback for MIMO Channels," *IEEE Communications Magazine*, Oct. 2004.

[42] B. Hassibi and B. M. Hochwald, "How Much Training is Needed in Multiple-Antenna Wireless Links?," *IEEE Transactions on Information Theory*, vol. 49, pp. 951–963, 2003.

[43] T. Halonen, J. Romero, and J. Melero, *GSM, GPRS and EDGE Performance*. John Wiley & Sons Ltd.; Second Edition, 2003.

[44] R. Chang and R. Gibby, "A theoretical study of performance of an orthogonal multiplexing data transmission scheme," *IEEE Transactions on Communication Technology*, vol. 16, pp. 529 –540, Aug. 1968.

[45] S. Weinstein and P. Ebert, "Data Transmission by Frequency-Division Multiplexing Using the Discrete Fourier Transform," *IEEE Transactions on Communication Technology*, vol. 19, pp. 628–634, Oct. 1971.

[46] A. Peled and A. Ruiz, "Frequency Domain Data Transmission Using Reduced Computational Complexity Algorithms," in *Proc. of the IEEE International Conference on Acoustics, Speech and Signal Processing (ICASSP)*, vol. 5, (Denver, USA), pp. 964–967, Apr. 9–11 1980.

[47] J. Lago-Fernandez and J. Salter, "Modelling Impulsive Interference in DVB-T: Statistical Analysis, Test Waveforms & Receiver Performance," tech. rep., BBC R&D, Apr. 2004. Retrieved Jan. 14, 2010.

[48] A. F. Mollisch, *Wireless Communications*. West Sussex, UK: John Wiley & Sons, July 2006.

[49] M. Johnson and S. G. Frigo, "The Design and Implementation of FFTW3," *Proceedings of the IEEE*, vol. 93, pp. 216–231, Feb. 2005.

[50] S. Ahmad, M. O. Swamy, and M. N. S. Bouguezel, "A General Class of Split-radix FFT Algorithms for the Computation of the DFT of Length-2m," *IEEE Transactions on Signal Processing*, vol. 55, pp. 4127–4138, Aug. 2007.

[51] J. G. Proakis, *Digital Communications*. McGraw-Hill Series in Electrical and Computer Engineering, McGraw-Hill Higher Education, 4 ed., Dec. 2000.

[52] D. Tse and P. Viswanath, *Fundamentals of Wireless Communication*. Cambridge University Press, 2005.

[53] M. Pätzold, *Mobile Fading Channels*. John Wiley & Sons, Ltd., 2002.

[54] A. Goldsmith, *Wireless Communications*. Cambridge University Press, 2005.

[55] P. Höher, "A Statistical Discrete-Time Model for the WSSUS Multipath Channel," *IEEE Transactions on Vehicular Technology*, vol. 41, pp. 461–468, Nov. 1992.

[56] S. Thoen, L. Van der Perre, and M. Engels, "Modeling the Channel Time-Variance for Fixed Wireless Communications," *IEEE Communications Letters*, vol. 6, pp. 331–333, aug 2002.

[57] W. Wang, T. Ottosson, M. Sternad, A. Ahlen, and A. Svensson, "Impact of Multiuser Diversity and Channel Variability on Adaptive OFDM," in *Proc. of the 58th IEEE Vehicular Technology Conference (VTC)*, (Orlando, USA), pp. 547–551, Oct. 6-9 2003.

[58] T. S. Rappaport, *Wireless Communications: Principles and Practice*. Prentice Hall, ISBN: 0130422320, 2 ed., Dec. 2001.

[59] H. Fattah and C. Leung, "An Overview of Scheduling Algorithms in Wireless Multimedia Networks," *IEEE Wireless Communications*, vol. 9, pp. 76–83, Oct. 2002.

[60] H. W. M. S. S. Boche, "Unifying View on Min-max Fairness and Utility Optimization in Cellular Networks," in *Proc. of the Wireless Communications and Networking Conference (WCN)*, vol. 3, pp. 1280–1285, IEEE, Mar. 13–17, 2005.

[61] S. Chan and M. Zukerman, "Is Max-min Fairness Achievable in the Presence of Insubordinate Users?," *IEEE Communications Letters*, vol. 6, pp. 120–122, Mar. 2002.

[62] H. Boche and M. Schubert, "Resource Allocation in Multiantenna Systems-achieving Max-min Fairness by Optimizing a Sum of Inverse SIR," *IEEE Transactions on Signal Processing*, vol. 54, pp. 1990–1997, June 2006.

[63] B. L. B. J. Y. Radunovic, "A Unified Framework for Max-min and Min-max Fairness With Applications," *IEEE/ACM Transactions on Networking*, vol. 15, pp. 1073–1083, Oct. 2007.

[64] M. M. Islam and M. Murshed, "Min-max Fairness Scheme for Resource Allocation in Cellular Multimedia Networks," in *Proc. of the International Conference on Information Technology: Coding and Computing (ICITCC)*, pp. 265–270, IEEE.

[65] F. P. Kelly, "Charging and Rate Control for Elastic Traffic," *European Transactions on Telecommunications*, vol. 8, pp. 33–37, 1997.

[66] Thyagarajan Nandagopal and Tae-Eun Kim and Xia Gao and Vaduvur Bharghavan, "Achieving MAC Layer Fairness in Wireless Packet Networks," in *Proc. of the International Conference on Mobile Computing and Networking*, (Boston, Massachusetts, United States), pp. 87 – 98, ACM, Aug. 6-11 2000.

[67] T. E. Kolding, "Link and System Performance Aspects of Proportional Fair Scheduling in WCDMA/HSDPA," in *Proc. of the Vehicular Technology Conference (VTC)*, vol. 3, (Orlando, USA), pp. 1717–1722, IEEE, Oct. 6–9, 2003.

[68] G. Caire, R. R. Muller, and R. Knopp, "Hard fairness versus proportional fairness in wireless communications: The single-cell case," *IEEE Transactions on Information Theory*, vol. 53, pp. 1366–1385, Apr. 2007.

[69] V. Vukadinovic and G. Karlsson, "Video Streaming in 3.5G: On Throughput-Delay Performance of Proportional Fair Scheduling," in *In Proc. of the Modeling, Analysis, and Simulation of Computer and Telecommunication Systems,(MASCOTS)*, (Monterey, California, USA), pp. 393–400, IEEE, Sept. 11–14, 2006.

[70] T. Bonald, "A Score-Based Opportunistic Scheduler for Fading Radio Channels," in *Proc. of the European Wireless Conference (EWC)*, (Barcelona, Spain), Feb.24–27 2004.

[71] B. Ghimire, G. Auer, and H. Haas, "Busy Bursts for Trading-off Throughput and Fairness in Cellular OFDMA-TDD," *Eurasip Journal on Wireless Communications and Networking*, vol. 2009, Article ID 462396, 14 pages, 2009.

[72] S. Chaudhury, H. Venkataraman, and H. Haas, "Uplink Capacity Comparison of Non-Perfect Frequency Synchronised Cellular OFDM Systems," in *Proc. of International Wireless Communications and Mobile Computing Conference (IWCMC)*, (Vancouver, Canada), July 3–6 2006.

[73] P. Moose, "A Technique for Orthogonal Frequency Division Multiplexing Frequency Offset Correction," *IEEE Transactions on Communications*, vol. 42, pp. 2908–2914, Oct. 1994.

[74] H. Tang, K. Y. Lau, and R. W. Brodersen, "Synchronization schemes for packet OFDM system," in *Proc. of the International Conference on Communications (ICC)*, vol. 5, pp. 3346–3350, IEEE, May 11–15, 2003.

[75] H. Minn, V. K. Bhargava, and K. B. Letaief, "A Robust Timing and Frequency Synchronization for OFDM Systems," *IEEE Transactions on Wireless Communications*, vol. 2, pp. 822–839, July 2003.

[76] A. Tyrrell, G. Auer, and C. Bettstetter, "Emergent Slot Synchronization in Wireless Networks," *IEEE Transactions on Mobile Computing*, no. 99, pp. 1–1.

[77] Y. Zhang, R. Hoshyar, and R. Tafazolli, "Timing and frequency offset estimation scheme for the uplink of OFDMA systems," *IET Communications*, vol. 2, pp. 121–130, Jan. 2008.

[78] Z. Zhang and C. Tellambura, "The effect of imperfect carrier frequency offset estimation on an OFDMA uplink," *IEEE Transactions on Communications*, vol. 57, pp. 1025–1030, Apr. 2009.

[79] M. Sternad, T. Svensson, T. Ottosson, A. Ahlen, A. Svensson, and A. Brunstrom, "Towards Systems Beyond 3G Based on Adaptive OFDMA Transmission," *Proceedings of the IEEE*, vol. 95, pp. 2432–2455, Dec. 2007.

[80] S.-E. Elayoubi, O. B. Haddada, and B. Fourestie, "Performance Evaluation of Frequency Planning Schemes in OFDMA-Based Networks," *IEEE Transactions on Wireless Communications*, vol. 7, pp. 1623–1633, May 2008.

[81] M. C. Necker, "Local Interference Coordination in Cellular OFDMA Networks," in *Proc. of the Vehicular Technology Conference (VTC)*, (Baltimore, USA), pp. 1741–1746, IEEE, Sept. 30 –Oct. 3, 2007.

[82] IST-4-027756 WINNER II, "D6.13.14 WINNER II System Concept Description." Retrieved June 25, 2008, from https://www.ist-winner.org/deliverables.html, Dec. 2007.

[83] Liciano Sarperi, Mythri Hunukumbure and Sunil Vadgama, "Simulation Study of Fractional Frequency Reuse in WiMAX Networks," *Fujitsu Scientific & Technical Journal*, vol. 44-3, pp. 318–324, July 2008.

[84] Z. Yuefeng and N. Zein, "Simulation Study of Fractional Frequency Reuse for Mobile WiMAX," in *Proc. of the Vehicular Technology Conference (VTC)*, (Marina Bay, Singapore), pp. 2592–2595, IEEE, May 11–14, 2008.

[85] J. S. Blogh and L. Hanzo, eds., *Third-Generation Systems and Intelligent Wireless Networking*. Wiley Interscience, West Sussex, UK: John Wiley & Sons, Ltd, May 2002.

[86] H. L. V. Trees, *Optimum Array Processing (Detection, Estimation, and Modulation Theory, Part IV)*. John Wiley & Sons, Inc., New York, 2002.

[87] R. Roy, A. Paulraj, and T. Kailath, "Estimation of Signal Parameters Via Rotational Invariance Techniques ESPRIT," in *Proc. of the Military Communications Conference*, vol. 3, (California, USA), pp. 1–41, IEEE, Oct. 5–9, 1986.

[88] F.-M. Han and X.-D. Zhang, "An Esprit-like Algorithm for Coherent DOA Estimation," *IEEE Antennas and Wireless Propagation Letters*, vol. 4, pp. 443–446, 2005.

[89] P. Stoica and N. Arye, "MUSIC, Maximum Likelihood, and Cramer-rao Bound," *Acoustics, Speech and Signal Processing, IEEE Transactions on*, vol. 37, pp. 720–741, May 1989.

[90] M. Mouhamadou and P. Vaudon, "Smart Antenna Array Patterns Synthesis : Null Steering and Multi-user Beamforming by Phase Control," *Progress In Electromagnetics Research*, vol. 60, pp. 95–106, 2006.

[91] F. A. Tobagi and L. Kleinrock, "Packet Switching in Radio Channels: Part II—The Hidden Terminal Problem in Carrier Sense Multiple-Access and the Busy-Tone Solution," *IEEE Transactions on Communications*, vol. 23, pp. 1417–1433, Dec. 1975.

[92] A. S. Tanenbaum, *Computer Networks (fourth edition)*. New Jersey, USA: Prentice-Hall Inc. , 2004.

[93] R. Rom, *Local Area and Multiple Access Networks*, ch. Collision Detection in Radio Channels, pp. 235–249. Computer Science Press Advances In Telecommunication Networks Series, NY, USA: Computer Science Press, Inc., 1986.

[94] Jin Wang, S. Premvuti and A. Tabbara, " A Wireless Media Access Protocol (CSMA/CD-W) for Mobile Robot Based Distributed Robotic Systems," in *Proc. of the International Conference on Robotics and Automation*, vol. vol. 3, (Nagoya, Japan), pp. 2561 – 2566, IEEE, May 21–27 1995.

[95] A. C. V. Gummalla and J. O. Jimb, "Wireless collision detect (wcd): Multiple access with receiver initiated feedback and carrier detect signal," in *Proc. of the International Conference on Communications (ICC)*, vol. 1, (New Orleans, LA, USA), pp. 397–401, IEEE, June 18–22 2000.

[96] D. S. Chan and T. Berger, "Collision Detection for Carrier Sense Multiple Access in Wireless Networks," in *Proc. of the 16th IEEE International Symposium on Personal, Indoor and Mobile Radio Communications (PIMRC)*, vol. 3, (Berlin, Germany), pp. 1495–1499, IEEE, 11-14 Sept. 2005.

[97] K. Xu, M. Gerla, and S. Bae, "How Effective Is the IEEE 802.11 RTS/CTS Handshake in Ad Hoc Networks," in *Proc. of the Global Telecommunications Conference (GLOBECOM)*, vol. 1, (Taipei, Taiwan), pp. 72–76, IEEE, Nov. 17–21, 2002.

[98] P. Karn, "MACA: A New Channel Access Method for Packet Radio," in *In Proc. of the ARRL Computer Networking Conference*, (Ontario, Canada), 1990.

[99] V. Bharghavan, A. Demers, S. Shenker, and L. Zhang, "MACAW: a media access protocol for wireless LAN's," in *SIGCOMM '94: Proc. of the conference on Communications architectures, protocols and applications*, (New York, NY, USA), pp. 212–225, ACM Press, 1994.

[100] S.-L. Wu, C.-Y. Lin, Y.-C. Tseng, and J.-L. Sheu, "A New Multi-channel MAC Protocol with On-demand Channel Assignment for Multi-hop Mobile *ad hoc* Networks," in *Proc. of the International Symposium on Parallel Architectures, Algorithms and Networks*, (Dallas, USA), pp. 232–237, IEEE, Dec.7-10, 2000.

[101] M. Seo, Y. Kim, and J. Ma, "A multi-channel MAC protocol with snooping for multi-hop wireless networks," in *Proc. of the International Symposium on Wireless Communication Systems*, pp. 268–272, Oct. 21–24, 2008.

[102] Z. J. Haas and J. Deng, "Dual Busy Tone Multiple Access (DBTMA)-A Multiple Access Control Scheme for ad hoc Networks," *IEEE Transactions on Communications*, vol. 50, pp. 975–985, June 2002.

[103] S. Wu, Y. Tseng, and J. Sheu, "Intelligent Medium Access for Mobile ad hoc Networks with Busytones and Power Control," in *Proc. of International Conference on Computer Communications and Networks (ICCCN 1999)*, (Boston, USA), pp. 71–76, IEEE, Oct. 11–13, 1999.

[104] R. Zhao, B. Walke, and M. Einhaus, "Constructing Efficient Multi-hop Mesh Networks," in *Proc. of the Conference on Local Computer Networks (LCN)*, (Sydney, Australia), pp. 166–173, IEEE, Nov. 15–17, 2005.

[105] R. Zhao, B. Walke, and G. Hiertz, "An Efficient IEEE 802.11 ESS Mesh Network Supporting Quality-of-Service," *IEEE Journal on Selected Areas in Communications*, vol. 24, no. 11, pp. 2005–2017, 2006.

[106] H. Haas and S. McLaughlin, eds., *Next Generation Mobile Access Technologies: Implementing TDD*. Cambridge University Press, ISBN: 13:9780521826228, Jan. 2008.

[107] B. Ghimire, H. Haas, and G. Auer, "Busy Burst Enabled Interference Avoidance in WINNER-TDD," in *Proc. of the International Symposium on Personal, Indoor and Mobile Radio Communications (PIMRC)*, (Athens, Greece), pp. 5 pages on CD–ROM, IEEE, Sept. 3–7, 2007.

[108] M. Debbah, P. Loubaton, and M. de Courville, "Asymptotic Performance of Successive Interference Cancellation in the Context of Linear Precoded OFDM Systems," *IEEE Transactions on Communications*, vol. 52, pp. 1444–1448, Sept. 2004.

[109] P. Patel and J. Holtzman, "Analysis of a Simple Successive Interference Cancellation Scheme in a DS/CDMA System," *IEEE Journal on Selected Areas in Communications*, vol. 12, pp. 796–807, June 1994.

[110] J. G. Andrews, "Interference Cancellation for Cellular Systems: A Contemporary Overview," *IEEE Wireless Communications Magazine*, vol. 12, pp. 19–29, April 2005.

[111] M. K. Varanasi and B. Aazhang, "Multistage Detection in Asynchronous Code-Division Multiple-Access Communications," *IEEE Transactions on Communications*, vol. 38, pp. 509–519, Apr. 1990.

[112] B. SIG, "Specification of the Bluetooth System." Retrieved from http://www.bluetooth.com/NR/rdonlyres/38C6F538-5B45-4811-A182-079C590B27A4/13551/CoreV40.zip on Jan 2010, Dec 2009.

[113] H. F. Harmuth, "Applications of Walsh Functions in Communications," *IEEE Spectrum*, vol. 6, pp. 82–91, Nov. 1969.

[114] K. J. Horadam, *Hadamard Matrices and Their Applications*. NJ, USA: Princeton University Press, 2007.

[115] A. Viterbi, *Principles of Spread Spectrum Communication*. Addison–Wesley, 1995.

[116] P. Agyapong, H. Haas, A. Tyrrell, and G. Auer, "Interference Tolerance Signaling Using TDD Busy Tone Concept," in *Proc. of the Vehicular Technology Conference (VTC)*, (Dublin, Ireland), pp. 2850–2854, IEEE, Apr. 22–25, 2007.

[117] IST-2003-507581 WINNER, "D5.4 v1.0 Final Report on Link Level and System Level Channel Models." Retrieved Apr. 15, 2007, from https://www.ist-winner.org/DeliverableDocuments/, Nov. 2005.

[118] A. Persson, T. Ottosson, and G. Auer, "Inter-Sector Scheduling in Multi-User OFDM," in *IEEE International Conference on Communications (ICC)*, vol. 10, (Istanbul), pp. 4415–4419, June 2006.

[119] R. Jain, D. Chiu, and W. Hawe., "A Quantitative Measure of Fairness and Discrimination for Resource Allocation in Shared Computer Systems," Tech. Rep. 301, DEC Technical Report, 1984.

[120] S. Singh and C. S. Raghavendra, "Power Efficient MAC Protocol for Multihop Radio Networks," in *Proc. of the 9th IEEE International Symposium on Personal, Indoor and Mobile Radio Communications (PIMRC)*, vol. 1, (Boston, USA), pp. 153–157, IEEE, Sept. 8–11, 1998.

[121] A. Michail and A. Ephremides, "Energy Efficient Routing for Connection-Oriented Traffic in ad-hoc Wireless Networks," in *Proc. of the 11th IEEE International Symposium on Personal, Indoor and Mobile Radio Communications (PIMRC)*, vol. 2, (London, UK), pp. 762–766, IEEE, Sept. 18–21, 2000.

[122] M. Etoh, T. Ohya, and Y. Nakayama, "Energy Consumption Issues on Mobile Network Systems," in *Proc. of the International Symposium on Applications and the Internet (SAINT)*, (Turku, Finland), pp. 365–368, IEEE, July/Aug. 2008.

[123] S. M. Heikkinen, H. Haas, and G. J. R. Povey, "Adjacent Channel Interference on the UTRA-TDD Air Interface," in *Colloquium on UMTS Terminals and Software Radio*, (Glasgow, Scotland), pp. 13/1 – 13/5, IEE, 26 Apr. 1999.

[124] Z. Bharucha and H. Haas, "Application of the TDD Underlay Concept to Home NodeB Scenario," in *Proc. of the 67th IEEE Vehicular Technology Conference (VTC)*, (Marina Bay, Singapore), pp. 56–60, May 11–14, 2008.

[125] S. Sinanović, N. Serafimovski, H. Haas, and G. Auer, "System Spectral Efficiency Analysis of a 2-Link Ad Hoc Network," in *Proc. of the 50th IEEE Global Telecommunications Conference (GLOBECOM)*, (Washington, USA), pp. 3684–3688, IEEE, Nov. 26–30 2007.

[126] IST-4-027756 WINNER II, "D1.1.2 v1.2 WINNER II Channel Models." Retrieved Feb. 5, 2008, from https://www.ist-winner.org/WINNER2-Deliverables/.